Development of bio-composites with novel characteristics through enzymatic grafting

By

Hafiz Muhammad Nasir Iqbal

Department of Life Sciences
Faculty of Science and Technology
University of Westminster
London, UK

A thesis submitted in partial fulfilment of the requirements of

the University of Westminster for the degree of

Doctor of Philosophy

June 2015

Abstract

Enzymatic grafting of biopolymers has recently been the focus of green chemistry technologies due to the growing environmental concerns, and subsequent legal restrictions. Over the last decade, research covering various applications of enzymes like lipases and laccases has been increased rapidly, particularly in the field of polymer science, to graft multi-functional polymers.

In this context, a series of bio-composites *e.g.* poly3-hydroxybutyrate [P(3HB)] grafted ethyl cellulose (EC) and bacterial cellulose (BC) [*i.e.,* P(3HB)-*g*-EC/BC] and keratin-*g*-EC bio-composites were successfully synthesised by introducing enzyme-based grafting where lipase and laccase were used as model bio-catalysts. Furthermore, various natural phenols *e.g.,* caffeic acid (CA), gallic acid (GA), *p*-4-hydroxybenzoic acid (HBA), and thymol (T) were grafted onto the newly developed P(3HB)-EC and keratin-EC-based composites under laccase-assisted environment. Subsequently, the resulting bio-composites were removed from their respective casting surfaces under ambient environment and characterised using different analytical and imaging techniques.

This project shows improvement in the thermo-mechanical properties of the bio-composites as compared to the individual components. The tensile strength, elongation at break point, and Young's modulus values of the bio-composites reached very high levels in comparison to the films prepared with untreated P(3HB) and keratin that were too fragile to be measured for any of the above mentioned characteristics. Morphological analysis of the newly developed bio-composites surfaces through SEM showed a uniform distribution of the P(3HB) and keratin within the backbone polymer (EC). Interestingly, untreated P(3HB) was hydrophobic in nature and after lipase treatment P(3HB) and P(3HB)-EC-based graft composites attained a higher level of hydrophilicity.

The phenol grafted bio-composites were critically evaluated for their antibacterial and biocompatibility features, as well as their degradability in a soil. In particular, the results of the antibacterial evaluation indicated that 20CA-*g*-P(3HB)-EC, 15GA-*g*-P(3HB)-EC, 15HBA-*g*-P(3HB)-EC, 15T-*g*-P(3HB)-EC, 15CA-*g*-keratin-EC, 15GA-*g*-keratin-EC, 10HBA-*g*-keratin-EC and 20T-*g*-keratin-EC exerted strong bactericidal and bacteriostatic activity against Gram$^+$ bacteria *Bacillus subtilis* NCTC 3610 and *Staphylococcus aureus NCTC* 6571 and Gram$^-$ bacteria *Escherichia coli NCTC* 10418 and *Pseudomonas aeruginosa NCTC* 10662 strains, respectively. This study shows further that at various phenolic concentrations the newly synthesised bio-composites remained cytocompatible with human keratinocyte-like HaCaT skin cells, as 100% cell viability was recorded after 5 days of incubation. From the degradation point of view, an increase in the degradation rate was recorded during the soil burial analyses.

This study provides novel and additional knowledge that encourage greater utilisation of biopolymers in the development of bio-composites with novel and sophisticated characteristics for potential applications.

Table of Contents

List of Figures

List of Tables

List of Abbreviations

Ala	Alanine
ASTM	American standard testing method
Arg	Arginine
Asp	Aspartic acid
B. subtilis	*Bacillus subtilis*
BC	Bacterial cellulose
CA	Caffeic acid
CALB	*Candida Antarctica Lipase B*
T_c	Crystallisation temperature
Cyst	Cystine
DSC	Differential scanning calorimetry
DMEM	Dulbecco's modified eagle's medium
DMA	Dynamic mechanical analyser
E.C	Enzyme Commission
E. coli	*Escherichia coli*
EC	Ethyl cellulose
FTIR	Fourier-transform infrared spectroscopy
GA	Gallic acid
Glu	Glutamic acid
T_g	Glass transition temperature
Gly	Glycine
GE	Grafting efficiency
GP	Grafting parameters
GY	Graft yield
HDI	High definition images
Ile	Isoleucine
Keratin-*g*-EC	Keratin grafted ethyl cellulose
Leu	Leucine
mcl-PHAs	Medium-chain-length PHAs
ΔH_m	Melting enthalpy
T_m	Melting temperature
MGM	Modified G medium
NR	Neutral red
ND	*Not detected*
OD	Optical density
Phe	Phenylalanine
PBS	Phosphate buffer saline
PHAs	Polyhydroxyalkanoates
P(3HP)	Poly(3-hydroxypropionate)
P(3HB)/PHB	Poly3-hydroxybutyrate
P(3HB)-*g*-EC	Poly3-hydroxybutyrate grafted ethyl cellulose
P(3HB)-*g*-BC	Poly3-hydroxybutyrate grafted bacterial cellulose
P(3HV)	Poly(3-hydroxyvalerate)
P(3HHx)	Poly(3-hydroxyhexanoate)
P(3HH)	Poly(3-hydroxyhexanoate)
P(3HO)	Poly (3-hydroxyoctanoate)
P(3HN)	Poly (3-hydroxynonanoate)
P(3HD)	Poly(3-hydroxydecanoate)

P(3HUD)or P(3HUd)	Poly(3-hydroxyundecanoate)
P(3HDD) or P(3HDd)	Poly(3-hydroxydodecanoate)
P(3HOD) or P(3HOd)	Poly(3-hydroxyoctadecanoate)
P(4HB)	Poly(4-hydroxybutyrate)
P(5HB)	Poly(5-hydroxybutyrate)
P(5HV)	Poly(5-hydroxyvalerate)
PLA	Poly lactic acid
HBA	*p*-4-hydroxybenzoic acid
Pro	Proline
P. aeruginosa	*Pseudomonas aeruginosa*
SEM	Scanning electron microscopy
Ser	Serine
scl-PHAs	Short-chain-length PHAs
S.E.	Standard error
S. aureus	*Staphylococcus aureus*
SDI	*Surface dipping and incorporation*
SR	Swelling ratio
Thr	Threonine
T	Thymol
TE	Tissue engineering
Tyr	Tyrosine
Val	Valine
WCA	Water contact angle
XRD	X-ray diffraction

List of Publications

Peer-reviewed Research Publications:

Iqbal, H.M.N., Kyazze, G., Locke, I.C., Tron, T., & Keshavarz, T. (2015). *In-situ* development of self-defensive antibacterial biomaterials: phenol-*g*-keratin-EC based bio-composites with characteristics for biomedical applications. *Green Chemistry,* 17, 3858-3869. (Impact factor = 8.020)

Iqbal, H.M.N., Kyazze, G., Locke, I.C., Tron, T., & Keshavarz, T. (2015). Poly(3-hydroxybutyrate)-ethyl cellulose based bio-composites with novel characteristics for infection free wound healing application. *International Journal of Biological Macromolecules,* 81, 552-559. (Impact factor = 2.858)

Iqbal, H.M.N., Kyazze, G., Tron, T., & Keshavarz, T. (2015). Laccase-assisted approach to graft multifunctional materials of interest: keratin-EC based novel composites and their characterisation. *Macromolecular Materials and Engineering,* 300, 712-720. (Impact factor = 2.661)

Iqbal, H.M.N., Kyazze, G., Locke, I.C., Tron, T., & Keshavarz, T. (2015). Development of novel antibacterial active, HaCaT bio-compatible and bio-degradable CA-*g*-P(3HB)-EC bio-composites with caffeic acid as a functional entity. *Express Polymer Letters,* 9, 764-772. (Impact factor = 2.761)

Iqbal, H.M.N., Kyazze, G., Locke, I.C., Tron, T., & Keshavarz, T. (2015). Development of bio-composites with novel characteristics: Evaluation of phenol-induced antibacterial, biocompatible and biodegradable behaviours. *Carbohydrate Polymers,* 131, 197-207. (Impact factor = 4.074)

Iqbal, H.M.N., Kyazze, G., Tron, T., & Keshavarz, T. (2014). "One-pot" synthesis and characterisation of novel P (3HB)-ethyl cellulose based graft composites through lipase catalysed esterification. *Polymer Chemistry,* 5(24), 7004-7012. (Impact factor = 5.520)

Iqbal, H.M.N., Kyazze, G., Tron, T., & Keshavarz, T. (2014). Laccase-assisted grafting of poly (3-hydroxybutyrate) onto the bacterial cellulose as backbone polymer: Development and characterisation. *Carbohydrate Polymers,* 113, 131-137. (Impact factor = 4.074)

Iqbal, H.M.N., Kyazze, G., Tron, T., & Keshavarz, T. (2014). A preliminary study on the development and characterisation of enzymatically grafted P (3HB)-ethyl cellulose based novel composites. *Cellulose,* 21, 3613-3621. (Impact factor = 3.573)

Iqbal, H.M.N., Kyazze, G., & Keshavarz, T. (2013). Advances in the valorization of lignocellulosic materials by biotechnology: An overview. *Bio-Resources,* 8(2), 3157-3176. (Impact factor = 1.425)

Iqbal, H.M.N., Kyazze, G., Tron, T., & Keshavarz, T. (2015). Laccase from *Aspergillus niger*: A novel tool to graft multifunctional materials of interests and their characterization. *Saudi Journal of Biological Sciences,* (Under review). (Impact factor = 1.257)

Peer-reviewed Book Chapter:

Iqbal, H.M.N., & Keshavarz, T. (2015). Keratin based materials in biotechnology. In V.K. Thakur, M. Thakur, & M.R. Kessler (Eds.). Handbook of Composites from renewable materials. Wiley-Scrivener, (Chapter 12).

Abstracts:

Iqbal, H.M.N., Kyazze, G., Tron, T., & Keshavarz, T. *Enzymatic grafting: A Novel Approach to Develop Multifunctional Materials of Interest* in 8th Energy, Materials, and Nanotechnology (EMN Fall meeting, 2014) Orlando, Florida, USA. 22nd – 25th November 2014.

Iqbal, H.M.N., Kyazze, G., Tron, T., & Keshavarz, T. *Synthesis and characterisation of novel keratin-cellulose based graft composites* in Annual PG-Fair, Faculty of Science and Technology, University of Westminster, London, UK. 29th April, 2014.

Iqbal, H.M.N., Kyazze, G., Tron, T., & Keshavarz, T. *Laccase-assisted bio-grafting of polyhydroxyalkanoates (PHAs) onto the ethyl cellulose (EC) backbone* in Annual PG-Fair, Faculty of Science and Technology, University of Westminster, London, UK. 25th April, 2013.

Iqbal, H.M.N., Tron, T., & Keshavarz, T. *Laccase bio-grafting a versatile modification tool from green chemistry technologies* in Annual PG-Fair, Faculty of Science and Technology, University of Westminster, London, UK. 26th April, 2012.

"The starting point of all achievement is desire"

Napoleon Hill

Acknowledgement

In the name of Allah, the most merciful, the most beneficent

AUTHOR'S DECLARATION

I declare that the present work was carried out in accordance with the Guidelines and Regulations of the University of Westminster. The work is original except where indicated by special reference in the text.

This thesis is entirely my own work and that where any material could be construed as the work of others, it is fully cited and referenced, and/or with appropriate acknowledgement given.

Until the outcome of the current application to the University of Westminster is known, the work will not be submitted for any such qualification at another university or similar institution.

Any views expressed in this work are those of the author and in no way represent those of the University of Westminster.

Signed: Date: 29th June 2015
Hafiz Muhammad Nasir Iqbal

Chapter 1

Introduction & literature review

1. Introduction and literature review

There has been a considerable interest in biopolymers and bio-based polymers in recent years due to their potential as alternative polymers to the traditional petroleum-based synthetic counterparts. Research is underway around the world on the development of 'greener' polymer technologies. In recent decades, there has been a growing search for new high-performance polymeric materials. The principle of 'going green' has directed this search towards eco-friendly materials. Words like renewability, recyclability and sustainability are emphasised in growing environmental awareness. The divergence from non-renewable to renewable materials is becoming the centre of interest for research in industrial communities around the globe. The fact is that environmental legislation is the driving force behind the development of these materials (Mohanty *et al*., 2000). The environmental impact of persistent plastic-based wastes is increasing global concerns as disposal methods are limited and no longer acceptable. In addition, the petroleum resources are finite and becoming increasingly costly. Originally petroleum-based plastics were designed to be durable and were synthesized from petrochemical resources, mainly crude oil. The shortage of synthetic raw materials and the depletion of petroleum resources has pushed up prices in essential sectors worldwide including energy, materials, and medical (Mani and Bhattacharya, 2001). The shortage and rise in the price of petrochemical resources have resulted in the strong demand for plastics based on renewable resources *i.e.* bio-based materials. Bio-based materials should ease disputes on eco- pollution and reliance on fossil resources (Mani and Bhattacharya, 2001; Huda *et al*., 2005). So focus has been shifted to polymers originating from bio-based renewable sources, which are often biocompatible and biodegradable (Plackett *et al*., 2003). Therefore, in this context, bio-based composite

materials are being engineered for target applications in different industries to address the growing environmental concerns where petroleum-based resources are unsustainable (Srubar *et al.*, 2012). On the other hand, bio-polymers have a number of advantages over petroleum-based polymers, such as being renewable, abundant and biodegradable while also providing competitive mechanical properties.

Since the last few decades, there has been a continuously increasing interest for development of stronger, stiffer, lighter-weight, and multifunctional engineering material for a variety of industrial and biotechnological applications. To compensate the demand for better performance, extensive research has been devoted to bio-polymers and different polymer based green composites. Research is underway on the commercial development of 'greener' polymer technologies; new materials with high performance at affordable costs. The principle of 'going green' has diverted this search towards eco-friendly materials. The development or selection of materials to meet the structural and design challenges calls for a compromise between conflicting visions/objectives which are often non-commensurate, and any improvement in one is at conflict with the other (Ashby, 2000).

Industrial ecology, eco-efficiency and green engineering are guiding the next generation of processes and products (Markarian, 2008). Bio-based polymers are moving into the mainstream applications changing the dynamics of 21st century materials. Biopolymers, bio-based and biodegradable are the words which are becoming more important in the world of industrial plastics. These materials have not only been a motivating factor for the materials scientists, but also they provide potential opportunities for improving the living standard (Nair and Laurencin, 2007). Before going into details, these words need to be distinguished with respect to their meaning. Generally speaking, a bio-based polymer is the term

used to describe a variety of materials. However, they fall into two principal categories (Christophe and Coszach, 2000).

(i) **Biopolymers** are polymers that are produced by biological systems either by living organisms such as microorganisms and plants. They are also called polymeric biomolecules, biological polymers, bio-based polymers or simply biopolymers.

(ii) **Bio-derived polymers** are polymers that are chemically synthesised, but their monomers are derived from biological starting materials such as amino acids and other biological monomers.

1.1. Biopolymers

Polymers that are produced by biological systems such as plants, animals or microorganisms through metabolic-based engineering reactions are called natural polymers. Carbohydrates such as cellulose and starch and proteins such as keratin and enzymes and polyhydroxyalkanoates (PHAs) such as poly-(3-hydroxybutrate) [P(3HB)] are all counted as biopolymers (Stevens, 2001). A summary of biopolymers or bio-based polymers is shown in Figure 1.1.

Biopolymers such as PHAs generated from renewable natural sources by micro-organisms are often biodegradable, biocompatible and non-toxic in nature. Therefore, preparations of green composites (see section 1.2, Bio-composites) using one or more individual bio-polymers are among the routes to improve some of the properties of biodegradable polymers (Miao and Hamad, 2013; Hooshmand *et al*., 2014). The structure of a biopolymer affects its functional characteristics where the functional capability is mostly dependent on the crystalline and/or amorphous nature of the materials. For example, cellulose or poly(β-D-glucose) is a structural polymer whose

properties arise in part from its crystalline nature. But physiochemical and/or biological treatments can transform it into a useful structural material for many potential applications (Skelton, 2006). Also chemically modified celluloses, *e.g.* ethyl cellulose and cellulose acetate, are found in a wide range of applications. Modified cellulose is used in the manufacture of paint, plaster, adhesives, cosmetics and pharmaceutical film coating and numerous other products (Stevens, 2001). A family of compounds known as PHAs have received much attention as bio-sustainable materials because they are produced more easily in quantity by fermentation of carbon–rich substrates using microorganisms particularly bacteria. Among the most promising and well-characterised bio-polymers, P(3HB) is of particular interest for the preparation of bio-based composite materials.
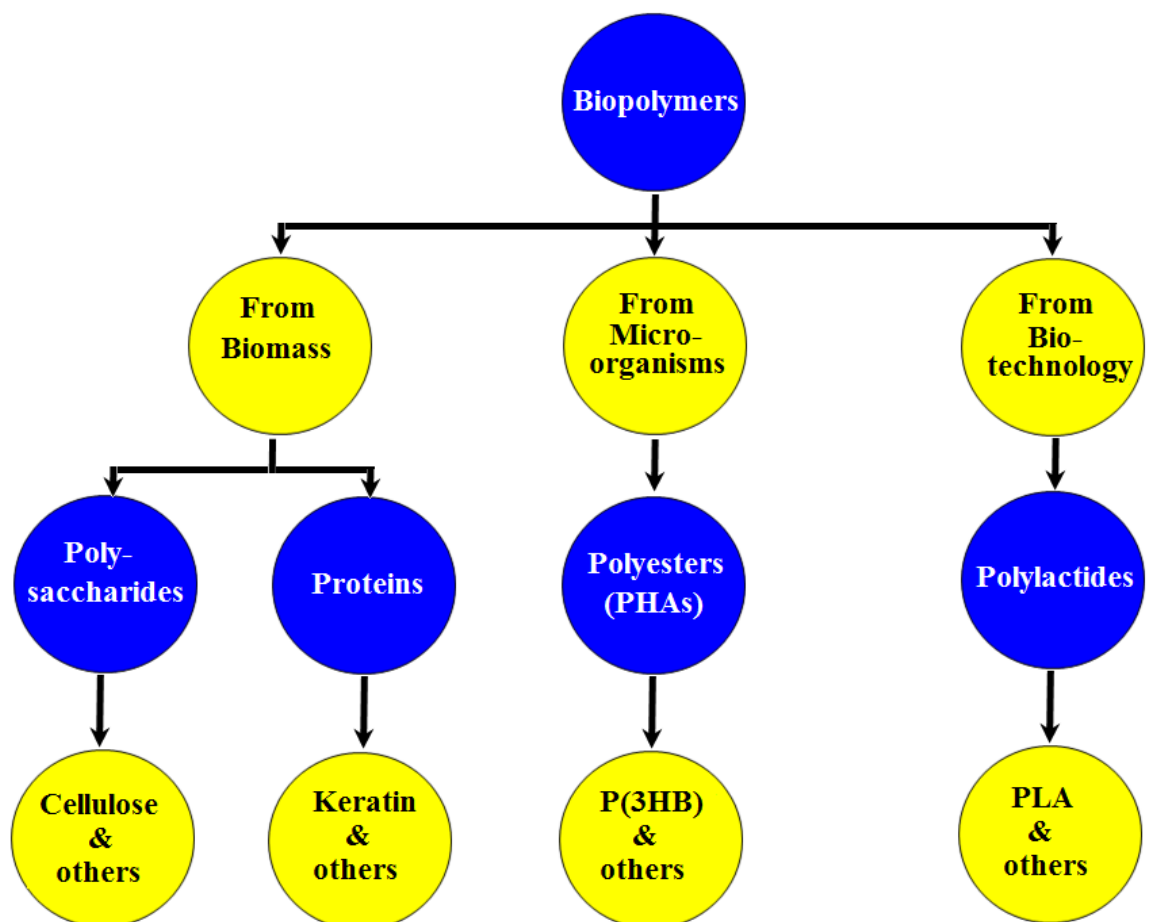
Figure 1.1 Classification of biopolymers.

There are still a number of issues including technical and processing that need to be addressed before the widespread use of bio-sustainable polymers is possible. A significant barrier to the widespread application of biopolymers in different sector is that their mechanical properties tend to compare unfavourably with existing petroleum-based polymers. For example, strength values are lower than those of the synthetic plastics so a component made from biopolymers would need to be thicker to compensate for lower mechanical properties. These shortcomings may be overcome by several means like grafting, blending and reinforcement with other suitable polymers. For example, P(3HB) graft composites with cellulose (P(3HB)-*g*-cellulose), impart new physiochemical and thermo-mechanical characteristics, decrease brittleness, and increase tensile strength of P(3HB).

1.1.1. Classification of biopolymers

Polymeric materials come from a variety of sources, ranging from familiar synthetic ones (petroleum-based) such as polystyrene to natural biopolymers such as cellulose, proteins, and microbial-based polyesters that are fundamental to biological structure and function (Wollerdorfer and Bader, 1998; Pandey *et al*., 2010). A wider spectrum of such materials has been classified accordingly as natural or synthetic based on their nature of origin. However, biopolymers or bio-based polymeric materials can be divided into three main categories according to their origin.

Category 1: Polymers directly extracted/removed from the biomass, for example, cellulose, starch and keratin.

Category 2: Polymers produced by classical chemical synthesis using renewable bio-based monomers. For example, poly lactic acid (PLA). The monomers themselves may be produced via fermentation of carbohydrate feedstock.

Category 3: Polymers produced by microorganisms or genetically modified species. To date, this group of bio-based polymers consist mainly of the PHAs, but developments with bacterial cellulose are in progress.

1.2. Bio-composites

The commonly accepted definition of a composite is a material that consists of two or more distinct materials/polymers in order to obtain tailor-made characteristics or to improve or impart ideal properties (specific strength, thermal properties, surface properties, bio-compatibility, and bio-degradability) that the individual homogeneous materials fail to demonstrate on their own. When composite materials comprise one or more phase(s) derived from a biological origin, they are described as bio-composites (Fowler *et al*., 2006; Auras *et al*., 2011). A broad definition of bio-composites is composite materials made up of natural or bio-derived polymers *e.g.* PHAs or PLA (John and Thomas, 2008). Table 1.1 lists the development of bio-composites using different materials and methods.

Table 1.1. Overview over bio-composites produced from different polymeric materials.

Polymer	Co-material	Methodology	References
Cellulose	Poly lactic acid	Extrusion and injection mold	Awal *et al*., 2015
Cellulose	Poly lactic acid	Compression mould	Church *et al*., 2015
Cellulose	High density polyethylene	Compression mould	Church *et al*., 2015
Carboxymethyl cellulose	Poly lactic acid	Ionic assembly	Chen *et al*., 2015
Cellulose	Polycaprolactone	Compression mould	Cocca *et al*., 2015
Curaua fibers	PHBV	Mill and injection	Beltrami *et al*., 2014
Wool fibres	Polypropylene	Compression mould	Conzatti *et al*., 2014
Bacterial cellulose	P3HB	Blending	Ruka *et al*., 2014
Wool keratin	Poly(vinyl alcohol)	Electron beam irradiation	Park *et al*., 2013
Hair keratin	Poly(vinyl alcohol)	Electron beam irradiation	Park *et al*., 2013
Oak wood flour	PHBV	Extrusion injection mold	Srubar *et al*., 2012
Cellulose	P3HB	Casting	Zhijiang *et al*., 2012
Bacterial cellulose	P3HB	Casting	Zhijiang and Guang, 2011
Cellulose	PHBV	Injection mould	Bledzki and Jaszkiewicz, 2010
Cellulose	Poly lactic acid	Injection mould	Bledzki and Jaszkiewicz, 2010
Cellulose	Polypropylene	Injection mould	Bledzki and Jaszkiewicz, 2010
Cellulose	P3HB	Compression mould	Cyras *et al*., 2009
Cellulose	P(3HB-co-3HH)	Compression mould	Zini *et al*., 2007

Fully sustainable bio-composite made up of bio/natural materials, and biodegradable polymers termed as green composites, are the centre of focus due to environmental

concerns and legislations. Recently bio-based composite materials have been engineered for target applications in different sectors such as bio-based packaging, bio-medical, pharmaceutical, textiles, paper and others (Klemm *et al*., 2001; Grunert and Winter, 2002; Gindl and Keckes, 2004; Svensson *et al*., 2005; Czaja *et al*., 2006), to address the growing environmental concerns of a globally unsustainable dependence on non-renewable petroleum-based resources (Srubar *et al*., 2012; Iqbal *et al*., 2013). Because of increasing environmental consciousness and demands of legislative authorities, the manufacture, use and removal of traditional synthetically produced polymers or composite structures are considered more critically (Herrmann *et al*., 1998). Bio-based materials that are derived from renewable resources having an accepted level of recyclability and a triggered biodegradability, along with commercial and environmental viability, are described as sustainable bio-based products. It means that the materials would remain stable in their intended lifetime but would degrade after disposal in suitable environment. The "green bio-composites" consist of biocompatible and biodegradable biopolymers (Mohanty *et al*., 2002). Biopolymers generated from renewable natural sources by micro-organisms are often biodegradable, biocompatible and non-toxic in nature. Therefore, manufacturing of green composites using one or more individual biopolymers is very desirable. Sustainability requirement is changing the dynamics of the materials industry, offering new opportunities and prospects. Innovations in the bio-plastic industry are providing a portfolio of sustainable and eco-efficient products to compete in the market presently dominated by synthetic plastics. The sustainability concept is shown in Figure 1.2.
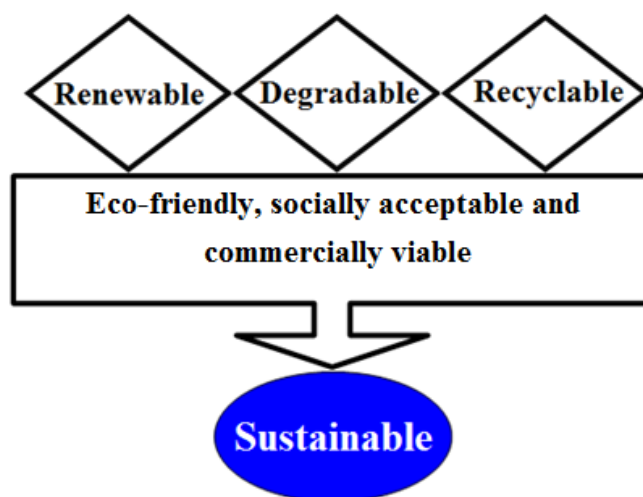
Figure 1.2 Concept of "sustainability" (modified from Mohanty *et al*., 2002).

1.3. What is grafting?

Grafting is a method in which the monomer building blocks of the bio-composites are covalently bonded (modified) onto the polymer chain to obtain the requisite properties. Grafting plays an important role in the modification of polymers to improve or impart ideal/new properties (specific strength, thermal properties, surface properties, bio-compatibility, and bio-degradability) that individual homogeneous materials fail to demonstrate on their own (Srubar *et al*., 2012). Effective modifications should include changes in chemical group functionality, surface charge, biocompatibility and biodegradability. Furthermore, enzymatic grafting is favourable over other physical and chemical grafting methods. By careful selection of the backbone material and monomer, it is possible to control the hydrophilic/hydrophobic balance of the grafted composites (Lao *et al*., 2010). There are several means to modify polymers properties to make them useful for a wider range of applications (Akaraonye *et al*., 2010). These techniques include alkaline hydrolysis, chemical, gamma radiation, photochemical, UV, plasma-induced techniques and enzymatic grafting (Mitomo *et al*., 1995; Kim *et al*., 2002; Ma *et al*., 2002; Grondahl *et al*., 2005; Lao *et al*., 2007; 2010).

The most common and in practice methods to initiate grafting processes are: (1) chemical, (2) photochemical and radiation, (3) plasma, and (3) enzymatic. However, the selection of a specific method from the above mentioned techniques strongly depends on the physicochemical nature and structure of the target polymers. Major grafting methods along with their core working process, merits and demerits are summarised in Table 1.2.

Table 1.2. Summary of major grafting methods and their core working principal, merits and demerits.

Grafting method	Working Principal	Merits	Demerits	References
Chemical	Generation of reactive free radicals/ions with chemicals	Simple and convenient method, alters surface properties, controlled synthesis, uniform distribution	Harsh chemicals, less sensitive, generation of extra by-products and a need of initiators	Roach *et al.*, 2007; Subhash *et al.*, 2010; Zhao *et al.*, 2010; Nady *et al.*, 2011; Krivoguz *et al.*, 2012
Photochemical and radiation	Generation of reactive free radicals by direct irradiation like UV, and gamma, along with chemicals	Alters surface properties, controlled synthesis, direct radical generation, no initiator required and elimination of washout steps	Harsh chemicals, highly sensitive, severe degradation of the pore structure of the target polymer and non-penetrative and only allows surface modification	Kubota *et al.*, 2001; Peng and Cheng, 2001; Gohil *et al.*, 2006; Huang *et al.*, 2009; Liu and Saunders, 2009; Vicente *et al.*, 2009; Nady *et al.*, 2011; Lv *et al.*, 2013
Plasma	Generation of ions, electrons, excited species, and free radicals	Modification of surface properties, controlled process	Temporary repellence and severe degradation or decomposition of the target polymer	Wavhal and Fisher, 2002; Kull *et al.*, 2005; Tsujii *et al.*, 2006; Vrlinic *et al.*, 2007; Nady *et al.*, 2011
Enzymatic	Generation of reactive free radicals by enzymes	High specificity, added-value, eco-friendly and convenient preparations and no or little use of harsh chemicals	Narrow pH, temperature and concentration range to work optimally	Hanefeld *et al.*, 2009; Hossain *et al.*, 2009; Aracri *et al.*, 2010; Iqbal *et al.*, 2015

1.4. Enzymatic grafting

Over the past decade, in vitro enzyme based catalysis has been established as an indispensable tool in polymer synthesis with a view of grafting where biotechnology is generating significant turnover and reducing negative environmental impact (Patel, 2007). Remarkably, oxidoreductases, transferases and hydrolases have been reported in enzymatic polymerisation, in vitro. Several excellent scholarly reviews have been dedicated to describing the sources, distribution, biochemical properties and general applications of lipases (Verma *et al*., 2008; Anobom *et al*., 2014; Gerits *et al*., 2014) and laccases (Riva, 2006; Kudanga *et al*., 2011; Giardina and Sannia, 2015). Briefly, lipases and laccases, in recent years, have appeared as green catalysts for synthesis and/or modification of polymers and polymerisation reactions owing to their wider substrate range, high activity and excellent stability. So far, a variety of polymer architectures have been developed using either enzymatic and/or chemo-enzymatic methods. Regardless of the type of polymerisation reaction, *Candida Antarctica Lipase B (CALB)*, also known as Novozym 435, dominates the literature related to lipase-assisted polymerisation. Moreover, it is also the most applied lipase in polymer applications so far due to its robustness, stability and simple removability. The enantioselectivity of hydrolases towards secondary alcohols and amines are well documented in the literature (Unelius *et al*., 1998; Ottosson *et al*., 2001; Yeniad *et al*., 2011).

A potential environmental benefit for using enzymes is that their selectivity may be exploited to eliminate the need for wasteful protection and de-protection steps. In the production of functional materials enzymes specificity may offer the potential to better control the polymer function through precise modifications in the polymer structure (Chen *et al*. 2000; Yamada *et al*., 2000).

Recently, laccase-assisted surface activation of polymers has raised interest with a view to grafting molecules of interest. It has been reported that "green" composites can be successfully fabricated by grafting and/or blending biodegradable polyester such as polyhydroxyalkanoates (PHAs) and/or bio-derived bio-polymers such as keratin with cellulosic materials, such as ethyl cellulose (EC) (Suthar *et al*., 2000; Zhang *et al*., 1997), bacterial cellulose (BC) (Zhijiang *et al*., 2011), cellulose esters (Yu *et al*., 2006), and recycled cellulose fibres (Bhardwaj *et al*., 2006). To meet with the high demand for materials with improved performance, extensive research has been carried out into bio-polymers and different polymer-based green composites. P(3HB) and keratin-based graft composites with ethyl cellulose (EC) such as P(3HB)-*g*-EC and keratin-*g*-EC which is the focus of the work presented in this thesis, to improve or impart new different physicochemical, thermal and mechanical properties.

1.5. Polyhydoxyalkanoates (PHAs)

PHAs belongs to a family of bio-polyesters produced by microbes under limited nutritional conditions (e.g. nitrogen or phosphate) Sudesh *et al*., 2000, Chen and Wu, 2005), or excess carbon source (Dawes and Senior, 1973; Lee, 1996; Ojumu *et al*., 2004; Keshavarz and Roy, 2010). The unbalanced nutritional supply causes the bacteria to accumulate PHAs in the form of granules as an internal energy storage, as shown in Figure 1.3.
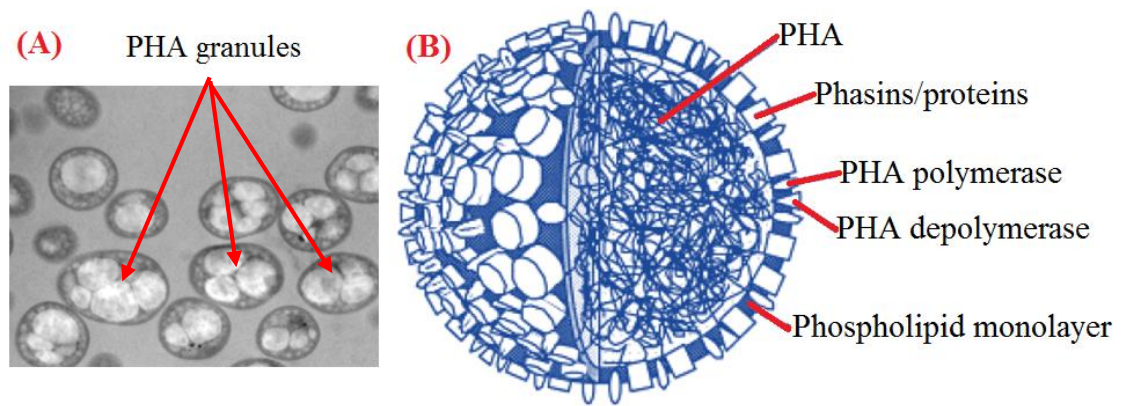
Figure 1.3 PHAs granules (A) and schematic of a PHA granule (B). The core consists of PHA polymer that is enwrapped by a phospholipid monolayer and proteins on the outside. The proteins consist of PHA polymerase, PHA depolymerase, structural proteins, and proteins of unknown function (modified from Zinn *et al*., 2001).

In 1888, Beijerinck first observed these intracellular granules within bacterial cells. During 1920s, a French microbiologist Maurice Lemoigne was the first who discovered a polyester, poly(3-hydroxybutyrate) [P(3HB)], as an intracellular granule in the Gram-positive bacterium *Bacillus megaterium* (Lemoigne, 1926; Lee, 1996). A wide spectrum of Gram-positive and Gram-negative bacteria (approximately over 300 species, examples of which include *Pseudomonas* spp. *Bacillus* spp. and *Methylobacterium* spp.) have been identified with the capability to biosynthesise PHAs. However, some bacterial species including *A. vinelandii* UWD, *A. eutrophus*, *A. latus* and a mutant *Azotobacter vinelandii* are also able to accumulate PHAs under non-limiting conditions (Chou *et al*., 1997; Ojumu *et al*., 2004; Keshavarz and Roy, 2010). Figure 1.4 shows the generic structural formula for the PHAs where x is 1 or higher, and R can be either hydrogen or hydrocarbon chains of up to C16 in length. Based on Figure 1.4, the main members of the PHAs family are presented in Table 1.3.
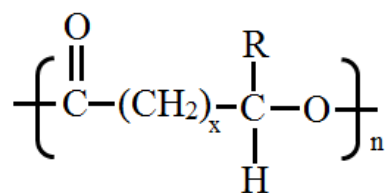
Figure 1.4 Generic chemical structure of the polyhydroxyalkanoates (PHAs).

Table 1.3. Main PHAs structures based on Figure 4.

Name	Abbreviation	x value	R group
Poly(3-hydroxypropionate)	P(3HP)	1	Hydrogen
Poly(3-hydroxybutyrate)	P(3HB)	1	Methyl
Poly(3-hydroxyvalerate)	P(3HV)	1	Ethyl
Poly(3-hydroxyhexanoate)	P(3HHx)	1	Propyl
Poly(3-hydroxyheptanoate)	P(3HHp)	1	Butyl
Poly (3-hydroxyoctanoate)	P(3HO)	1	Pentyl
Poly (3-hydroxynonanoate)	P(3HN)	-	Hexyl
Poly(3-hydroxydecanoate)	P(3HD)	1	Heptyl
Poly(3-hydroxyundecanoate)	P(3HUD)or P(3HUd)	1	Octyl
Poly(3-hydroxydodecanoate)	P(3HDD) or P(3HDd)	1	Nonyl
Poly(3-hydroxyoctadecanoate)	P(3HOD) or P(3HOd)	1	Pentadecanoyl
Poly(4-hydroxybutyrate)	P(4HB)	2	Hydrogen
Poly(5-hydroxybutyrate)	P(5HB)	2	Methyl
Poly(5-hydroxyvalerate)	P(5HV)	3	Hydrogen

The types of monomer being synthesised by the bacterium are determined by the carbon source used in the fermentation medium. It has now been well established that

the major monomer has the same chain length as the carbon source. Monomers containing odd numbers of carbon atoms are synthesised when a carbon source with odd numbers of carbon atoms is utilised, while monomers containing even numbers of carbon atoms are synthesised from carbon sources with even numbers of carbon atoms. For example, when a bacterium is cultivated with noctane (8 carbon atoms) as the only carbon source, the produced PHAs consist mainly of 3-hydroxyoctanoate units (8 carbon atoms), with small amounts of 3 hydroxyhexanoate units (6 carbon atoms) (De Smet *et al.*, 1983). More than 100 different monomers can be combined within this family to give materials with different properties; they can be either thermoplastic or elastomeric materials. PHAs have attracted great scientific and technological interest due to their good biocompatibility, biodegradability and thermoplastic properties (Stevens, 2008; Bettinger, 2011) and are expected to contribute to the construction of environmentally sustainable products.

Polymers from the aforementioned polyester family exhibit a wider range of structural, physicochemical and thermo-mechanical properties. Depending on the length of the alkyl group, R, PHAs can be categorised into short-chain-length PHAs (scl-PHAs) and medium-chain-length PHAs (mcl-PHAs). The scl-PHAs, which contain 3-5 carbon atoms, are thermoplastic exhibiting a high degree of crystallinity. The mcl-PHAs, which contain 6-14 carbon atoms, are elastomers with a low degree of crystallinity. With variations in the length of R, PHAs change their properties. Grafting/blending of different PHA monomers allows optimising their properties for various applications and in particular for a biomedical sector where biocompatibility, biodegradability, and thermo-mechanical properties are considered critically. Various applications of PHA and their polymer blends are listed in Table 1.4. To date, approximately 150 different types of biosynthetic PHAs have been reported, making them the largest group of

natural polyesters (Zhang *et al*., 2006; Keshavarz and Roy, 2010; Li and Loh, 2015; Rehm, 2015). PHA nomenclature and classification may still evolve as new structures continue to be discovered. So far several PHAs including Poly(3-hydroxybutyrate) [P(3HB)], copolymers of 3-hydroxybutyrate and 3-hydroxyvalerate, P(3HB-co-3HV), poly(4-hydroxybutyrate) [P(4HB)], copolymers of 3-hydroxybutyrate and 3-hydroxyhexanoate P(3HB-co-3HHx) and poly(3-hydroxyoctanoate, P(3HO) are available in sufficient quantity for research purposes (Chen and Wu, 2005; Bettinger, 2011).

Table 1.4. Application of PHAs and their blends/bio-composites in various fields (Adopted from Babu *et al*., 2013).

PHA polymer type	Applications	Reference
P(3HB), P(3HB-co- 3HHX) and blends/bio-composites	Scaffolds, nerve regeneration, soft tissue, artificial esophagus, drug delivery, skin regeneration, food additive	Yang *et al*., 2002; Chen and Qiong, 2005; Clarinval and Halleux, 2005; Bayram *et al*., 2008; Tang *et al*., 2008
mcl-PHA/scl-PHA	Cardiac tissue engineering, drug delivery, cosmetics, drug molecules	Sodian *et al*., 2000; Wang *et al*., 2003; de Roo *et al*., 2002; Zhao *et al*., 2003; Ruth *et al*., 2007
P(4HB) and P(3HO)	Heart valve scaffolds, food additive	Clarinval and Halleux, 2005; Valappil *et al*., 2006
P(3HB-co-4HB), P(3HB-co-3HV)	Drug delivery, scaffolds, artificial heart values, patches to repair gastrointestinal tracts, sutures	Williams *et al*., 1999; Türesin *et al*., 2001; Freier *et al*., 2002; Volova *et al*., 2003; Kunze *et al*., 2006; Chen *et al*., 2008;
PHB, Mirel P103	Commodity applications, shampoo and cosmetic bottles, cups and food containers	Amass *et al*., 1998; Walle *et al*., 2001; Philip *et al*., 2007

1.5.1. Poly(3-hydroxybutyrate)

Poly(3-hydroxybutyrate) [P(3HB)] belongs to scl-PHAs type and is the most often used PHA since its discovery in 1926 by Lemoigne. It represents the simplest member of the PHA family, with its chemical structure shown in Figure 1.5. Mechanical properties of P(3HB) are comparable to that of the synthetic polymers such as polypropylene (Engelberg and Kohn, 1991). Physical properties of P(3HB) are shown in Table 1.5.
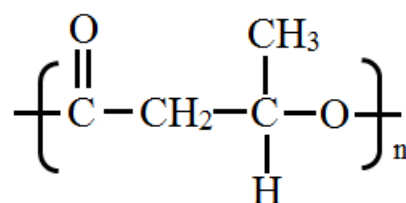
Figure 1.5 Chemical structure of P(3HB).

Table 1.5. Physical properties of P(3HB) (Misra *et al.*, 2006).

Properties	Values
T_m (°C)	175-179
T_g (°C)	4
Crystallinity (%)	60-80
Tensile strength (MPa)	40
Young's Modulus (GPa)	1.1 – 3.5
% Elongation at break	5-6

Where; T_m = Melting temperature and T_g = Glass transition temperature

P(3HB) is an amorphous to highly crystalline material with a degree of crystallinity of 30-90% (Sudesh *et al.*, 2000), due to the presence of a short methyl side chain within its structure (Kawaguchi and Doi, 1992). In spite of its relatively brittle and stiff properties, with a strain at break typically less than 5%, P(3HB) can be fabricated with other suitable natural and/or synthetic polymers to achieve satisfactory flexibility (Misra *et al.*, 2006). The properties of P(3HB) strongly depend upon various factors including the type of microbial culture, production and extraction protocols. Due to its high crystallinity, P(3HB) exhibits a very slow degradation rate of 3.6 wt% per week in activated sludge, 1.9 wt% per week in soil, 1.5 wt% per week in lake water, and 0.8 wt% per week in Indian Ocean sea water (Akmal *et al.*, 2003; Liu *et al.*, 2014). Beside the processing conditions, the microstructure and properties of the PHA materials themselves can significantly affect the degradation rates (Abe and Doi, 1999; Plackett, 2011). Thus, it has been investigated for tissue engineering applications that require a longer retention time or a high stability in the surrounding environment (Chen *et al.*, 2013, Chen and Wu, 2005), e.g., bone repair (Doyle *et al.*, 1991, Luklinska and Bonfield, 1997), nerve conduits (Hazari *et al.*, 1999; Young *et al.*, 2002), and pericardial substitutes (Duvernoy *et al.*, 1995, Kalangos and Faidutti, 1996). *In vitro* tests have shown that P(3HB) is biocompatible with various cell lines, including osteoblasts, epithelial cells and rabbit chondrocytes (Doyle *et al.*, 1991, Zheng *et al.*, 2005).

The material properties of P(3HB) can be fine-tuned for specific applications by incorporating it with a second monomer unit. There are two approaches: (i) co-synthesis of P(3HB) with hydroxyalkanoate monomeric units of higher chain length, by co-feeding of the culture with different carbon sources. Some common examples are poly(3-hydroxybutyrate-co-3-hydroxyvalerate) [P(3HB-co-3HV)], which are also

available commercially as Biopol (Köse *et al*., 2005; Sun *et al*., 2005; Weng *et al*., 2011), poly(3-hydroxybutyrate-co-3-hydroxyhexanoate) [P(3HB-co-3HHx)] (Doi *et al*., 1995; Wang *et al*., 2005) and poly(3-hydroxybutyrate-co-4-hydroxybutyrate) [P(3HB-co-4HB)] (Ying *et al*., 2008); (ii) physical blending of P(3HB) with higher chain length PHAs, e.g., P(3HV) (Satoh *et al*., 1994; Gassner and Owen, 1996), P(3HHx) (Deng *et al*., 2002; Deng *et al*., 2003; Kai *et al*., 2003; Zheng *et al*., 2005) and P(3HO) (Dufresne and Vincendon, 2000; Basnett *et al*., 2013). The physical and thermal properties of microbial copolyesters can be regulated by varying their molecular weights and compositions. In general, the resulting copolyesters are more flexible and elastic than P(3HB) (Barker *et al*., 1990). The blending approach has several advantages in comparison to synthesising new copolyesters, including the ease of preparation and optimisation of its final properties (Ha and Cho, 2002). Blending reduces the crystallinity of P(3HB) and as a result of macrophase separation and the effective surface area of the blended material, increases the surface erosion rate (Satoh *et al*., 1994, Ha and Cho, 2002).

1.6. Cellulose

Cellulose is a most abundant, renewable and most widely used polymer in the history of mankind. During the last few years, the development of biopolymers with multi-functional characteristics has gained considerable attention. There has also been a great interest in utilising cellulose as a reinforcement material to impart new or improve the existing mechanical characteristics of other polymers including P(3HB) (De Smet *et al*. 2011). Cellulose is a major constituent of the plant biomass. It is a homogenous linear polymer of D-glucopyranose sugar units (Sánchez, 2009; Kumar *et al*. 2009; Bertero *et al*. 2012), that are linked in a β configuration. The average cellulose chain has a degree of polymerisation of about 9,000 to 10,000 units.

Cellulose possesses excellent mechanical properties such as tensile or elastic modulus strength around 16.9 GPa and a tensile strength around 2 GPa. About 65 % or more of the cellulose is highly oriented, crystalline, and not accessible to water or other solvents. Cellulose is protected from degradation because of its close association to a sheath of matrix polymers that include lignin and hemicellulose (Figure 1.6).
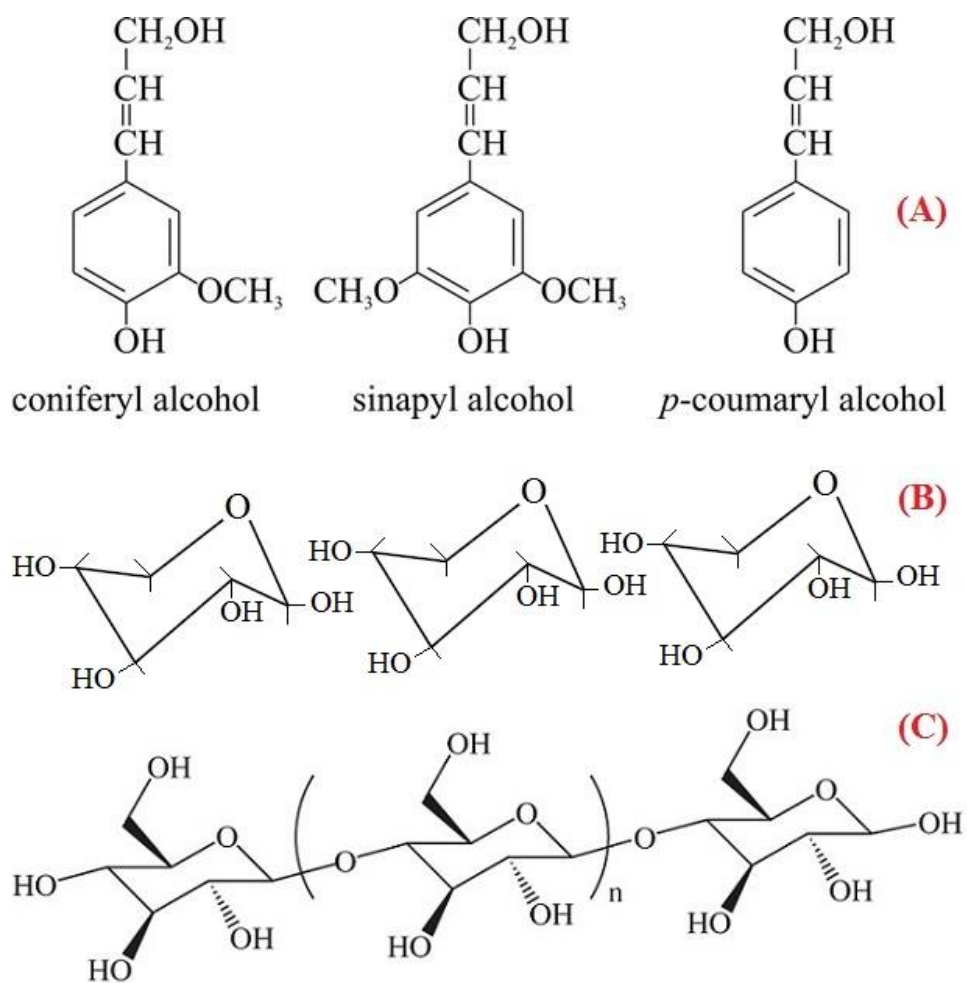
Figure 1.6 Chemical structure of lignocellulosic material; (A) lignin; (B) hemicellulose; and (C) cellulose (Iqbal *et al*., 2013).

Ethyl cellulose (EC) (as a chemically modified cellulose) exhibits excellent plasticity, good solubility in organic solvents, biocompatibility, high mechanical intensity, good heat-resistance, cold-resistance and stability (Yuan *et al*., 2007; Zhu *et al*., 2010). Copolymers formed with ethyl cellulose as a hydrophobic backbone exhibit a number of very interesting properties such as biocompatibility and biodegradability (Lao *et al*., 2007; Yan *et al*., 2009; Yuan *et al*., 2007; Yu *et al*., 2012). Apart from plants, cellulose is also produced by bacterial genera *e.g. Rhizobium spp. Agrobacterium spp. Acetobacter spp. Alcaligenes spp.* (Vandamme *et al*., 1998). The *Acetobacter xylinum* strain is able to produce cellulose at a temperature range of 25-30°C and pH range of 4.5-7.5 (Son *et al*., 2001). Many substrates have been analysed for their potential to work as a carbon source in the production of bacterial cellulose including monosaccharides *e.g.* D-glucose, disaccharides *e.g.* lactose, polysaccharides *e.g.* starch, organic acids *e.g.* gluconic acid, and alcohols *e.g.* ethylene glycol (Jonas and Farah, 1998). Bacterial cellulose (BC) is a straight chain polysaccharide with the same chemical structure as cellulose derived from plants. However, bacterial cellulose has the advantage of being devoid of lignin, pectin, hemicellulose and other biogenic products that are normally associated with plant cell wall (Jonas and Farah, 1998; Soykeabkaew *et al*., 2009). Due to the high purity and special physicochemical characteristics, bacterial cellulose has applications in a wide range of sectors including food, bio-medical (*e.g.* wound care) and tissue engineering (*e.g.* nano-composites) (Klemm *et al*., 2001; Grunert and Winter, 2002; Gindl and Keckes, 2004; Svensson *et al*., 2005; Czaja *et al*., 2006; Silva *et al*., 2014). Therefore, and in the light of the above-discussed characteristics, bacterial cellulose would appear to be an interesting candidate for the development of high-strength bio-composites (Piao, 2006; Kalia *et al*., 2011).

Owing to the aforementioned properties of both forms of cellulose and more importantly their biocompatibility and biodegradability under natural environment, various forms of cellulose including pure and/or chemically modified *i.e.,* ethyl cellulose have been widely used in the synthesis of novel composites (Klemm *et al*., 2001). For this reason, the development of bio-based composites has been a subject of interest in materials science from both ecological and environmental perspectives (Bajpai *et al*., 2013). Among the possible alternatives, the development of composites using cellulose as reinforcing element is currently receiving increasing attention. There are various methods of manufacturing bio-based composites depending on the processing techniques e.g. surface casting, ultrasonic-assisted casting, pultrusion, extrusion, injection moulding, press moulding, hand lay-up, filament winding, sheet moulding compounding and enzymatic grafting (Fowler *et al*., 2006; Tyagi, 2015). Synthetic fibres, such as glass and carbon fibres, are brittle and are often broken into smaller fragments (Hancox, 2001), while cellulose is flexible and will not fracture when they are processed over sharp curvatures. This permits a high volume fraction filling during processing of cellulose with other polymers, which results in improved mechanical properties as compared to the abrasive synthetic polymers. All of the aforementioned features enable cellulose to maintain the desired characteristics for good performance of the prepared composites (Shaw, 2002; Tserki *et al*., 2005). Moreover, cellulose offers high ability for surface modification, an eco-friendly approach, a non-toxic nature, easy handling, and it presents no health problems while most synthetic polymers do, which cause skin irritations and respiratory disease (Premalal *et al*., 2002; Yang *et al*., 2004). Cellulose-based composites can be used for different applications including automotive (Ashori, 2008; Alves *et al*., 2010), building (MacVicar *et al*., 1999), packaging (Espert *et al*., 2004) and medicine (Wan

et al., 2007; Miao *et al.*, 2011; Wang and Chen, 2011; Mathew *et al.*, 2012; Ul-Islam *et al.*, 2012).

1.7. Keratin

Keratin derives from the Greek word "kera" which means horn. In 1950s, the word keratin first appeared in the literature to define a material made up of hard tissues such as animal hoofs and horns. In 1905, a United States patent was issued describing the process of keratin extraction from animal hoofs with the help of lime (Jillian and Van Dyke, 2010). Since then many research-based methods have been developed, with the aim, to extract keratin mainly using oxidative and reductive approaches (Khosa and Ullah, 2013). Initially, these technologies were applied to extract keratin from animal based sources such as horns, hooves, chicken feathers and, finally human hairs (Jillian and Van Dyke, 2010). These keratin-rich sources are difficult to degrade as the polypeptide in their structure is tightly packed in α-helix (α-keratin) or β-sheet (β-keratin) into super coiled chains which are strongly stabilised by several hydrogen bonds and hydrophobic interactions, in addition to the di-sulphide bonds (Kreplak *et al.*, 2004; Brandelli, 2008).

In nature, chicken feather is perhaps the most abundant and easily available keratinous biopolymer (Khosa and Ullah 2013). A typical feather is shown in Figure 1.7. Keratin-based chicken feather from butchery account for more than 5 million tons per year worldwide in the form of waste material (Aluigi *et al.*, 2011; Ghosh and Collie, 2014). Apart from its minor usage in low grade products such as glue, corrugated paper, cardboard, animal feed, and fertilisers etc., the landfill disposal of poultry feather poses a significant ecological and environmental threat. On the other hand, from

economic and environmental point of view it is also desirable to establish an effective process for the application of such abandoned natural resource (Wang and Cao, 2012).
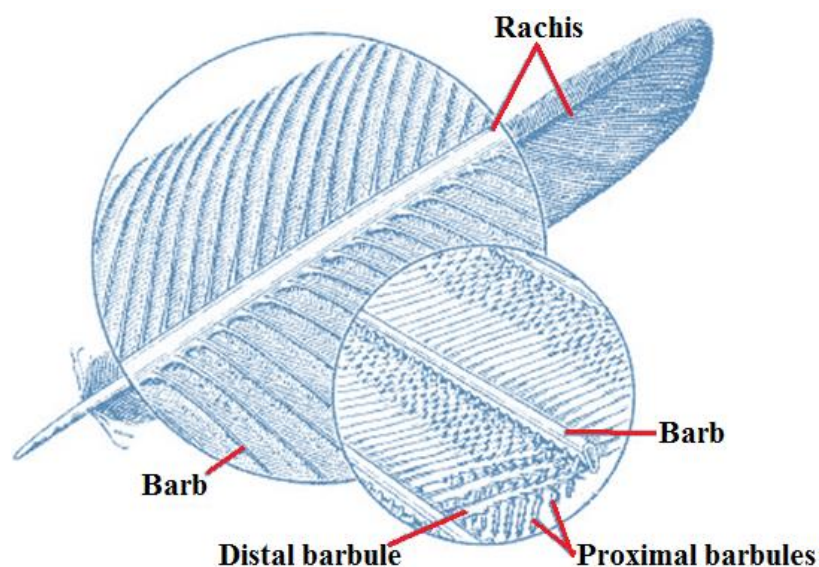
Figure 1.7 A typical feather (adapted with modification from Bartels, 2003).

The presence of multi-functional groups in keratin, such as di-sulphide, amino, thiol, phenolic and carboxylic, make it reactive under appropriate reaction conditions. Under reducing environment, the amino and some of other groups mentioned above in the keratin make its surface positive, and thus solubilisation takes place (Khosa and Ullah 2013). With unique properties of bio-degradability and non-toxic nature, keratin is among versatile biopolymers that can be modified and developed into various products of interests. Thus, notable amount of information on the characteristics and hydrolysis of keratin has become available where recalcitrant keratinous wastes are converted into valuable products (Aluigi *et al*., 2011; Ullah *et al*., 2011; Khosa and Ullah 2013). The knowledge on keratin-rich wastes has been robustly increased and their use in cosmetics or in medicines to enhance drug delivery, and production of biodegradable

films, are amongst the outstanding and emerging biotechnological and biomedical applications (Brandelli, 2008; 2010; Khosa and Ullah, 2013).

1.8. Enzyme as a potential grafting tool

1.8.1. Lipase

Lipases (triacylglycerol acyl hydrolases or carboxylic ester hydrolases, E.C. 3.1.1.3) belongs to the class of hydrolases that act on the carboxylic ester bonds and form the 3rd largest group of commercialised enzymes after peptidases and carbohydrases (Casas-Godoy *et al*., 2012). They hydrolyse a wide range of reactions that include hydrolysis, alcoholysis, esterification, trans-esterification and inter-esterification reactions (Atadashi *et al*., 2013; Dhake *et al*., 2013; Silva *et al*., 2014). Lipases also catalyse the synthesis of the esters formed from the hydroxyl and carboxylic groups. This versatility makes lipases the enzyme of choice for potential applications in various industrial and modern biotechnological sectors (Gupta *et al*., 2004; Aravindan *et al*., 2007). The reasons for the enormous biotechnological potential of microbial lipases include the facts that they are (i) stable in organic solvents, (ii) do not require cofactors, (iii) possess a broad substrate specificity, and (iv) exhibit a high enantioselectivity. As lipases do not require any cofactors, in the absence/presence of traces of water, they are capable of reversing the reaction that leads to the esterification and inter-esterification (Macrae, 1983; Sharma *et al*., 2001). The esterification by the lipases appears to be an attractive alternative to the green chemistry technologies in comparison to the use of bulk chemicals for esterification, as there are major drawbacks in these chemical processes. Lipase acts on the substrate in a specific or non- specific manner. The hydrophobic patches on the surface of lipases are responsible for the strong interactions with the hydrophobic

substrates. Besides the lipolytic activity, lipases possess esterolytic activity, thus, have a wide substrate range. The chemo-, regio-, and enantio-specific behaviour of these enzymes have attracted extensive scientific and industrial research (Saxena *et al.*, 2003).

1.8.1.1. Mechanism of action

Lipases can catalyse the hydrolysis and/or synthesis of the ester bond(s) that is, esterification reaction (Andualema and Gessesse, 2012), including inter- or trans-esterification reactions in non-aqueous media (Macrae and Hammond 1985; Houde *et al.*, 2004). In contrast to non-aqueous media, only few lipases can catalyse ester synthesis in aqueous media due to the high level of water content in aqueous media (Briand *et al.* 1994; Lecointe *et al.* 1996; Sun and Liu, 2015). The active site of lipases is composed of the catalytic triad serine, aspartate/glutamate, and histidine (Brady and others 1990). Serine acts as a nucleophile and aspartate or glutamate as a catalytic acid residue that forms hydrogen bonds with histidine (Jaeger *et al.*, 1999; Andualema and Gessesse, 2012). The mechanism of lipase catalysed esterification involves the formation of two intermediates as shown in Figure 1.8. The first intermediate is formed when serine residue of the catalytic triad attack the substrate as a nucleophile. Subsequently, the intermediate loses a water (H_2O) molecule to give an acyl-enzyme complex. Nucleophilic attack by an alcohol causes the addition of a hydroxyl group to the carboxyl group, producing a second intermediate, which then rearranges, releasing the ester molecule and regenerating the active site serine of lipase. Both of the intermediates possess an oxyanion that is stabilised by hydrogen bonds to protein atoms of the oxyanion (Grochulski *et al.*, 1994; Jaeger *et al.*, 1999; Kanwar *et al.*, 2007).
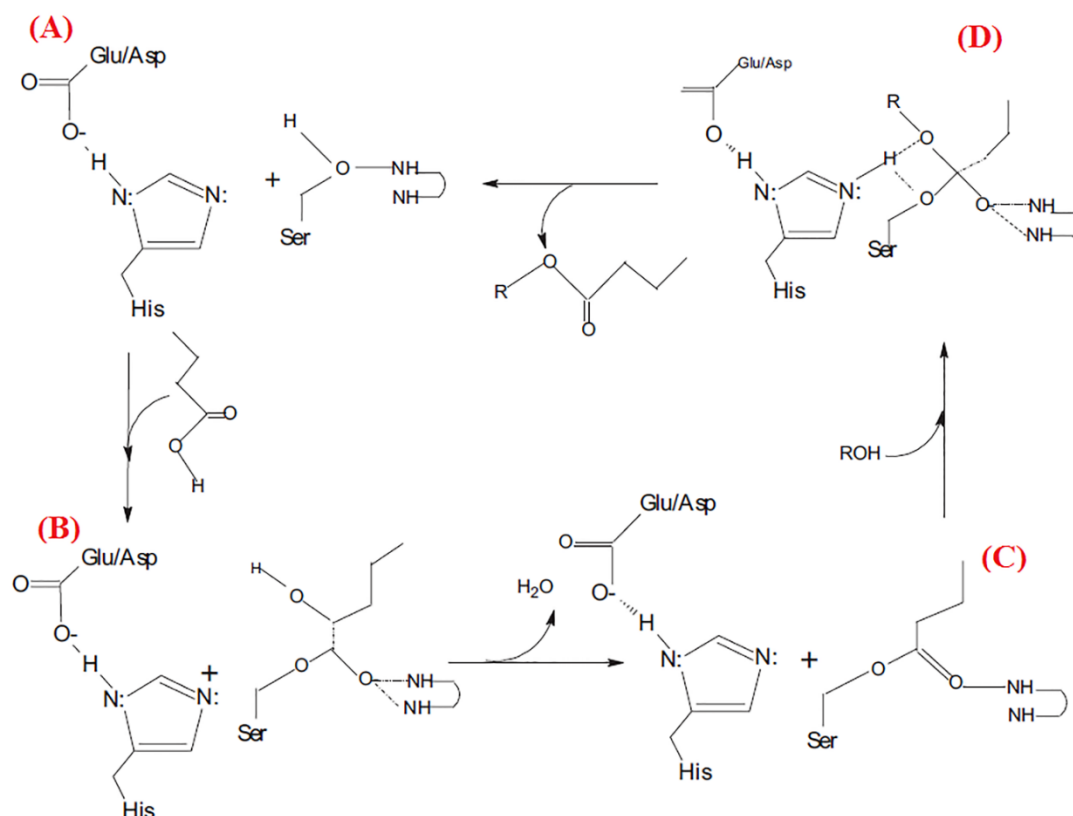
Figure 1.8 Mechanism of lipase-catalysed esterification. (A) Binding of substrate, activation of nucleophilic serine residue by neighbouring histidine and nucleophilic attack of the substrate's carbonyl carbon atom by Ser, (B) Transient tetrahedral intermediate that loses a water molecule to give an acyl enzyme complex, (C) An alcohol molecule attacks the acyl enzyme complex (nucleophilic attack) to give second intermediate, and (D) second tetrahedral intermediate that releases an ester molecule to convert the lipase to its native form (adapted from Verma *et al*., 2008).

1.8.2. Laccase

Laccase (EC 1.10.3.2, p-diphenol:dioxygen oxidoreductase) is a blue copper oxidoreductase capable of reacting with a large variety of suitable substrates, such as phenols, polyphenols, anilines, aryl diamines, methoxy-substituted phenols, hydroxyindols, benzenethiols, inorganic/organic metal compounds and many others with the simultaneous reduction of molecular oxygen to water (Claus, 2004). Laccase

catalyses the four-electron reduction of oxygen (O_2) to water coupled with oxidation of the aforementioned substrates. Laccase was first extracted from the exudates of a Japanese lacquer tree, *Rhus vernicifera*, in the presence of air by Yoshida in 1883, and named laccase 10 years later, after isolation and purification (Bertrand, 1894). Since then, new and novel sources of laccases have been reported continuously from insects, bacteria, terrestrial and marine fungi (Campos *et al*., 2001; Zille, 2005; Mustafa *et al*., 2005; Pereira *et al*., 2005; Baldrian, 2006; Hoegger *et al*., 2006; Riva, 2006; Alcalde, 2007; Araújo *et al*., 2008; Kunamneni *et al*., 2008; Desai and Nityanand, 2011; Jeon *et al*., 2010). Their high availability at a reasonable price and broad oxidative capabilities make them a powerful tool for surface modification of polymers. These characteristics make them attractive candidates for a wide range of applications (Riva, 2006; Widsten and Kandelbauer, 2008). Over the last decade, a number of industrial applications for laccases have been proposed in many areas by several authors and they include paper processing, prevention of wine decolouration, detoxification of environmental pollutants, oxidation of dyes and their precursors, and enzymatic conversion of chemical intermediates (Bhat, 2000; Rodríguez-Couto and Sanroman, 2006).

1.8.2.1. Mechanism of action

Laccases are glycoproteins, containing four copper atoms in their active site and are often referred to as blue-coloured oxidoreductases (Kunamneni *et al*., 2008; Dwivedi *et al*., 2011). Figure 1.9 illustrates a schematic diagram of an active site of laccase CotA from *Bacillus subtilis*. Laccases are type 4 copper proteins, which are composed of a mononuclear type 1 copper centre and a tri-nuclear centre, a combination of type 2 and type 3 centres (Fig. 1.9) (Claus, 2004). A tri-nuclear site is responsible for oxygen binding and concomitant reduction to water as the final by-

product in a four-electron transfer process (Bourbonnais *et al*., 1992; 1997; Robles *et al*., 2000; Zille, 2005; Riva, 2006; Morozova *et al*., 2007; Kunamneni *et al*., 2008; Jeon *et al*., 2010; Kudanga *et al*., 2011). Laccases are also known as di-oxygen-binding proteins and play a key role in many biological processes via the activation of the oxygen and oxidation of various substrate molecules. The catalytic mechanisms behind oxidation of a substrate typically generate radicals by the reaction of a reduced Cu^+ centre with molecular oxygen, which may also be incorporated in the substrate (Hatcher and Karlin, 2004; Rosenzweig and Sazinsky, 2006). These free radicals are capable to spontaneously rearrange and perform further fission of C–C or C–O bonds of the alkyl side chains, or to cleave the aromatic rings, resulting in de-polymerisation, re-polymerisation, demethylation or quinone formation (Kunamneni *et al*., 2008). The redox potential of laccases depends on the structure and properties of the copper centres. The simplified scheme of laccase-catalysed redox cycles for substrate oxidation is illustrated in Figure 1.10. Generally, fungal laccases (particularly from white-rot fungi) have a high-redox potential, whereas, bacterial laccases and laccases extracted from plants have a low-redox potential (Mikolasch and Schauer, 2009). Previous studies have indicated that the catalytic efficiency of laccases for some reducing substrates depends linearly on the redox potential of the T1 copper, showing the higher the redox potential of the T1 site is, the higher the catalytic efficiency of the laccase presents (Xu *et al*., 1996; 2000).
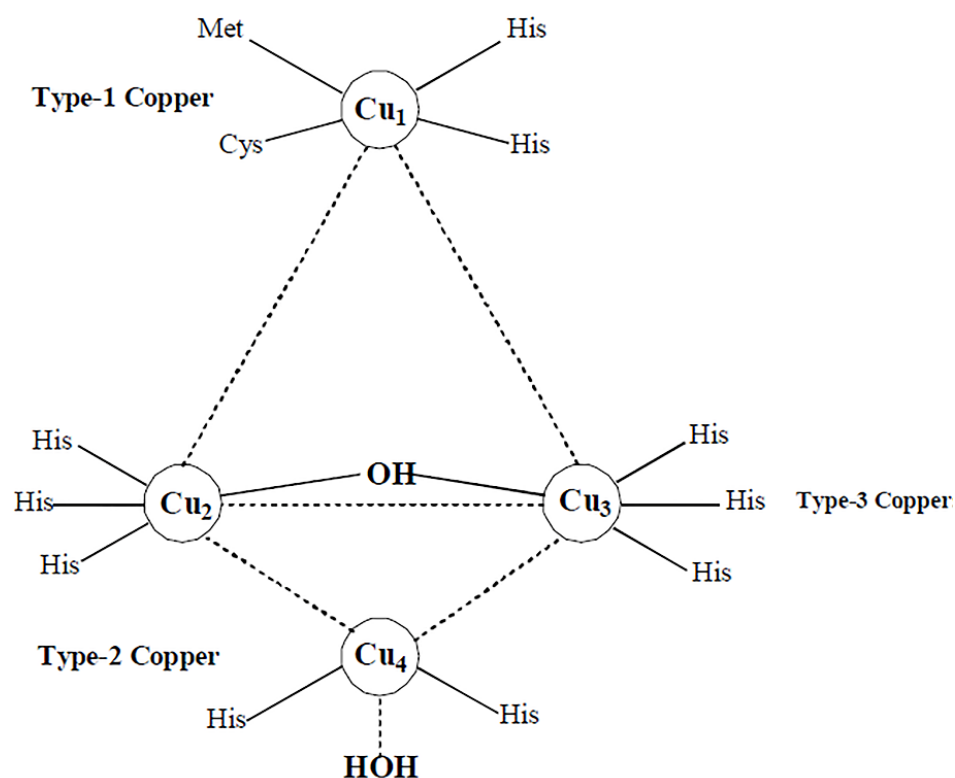
Figure 1.9 Active site of laccase CotA from *Bacillus subtilis* (adapted from Enguita *et al.*, 2003).
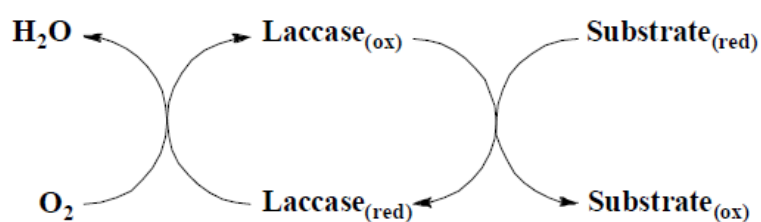
Figure 1.10 Scheme of laccase-catalysed redox cycles for substrate oxidation.

1.9. Properties of Bio-composites for Bio-medical applications

1.9.1. Biocompatibility

A unifying property of biomaterials is biocompatibility. According to the European Society for Biomaterials, the commonly accepted definition of biocompatibility is

"The ability of a material to perform with an appropriate host response in a specific application" (Williams, 1987). No particular parameters or tests are specified in the broad definition. The ultimate goal of biocompatible materials in regenerative medicine is to assist in the reconstruction of any tissue or organ in situ from scratch. Such interpretation of biocompatibility may seem futuristic, but is, in fact, much closer than one would expect. Throughout the history, the idea of inserting foreign objects into the human body has developed steadily. *In vitro* cell studies are ideal extensions of biomaterials-based research as they allow direct observation of cell interaction with the test composites. It is generally recognised that cell interaction with a test surface is a simplification of physiological conditions that usually involves full immersion of the cell in a culture environment. Although, *in vitro* growth of cells on a surface cannot be expected to fully reflect *in vivo* responses, it is, nonetheless, a widely used approach for studying biomaterial surface effects on cell functionality (Ratner, 2004). The versatility of *in vitro* cell studies is affirmed by the vast amount of well-established techniques. Apart from the typical biochemical quantification methods, new microscopic-based techniques are emerging steadily owing to their wider coverage and depiction of cell morphology in relation to biomolecules.

It is often considered necessary to match, as much as possible, the physicochemical and mechanical characteristics of the support biomaterials surrounding tissues. Prior to the design and/or development of bio-composite biomaterials their physicochemical, mechanical, morphological, and toxicological characteristics must be evaluated carefully, and critically with regard to the biomedical-based applications. Over the last decade, substantial efforts have been made to develop bio-composites with novel characteristics to optimise both, *in vitro* and *in vivo* performances while retraining the anticipated bulk properties. On the other hand, many researches have shown evidences

that apart from the surface chemistry, topography also has important effect on regulating cell behaviour in terms of cell adhesion, activation, proliferation, alignment and orientation (Brown *et al*., 1998; Ng and Swartz, 2003; Garcia *et al*., 2006; Rhee and Grinnell, 2007). However, there are several factors including composition, energy, oxidation level, surface charge, and morphology which need to be considered with regard to cell-matrix interactions (Silver and Christiansen, 1999; Davis and Senger, 2005). These interactions together with focal adhesions and cells ability to stimulate signalling pathways regulate cell adhesion, proliferation and survival within the matrix (Metcalfe and Ferguson, 2007), culminating in vascularisation of the matrix. Cell attachment, migration, proliferation and differentiation are phenomena related to development and wound healing. Although much is known in this area, the mechanisms regulating these processes are not fully understood.

As far as the use of tools and materials in medicine are concerned, owing to the emergence of novel green technologies, the benefits of carefully selected and crafted materials have been well established. Over the last 50 years innovative devices such as joint replacements, pacemakers, lenses, cochlear implants, artificial heart valves, and blood vessels have significantly extended the lifetime and life quality of patients (Ratner, 2004). These devices are termed "implantable medical devices", and the materials suitable for producing them are termed "biomaterials". Although highly successful in several clinical applications, the design of such materials is far from its optimum (Whitesides, 2005). Consequently, the anticipation and inspiration for further research in biomaterials with novel characteristics intensifies. The interdisciplinary research area is more active and innovative than ever, and ranges from physics and chemistry through to molecular and cell biology and medicine.

1.9.2. Biodegradability

Biodegradation is mainly the degradation of an organic material caused by biological activity (biotic degradation), of microorganisms' enzymatic action. Over the last two decades, biodegradable polymers have been the topic of many studies. As shown above in Figure 1.1, biodegradable polymers can be mainly classified as agro-polymers (biomass-based) and polyesters. Since the last few decades, there has been a continuously increasing interest for bio-based products due to the decreasing reserve of fossil fuel and the growing concern for the environment. The environmental impact of persistent plastic-based wastes is increasing global concerns and disposal methods are limited. In addition, the petroleum resources are finite and becoming increasingly costly. As described earlier, in practice, most of the synthetic polymers are petroleum-based and are not biodegradable. Therefore, in this context, biodegradable biopolymers or bio-based polymers, contribute significantly to the sustainable development of wider range of disposal polymers with minor adverse environmental impact. According to Narayan (2001), biodegradation is an important factor that should be considered during the design, and the products must be engineered from "conception to reincarnation", the so-called "cradle-to-cradle" approach. Moreover, the choice of the designed materials relate to the intended biotechnological and biomedical applications. In recent years, with increasing scientific knowledge and consciousness people are more aware that efforts have to be made to re-balance the carbon cycle by reducing the amount of carbon dioxide (CO_2) production. The carbon cycle is a complex process by which carbon is exchanged between the four main reservoirs of carbon on the planet Earth *i.e.,* the lithosphere, the biosphere, the hydrosphere, and the atmosphere (CO_2). Part of the "going green" concept is based on the development of products based on renewable and biodegradable resources.

According to ASTM standard D-5488-94d and European Standard EN 13432-2000, the term ''biodegradable'' is defined as: ''capable of undergoing decomposition into carbon dioxide, methane, water, inorganic compounds, and biomass''. The end-products are CO_2, new biomass, and water (in the presence of oxygen, i.e. aerobic conditions) or methane (in the absence of oxygen, i.e., anaerobic conditions). The predominant mechanism is the enzymatic action of microorganisms, which can be measured by standard tests over a specific period of time, reflecting best processing conditions. Different media (liquid, inert, or compost medium) are considered for the analysis of biodegradability.

Biodegradation involves living microorganisms, promoted by their enzymes, and can occur under aerobic and anaerobic conditions leading to complete or partial removal of the target material from the environment. Linear polymers are generally more biodegradable than branched polymers. Several researchers have examined the biodegradability of aliphatic homo- and co-polyesters based materials including P(3HB)-based bio-composites in various environments such as soil, freshwater, and seawater (Doi, 1990; Abe *et al*., 1999; Rizzarelli *et al*., 2004; Tokiwa and Calabia 2004; Lenz and Marchessault 2005; Volova *et al*., 2010; Boyandin *et al*., 2012; Burlein *et al*., 2014). Meargret *et al*., 1992 isolated more than 300 microbial strains from the soil which have potential to degrade P(3HB), in vitro. The most attractive property of P(3HB) with respect to ecology is that it can be degraded by microorganisms finally to CO_2 and H_2O (Lenz and Marchessault, 2005). This property of P(3HB) allows to develop biodegradable products for potential applications (Lenz and Marchessault, 2005; Nigmatullin *et al*., 2015).

The process of biodegradation can occur at different rates depending on the material components and cross-linking behaviour. *In situ* biodegradation cannot be neglected

since it will affect the material's physicochemical and mechanical characteristics leading to loss of integrity and ultimately to functional failure. Moreover, in terms of biological response the degradation process may result in the release of bio-products with different properties from the bulk material. Within the body, biomaterial degradation is mostly accomplished based on the phagocytic activity. A well-known example in recent medical history is the in vivo degradation of silicone gel breast implants (Braybrook, 1997). Therefore, the comparison of the results obtained from different standards seems to be difficult or impossible. We must also take into account the amount of mineralisation as well as the nature of the residues (commonly called ''by-products'') left after biodegradation (Avella *et al*., 2001).

1.10. Biomedical and biotechnological applications

The use of biopolymers based bio-composites for biomedical and biotechnological applications has many intrinsic advantages such as biocompatibility, biodegradability, renewability, sustainability, and non-toxicity. In recent years, from a biological point of view, a wide spectrum of (bio)-polymers based bio-composites have been engineered for target applications. Some of the major examples include polyesters (P(3HB), keratin, cellulose and many others. All of the aforementioned biopolymers are characterised and well organised/developed into value-added structures, thus can provide a proper route to emulate bio-systems - a biomimetic approach. Herein, Figure 1.11 illustrates an overview of the recent uses of biopolymers for biomedical and biotechnological applications.
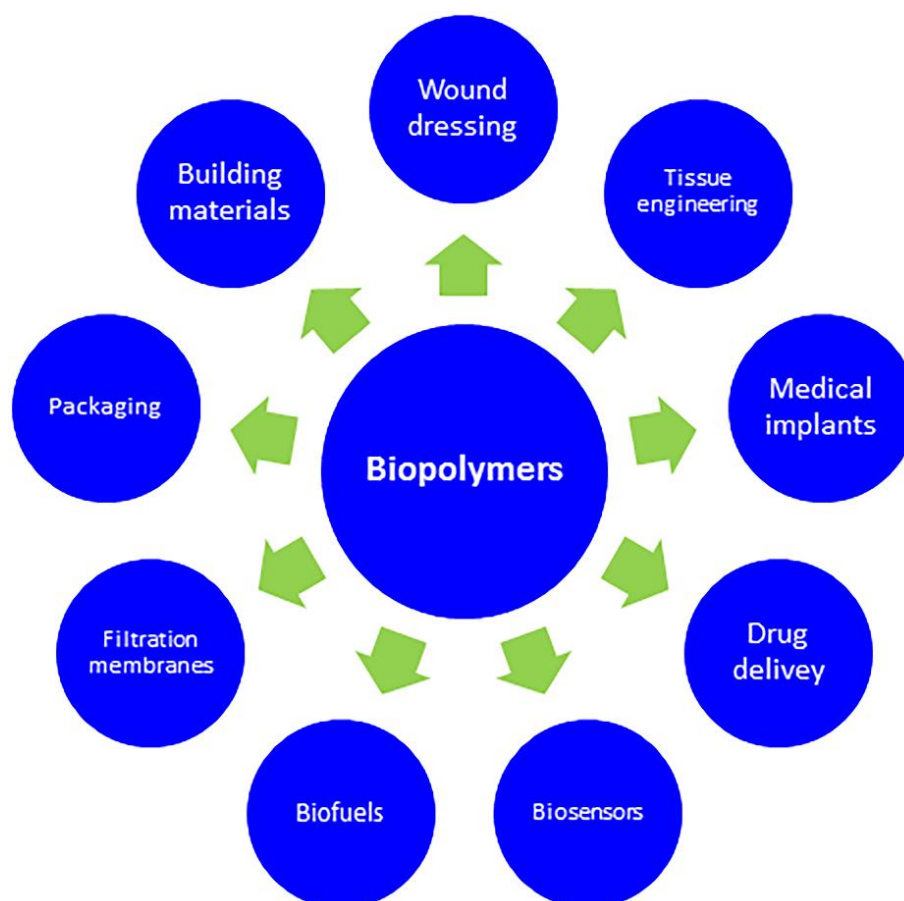
Figure 1.11 Use of biopolymers for various biomedical and biotechnological based applications.

1.10.1. Potential applications

1.10.1.1. Wound healing

Wound healing is an intricate process where the damaged skin needs to be repaired either by itself or through external aid. Driven by the major factors mentioned above, there is an urgent need for advanced wound care products. In this regard, new technology will dramatically accelerate the development of innovative dressing materials for wound healing. A superlative dressing must provide a suitable environment to the wound surfaces in which healing can take place at the maximum rate (Thomas, 1990). Apart from the basic covering function, in practice, dressings

are being developed to facilitate infection free wound healing. Because of increasing awareness and demands of legislative authorities the characteristics of (i) haemostatic, (ii) absorption of exudates, (iii) provision and maintenance of a suitable environment (moisture, water and adequate gaseous exchange), (iv) functional adhesion, (v) painlessness, and (vi) cost-effectiveness have been recognised and considered more critically. The ongoing research around the globe using polymer membranes as medical dressings/bandage is still in its early stages (Coffee, 1998; Smith *et al.*, 2001; Dabney, 2002; Wnek *et al.*, 2003; Kenawy *et al.*, 2003; Min, *et al.*, 2004; Yao *et al.*, 2007). In recent years, various medical and cosmetic applications of cellulose based bio-composites have drawn plenty of research attention in this field. Various potentials of cellulose originate from its unique properties such as strength, high liquid absorbency, biocompatibility, biodegradability and non-toxic nature. These characteristics make it an ideal option for specific demands of skin repair.

A well organised and structured composite materials can be obtained using polymers from a wider range of materials, such as cellulose and its derivatives (Kim *et al.*, 2001; 2006; Canejo *et al.*, 2008), PLA (Yang *et al.*, 2005), keratin (Min *et al.*, 2004), collagen (Buttafoco *et al.*, 2006), polyurethanes (Zhuo *et al.*, 2008), and ceramics (Franco *et al.*, 2012). Another approach reported by Wang and Cheng (2011) suggests a suitable method to prepare all-cellulose composites with characteristics for biomedical applications. Cellulose nanowhiskers are able to develop a porous network through their unique hydrogen bonding system with the host polymer matrix. Moreover, by analysing the controlled release of a model molecule such as bovine serum albumin from these nano-composites, these authors demonstrated their great potential as drug delivery systems, thus providing a useful option for skin tissue

repair, and wound dressings. Beyond the improvement of the typical properties, composites can include additional properties, for instance, antibacterial characteristics. The incorporation of antibacterial agents such as phenols (Iqbal *et al*., 2015), silver nanoparticles (Son *et al*., 2006) or polypeptides (Miao *et al*., 2011) to kill bacterial pathogens has also been reported. Son and co-workers (2006) have described the production of composites using cellulose acetate/silver nitrate that exhibited a strong antimicrobial activity which is necessary when considering wound dressing applications.

1.10.1.2. Tissue engineering

Tissue engineering (TE) is an interdisciplinary field that applies the principles of engineering and biological (biomedical) sciences to develop suitable alternatives that maintain, improve, or restore biological function of a tissue or a whole organ" (Langer and Vacanti, 1993). It has also been classified as "understanding the principles of tissue growth, and applying this to produce functional replacement, repair, maintenance, and/or enhancement of tissue function for clinical use" (MacArthur and Oreffo, 2005). Most definitions of tissue engineering cover a broad range of applications, in practice the term is closely associated with applications that repair or replace portions or whole tissues *i.e*., skin, muscle, cartilage, bone, blood vessels etc. So far major developments in this multidisciplinary field have yielded a novel set of tissue replacement implements and implementation strategies. In 2003, the NSF published a report entitled "The Emergence of Tissue Engineering as a Research Field", which gives a detailed description of the history of TE (Viola *et al*., 2003).

For centuries, physicians have attempted to cover/treat wounds with grafts from a variety of sources. By the early decades of the 20th century, researchers were

investigating the immunologic basis for rejection of skin allografts though there was no apparent progress toward any practical solution (Duquesnoy, 2002). During World War II due to the increasing number of burn victims, Peter Medawar made important contributions both to further progress the understanding of the immunology of graft rejection (Duquesnoy, 2002), and the *in vitro* culture of epithelial cells drawn from a patient. Using the technique, one sample of cells was sufficient to generate a thick, multi-layered skin to resurface the entire body of a burn victim. Later by 1953, Billingham and Reynolds demonstrated in animal models that the products of a culture of epidermal cells could be applied to a graft bed to reconstitute an epidermis (Billingham and Reynolds, 1953). Despite these early successes, more efficient means of cultivation were needed. Overgrowth of certain cell types, such as fibroblasts, suggested that existing culture techniques would not be effective in producing large quantities of the desired cells types. Green and co-workers, described the co-culture method, a technique for the serial cultivation of human epidermal keratinocytes from small biopsy samples (Green *et al*., 1979). In 1979, Green and colleagues demonstrated that cultured cells can be grown in sheets in a petri dish and transferred intact, rather than as disaggregated cells, to a graft wound bed (Green *et al*., 1979).

Recent advances in the biomaterials and biomimetic environments have created potential opportunities to fabricate tissues in the laboratory. Apart from biocompatibility and non-toxicity, the biodegradability of extracellular matrices is also recognised as a requisite property for TE. Over the last few years there has been an increasing research interest in developing novel materials including composites, blends, micro/nano- scale fibres and/or scaffolds etc. for cell seeding, proliferation and differentiation prior to the regeneration of biologically functional tissues. As described above, a range of biomaterials has been developed in recent years. They have variety

of designed characteristics that includes physical, chemical, and mechanical depending mostly in the final application (Czaja *et al*., 2007). The final product's success strongly depends on the cellular adhesion and growth onto the polymer surface, thus biopolymer's chemical surface can dictate cellular response by interfering in cellular adhesion, migration, and proliferation. On the other hand, to regenerate tissues, three specific points are taken into account: the culture, the support, and the growth factors. Cells synthesise a matrix for the new tissues, support holds and keeps the appropriate environment for the growth while the growth factors facilitate and promote the cell regeneration (Ikada, 2006). Since the surface-cell interaction is fully understood at a cellular level, new biomaterials and products can be easily developed (Kumari *et al*., 2001).

1.11. Overall aim

The overall aim of this research project was enzymatic *i.e.,* lipase and laccase-assisted grafting, of various biopolymers by a simple and eco-friendly procedure to develop novel bio-composites with improved or new multi-functional characteristics.

In order to achieve the aforementioned aim, research was directed through the following objectives.

1.12. Objectives

- ➤ To develop new types of EC-based bio-composites consisting of P(3HB) as a side chain biopolymer using lipase and laccase as green biocatalysts. Additionally, BC was also explored as an alternative type of cellulose. The purpose of this work was to fabricate and modify the native properties of the biopolymer P(3HB) along with EC/BC, and to study morphological, thermo-mechanical and wettability characteristics with different instrumental techniques.

- ➤ To develop bio-composites consisting of EC and keratin under laccase-assisted environment. The purpose was to improve the mechanical properties and, simultaneously, to modulate the hydrophobic/hydrophilic balance of the newly developed keratin-EC-based bio-composites.

- ➤ To graft various natural phenols, including caffeic acid, gallic acid, *p*-4-hydroxybenzoic acid and thymol, as functional entities onto the previously developed P(3HB)-EC, and keratin-EC-based bio-composites.

➢ To investigate the bactericidal and bacteriostatic activities of the phenol-*g*-P(3HB)-EC and phenol-*g*-keratin-EC bio-composites against various bacterial strains including *Bacillus subtilis* NCTC 3610, *Staphylococcus aureus* NCTC 6571, *Escherichia coli* NCTC 10418 and *Pseudomonas aeruginosa* NCTC 10662.

➢ To investigate the biocompatibility of the phenol-*g*-P(3HB)-EC and phenol-*g*-keratin-EC bio-composites against human keratinocytes-like (HaCaT) cell line.

➢ To investigate, as a preliminary study, the soil burial degradation features of the newly developed bio-composites. The purpose was to initiate future studies on the developed bio-composites.

Chapter 2

Materials and Methods

2. Materials and Methods
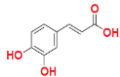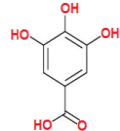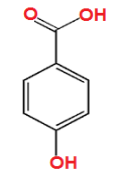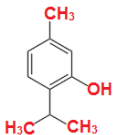
2.1. Chemicals and reagents

All the chemicals and/or reagents used for microbial maintenance and fermentation were mainly obtained from Sigma-Aldrich Company Ltd., UK; VWR Chemicals (Leicestershire, UK), and DIFCO (BD Ltd., Oxford, UK). EC was obtained from Sigma-Aldrich Company Ltd., UK and used as-received according to the material safety data sheet provided by the company. Chicken feathers were kindly provided by the Department of Bioengineering, Faculty of Engineering, Ege University, Izmir, Turkey. Four different natural phenols *i.e.,* caffeic acid (CA); gallic acid (GA); *p*-4-hydroxybenzoic acid (HBA); and thymol (T) were obtained from Sigma-Aldrich Company Ltd., UK. Table 2.1 illustrates the physiochemical characteristics of the phenolic contents used in the present study. To evaluate bio-compatibility, Dulbecco's modified eagle's medium (DMEM), phosphate buffer saline (PBS), streptomycin and penicillin were obtained from Lonza, Wilford Industrial Estate, Nottingham, UK. Fetal calf serum was received from Labtech International Ltd., Bellbrook Industrial Estate, East Sussex, UK. Neutral Red (NR) dye was obtained from Sigma-Aldrich Company Ltd., UK and used as-received for *in-vitro* human keratinocyte-like HaCaT cell viability assay. All of the chemicals and/or reagents were of analytical laboratory grade and used as-received without further purification unless otherwise stated.

2.2. Enzymes

Two fungal enzymes *i.e.,* lipase from *Rhizopus oryzae* with a unit activity ≥ 25 U/mg and laccase from *Trametes versicolor* with a unit activity ≥ 10 U/mg were obtained from Sigma-Aldrich Company Ltd., UK. These enzymes were used as model catalysts to prepare graft composites under an ambient environment.

Table 2.1 Physiochemical characteristics of natural phenols used in this study for grafting purposes using laccase as a model catalyst.

Natural phenols	Appearance	Molecular formula	Molecular mass (g/mol)	Density (g/cm³)	Melting point (°C)	Functional groups	Structure
Caffeic acid	Yellow solid	$C_9H_8O_4$	180.16	1.478	223 to 225	Hydroxyl and carboxylic	
Gallic acid	White or yellow-white powder	$C_6H_2(OH)_3$ COOH	170.12	1.694	260	Hydroxyl and carboxylic	
p-4-hydroxy benzoic acid	White crystalline	$C_7H_6O_3$	138.121	1.460	214.5	Hydroxyl and carboxylic	
Thymol	White crystalline	$C_{10}H_{14}O$	150.22	0.960	49-51	Hydroxyl	

2.3. Microorganisms and cell line

The bacterial strains *i.e., Bacillus subtilis* NCTC 3610, *Staphylococcus aureus* NCTC 6571, *Escherichia coli* NCTC 10418, *Pseudomonas aeruginosa* NCTC 10662, and *Acetobacter xylinus* ATCC 700178 were obtained from the bacterial culture collection unit of the University of Westminster, London, United Kingdom (UK). For bio-compatibility evaluation in later stages of the study human keratinocyte-like HaCaT cell line was obtained from the cell culture collection unit of the University of Westminster, London, UK.

2.4. Stock cultures and maintenance

In order to obtain single bacterial colonies, each of the collected bacterial strains were sub-cultured, using streak plate method on sterile nutrient agar plates under sterilised

environment. After the stipulated time period (24 h), the fully grown cultures were then stored at 4 °C and revived periodically for further use in the subsequent studies. Following that a single pure colony from each of the aforementioned strains except *A. xylinus* ATCC 700178 was grown overnight in 50 mL sterile nutrient broth under temperature controlled environment at 30 °C and 120 rpm. Whereas, the pure culture of *A. xylinus* ATCC 700178 was maintained in nutrient liquid medium. The constituents of the sterile nutrient agar and nutrient broth are presented in Tables 2.2 and 2.3, respectively whereas the main ingredients of the maintenance liquid medium are given in Table 2.4. The initial bacterial concentration was maintained approximately at 10^5 CFU/mL in the freshly prepared spore suspension by comparing OD_{600} using McFarland standard method.

Table 2.2 Composition of nutrient agar for maintenance of bacterial cultures.

Ingredients	Concentration (g/L)
'*Lab-Lemco*' Powder	1.00
Yeast extract	2.00
Peptone	5.00
Sodium chloride	5.00
Agar	15.00

Table 2.3 Composition of nutrient broth used for the preparation of spore suspension.

Ingredients	Concentration (g/L)
'*Lab-Lemco*' Powder	1.00
Yeast extract	2.00
Peptone	5.00
Sodium chloride	5.00

Table 2.4 Composition of liquid medium for maintenance of *A. xylinus* ATCC 700178.

Ingredients	Concentration (% w/v)
Glucose	4.0
Yeast extract	0.1
Polypeptone	0.7
$Na_2HPO_4 \cdot 12H_2O$	0.8

Table 2.5 Composition of MGM used for the production of P(3HB) from *B. subtilis* NCTC 3610

Ingredients	Composition (g/L)
$FeSO_4$	0.0050
$(NH_4)_2SO_4$	2.0000
$MnSO_4 \cdot H_2O$	0.0030
$MgSO_4 \cdot 7H_2O$	0.4100
K_2HPO_4	0.5000
$CaCl_2 \cdot 2H_2O$	0.1000
$CuSO_4 \cdot 5H_2O$	0.0005
$ZnSO_4 \cdot 7H_2O$	0.0005
$CoCl_2$	0.0050
Yeast extract	2.5000
Sucrose	20.0000

2.5. Production and extraction protocols of P(3HB)

The Gram-positive *B. subtilis* NCTC 3610 was used for the production of P(3HB). P(3HB) production was carried out in 500 mL Erlenmeyer flasks containing a 150 mL of a reported modified G medium (MGM), (Akaraonye *et al*., 2010). The concentrations of the MGM ingredients are presented in Table 2.5. Prior to inoculation, the prepared MGM was sterilised at 121 °C and pressure (103 kPa) for 15 min and after cooling inoculated with freshly prepared homogeneous bacterial spore suspension of *B. subtilis* NCTC 3610. The inoculation was carried out in a laminar air

flow cabinet. Sucrose was sterilised separately before adding into each of the flasks along with the inoculum. The inoculated flasks were kept at 30 °C in a temperature controlled rotary incubator for 72 h at 200 rpm. After the stipulated fermentation time period (72 h) the P(3HB) was extracted from the fermented bacterial culture using as-reported, the chloroform-hypochlorite dispersion method (Rai *et al*., 2011). Briefly, the bacterial cells were harvested from the culture by centrifugation at $5,000 \times g$ for 10 min. The resultant pellets were collected from the bottom of the centrifuge tube and stored at -20 °C for 24 h. The fully frozen cells were then lyophilised for up to 48 h in a freeze drier at -47 °C and at a pressure of 133 mbar. Following that a dispersion solution containing 50 mL of chloroform and 50 mL of 30% sodium hypochlorite solution was used to extract P(3HB) from the freeze-dried pellets. The freeze-dried cells (1 g) were added to the dispersion solution (100 mL) and incubated in shaker (100 rpm) at 38 °C for 1 h. Three different phases were obtained from the above incubated solution after it had been centrifuged at $4,000 \times g$ for 10 min. P(3HB) was recovered from the bottom phase by precipitation using 10 volumes of ice-cold methanol. Figure 2.1 depicts a schematic diagram of different steps adapted to extract P(3HB). After that freshly extracted P(3HB) was stored in air tight desiccated jars to keep P(3HB) moisture free and used further in subsequent graft synthesis experiments.
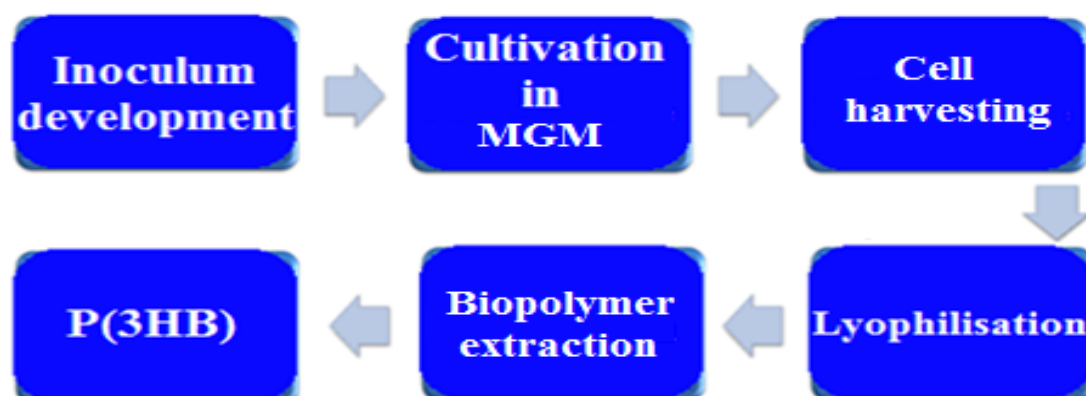
Figure 2.1 Schematic diagram of different steps adopted to extract P(3HB) from 72 h fermented *B. subtilis* NCTC 3610 culture using a modified G medium (MGM).

2.6. Preliminary processing of the chicken feathers

The chicken feathers were washed three times with hot water and ethylene alcohol to avoid any microbial/dust contamination. Then, they were dried at 60 °C and cut into small fragments with lengths of 1–2 mm. Ten grams of clean feathers were then dissolved in an aqueous solution of 3% wt. sodium hydroxide (NaOH) at 50 °C for 24h. After the stipulated time (24 h) the keratin hydrolysate was filtered in order to separate the insoluble parts of feathers. The hydrolysate was submitted to dialysis for 48 h to remove excess chemicals. After 48 h of dialysis, 2 N Hydrogen Chloride (HCl) was poured into the keratin hydrolysate in order to extract the keratin in the form of a precipitate. The precipitated keratin was centrifuged at $4,000 \times g$ for 10 min, washed with distilled water, and dried by lyophilisation at -47 °C and at a pressure of 133 mbar until fully dried. The dried keratin powder was stored in air tight desiccated jars to keep moisture free and used in the subsequent graft synthesis experiments (Figure 2.2). The amino acids present in chicken feather are mainly aspartic acid, glutamic acid, arginine, proline, glycine, phenylalanine, alanine, cystine, valine, isoleucine, leucine, tyrosine, threonine and serine among others (Schmidt, 1998; Martínez-Hernández *et al*., 2005) (For further details, see Table 2.6). Table 2.6 gives the content ratio against each amino acid present in the keratin solution.
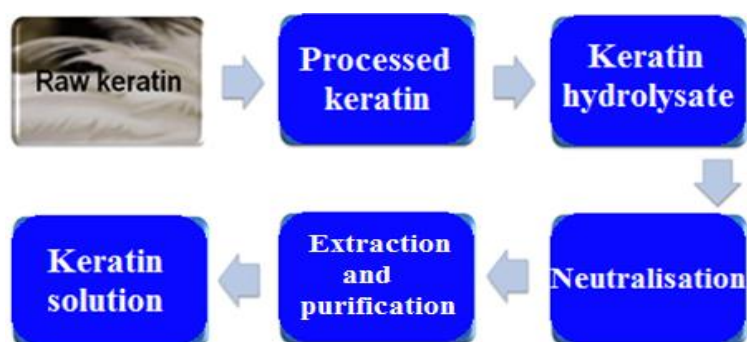
Figure 2.2 Schematic diagram of different processing steps adopted to extract keratin using raw keratin from chicken feathers.

Table 2.6 Amino acid contents present in the keratin solution from chicken feather (Martínez-Hernández *et al*., 2005).

Functionality	Amino acid	Symbol	Content (as % mole)
Negatively charged	Aspartic acid	Asp	05
	Glutamic acid	Glu	07
Positively charged	Arginine	Arg	05
Conformationally special	Proline	Pro	12
	Glycine	Gly	11
	Phenylalanine	Phe	04
	Alanine	Ala	04
	Cystine	Cyst	07
Hydrophobic	Valine	Val	09
	Isoleucine	Ile	05
	Leucine	Leu	06
	Tyrosine	Tyr	01
Hydrophilic	Threonine	Thr	04
	Serine	Ser	16

2.7. Production and extraction of bacterial cellulose (BC)

A. xylinus ATCC 700178 was grown in the liquid medium containing 4% (w/v) glucose, 0.1% (w/v) yeast extract, 0.7% (w/v) polypeptone, 0.8% (w/v) $Na_2HPO_4 \cdot 12H_2O$, and 1.4% (v/v) ethanol. The pH of the medium was adjusted to 5.5 before inoculation. Batch cultures in flasks were incubated at 26 °C for seven days under continuous shaking at 130 rpm. Hydrated BC pellicles were harvested from 7 days old fermented culture, washed three times with sterilised water and kept immersed overnight (24 h) in sterilised water to remove excess chemicals. After the stipulated period (24 h), the BC pellicles were withdrawn and homogenised at 10,000rpm for 1 min and centrifuged at $4,000 \times g$ for 20 min. After that the precipitated BC pellets were treated with 0.1 N sodium hydroxide (NaOH) at 80 °C for 20 min in

order to eliminate the attached bacterial cells (Bae *et al*., 2004). The above NaOH treated BC was then rinsed with sterilised water. This procedure was repeated three times and finally BC was dried at 80 °C in an oven at least for 8 h until fully dried. The dried BC was stored in air tight desiccated jars to keep moisture free and used in the subsequent graft synthesis experiments.

2.8. Preparation of graft composites

2.8.1. "One-pot" synthesis of P(3HB)-*g*-EC composites using lipase

Freshly isolated P(3HB) and ethyl cellulose (EC) were used to prepare graft composites of P(3HB) and EC with different P(3HB) to EC ratios *i.e.,* P(3HB): EC; 0:100, 25:75, 50:50, 75:25 and 100:0, respectively. A fungal lipase from *R. oryzae* with a unit activity of ≥ 25 U/mg was used as a model catalyst for grafting purposes. The reaction mixture comprised of P(3HB) and EC was prepared by the addition of lipase using sodium phosphate buffer of pH 4.5. The above reaction mixture was then incubated at 25 °C and 120 rpm for 30 min. After the stipulated reaction period (30min) the above lipase treated reaction mixture was poured into a sterile labelled petri plate followed by incubation under temperature controlled environment at 50 °C for 24 h. The grafted composites were then removed from their respective casting surfaces (petri plate) and assigned IDs subject to P(3HB) to EC ratios, as shown in Table 2.7. All of the collected composites were then characterised using different analytical and imaging techniques including Fourier-transform infrared spectroscopy (FT-IR), scanning electron microscopy (SEM), X-ray diffraction (XRD), differential scanning calorimetry (DSC), dynamic mechanical analyser (DMA) and water contact angle analyser (WCA). Figure 2.3 illustrates a schematic representation of preparation and evaluation of lipase-assisted P(3HB)-EC based graft composites.
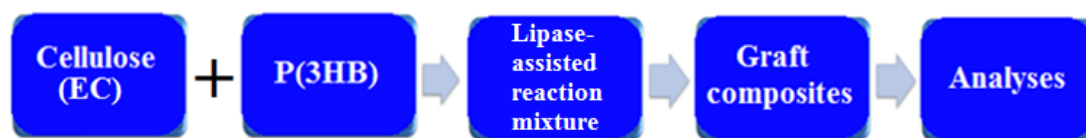
Figure 2.3 Schematic representation of preparation and evaluation of lipase-assisted P(3HB)-EC based graft composites.

Table 2.7 Designation of IDs to the newly developed P(3HB)-EC based graft composites prepared using different P(3HB) to EC ratios (P(3HB): EC). Lipase from *R. oryzae* with a unit activity of ≥ 25 U/mg was used as a model catalyst for grafting purposes.

Backbone polymer	Grafted polymer	P(3HB): EC	Composite ID
EC	P(3HB)	100: 0	P(3HB)-*g*-EC^A
EC	P(3HB)	75: 25	P(3HB)-*g*-EC^B
EC	P(3HB)	50: 50	P(3HB)-*g*-EC^C
EC	P(3HB)	25: 75	P(3HB)-*g*-EC^D
EC	P(3HB)	0: 100	P(3HB)-*g*-EC^E

2.8.2. "One-pot" synthesis of keratin-*g*-EC composites using laccase

The freshly isolated keratin (section 2.6) and EC were used to prepare the graft between keratin and EC with different keratin to EC ratios *i.e.,* keratin: EC; 0:100, 25:75, 50:50, 75:25 and 100:0, respectively. A fungal laccase from *T. versicolor* with a unit activity of ≥ 10 U/mg was used as a grafting tool. Briefly, the reaction mixture comprised of keratin and EC was prepared using laccase and sodium malonate buffer of pH 4.0 followed by incubation at 120 rpm for 30 min at 25 °C. The control samples were prepared in the absence of laccase using sodium malonate buffer of pH 4.0 alone. The above laccase treated reaction mixture was then poured into the sterile labelled petri plate followed by incubation at 50 °C for 24 h. The newly developed composite

films were then removed from their respective casting surfaces (petri plate) and assigned IDs subject to keratin to EC ratios, as shown in Table 2.8. All of the collected composites were then characterised using different analytical and imaging techniques including Fourier-transform infrared spectroscopy (FT-IR), scanning electron microscopy (SEM), X-ray diffraction (XRD), differential scanning calorimetry (DSC), dynamic mechanical analyser (DMA) and water contact angle analyser (WCA). Figure 2.4 depicts a schematic representation of preparation and evaluation of laccase-assisted keratin-EC based graft composites.
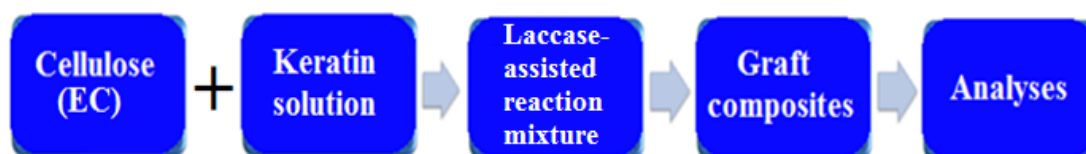
Figure 2.4 Schematic representation of preparation and evaluation of laccase-assisted keratin-EC based graft composites.

Table 2.8 Designation of IDs to the newly developed keratin-EC based graft composites prepared using different keratin to EC ratios (keratin: EC). A fungal laccase from *T. versicolor* with a unit activity of ≥ 10 U/mg was used as a model catalyst for grafting purposes.

Backbone polymer	Grafted polymer	Keratin: EC	Composite ID
EC	keratin	100: 0	keratin-*g*-EC^A
EC	keratin	75: 25	keratin-*g*-EC^B
EC	keratin	50: 50	keratin-*g*-EC^C
EC	keratin	25: 75	keratin-*g*-EC^D
EC	keratin	0: 100	keratin-*g*-EC^E

2.8.3. Preparation of P(3HB)-*g*-EC/BC composite using laccase

P(3HB) and EC/BC were treated with laccase using sodium malonate buffer of pH 4.0 at room temperature and stirred continuously for 20 min. The above treated mixture was then poured into a sterile labelled Petri plate followed by incubation in hot air oven at 50 ºC for 3 h. The resulting enzymatically grafted composites were designated as P(3HB)-*g*-EC (prepared in the presence of laccase), P(3HB)-*g*-EC* (prepared in the absence of laccase using sodium malonate buffer alone and considered as a control sample), P(3HB)-*g*-BC (prepared in the presence of laccase), P(3HB)-*g*-BC* (prepared in the absence of laccase using sodium malonate buffer alone and considered as a control sample). Three different vaporisation rates (fast, medium and slow) were tested for preparation of the composite samples. The fast rate involved placing the samples under a vacuum during drying at -46 ºC and 133 mbar pressure. The medium vaporisation rate was achieved by drying the samples in an oven at 80 ºC. The slow vaporisation rate was achieved by placing the sample in a covered Petri dish with only a small gap between the edges of the dish in an oven at 50 ºC for 3 h. In the fast vaporisation rate, the composites were severely shrivelled after desiccation. At the medium rate, the grafted composites contained some visible air bubbles trapped inside the samples. Whereas, at the slow vaporisation rate, the composites were smooth and did not have any trapped bubbles. Therefore. the slow vaporisation rate was followed throughout the further experiments. All of the collected composites were then characterised using different analytical and imaging techniques as described in the section 3.8.1. Figure 2.5 depicts a schematic representation of preparation and evaluation of laccase-assisted P(3HB)-EC/BC based graft composites.
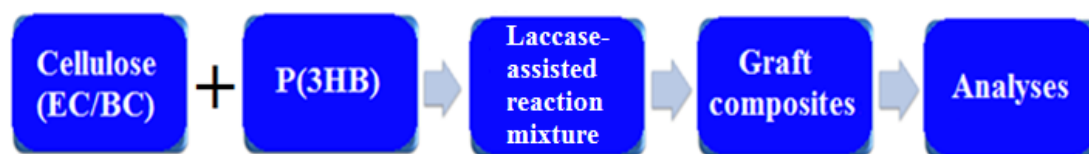
Figure 2.5 Schematic representation of preparation and evaluation of laccase-assisted P(3HB)-EC/BC based graft composites.

2.9. Characterisation of the graft composites

2.9.1. Fourier Transform Infrared Spectroscopy (FT-IR)

FT-IR spectroscopy was used primarily to identify the structural and elemental groups of the P(3HB), keratin, EC/BC and their grafted composites *i.e.,* P(3HB)-*g*-EC (prepared using lipase as described in the section 2.8.1), keratin-*g*-EC (prepared using laccase as described in the section 2.8.2) and P(3HB)-*g*-EC/BC (prepared using laccase as described in the section 2.8.3). Each of the individual polymer and their grafted composites were placed directly onto the diamond crystal, and infrared absorption spectra were recorded from the wavenumber region of 4000-500 cm^{-1} using a Perkin Elmer System 2000 FT-IR spectrophotometer. All spectra were collected with 64 scans and 2 cm^{-1} resolution and assigned peak numbers.

2.9.2. Scanning Electron Microscopy (SEM)

Surface morphologies and microstructure of the individual polymers *i.e.,* P(3HB), keratin and EC/BC and their grafted composites *i.e.,* P(3HB)-*g*-EC (prepared using lipase as described in the section 2.8.1), keratin-*g*-EC (prepared using laccase as described in the section 2.8.2) and P(3HB)-*g*-EC/BC (prepared using laccase as described in the section 2.8.3) were studied in ultra-high vacuum mode at an accelerating voltage of 5 kV in a field emission gun scanning electron microscope (Philips, XL-30, FEG SEM; EFI, Netherlands). The samples were placed on the 8mm

diameter aluminium stubs and gold coated for 2 min using the gold spluttering device (EMITECH-K550). High definition images (HDI) were then recorded at different magnifications to study the surface morphologies of each sample. The operating pressure of 7×10^{-2} bar and deposition current of 20 mA for 2 minutes was used for current analysis.

2.9.3. X-ray Diffraction (XRD)

X-ray diffraction technique was adopted to investigate the crystalline structures of the individual and grafted composites with a thin film attachment using a Brüker D-8 Advance X-ray diffractometer equipped with Ni filtered Cu K radiation. The samples were scanned at 2θ values ranging from 10 °C to 100 °C with a scan speed of 5 °C/min. The data was obtained with the help of a MDI/JADE6 software package attached to the Brüker D-8 Advance XRD instrument.

2.9.4. Differential Scanning Calorimetry (DSC)

A Pyris Diamond Differential scanning calorimeter (Perkin-Elmer Instruments, USA) was used to measure the thermal properties of the individual and grafted composites. The thermal profiles were determined using DSC~3-7 mg of sample weight. Samples (DSC~3-7 mg in weight) were encapsulated in standard aluminium pans to avoid contamination of the ampoules. The temperature scanning range was set from -50 ℃ to 250 ℃ and the scanning rate was 20 ℃/min under nitrogen atmosphere. In order to remove prior thermal history, specimens were initially heated to 250 ℃ at 20 ℃/min and then held for 1 min at 250 ℃ to ensure complete melting. The experimental data was collected for both a cooling scan at 20 ℃/min to -50 ℃ and a subsequent heating scan at 20 ℃/min to 250 ℃.

2.9.5. Dynamic Mechanical Analyser (DMA)

The mechanical profiles in terms of DMA measurements *i.e.,* Young's modulus, tensile strength and elongation at break point of the individual polymers and their grafted composite were carried out using a Perkin–Elmer Dynamic Mechanical Analyser. Prior to load on a crosshead, the test sample was cut into a rectangular shape with 8 mm × 4 mm × 0.25 mm dimensions. The load was set within the range of 1-6000 mN and the crosshead speed was set at a constant tensile rate of 200 mNmin^{-1}. All tests were conducted at ambient temperature and an average value of four repeated tests was taken for each treatment.

2.9.6. Water Contact Angle (WCA)

The water contact angles of the individual polymers and grafted composites were measured on the air surface of their films using pendant drop method using a KSV Cam 200 optical contact angle analyser at room temperature (KSV instruments Ltd., Finland). Approximately 200 μL of de-ionized water was dropped onto the surface of each sample at a contact time of 5 s by means of a gas tight micro-syringe followed by capturing the images using the Windows based KSV-Cam software in order to monitor the contact angle. Ten independent determinations at different sites of the sample were averaged. The results are presented as mean ± S.E. (standard error) of means. The S.E values are displayed as Y-error bars on the figures.

2.10. Grafting of natural phenols

Prior to grafting, phenolic solutions of caffeic acid (CA, $C_9H_8O_4$; MW, 180.16); gallic acid (GA, $C_7H_6O_5$; MW, 170.12); *p*-4-hydroxybenzoic acid (HBA, $C_7H_6O_3$; MW, 138.12); and thymol (T, $C_{10}H_{14}O$; MW, 150.22) with different mM concentrations (0 to 20 mM) were prepared. CA, GA, HBA and T were dissolved separately in 250 mL

of sodium malonate buffer pH 4.0, then reacted with laccase (unit activity $\geq$ 10 U/mg) for 2 h at 50 $^{\circ}$C under constant stirring at 100 rpm. Subsequently the surface dipping and incorporation (SDI) technique was adopted to graft the aforementioned phenolic contents as antimicrobial agents onto the previously developed P(3HB)-*g*-EC (prepared using lipase as described in the section 2.8.1), keratin-*g*-EC (prepared using laccase as described in the section 2.8.2) and P(3HB)-*g*-EC (prepared using laccase as described in the section 2.8.3).

Table 2.9 Designation of IDs to the newly synthesised phenol grafted P(3HB)-EC composites subject to the concentration of phenol used for grafting purposes using laccase.

Phenolic component	Concentration (mM)	Composite ID
CA	05	5CA-*g*-P(3HB)-EC
CA	10	10CA-*g*-P(3HB)-EC
CA	15	15CA-*g*-P(3HB)-EC
CA	20	20CA-*g*-P(3HB)-EC
GA	05	5GA-*g*-P(3HB)-EC
GA	10	10GA-*g*-P(3HB)-EC
GA	15	15GA-*g*-P(3HB)-EC
GA	20	20GA-*g*-P(3HB)-EC
HBA	05	5HBA-*g*-P(3HB)-EC
HBA	10	10HBA-*g*-P(3HB)-EC
HBA	15	15HBA-*g*-P(3HB)-EC
HBA	20	20HBA-*g*-P(3HB)-EC
T	05	5T-*g*-P(3HB)-EC
T	10	10T-*g*-P(3HB)-EC
T	15	15T-*g*-P(3HB)-EC
T	20	20T-*g*-P(3HB)-EC

Briefly, each of the pre-weight composites were dipped in a glass basin containing 50mL of pre-dissolved CA, GA, HBA and T, separately, in the presence of laccase for 60 min of reaction time at 30 °C under constant stirring at 100 rpm. Control samples were also treated in the same way using sodium malonate buffer alone without adding any of the aforementioned natural phenol. After the stipulated reaction time (60 min) the weight of each composite was recorded in the swollen state followed by incubation at 50 °C until fully dried. Afterwards all of the composites were washed three times with sodium malonate buffer to eliminate any of the un-reacted phenolic contents, and then again dried at 50 °C and final dry weight after immersion was recorded to calculate the grafting parameters. All of the samples were prepared in triplicates. Means and standard errors of means (Mean ± S.E) were calculated for each treatment. The newly synthesised graft composites between the tested phenols *i.e.,* CA, GA, HBA and T and previously developed P(3HB)-*g*-EC composite (prepared using lipase as described in the section 3.8.1) were assigned IDs subject to the concentration of the phenol used, as shown in Table 2.9. Table 2.10 illustrating IDs of the composites prepared using the aforementioned natural phenols and previously developed keratin-*g*-EC composite (prepared using laccase as described in the section 2.8.2). The newly synthesised graft composites between the tested phenols *i.e.,* CA, GA, HBA and T and previously developed P(3HB)-*g*-EC composite (prepared using laccase as described in the section 2.8.3) were assigned IDs subject to the concentration of the phenol used, as shown in Table 2.11.

2.11. Fourier Transform Infrared Spectroscopy (FT-IR)

Primarily to investigate the structural and elemental groups of the grafted composites *i.e.,* CA-*g*-P(3HB)-*g*-EC, GA-*g*-P(3HB)-*g*-EC, HBA-*g*-P(3HB)-*g*-EC, T-*g*-P(3HB)-*g*-EC, CA-*g*-keratin-*g*-EC, GA-*g*-keratin-*g*-EC, HBA-*g*-keratin-*g*-EC and T-*g*-

keratin-*g*-EC along with their individual counterparts *i.e.,* CA, GA, HBA, T, P(3HB)-*g*-EC and keratin-*g*-EC, respectively, an FT-IR spectroscopy was used, in this study. Prior to record the spectra against each sample, the above mentioned grafted composites and individual counterparts were placed directly on the diamond crystal of a Perkin Elmer System 2000 FT-IR spectrophotometer. An IR absorption spectra were recorded using the wavelength ranging from 4000 to 500 cm^{-1} using a Perkin Elmer System 2000 FT-IR spectrophotometer. All spectra were collected with 64 scans and 2 cm^{-1} resolution and assigned peak numbers.

Table 2.10 Designation of IDs to the newly synthesised phenol grafted keratin-EC composites subject to the concentration of phenol used for grafting purposes using laccase.

Phenolic component	Concentration (mM)	Composite ID
CA	05	5CA-*g*-keratin-EC
CA	10	10CA-*g*-keratin-EC
CA	15	15CA-*g*-keratin-EC
CA	20	20CA-*g*-keratin-EC
GA	05	5GA-*g*-keratin-EC
GA	10	10GA-*g*-keratin-EC
GA	15	15GA-*g*-keratin-EC
GA	20	20GA-*g*-keratin-EC
HBA	05	5HBA-*g*-keratin-EC
HBA	10	10HBA-*g*-keratin-EC
HBA	15	15HBA-*g*-keratin-EC
HBA	20	20HBA-*g*-keratin-EC
T	05	5T-*g*-keratin-EC
T	10	10T-*g*-keratin-EC
T	15	15T-*g*-keratin-EC
T	20	20T-*g*-keratin-EC

Table 2.11 Designation of IDs to the newly synthesised phenol grafted P(3HB)-EC composites subject to the concentration of phenol used for grafting purposes using laccase.

Phenolic component	Concentration (mM)	Composite ID
CA	05	5CA-*g*-P(3HB)-EC
CA	10	10CA-*g*-P(3HB)-EC
CA	15	15CA-*g*-P(3HB)-EC
CA	20	20CA-*g*-P(3HB)-EC
GA	05	5GA-*g*-P(3HB)-EC
GA	10	10GA-*g*-P(3HB)-EC
GA	15	15GA-*g*-P(3HB)-EC
GA	20	20GA-*g*-P(3HB)-EC
HBA	05	5HBA-*g*-P(3HB)-EC
HBA	10	10HBA-*g*-P(3HB)-EC
HBA	15	15HBA-*g*-P(3HB)-EC
HBA	20	20HBA-*g*-P(3HB)-EC
T	05	5T-*g*-P(3HB)-EC
T	10	10T-*g*-P(3HB)-EC
T	15	15T-*g*-P(3HB)-EC
T	20	20T-*g*-P(3HB)-EC

2.12. Evaluation of grafting parameters

The effect of different phenolic concentrations used on the grafting process between CA, GA, HBA, and T and P(3HB)-*g*-EC and keratin-*g*-EC base was investigated in terms of grafting parameters *i.e.,* graft yield (%GY), grafting efficiency (%GE) and swelling ratio (%SR). Graft yield was calculated in percentage by Equation (1), grafting efficiency was calculated in percentage by Equation (2) and swelling ratio was calculated in percentage by Equation (3), as reported earlier by Sabaa *et al*., 2010.

$$Graft\ yield\ (\%GY) = \frac{Wf - Wi}{Wi} \times 100 \qquad (1)$$

$$Grafting\ efficiency\ (\%GE) = \frac{Wf - Wi}{Ws - Wi} \times 100 \qquad (2)$$

$$Swelling\ ratio\ (\%SR) = \frac{Ws - Wi}{Wi} \times 100 \qquad (3)$$

Where, Wi = initial weight before immersion; Wf = final dry weight after immersion; and Ws = weight of a sample in the swollen state

2.13. Evaluation of anti-bacterial potential

To evaluate the anti-bacterial potential of the aforementioned composites with natural phenols as functional entities, the AATCC Anti-Bacterial Test Method was adapted (Elegir *et al*., 2008). The anti-bacterial characteristics of the composites were tested against various Gram-positive bacterial strains (*B. subtilis* NCTC 3610 and *S. aureus* NCTC 6571) and Gram-negative bacterial strains (*E. coli* NCTC 10418 and *P. aeruginosa* NCTC 10662). For this purpose, the selected bacterial strains were grown from their respective spore or agar slopes and subsequently a suspension containing 10^5 CFU/mL was spread onto the surfaces of the test composites, all of the composites were heat sterilised at 90 °C for 30 min. The inoculated test composites were placed onto the sterile moisture pads followed by incubation in a temperature controlled incubator at 30 °C for 24 h. The moisture pads were prepared into 90 mm petri dishes by placing sterile sponges which contained approximately 20 mL of sterile phosphate buffer to avoid the drying of the test composites during incubation period. Figure 2.6 depicting a schematic representation of preparation of moisture pad. After the stipulated incubation time period (24 h) the bacterial cells from the control and test samples were washed very gently twice using 50 mL phosphate buffer (pH, 7.0). The

viable cell number in each of the washed suspension was determined by conventional spread-plate method and plate counter agar was used to calculate the CFU/mL by serial dilution. The plate counter agar nutrients and their concentrations were: tryptone, 5.0; yeast extract, 2.5; glucose, 1.0 and agar, 9.0. After 24 h incubation on plate counter agar medium at 30 $^{\circ}$C, the replicates were examined and the results were expressed as mean colony forming units per mL (CFU/mL). In comparison with the control (initial bacterial count *i.e.,* 10^5 CFU/mL) the CFU/mL values were used to calculate the antibacterial efficacy of the test composites by using the following equation (4).

$$Log\ reduction = Log\ CFU\ Control\ sample - Log\ CFU\ Treated\ sample \qquad (4)$$

Due to the intrinsic variability of the antibacterial test results, at least a 2 log reduction was considered necessary to claim an antibacterial activity, as reported by Elegir et al., 2008.
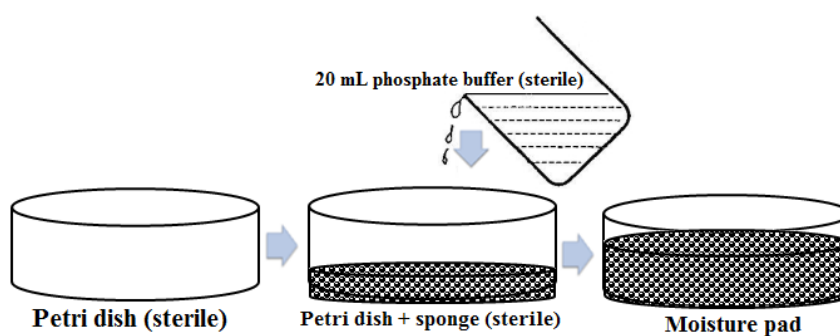
Figure 2.6 Schematic representation of preparation of moisture pad used to avoid the drying of the test composites during incubation period.

2.14. *In-vitro* bio-compatibility evaluation

2.14.1. Cell culture and maintenance

Human keratinocytes-like (HaCaT) skin cell line was cultured in a sterilised Dulbecco's modified eagle's medium (DMEM, Lonza, Wilford Industrial Estate,

Nottingham, UK) supplemented with 10% fetal calf serum (Labtech International Ltd., Bellbrook Industrial Estate, East Sussex, UK), 100 mg/mL streptomycin (Lonza, Wilford Industrial Estate, Nottingham, UK) and 100 mg/mL penicillin (Lonza, Wilford Industrial Estate, Nottingham, UK) at 37 °C in a humidified atmosphere of 5% CO_2. After 24 h of initial incubation the culture medium was changed to remove any dead cells and also to promote cell growth. The confluent cells were subjected to trypsinisation and recovered by centrifugation at $1000 \times g$ for 10 min. The cell pellets were re-suspended homogenously into the culture medium and then transferred into a 75 cm^2 tissue culture flask for further passages.

2.14.2. *In-vitro* cell viability assay

HaCaT cells were adopted to evaluate the cytotoxicity of the newly synthesised composites, and the cell viability was determined quantitatively using neutral red (Sigma-Aldrich, UK) uptake assay. Prior to in vitro testing, the test samples (1 cm^2 in area) were sterilised using UV radiation for 30 min on each side and placed in a 24-well tissue culture plates. After cell counting, HaCaT cells were seeded in 24-well tissue culture plates containing test composites (1cm^2 in area) at a density of 1×10^5 cells per well. After incubating for 1, 3 and 5 days respectively, the culture medium (DMEM) was removed and the specimens were rinsed with phosphate buffer saline (PBS, Lonza, Wilford Industrial Estate, Nottingham, UK) three times in order to remove the unattached cells. Cell viability of the adherent cells was measured by adding 1 mL/well culture medium containing 5 mg/mL NR dye and incubated for 3 h to allow the viable cells to uptake the dye. After the stipulated incubation time (3 h), the test specimens were washed three times with a mixture solution containing 1% $CaCl_2$ and 0.5 % formaldehyde. This was followed by 10 min incubation at an ambient temperature under lysate solution containing 1% acetic acid and 50% ethanol solution

to extract the dye taken up by the viable cells. Subsequently 100 μL from each well was transferred into new 96-well cell culture plates and optical density (OD value) of the extracted supernatant was measured with a Thermomax microplate reader (Alpha Laboratories Ltd., Eastleigh, Hampshire, UK) at 540 nm using Softmax Pro version 4.8 software. Percentage cell viability of the test composites was calculated using the following equation (5).

$$HaCaT \ viability \ (\%) = \frac{OD \ Test \ composite - OD \ Negative \ control}{OD \ Positive \ control} \times 100 \qquad (5)$$

In this experiment, standard tissue culture plastic was used as a positive control whereas a graft composite without cell culture was used as negative control to normalise the absorption of the neutral red dye by the graft composite itself.

2.14.3. Adherent morphology – Cell adhesion

The adherent morphology of HaCaT cell line seeded onto the test composites was observed using Nikon light microscope. After 1, 3 and 5 days of incubation at 37 ℃ in a humidified atmosphere of 5% CO_2 cells were washed with PBS in order to remove the un-attached cells and then fixed with 4% (w/v) paraformaldehyde in PBS for 30min at an ambient temperature. The samples were then washed with PBS and this was followed by adding 5 mg/mL neutral red dye to stain HaCaT cells for 1 h. After the stipulated time, the stained cells were washed three times with PBS for 15 min at an ambient temperature. Following that high definition images (HDI) were captured with DCMI-15 Nikon light microscope camera using ScopeTeck, ScopePhoto Windows based version x86, 3.1.475 software at 100× magnification.

2.15. Bio-degradability evaluation

2.15.1. Soil burial test

American standard testing method (ASTM D6400-99) which includes European standards (CEN/TC 261/SC 4N 99 and ISO 14855) procedure was adopted to conduct a soil burial test. The biodegradability of the composites as a function of time dependent weight loss was performed as described earlier by Wattanakornsiri *et al.*, 2012, with minor modifications. Briefly, about $30 \times 30 \times 1$ mm in sizes test specimens were cut from each of the composite, dried and equilibrated at room temperature in desiccators, and weighed to determine the reference weight (control). The soil burial test was carried out over a period of 6 weeks (42 days) under ambient environment (30 ± 5 °C). A garden type soil was placed into plastic containers (pots) with 25 cm in diameter and 20 cm in height with tiny holes perforated at the bottom and on the sides of the containers to increase air and water circulation to promote the microbial action of the microorganisms which are normally present in the soil at 40-50% moisture. A set of triplicate composites were buried under a soil surface of approximately 8-10cm. During every 7 days of burial, each set was removed, washed with distilled water, dried under ambient environment (30 °C) and subsequently weighed to determine the loss in weight, being recorded every week for 6 weeks. The percentage of weight loss was calculated using the following equation (6).

$$Loss\ in\ weight\ (\%) = \frac{Control\ weight - Loss\ in\ weight}{Control\ weight} \times 100 \qquad (6)$$

2.16. Statistical analysis

All of the quantitative data analyses were performed in triplicate; statistically evaluated results are presented as mean ± S.E. (standard error) of means with n = 3. The S.E values are displayed as Y-error bars in figures.

Chapter 3

In situ development and characterisation of
novel bio-composites through enzymatic
grafting

3.0. Summary

In this chapter, the results of *in-situ* development, characterisation, and analysis of newly synthesised bio-composites are discussed. A series of bio-composites *e.g.* poly3-hydroxybutyrate [P(3HB)] grafted ethyl cellulose (EC) and bacterial cellulose (BC) [*i.e.,* P(3HB)-*g*-EC/BC] were successfully synthesised by introducing enzyme-based grafting where lipase from *Rhizopus oryzae* and laccase from *Trametes versicolor* were used as model bio-catalysts. Subsequently, the resulting bio-composites were removed from the casting surfaces under ambient environment. Finally, the target bio-composites were characterised in detail by Fourier-transform infrared spectroscopy (FT-IR), scanning electron microscopy (SEM), X-ray diffraction (XRD), and thermo- mechanical behaviour of the grafted composites was investigated by differential scanning calorimetry (DSC) and dynamic mechanical analyser (DMA) measurements, respectively. Furthermore, hydrophobic and hydrophilic characteristics of the composites were studied through drop contour analysis using water contact angle (WCA). However, the set of techniques that are used here may also apply to other biological and synthetic materials.

3.1. Introduction

Polyhydoxyalkanoates (PHAs) are a family of intracellular bio-polymers synthesised by variety of microorganisms especially bacteria as intracellular carbon and energy storage granules, under unbalanced growth conditions (Sevastianov *et al*., 2003). More than 100 different monomers can be combined within this family to provide polymers with different properties; including thermo-plastic and elastomeric materials. PHAs have attracted great scientific and commercial interests due to their good biocompatibility, biodegradability and thermo-plastic properties and are

expected to contribute to the construction of environmentally sustainable society. Currently, over 150 different types of PHAs have been reported (Keshavarz and Roy, 2010; Rehm, 2015). PHA nomenclature and classification will still evolve as new structures continue to be discovered. So far several PHAs including poly(3-hydroxybutyrate) [P(3HB)], and other co-polymers are available in sufficient quantity for research purposes (Chen and Wu, 2005; Rehm, 2015).

To obtain the desired functionality with natural polymers, it is generally necessary to graft appropriate moieties onto a preformed polymer backbone (Nasef, 2014; Roy and De, 2014). Among the most promising and well-characterised biopolymers, P(3HB) is of particular interest to prepare composites that can be synthesised by combining with another suitable homo-, or co-polymers. This polymer is the focus of the work presented here, to produce composites with cellulose to improve or impart new physiochemical and thermo- mechanical properties, decrease brittleness, and increase tensile strength of P(3HB) with varied cellulosic contents in the grafted material. It has been reported that "green" composites can be successfully fabricated by grafting or blending biodegradable polyesters with cellulosic materials such as EC, bacterial cellulose (BC), cellulose esters, cellulose triacetate, and recycled cellulose fibres (Zhang *et al*., 1997; Bhardwaj *et al*., 2006; Yu *et al*., 2006; Zhijiang *et al*., 2011; Carlsson *et al*., 2012; Yu *et al*., 2012; Iqbal *et al*., 2014a). Among them, EC as a chemically modified cellulose exhibits excellent plasticity, good solubility in organic solvents, biocompatibility, high mechanical strength, good heat-resistance, cold-resistance and stability (Yuan *et al*., 2007; Zhu *et al*., 2010; Iqbal *et al*., 2014b).

Green chemistry has many challenges for successful implementation of innovative technologies to accomplish pollution prevention that reduce or eliminate the use or generation of hazardous substances during the entire manufacturing processes. The

environmental impact of persistent chemical or petroleum based technologies is increasing global concerns (Cao *et al.*, 2014; Andrady *et al.*, 2015). Environmental pollution awareness and the demand for green chemistry technologies have drawn considerable attention from both academia and industry to develop eco-friendly processing designs. In this context, recently bio-based composites are being engineered for target applications in different industries to address growing environmental concerns of unsustainable dependence on petroleum based resources (Iqbal *et al.*, 2013). Bio-polymers generated from natural sources are often biodegradable, biocompatible and non-toxic. Therefore, preparations of green composites using one or more individual bio-polymers are among the measures to improve the properties of biodegradable polymers (Miao and Hamad, 2013; Hooshmand *et al.*, 2014).

Grafting is a method where monomers are covalently bonded (modified) onto a polymer chain to obtain the requisite properties. There are several means to modify the existing polymer properties to make them suitable and useful for wider range of applications. These techniques include alkaline hydrolysis, chemical modification, gamma radiation, photochemical modification, UV radiation, reversible addition-fragmentation chain transfer (RAFT), free radical based polymerisation, plasma-induced techniques, and enzymatic grafting (Chen *et al.*, 2000; Kim *et al.*, 2002; Grøndahl *et al.*, 2005; Lao *et al.*, 2007; Roy *et al.*, 2013; Xiao *et al.*, 2014; Pei *et al.*, 2015).

Enzymatic grafting of bio-polymers is favourable over other physical and chemical grafting methods. The principle involved is that enzymes offer clean and safe alternatives to current practices as an active starting material in the grafting reaction and work under safe conditions (Aljawish *et al.*, 2012; Iqbal *et al.*, 2014b). There are

several advantages for the use of enzymes in polymer modifications, with respect to health and safety. Enzymes offer the potential for eliminating the hazards associated with reactive reagents. A potential environmental benefit for using enzymes is that their selectivity may be exploited to eliminate the need for wasteful protection and de-protection steps. These facts have stimulated the investigation for alternatives to convert polyester materials into value-added products of interests (Ghanbarzadeh and Almasi, 2013; Iqbal *et al*., 2014c).

Lipases (carboxylic ester hydrolases) belong to the class of hydrolases that act on the carboxylic ester bonds. They hydrolyse a wide range of reactions including hydrolysis, alcoholysis, esterification, trans-esterification and inter-esterification type reactions (Atadashi *et al*., 2013; Dhake *et al*., 2013; Silva *et al*., 2014). Lipases also catalyse the synthesis of the esters formed from the hydroxyl and carboxylic groups. This versatility makes lipases the enzymes of choice for potential applications in various industrial and modern biotechnological sectors. Interestingly, lipases do not require any cofactor and due to this unique feature, in the absence/presence of traces of water, lipases are capable of reversing the reaction that leads to the esterification and inter-esterification (Sharma *et al*., 2001). There are major drawbacks of such chemical processes. The esterification by lipases appears to be an attractive alternative by the green chemistry technologies to replace the pre-existing bulk chemical routes. Here, in the esterification reactions, lipases act on the substrate in a specific or non-specific manner. The hydrophobic patches on the surface of lipases are responsible for the strong interactions with the hydrophobic substrates. Besides the lipolytic activity, lipases also possess esterolytic activity, thus, have a wide substrate range. The chemo-, regio-, and enantio-specific behaviour of these enzymes have attracted notable scientific and industrial research (Saxena *et al*., 2003).

Laccase (EC 1.10.3.2, p-diphenol:dioxygen oxidoreductase) is a blue copper oxidase capable of reacting with a large variety of suitable substrates. Their commercial availability, broad oxidative capabilities and potential as a powerful tool for surface modifications make them attractive candidates for a wide range of applications (Riva, 2006). There is now a new wave of interest in laccase mediated surface activation with a view to grafting molecules of interest.

In the present work, novel graft composites were prepared by combining the advantages of EC and the freshly isolated P(3HB) using lipase and laccase. To date there is no report in literature explaining the lipase-catalysed and laccase-assisted grafting of P(3HB) and EC/BC. The enzyme-based synthesis of such green composites opens the doors to effective polymer reinforcement without the environmental and economic restraints of petroleum-based alternatives.

3.2. Results and Discussion

3.2.0. PART – 1 ("One-pot" synthesis and characterisation of P(3HB)-EC-based bio-composites through lipase-catalysed esterification)

3.2.1. Fourier-transform infrared spectroscopy (FT-IR)

The structural element of the untreated P(3HB) and P(3HB)-EC-based bio-composites were characterised using FT-IR spectroscopy to confirm the structural changes of the grafted composites comprising them. The changes in the structural elements during lipase treatment were confirmed from the FT-IR spectra by detecting the vibration of chemical bonds as shown in Figure 3.1. Two regions in FT-IR spectra are of particular interest between 2,800 and 3,600 cm^{-1} and between 1,000 and 1,800 cm^{-1}. The

untreated P(3HB) showed bands corresponding to the C=O region and the CH_3, CH_2, CH regions (2,850-3,000 cm^{-1}). The band at 1,717 cm^{-1} arises from the stretching vibration of C=O group, while the bands at 2,932 and 2,976 cm^{-1} are assigned to the CH_3 symmetric stretching. The bands at 1,278 and 1,260 cm^{-1} are assigned to the C-O-C stretching modes. The lipase treated P(3HB) showed a broad peak in the region of 3,500-3,200 cm^{-1} that is attributed to -OH group and a new peak in the region of 1,600-1,650 cm^{-1} (Figure 3.1). An increase in the intensity of bands at 1,717 cm^{-1} with the increasing P(3HB) content ratio in the graft composites was also recorded. Table 3.1 shows an overview of infrared band signals that confirm important shifts in the untreated P(3HB), EC and P(3HB)-EC based lipase-assisted graft bio-composites. However, earlier studies conducted by Zhao *et al*., (2002) and Wang *et al*., (2003) did not report any obvious changes in the FT-IR spectra of the polyhydroxybutyrate (PHB) and poly(hydroxybutyrate-co-hydroxyhexanoate) (PHBHHx) films including new band emerging prior and after lipase treatment; but, the presence of carboxyl groups was noted by X-ray photoelectric spectroscopy (Wang *et al*., 2003). It is worth mentioning that in the case of the addition of cellulose, the intensities of the absorption bands at 1,717 cm^{-1} and 1,278 cm^{-1} relative to the P(3HB) content ratio decreased. As described by previous researchers (Guzmán and co-workers, 2011), lipase-assisted modification of the P(3HB) causes a reduction in the crystallinity, thus yield more amorphous materials, which lead to decreases in the intensities of the crystalline bands near 1,700 and 1,200 cm^{-1} (Furukawa *et al*., 2006). This reduction in the crystallinity was also confirmed in later experiments characterised by X-ray diffraction analyses. It also exhibited a more pronounced absorption in the region of 1,260-1,000 cm^{-1} as a result of the C-O stretching frequency of the poly-hydroxyl groups contributed by EC. The peak at 1,050-1,100 cm^{-1} region is due to the stretching of the C-O-C linkage of

74

ethyl cellulose molecules. The high intensity of the 3,358 cm^{-1} band in the graft composite showed an increase of hydrogen-bonded groups at that distinct band region (Zhang *et al.*, 1997). Figure 3.2 illustrates a schematic representation of the proposed mechanism of graft formation through lipase catalysed esterification between P(3HB) and EC.
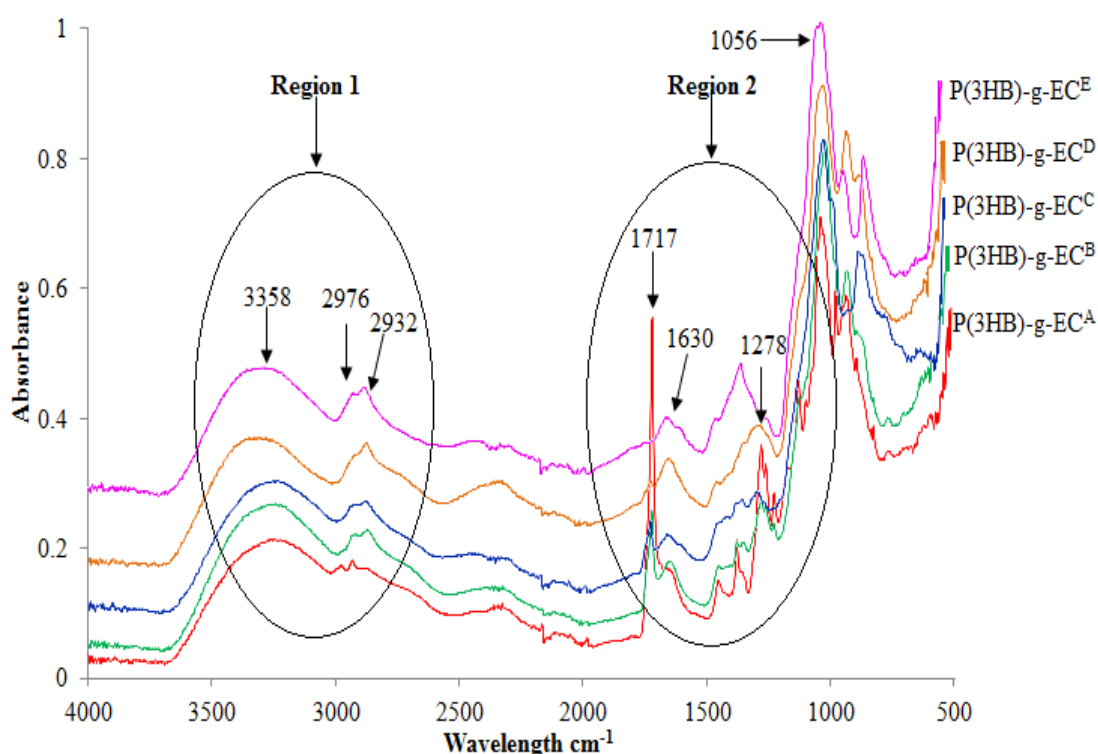
Figure 3.1 FT-IR spectra of P(3HB) and P(3HB)-EC-based lipase-assisted bio-composites *i.e.,* P(3HB)-*g*-EC^{A}, P(3HB)-*g*-EC^{B}, P(3HB)-*g*-EC^{C}, P(3HB)-*g*-EC^{D}, and P(3HB)-*g*-EC^{E} prepared using different P(3HB) to EC ratios.

Where, ^{A}*: P(3HB): EC, 100:0;* ^{B}*: P(3HB): EC, 75:25;* ^{C}*: P(3HB): EC, 50:50;* ^{D}*: P(3HB): EC, 25:75 and* ^{E}*: P(3HB): EC, 0:100.*

Table 3.1 Overview of Infrared Bands of P(3HB) and P(3HB)-EC-based lipase-assisted bio-composites.

Band Position [cm^{-1}]			Band assignment
P(3HB)	P(3HB)-*g*-EC	EC	
1,721			C=O
2,867			CH$_3$
	1,717		C=O
	2,932		CH$_3$
	2,976		CH$_3$
	1,278		C-O-C
	3,500-3,200		OH
		1,056	C-O-C
		3,358	OH
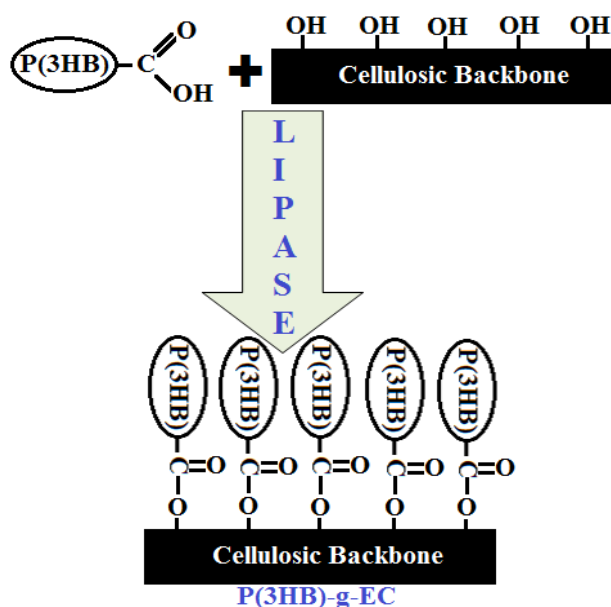
Figure 3.2 A schematic representation of proposed mechanism of graft formation through lipase catalysed esterification between P(3HB) and EC (Iqbal *et al*., 2014a).

3.2.2. Scanning electron microscopy (SEM)

Scanning electron microscopy investigation was performed on the individual polymers *i.e.,* P(3HB) and EC and their grafted composites *i.e.,* P(3HB)-*g*-EC to evaluate their surface morphologies. The morphology of the resulting composites surfaces prepared using lipase under an ambient environment with different P(3HB): EC ratios are shown in the Figure 3.3 (A-F). It was observed that the untreated P(3HB)

has a porous coralloid surface as shown in the Figure 3.3 (A). This was in agreement with the findings of Deng and co-workers, who have also observed a similar coralloid surface with large pores in P(3HB) based scaffold (Deng *et al*., 2002). Interestingly, as the content ratio of P(3HB) increased in addition with EC in the grafted composites the distribution of pores on the composite surface was decreased, and finally a pore free and continuous surface was observed in case of the graft composite prepared with P(3HB) to EC ratio 25: 75 in the presence of lipase (Figure 3.3, E). Similarly, Kai *et al*., 2003 reported that the treatment of the P(3HB) scaffold with lipase converted the coralloid surface of the P(3HB) to a regular one. Also, the lipase treated P(3HB) film has been reported to result in a reduced pore size giving the appearance of smooth polymer surface (Yang *et al*., 2002; Wang *et al*., 2003). The lipase treatment may bring two changes to the polymers surface: one is the change of chemical structures; another is its physical properties, and this is because lipase treatment could produce many hydroxyl groups resulting from the hydrolysis of the ester bonds in P(3HB), and thus contributing to the improved polymer properties (Yang *et al*., 2002; Zhao *et al*., 2002; Kai *et al*., 2003; Alejandra *et al*., (2012). The results obtained in the present study showed obvious differences in the surface properties which are apparent and consistent with the P(3HB) content. A continuous, porous surface structure is apparent in untreated P(3HB) while, in the case of grafted composites prepared in the presence of lipase with different P(3HB) to EC content ratios, the morphological appearance completely changed which clearly revealed the enzyme action during the graft formation process. It has also been reported in literature that the graft copolymerisation modified the surface morphology; physical, chemical, and microstructural characteristics of grafted materials (Joshi and Sinha, 2006).
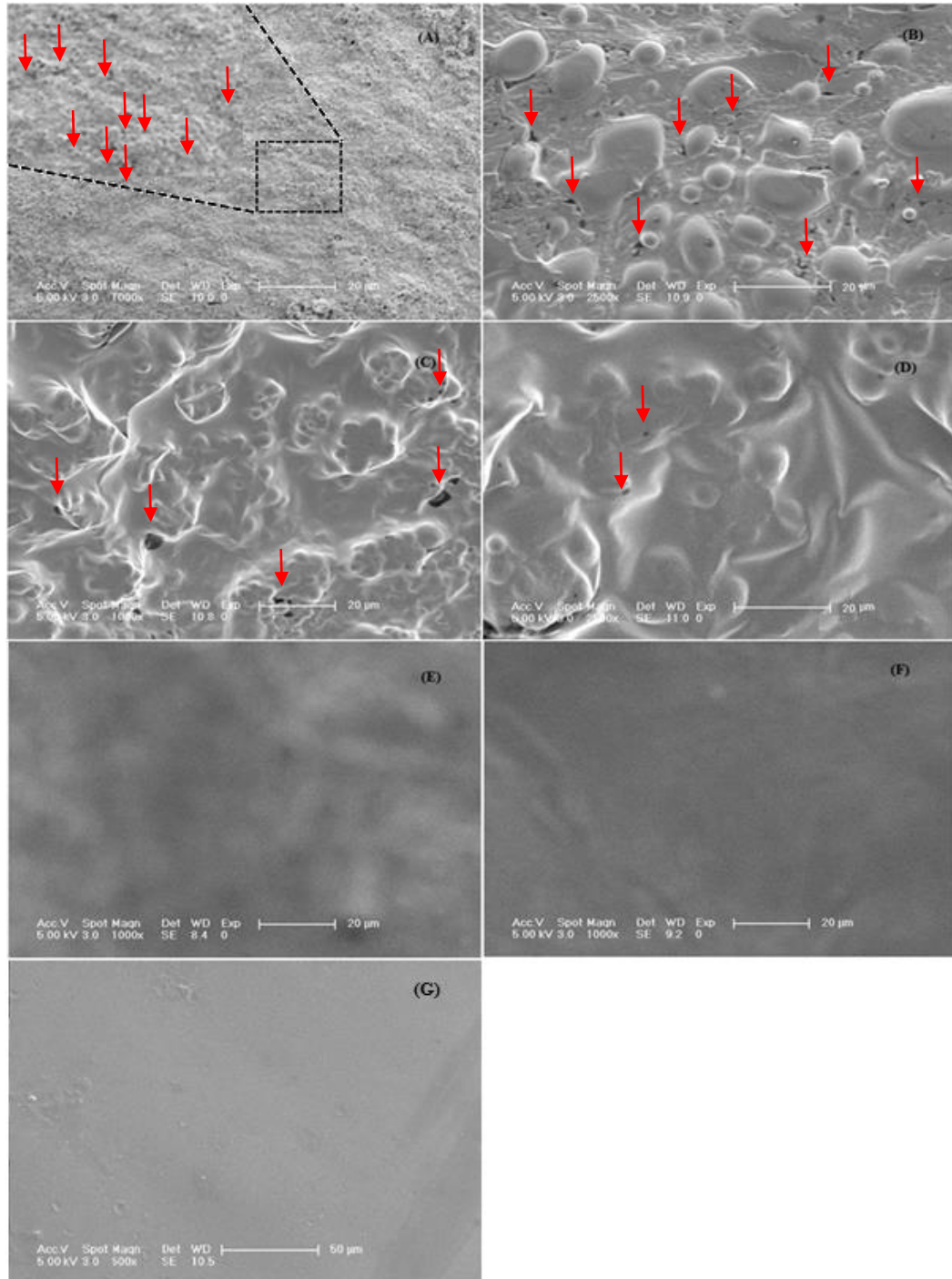
Figure 3.3 SEM micrograph of untreated P(3HB) and P(3HB)-EC-based bio-composites prepared using lipase with different P(3HB) to EC ratios. The red arrows point to gaps and pores formed on the surface.

Where, (A): Untreated P(3HB); (B): P(3HB): EC, 100:0; (C): P(3HB): EC, 75:25; (D): P(3HB): EC, 50:50; (E): P(3HB): EC, 25:75; (F): P(3HB): EC, 0:100 and (G): untreated EC

3.2.3. X-ray diffraction (XRD)

In the present study, XRD analyses were carried out to investigate the micro-structural changes that happens during the graft formation process between P(3HB) and EC in the presence of lipase. Figure 3.4 (A-E) illustrates XRD patterns obtained for the grafted composites prepared with different P(3HB) to EC ratios. For EC, a main scattering peak was identified at 2-Theta value of 20°, which is assigned to the reflexion planes of cellulose I (Tokoh *et al*., 1998). In comparison to the EC the X-ray diffraction pattern of the P(3HB) showed distinct peaks at 2-Theta values of 28°, 32°, 34°, 39°, 46°, 57°, 64°, 78°, and 84° that represent the crystalline nature of the P(3HB) due to its orthorhombic system (Yokouchi *et al*., 1973; Sato *et al*., 2004). It has also been reported in literature that Poly(3-hydroxybutyrate) P(3HB) shows high crystallinity because of the perfect stereo-regularity produced by bacteria (Sato *et al*., 2004). Wider peaks were observed in the graft composites prepared with P(3HB): EC 100:0, 75:25 and 50:50 in the presence of lipase as a grafting catalyst, as compared to the sharp peaks of the untreated P(3HB) at some specific region of 2-Theta values. This is possibly due to the lipase action (Figure 3.4, A-C). This shift from sharp to the wider peaks clearly indicates the breakdown of some crystalline domains at 2-Theta values of 14°, 17°, 22°, and 26°. The penetration and interaction of P(3HB) into the cellulosic backbone slightly disturb the native hydrogen bonding interactions in the cellulose chains and eventually result in a lower crystallinity of the composites. The major diffraction peaks for both P(3HB) and cellulose were observed in the diffractogram of the P(3HB)-*g*-cellulose composites prepared with P(3HB):EC; 75:25, 50:50 and 25:75 (Figure 3.4, B-D).
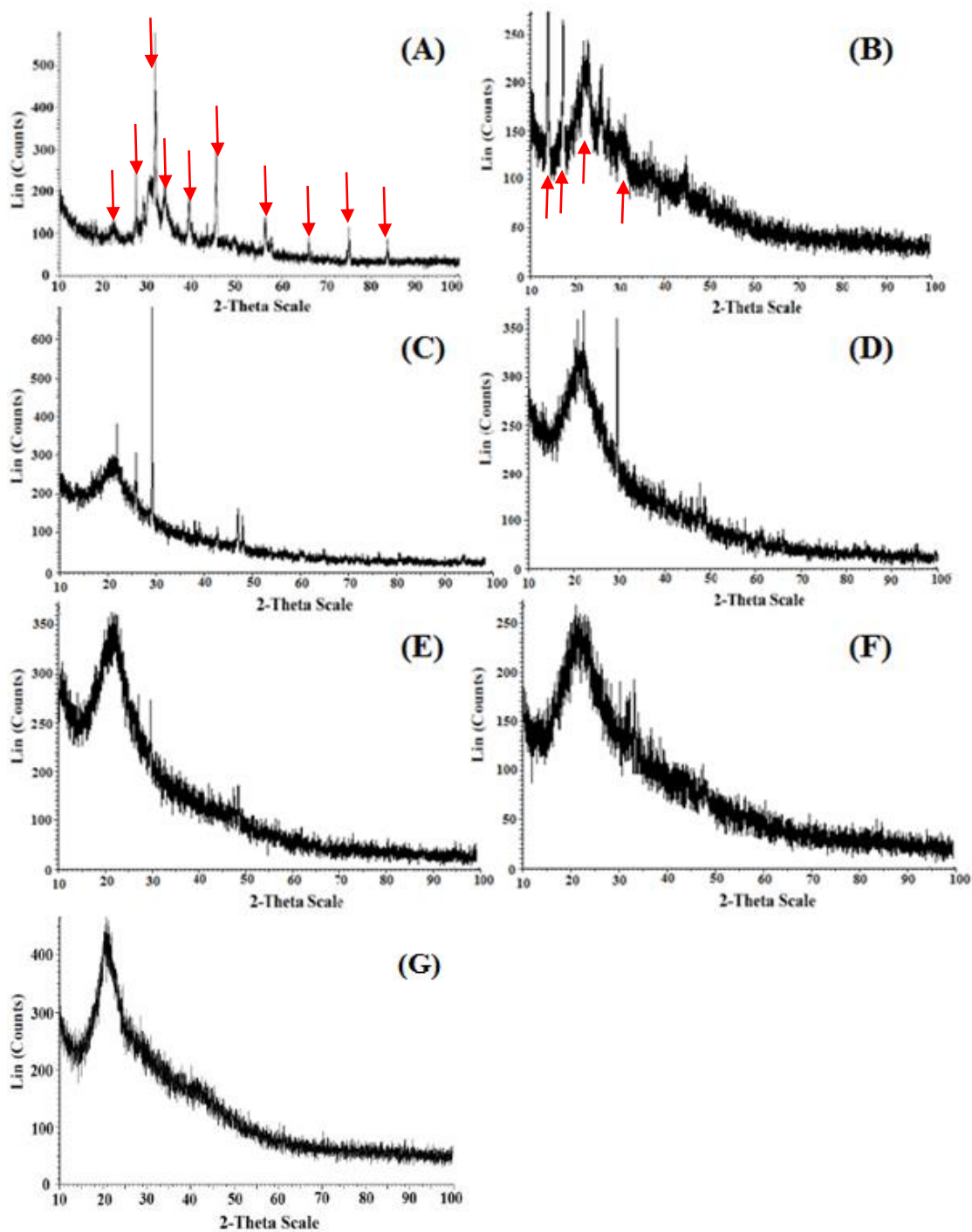
Figure 3.4 Typical X-ray diffracogram of untreated P(3HB), EC and P(3HB)-EC-based bio-composites prepared using lipase with different P(3HB) to EC ratios. The red arrows point to a change in the peaks.

Where, (A): Untreated P(3HB); (B): P(3HB): EC, 100:0; (C): P(3HB): EC, 75:25; (D): P(3HB): EC, 50:50; (E): P(3HB): EC, 25:75; (F): P(3HB): EC, 0:100 and (G): untreated EC.

3.2.4. Differential Scanning Calorimetry (DSC)

Thermal profile of the lipase-assisted grafted composites prepared with different P(3HB) to EC ratios obtained from the DSC analyses are shown in Table 3.2. As shown in Table 3.2, the untreated P(3HB) showed thermal properties (T_g, 9 °C; T_m, 174 °C and T_c, 135 °C) with melting enthalpy (ΔH_m) of 64 J/g, which are comparable with the earlier reported range of different thermoplastic bacterial PHAs polymers (Valappil *et al*., 2007; Alejandra *et al*., 2012). In comparison to the untreated P(3HB) a decrease in the T_g, T_m and T_c values from 9 °C to 3 °C, 174 °C to 142 °C, and 135 °C to 58 °C , respectively was observed in case of the composite prepared only with P(3HB) using lipase as a catalyst. One possible explanation of this initial reduction in the T_g and T_m values may be due to the lipase cleavage of the individual segments into short chains which is not enough to reach the critical T_g and T_m values. In an earlier study, a similar kind of reduction phenomenon in the T_m value of the poly(3-hydroxybutyrate) P(3HB) treated with lipase enzyme, that increases with the reaction time, was also observed by Alejandra *et al*., (2012). However, in case of the grafted composites the re-joining and/or reorganisation of smaller chains, resulting from chain scission, during the reaction phase would cause an increase in the T_g and T_m due to the better impregnation of cellulosic component as reinforcement, and also because of the formation of new cross-linking of P(3HB) within the cellulosic backbone. This reorganisation of smaller chain segments lead into more compact structures and therefore contribute to the increase in the X_c values (Luzuriaga *et al*., 2006; Alejandra *et al*., 2012). Based on the data reported in the literature T_m is directly linked to the size of the crystalline domains of the polymers therefore, herein, the parameter T_c is used to measure the overall rate of crystallisation, and the smaller the T_c, the greater the rate of crystallisation (Yu *et al*., 2012). Based on these literature evidences and

above discussed data, it appears that strong interactions occurred between P(3HB) and cellulose molecules. This clearly indicates the formation of the composite and supports the FT-IR and XRD confirmations.

Table 3.2 DSC-thermal properties of P(3HB), EC and P(3HB)-EC-based bio-composites prepared using lipase with different P(3HB) to EC ratios.

S. No.	Sample ID	T_g (°C)	T_m (°C)	T_c (°C)	ΔH_m (J/g)
1	P(3HB)*	9±0.05	174±0.45	135±0.18	64±0.02
2	P(3HB)-g-EC^A	3±0.09	142±1.75	58±1.06	32±0.85
3	P(3HB)-g-EC^B	17±0.65	180±3.25	76±1.78	48±0.66
4	P(3HB)-g-EC^C	22±0.99	195±2.99	92±2.12	42±0.38
5	P(3HB)-g-EC^D	19±0.85	191±3.33	85±2.65	45±0.86
6	P(3HB)-g-EC^E	ND	186±2.15	52±1.09	80±0.98
7	EC*	ND	188±0.09	48±0.05	86±0.69

T_g = Glass transition temperature; T_m = Melting temperature; T_c = Crystallisation temperature and ΔH_m = melting enthalpy

* Untreated

ND: not detected

Where, ^{A}: P(3HB): EC, 100: 0; ^{B}: P(3HB): EC, 75: 25; ^{C}: P(3HB): EC, 50: 50; ^{D}: P(3HB): EC, 25: 75 and ^{E}: P(3HB): EC, 0: 100.

3.2.5. Dynamic Mechanical Analyser (DMA)

To investigate the mechanical characteristics of the grafted composites, the tensile tests were performed according to ASTM D-882-97 standard test method. Table 3.3 provides the results of mechanical profile of P(3HB)-*g*-EC (prepared with different P(3HB): EC including; 100:0; 75:25; 50:50; 25:75 and 0:100) calculated from the stress-strain curves. The untreated P(3HB) film was too fragile to measure its mechanical properties. However, the composites prepared with P(3HB) and EC using P(3HB): EC ratio 100:0 in the presence of lipase was fairly flexible judged from tensile strength (31 ± 0.88 MPa), elongation at break (3.5 ± 0.22 %) and Young's modulus (0.22 ± 0.42 GPa) as compare to the untreated P(3HB) film. The P(3HB)-*g*-EC composite showed simultaneous improvement in the tensile strength and % elongation at break point as compare to its individual counterpart of P(3HB) because the high strength of EC allowed the mechanical properties of P(3HB)-*g*-EC composite to improve. As shown in Table 3.3, P(3HB) supplemented with 50 wt% of EC showed 78±0.21MPa of tensile strength, 31.0 ± 0.38 % of elongation, and 2.35 ± 0.54 GPa of Young's modulus (Table 3.3). This implies that the fragility of P(3HB) was effectively improved by the incorporation of cellulose. The mechanisms responsible for the improved mechanical performance are likely related to the dispersion state and also the nature of the polymers used (Yu *et al*., 2012). In the last decade several authors have shown that lipase treatments can improve various properties including mechanical, bio-compatibility and hydrophilicity of different microbial polyesters through various cross-linking reactions (Zhao *et al*., 2002; Wang *et al*., 2003).

Table 3.3 DMA-mechanical properties of P(3HB), EC and P(3HB)-EC-based bio-composites prepared using lipase with different P(3HB) to EC ratios.

S. No.	Sample ID	Tensile strength (MPa)	Young's modulus (GPa)	Elongation at break (%)
1	P(3HB)*	ND	ND	ND
2	P(3HB)-g-EC^A	31 ± 0.88	0.22 ± 0.42	3.5 ± 0.22
3	P(3HB)-g-EC^B	51 ± 0.15	0.84 ± 0.29	8.0 ± 0.25
4	P(3HB)-g-EC^C	78 ± 0.21	2.35 ± 0.54	31.0 ± 0.38
5	P(3HB)-g-EC^D	108 ± 0.33	2.86 ± 0.35	19.0 ± 1.10
6	P(3HB)-g-EC^E	121 ± 0.55	3.5 ± 0.75	9.0 ± 0.15
7	EC*	122 ± 9.85	3.38 ± 0.85	8.2 ± 1.25

Untreated

ND: Not detected

Where, ^{A}: P(3HB): EC, 100: 0; ^{B}: P(3HB): EC, 75: 25; ^{C}: P(3HB): EC, 50: 50; ^{D}: P(3HB): EC, 25: 75 and ^{E}: P(3HB): EC, 0: 100

3.2.6. Water contact angle (WCA)

The hydrophobic/hydrophilic characteristics of the solid materials can be explained by the theory of intermolecular forces, and be estimated by means of contact angle measurement. Therefore, in the present study, a drop contour analysis was used to investigate the water contact angle and the surface tension properties of the newly

synthesised graft composites and their individual counterparts *i.e.,* P(3HB) and EC. The results obtained for characteristic water contact angle and surface tension of all of the tested samples are presented in Figure 3.5. The water content angle and surface tension properties of the untreated P(3HB) were 68° and 21 mN/m. Interestingly, the composites prepared with different P(3HB)-EC ratio using lipase exhibited a more than two-fold decrease in the contact angle measurement in comparison to the untreated P(3HB). This could be due to hydrolysis caused by lipase. Based on the data obtained after DSC analyses a reduction in the T_g and T_m was observed for P(3HB) treated with lipase. This implied a reduction in crystallinity of the P(3HB) on modification to yield more amorphous and hydrophilic materials as evident by XRD and WCA analyses. It was believed that the lipase treatment should produce many hydroxyl groups resulted from the hydrolysis of the ester bonds, as lipase can hydrolyse the ester linkages of the polyesters used here during the initial phase of the reaction, thus contribute to the improved hydrophobic/hydrophilic characteristics of the as-prepared composites. Such characteristics are sought for successful tissue development and/or implantation in a host. Increased hydrophilicity of the lipase treated P(3HB) and P(3HB) containing graft composites was also demonstrated by an increase in the surface tension properties from 21 to 118 mN/m (Figure 3.5). It has also been reported in literature that the grafted polymers with more hydroxyl groups of short chains exhibit more hydrophilic than other co-polymers (Carlsson *et al*., 2012).
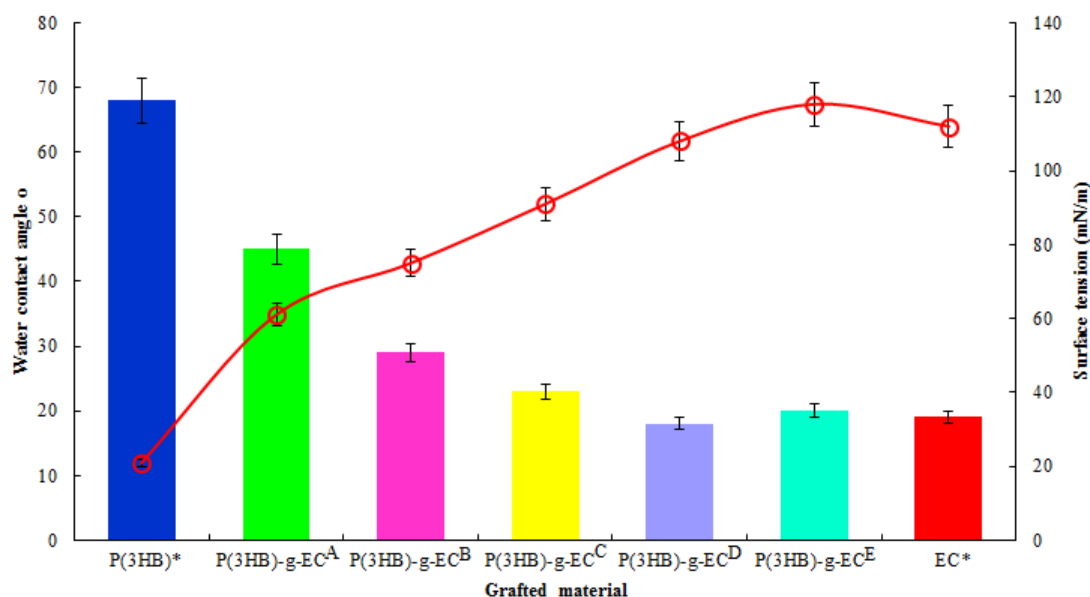
Figure 3.5 Water contact angle (bars in colour) and surface tension (red line) measurements of P(3HB), EC and P(3HB)-EC-based graft bio-composites prepared using lipase with different P(3HB) to EC ratios.

* Untreated

Where, (A): P(3HB): EC, 100: 0; (B): P(3HB): EC, 75: 25; (C): P(3HB): EC, 50: 50; (D): P(3HB): EC, 25: 75 and (E): P(3HB): EC, 0: 100.

3.3. Concluding remarks

In the present work, the crystallisation, thermo- mechanical, morphology and wettability characteristics of lipase assisted composites of P(3HB) grafted with EC using different P(3HB) to EC ratios were presented have been obtained. It has been shown that the crystallisation rate, crystallinity, thermo- mechanical strength and wettability features of the grafted P(3HB)-EC are significantly improved as compared to the untreated counterparts, during the grafting reaction.

Lipase-catalysed esterification reactions are versatile and promising methods to prepare graft composites using polyester type bio-degradable materials like P(3HB) with cellulosic materials. The results obtained in the present study should be useful for expanding the availability of cellulosic material as a major component to design novel composites furnished with high functionality. Lipase-assisted synthesis appears to be an attractive green chemistry alternative approach to replace the existing bulk chemical processing. In conclusion, the results obtained in the present study and the data discussed in this chapter suggest the newly synthesised P(3HB)-*g*-EC as a potential candidate for potential applications.

3.4.0. PART – 2 (Development and characterisation of enzymatically grafted P(3HB)-EC and P(3HB)-BC-based bio-composites)

3.4.1. Fourier Transform Infrared spectroscopy (FT-IR)

FT-IR spectroscopy was used in the characterisation studies to confirm the structural changes of the grafted composites. The strong and broad infrared absorption found at 3,450 cm^{-1} for P(3HB) was shifted to 3,358 cm^{-1} for P(3HB)-*g*-EC (Figure 3.6). This implied the presence of –OH groups in the EC and hydrogen bonding between those –OH groups. The peak assigned to the O–H stretching vibration at 3,358 cm^{-1} in the P(3HB)-*g*-EC composite was due to the contributions from the –OH group of EC that was not present in the FT-IR spectrum of the composite prepared in the absence of laccase. The higher intensity of the 3,358 cm^{-1} band in the graft composite showed an increase of hydrogen-bonded groups (Zhang *et al*., 1997). This also implied that the terminal hydroxyl groups of P(3HB) were utilised in reaction with hydroxyl groups of EC through laccase reaction. Furthermore, a shift in the characteristic band 2,980 to 2,867 cm^{-1} for P(3HB) occurred in the P(3HB)-*g*-EC as shown in Figure 3.6, belonging to the CH$_3$ stretching vibration from alkyl groups of P(3HB). Figure 3.7 depicts the FT-IR spectra of P(3HB), BC, P(3HB)-*g*-BC and P(3HB)-*g*-BC* film. For pure PHB (Figure 3.7), the peak at 3,358 cm^{-1} refers to hydroxyl end groups while, peaks at 2,926cm^{-1}, and 2,867 cm^{-1} are due to the stretching vibration of aliphatic C–H bond (Mansur *et al*., 2008). A sharp band observed at 1,721 cm^{-1} is assigned to C=O stretching vibration.
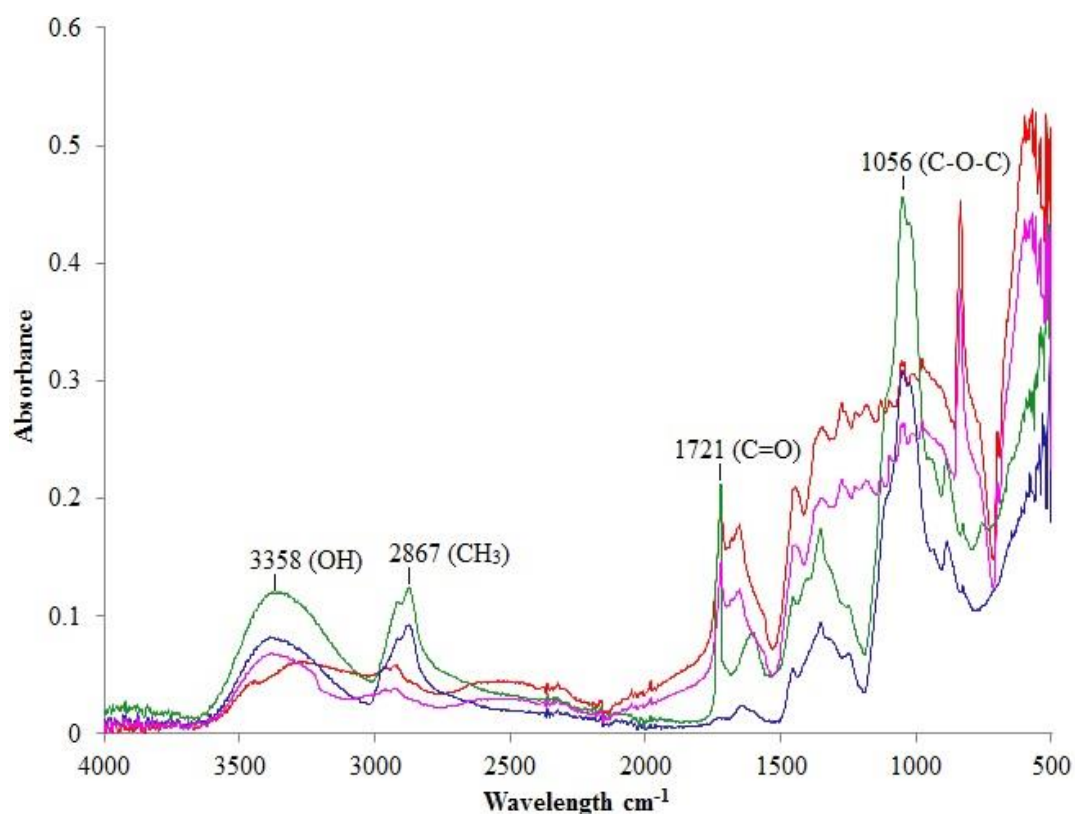
Figure 3.6 FT-IR spectra of the pure P(3HB) (Red line); EC (Blue line); P(3HB)-*g*-EC (prepared using laccase) (Green line) and P(3HB)-*g*-EC* (prepared in the absence of laccase) (Pink line).
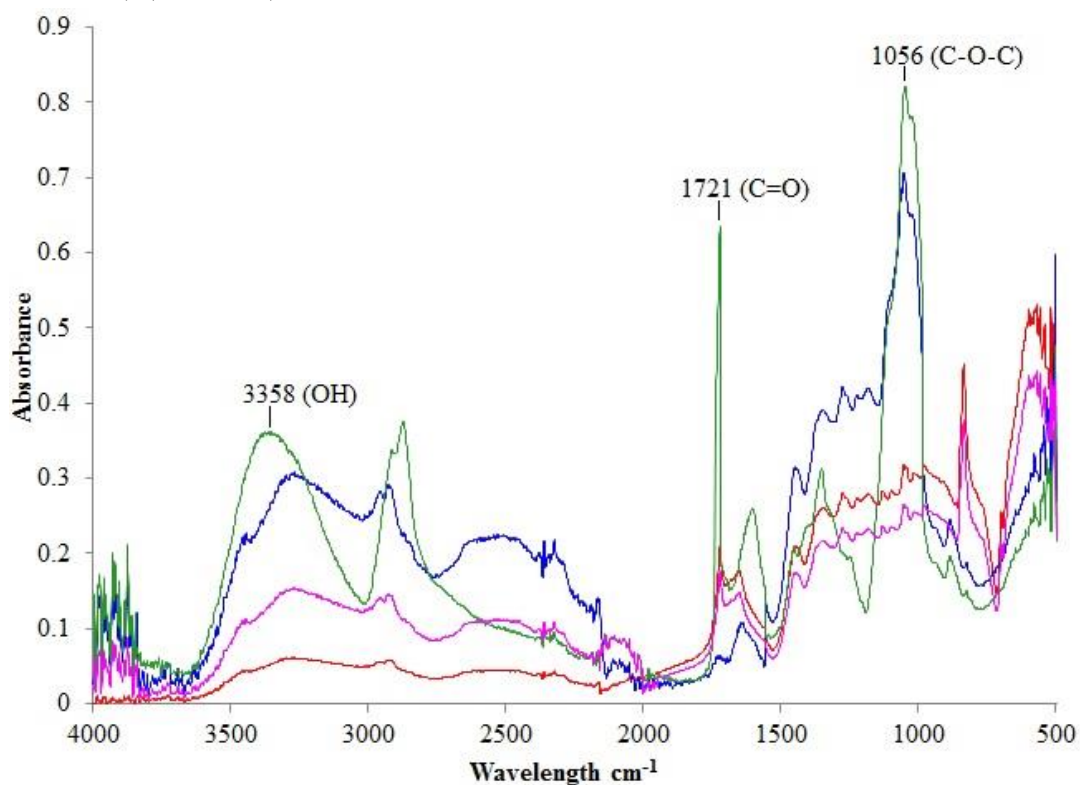
Figure 3.7 FT-IR spectra of the pure P(3HB) (Red line); BC (Blue line); P(3HB)-*g*-BC (prepared using laccase) (Green line) and P(3HB)-*g*-BC* (prepared in the absence of laccase) (Pink line).

In the case of pure BC (Figure 3.7), a band at 2,867 cm^{-1} is attributed to the aliphatic C–H stretching vibrational mode of bacterial cellulose. A sharp and steep band observed at 1056 cm^{-1} is due to the presence of C–O–C stretching vibrations. The bands with characteristic peaks at 1,260, 1,353, 1,456, 1,721, and 2,926 cm^{-1} in the P(3HB)-g-BC composite were particularly attributed to the bending modes of C-H, stretching vibration of C=O in ester, and symmetric and asymmetric stretching vibration of CH$_3$ of P(3HB), respectively (Liu *et al*., 2009). Previously, FT-IR spectroscopy has been used to prove the existence of hydrogen bonding interactions in the different composites based on cellulose/PHBV blends at different compositions (Hameed *et al*., 2011). A broad peak between 3,376 and 3,500 cm^{-1} indicates cellulose O–H vibration (Freire *et al*., 2006), while the peak at 1,050-1,100 cm^{-1} region is due to the stretching of the C–O–C linkage of ethyl cellulose molecules (Hinterstoisser and Akerholm, 2003; Mohammed-Ziegler *et al*., 2008). The band at 934 cm^{-1} is due to the C–COO^{-} stretching vibration of the molecules containing de-protonated carboxylic groups (Kudelski, 2002). Figure 3.8 illustrates a tentative schematic mechanism of graft formation between P(3HB) and laccase assisted functionalised cellulose through hydrogen bonding-type interaction.
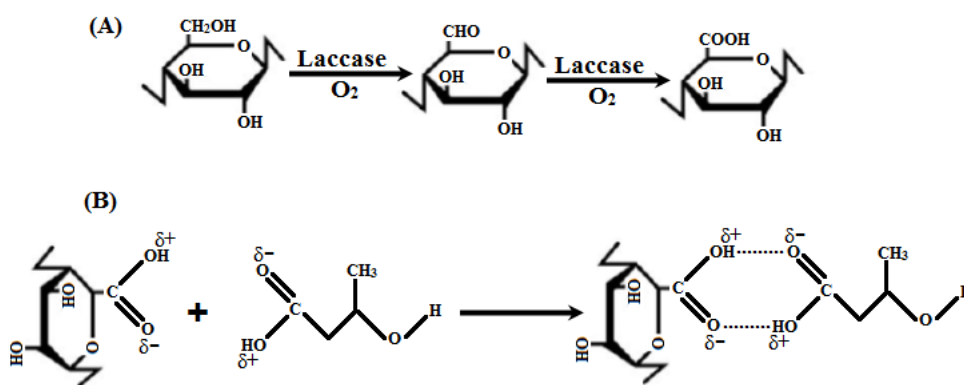
Figure 3.8 A tentative schematic representation: **(A)** laccase assisted cellulose surface functionalisation to form C6-carboxylate group via C6-aldehyde group; **(B)** proposed mechanism of graft formation through hydrogen bonding between P(3HB) and functionalise cellulose (Iqbal *et al*., 2014b).

3.4.2. Scanning electron microscopy (SEM)

Evaluation by SEM was investigated to observe any modification of the polymer surface by laccase-assisted grafting polymerisation reaction. SEM micrographs (Figure 3.9) confirm the morphological topographies of the surfaces of P(3HB), EC, P(3HB)-*g*-EC (prepared using laccase) and P(3HB)-*g*-EC* (prepared in the absence of laccase) observed using SEM, which showed the well dispersed P(3HB) in the backbone polymer of ethyl cellulose (part C of the Figure 3.9). In comparison to the P(3HB)-*g*-EC (part C of the Figure 5.4) P(3HB)-*g*-EC* (part D of the Figure 3.9) showed clear aggregates of P(3HB) on the top surface of the cellulose membrane. This, again, reveals the action of laccase in part C. In parallel to the above discussed graft composite, a set of selected SEM micrographs of the surfaces of P(3HB), BC and P(3HB)-*g*-BC composite polymers were also studied and the representative SEM micrographs are shown in Figure 3.10. This figure presents the morphological characteristics of the individual P(3HB), BC and the grafted P(3HB)-*g*-BC composite. SEM analysis revealed the clear nano-fibrils of BC. This is shown on the surface topographic scan (Figure 3.10), while the SEM micrograph of P(3HB)-g-BC shows that the P(3HB) completely filled the pores between the individual BC and the vacant spaces between the BC sheets. The SEM micrograph for P(3HB)-g-BC also provides evidence of the strong interaction between the BC nano-fibrils and the P(3HB) matrix, as shown by the good dispersion of P(3HB), without noticeable aggregates. The SEM photomicrograph of P(3HB)-*g*-BC* in Figure 3.10 (D) shows that the P(3HB) in this composite tends to agglomerate into bundles and is unevenly distributed in the matrix. In an earlier study, Luo *et al*., 2009 observed a similar kind of rougher surface topography during the synthesis of Poly(3-hydroxybutyrate-co-3-hydroxyhexanoate) (PHBHHx) and poly(3-hydroxybutyrate-co-4-hydroxybutyrate) (P3HB4HB) based

films. It has also been reported in literature that the graft copolymerisation modifies the surface morphology; physical, chemical, and microstructural characteristics of the grafted materials (Joshi and Sinha, 2006), which in turn affects their biocompatibility and biodegradability.
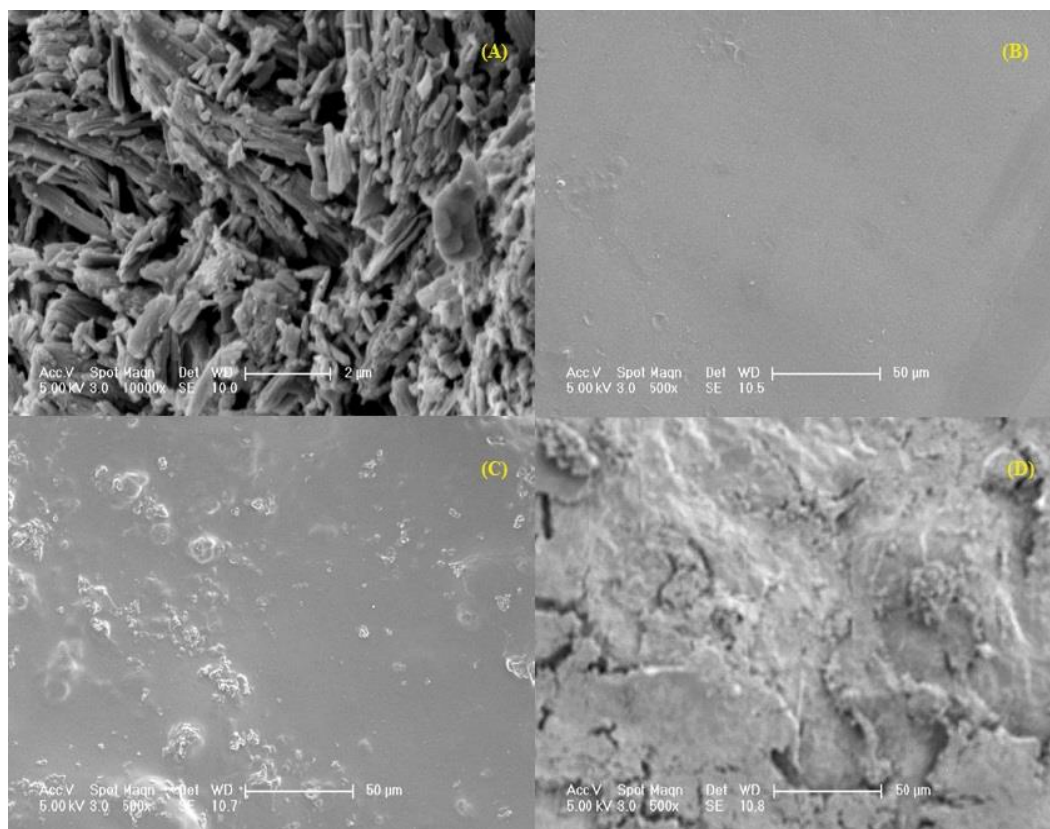

Figure 3.9 Scanning Electron Microscopy of untreated P(3HB) (A), EC (B), P(3HB)-*g*-EC (prepared using laccase) (C) and P(3HB)-*g*-EC* (prepared in the absence of laccase) (D).
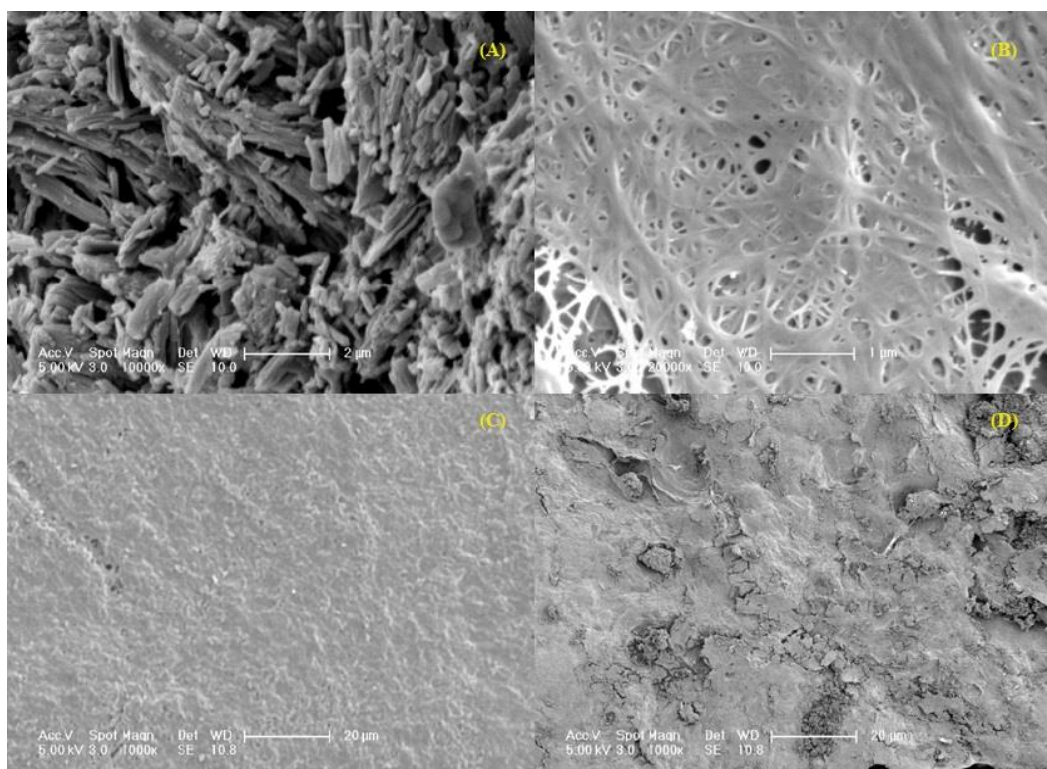
Figure 3.10 Scanning Electron Microscopy of pure P(3HB) (A), BC (B), P(3HB)-*g*-BC (prepared using laccase) (C) and P(3HB)-*g*-BC* (prepared in the absence of laccase) (D).

3.4.3. Differential scanning calorimetry (DSC)

The thermal behaviour of the individual polymers and their enzymatically grafted composite *i.e.,* P(3HB), EC, BC, P(3HB)-*g*-EC, P(3HB)-*g*-EC*, P(3HB)-*g*-BC and P(3HB)-*g*-BC* were compared to investigate their thermal properties. Thermal properties such as glass transition temperature (T_g), melting temperature (T_m), and crystallisation temperature (T_c) were measured using Differential Scanning Calorimetry (DSC). The results obtained after DSC analysis are summarised in Tables 3.4 and 3.5. The results show a dramatic change in the glass transition temperature (T_g) of P(3HB)-*g*-EC composite as compared to the P(3HB) alone. This occurs when the mobility of the amorphous region is restricted due to the presence of fillers of

93

crystalline nature. Like T_g there was also an increase in the melting temperature (T_m) of the P(3HB)-g-EC composite. In the DSC first heating scan, all of the tested samples reveal a glass transition temperature T_g from 9°C to 39°C and endo-thermal melting peak T_m of 174°C to 198°C. This is comparable with the T_m range of different thermoplastic PHAs polymers which are usually stored at room temperature (Barham *et al.*, 1984; Baltieri *et al.*, 2003; Dai *et al.*, 2008; Serafim *et al.*, 2008).

Table 3.4 DSC-thermal properties of the individual polymers P(3HB), EC and their grafted composites i.e., (P(3HB)-*g*-EC and P(3HB)-*g*-EC*.

Samples	T_g (°C)	T_{onset} (°C)	T_m (°C)	T_{offset} (°C)	T_c (°C)	ΔH_m (J/g)
P(3HB)	9±0.05	152±0.41	174±0.45	181±0.58	135±0.18	64±0.02
EC	ND	165±0.89	188±0.09	202±0.62	48±0.05	86±0.69
P(3HB)-g-EC	39±0.16	155±0.55	185±0.41	198±0.31	78±0.06	59±0.03
P(3HB)-g-EC*	8±0.06	150±0.69	169±1.10	192±0.28	110±0.74	73±0.65

Where, P(3HB) = Poly(3-hydroxybutyrate); EC = Ethyl cellulose; P(3HB)-g-EC = Poly(3-hydroxybutyrate) grafted ethyl cellulose (prepared using laccase); and P(3HB)-g-EC* = Poly(3-hydroxybutyrate) grafted ethyl cellulose (prepared in the absence of laccase).

From the T_g and T_m data of the individual polymers *i.e.,* P(3HB), EC and BC and their grafted composite samples respectively, it was noted that in the presence of laccase, the T_g and T_m drop to lower values in case of individual polymers and to higher values in the grafted composites *i.e.,* P(3HB)-*g*-EC and P(3HB)-*g*-BC. One possible

explanation of this initial reduction in the T_g and T_m may be due to the laccase cleavage of the individual segments into short chains which is not sufficient to reach the critical molecular weight to give the typical values related to T_g and T_m as shown above in Table 3.4. While in the case of P(3HB)-*g*-EC and P(3HB)-*g*-BC the re-joining of short segments during co-polymerisation reaction would cause a dramatic increase in T_g and T_m due to the better impregnation of thermally stable cellulosic component as a reinforcement into the P(3HB) matrix. The increase in the T_g might be due to the new cross-linking of P(3HB) within the EC and/or BC backbone which would inhibit the mobility of the P(3HB) segments. In comparison to the pure P(3HB), the addition of cellulosic contents in the P(3HB)-*g*-EC, the crystallisation temperature (T_c) gradually reduces from 135 °C to 78 °C and 88 °C for the P(3HB)-*g*-EC and P(3HB)-*g*-BC, respectively (Table 3.5).

Table 3.5 DSC-thermal properties of the individual polymers *i.e.,* P(3HB) and BC, and their grafted composites *i.e.,* P(3HB)-*g*-BC and P(3HB)-*g*-BC*.

Sample ID	T_g (°C)	T_{onset} (°C)	T_m (°C)	T_{offset} (°C)	T_c (°C)	ΔH_m (J/g)
P(3HB)	9±0.05	152±0.41	174±0.45	181±0.58	135±0.18	64±0.02
BC	22±0.20	172±0.33	198±0.38	207±0.45	43±0.05	92±0.03
P(3HB)-g-BC	30±0.09	164±0.42	190±0.29	202±0.34	88±0.05	73±0.04
P(3HB)-g-BC*	23±0.12	155±0.39	177±0.85	188±0.42	118±0.95	98±0.26

Where, P(3HB) = Poly(3-hydroxybutyrate); BC = Bacterial cellulose; P(3HB)-g-BC = Poly(3-hydroxybutyrate) grafted bacterial cellulose (prepared using laccase); and P(3HB)-g-BC* = Poly(3-hydroxybutyrate) grafted bacterial cellulose (prepared in the absence of laccase).

3.4.4. Dynamic Mechanical Analyser (DMA)

To investigate the mechanical characteristics of the individual polymers and grafted composites, the stress-strain analyses were performed according to ASTM D-882-97 standard test method. The stress-strain behaviour in uniaxial tension of the individual polymers and the grafted composites was recorded to measure the mechanical properties and the associated data along with the standard deviations (Tables 3.6 and 3.7). The P(3HB)-g-EC composite showed simultaneous improvement in the tensile strength and the Young's modulus as compared to its individual counterpart P(3HB). This is because the high strength of EC allowed the mechanical properties of P(3HB)-g-EC composite to improve or enhance as compared to the pristine P(3HB). In comparison to the pure P(3HB), an increase in the tensile strength and Young's modulus (up to values of 68.3 MPa and 0.99 GPa,) were recorded respectively in the case of P(3HB)-g-EC. This is possibly due to the loading of EC as a reinforcement material within the P(3HB) matrix. The elongation at the break point calculated from the slope of the curve was 8.2% for the native EC, 13.2% for P(3HB)-g-EC and 7.0% for the P(3HB)-g-EC* composite. This behaviour can be due to the combination of P(3HB) with cellulose fibrils with good interfacial adhesion, and the formation of strong interactions between P(3HB) and EC.

However, in the case of BC and P(3HB)-g-BC, in the beginning at low strain values, the stress-strain behaviour was linear elastic. Based on the data reported in literature the strain-hardening region is termed as plastic region (Henriksson *et al*., 2008). A simultaneous improvement was recorded in the mechanical properties of the laccase assisted graft composite prepared from P(3HB) with BC as compared to its individual counterpart, of P(3HB). This is because the inherently high strength of BC allowed the mechanical properties of P(3HB)-g-BC composite to improve. On the other hand,

mechanical properties of the graft composite prepared from P(3HB) with BC showed a notable increase in the tensile strength (64.5MPa), elongations at break (15.7%) and Young's modulus (0.98 GPa) as compared to the P(3HB) alone which was too brittle to measure any of the above mentioned characteristics. Unlike native BC which is flexible, P(3HB) is crystalline and brittle in its nature, therefore, it has much lower mechanical values. In the present study, as concluded from the T_g and XRD measurements, the interactions between the P(3HB) and BC, alter the thermal and physical properties of the P(3HB) and BC, respectively.

Table 3.6 Mechanical properties of the individual polymers *i.e.,* P(3HB), and EC and their grafted composites *i.e.,* P(3HB)-*g*-EC and P(3HB)-*g*-EC*.

Samples	Tensile strength (MPa)	Young's modulus (GPa)	Elongation at break (%)
P(3HB)	ND	ND	ND
EC	122 ± 9.85	3.38 ± 0.85	8.2 ± 1.25
P(3HB)-*g*-EC	68.3± 2.25	0.99± 1.65	13.2± 1.05
P(3HB)-*g*-EC*	36.2± 3.2	1.55± 1.11	7.0± 0.45

Where, P(3HB) = Poly(3-hydroxybutyrate); EC = Ethyl cellulose; P(3HB)-g-EC = Poly(3-hydroxybutyrate) grafted ethyl cellulose (prepared using laccase); and P(3HB)-g-EC = Poly(3-hydroxybutyrate) grafted ethyl cellulose (prepared in the absence of laccase).*

ND: Not detected.

Table 3.7 DMA-mechanical properties of the individual polymers *i.e.,* P(3HB) and BC, and their grafted composites *i.e.,* P(3HB)-*g*-BC and P(3HB)-*g*-BC*.

Sample ID	Tensile strength (MPa)	Young's modulus (GPa)	Elongation at break (%)
P(3HB)	ND	ND	ND
BC	139 ± 5.55	3.50 ± 0.39	9.22 ± 0.99
P(3HB)-*g*-BC	64.5± 2.33	0.98± 2.53	15.7± 2.65
P(3HB)-*g*-BC*	42.3± 1.31	2.41± 1.39	7.65± 0.33

Where, P(3HB) = Poly(3-hydroxybutyrate); BC = Bacterial cellulose; P(3HB)-g-BC = Poly(3-hydroxybutyrate) grafted bacterial cellulose (prepared using laccase); and P(3HB)-g-BC* = Poly(3-hydroxybutyrate) grafted bacterial cellulose (prepared in the absence of laccase).

ND: Not detected.

3.4.5. X-ray diffraction (XRD)

Figure 3.11 illustrates XRD patterns obtained for P(3HB), EC, P(3HB)-*g*-EC and P(3HB)-*g*-EC* respectively. XRD pattern for P(3HB) showed some distinct peaks at 2-Theta values of 28º, 32º, 34º, 39º, 46º, 57º, 64º, 78º, and 84º that represent the crystalline nature of the P(3HB). On the other hand, EC had broader diffraction with a broad peak at 20º in the XRD-patterns that represents the highly amorphous nature of EC (Zhu *et al*., 2010). While part C of the figure 3.11, (P(3HB)-*g*-EC) shows that,

the crystallinity of the P(3HB) decreased during graft formation reaction with EC. The disappearance of some distinct peaks at 2-Theta values of 32°, 34°, 46°, 57°, 64°, 78° and 84° in the XRD pattern of P(3HB)-g-EC confirms this reduction in crystallinity. The distinct peaks mostly from the region of 13-29° belonged to an orthorhombic crystal system of P(3HB). Ethyl cellulose (EC) as an amorphous polymer can suppress and break the crystalline domains of crystalline polymers (Yuan *et al*., 2007; Yan *et al*., 2009; Zhu *et al*., 2010), thus the crystallisation of P(3HB) in P(3HB)-*g*-EC would be restricted, resulting in the imperfection of P(3HB). The reduction in the crystallinity is mainly because of the new cross-linking of P(3HB) within the EC backbone that changes the morphology and destroys the crystallites. Characteristic XRD diffractogram of the pure P(3HB), BC, P(3HB)-*g*-BC and P(3HB)-*g*-BC* composite is given in Figure 3.12. The changes in the crystallinity of the pure P(3HB), caused by incorporation of the BC, were investigated by X-ray diffraction. For the BC, a main scattering intensity peak can be identified at 2-Theta value of 21.2° as shown in the figure 5.7, which is assigned to the reflexion planes of cellulose I (Tokoh *et al*., 1998). In the X-ray diffraction pattern of the P(3HB)-*g*-BC composite (Figure 3.12), a change in the characteristic peaks of both P(3HB) and BC was observed, which means the reduction in the crystalline and amorphous nature of the P(3HB) and BC, respectively. Compared with pure P(3HB), P(3HB)-*g*-BC has some changes at the 2-Theta values and the peaks of the P(3HB) in the composite P(3HB)-*g*-BC were sharper and clearer than those in the pure P(3HB). The results obtained through XRD analyses evidently support that the extent of crystallisation of P(3HB) can be greatly reduced by homogeneous incorporation of amorphous cellulose into the polymeric matrix. Furthermore, there might be an interaction between the enzymatically treated cellulose and P(3HB), the motion of the P(3HB) side chains was restricted and subsequently

caused the reduction of crystallinity in P(3HB)-*g*-EC/P(3HB)-*g*-BC. A similar phenomenon was reported earlier by Lin *et al.,* 2011, during the preparation of acetylated cellulose nanocrystals/poly(lactic acid) nanocomposites.
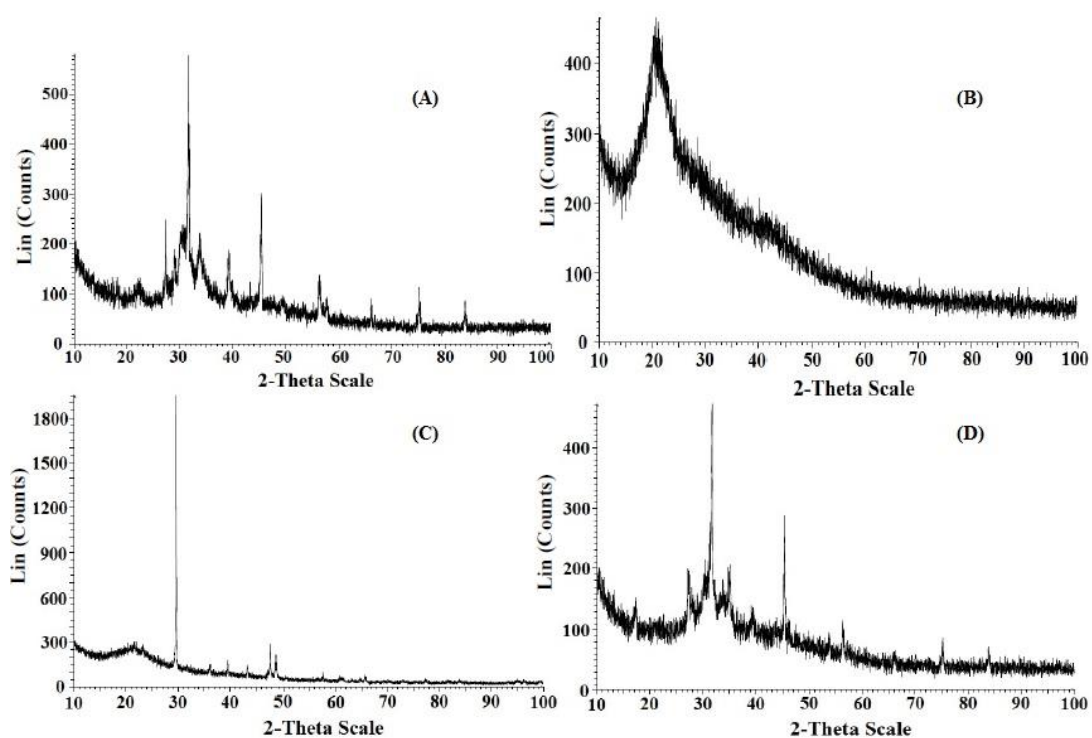
Figure 3.11 XRD diffractogram for the pure P(3HB) (A), EC (B), and grafted composites P(3HB)-*g*-EC (prepared using laccase) (C) and P(3HB)-*g*-EC* (prepared in the absence of laccase) (D).
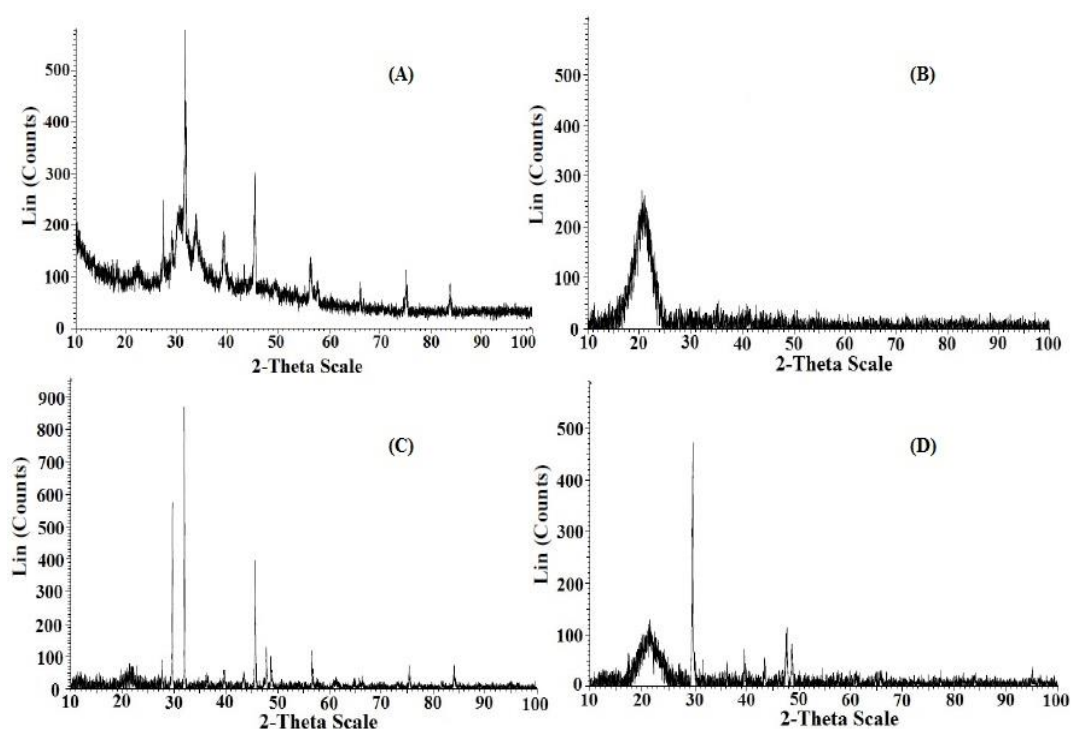
Figure 3.12 XRD diffractogram for the pure P(3HB) (A), BC (B), and grafted composites P(3HB)-*g*-BC (prepared using laccase) (C) and P(3HB)-*g*-BC* (prepared in the absence of laccase) (D).

3.4.6. Water contact angle (WCA)

The drop contour analysis was used for determining the surface tension and the water contact angle characteristics of the newly synthesised composites. The characteristic contact angle and surface tension of the P(3HB), EC, and the resulting composite *i.e.,* P(3HB)-*g*-EC and P(3HB)-*g*-EC* are shown in Figures 3.13, respectively. For pure EC, the water contact angle value was very small (19º). This means EC has very high hydrophilicity. However, for the pure P(3HB), and P(3HB)-*g*-EC composite, the contact angle values were 68º and 42º respectively (Figure 3.13). On the other hand, the surface tension value of the pure P(3HB) was about 20.5 mN/m which increased up

to 62.3 mN/m with the reinforcement of hydrophilic EC into the P(3HB) matrix in the case of P(3HB)-*g*-EC grafted composite. Hence, the increase in the amount of EC incorporation indicates that the hydrophilic property of P(3HB)-*g*-EC composite is much better than the pure P(3HB). Figure 3.14 illustrates the contact angles and surface tension characteristics of the individual polymers [(P(3HB) and BC)] and their resulting graft composites [P(3HB)-*g*-BC and P(3HB)-*g*-BC*], respectively determined by deionized water via the static contact angle measurement. It was found that P(3HB) has larger water contact angle *i.e.,* 68° whereas comparative to the P(3HB), BC has lower contact angle value of 15°, which means BC has very high hydrophilicity. The P(3HB)-*g*-BC with more hydroxyl groups of side chains exhibited more hydrophilic features than its individual P(3HB) counterpart which was hydrophobic in nature. On the other hand, the surface tension properties of the pure P(3HB) was about 20.5 mN/m which increased up to 59.2 mN/m with the reinforcement of hydrophilic BC into the P(3HB) matrix in the case of P(3HB)-*g*-BC grafted composite. It has also been reported in literature that the grafted polymers with more hydroxyl groups of short chains exhibited more hydrophilic than other copolymers (Yu *et al.,* 2012).
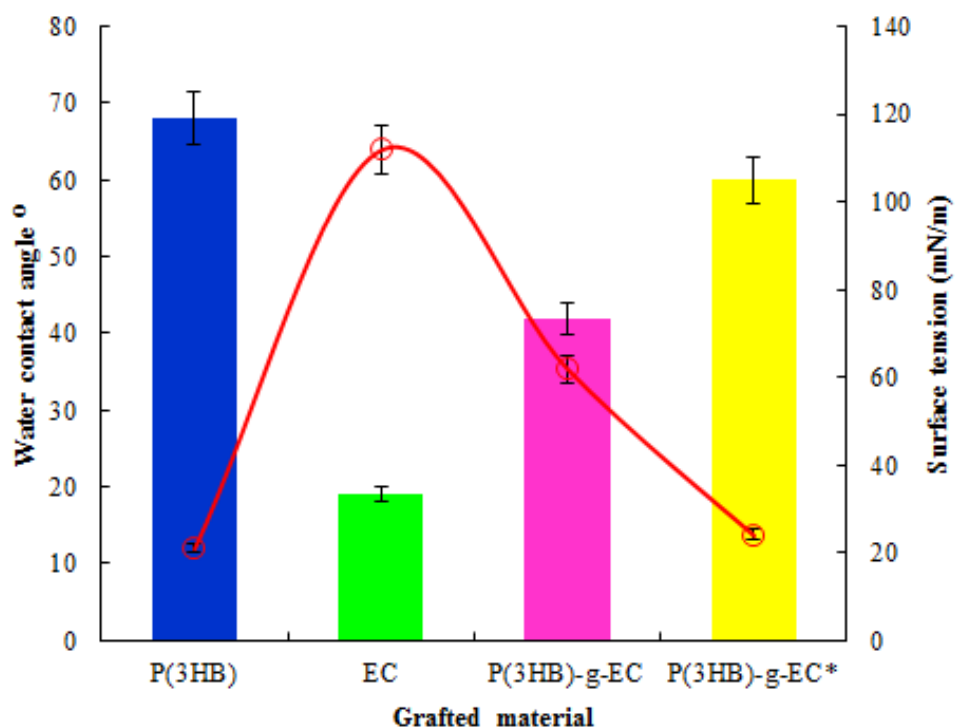
Figure 3.13 Static water contact angle (bars in colour) and surface tension (red line) measurements of P(3HB), EC, and grafted bio-composites *i.e.,* P(3HB)-*g*-EC (prepared using laccase) and P(3HB)-*g*-EC* (prepared in the absence of laccase).
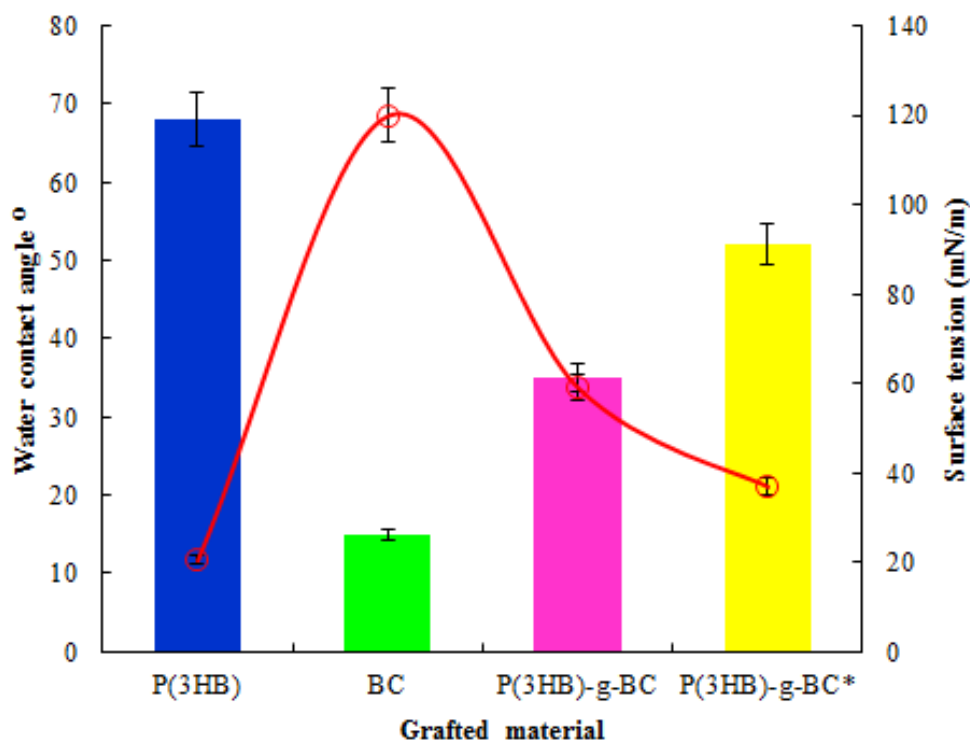
Figure 3.14 Static water contact angle (bars in colour) and surface tension (red line) measurements of P(3HB), BC and their grafted bio-composites *i.e.,* P(3HB)-*g*-BC (prepared using laccase) and P(3HB)-*g*-BC* (prepared in the absence of laccase).

103

3.5. Concluding remarks

The newly enzyme-assisted grafted composites exhibit multifunctional characteristics such as good tensile strength and mechanical strength along with low crystallinity. This is due to their unique graft structure. The main benefits of laccase assisted grafting are the absence of harmful solvents and chemicals, the mild eco-friendly environment, and energy saving reaction conditions. The above discussed newly synthesised composites are expected to find potential applications in various industrial and bio-medical and/or pharmaceutical sectors, where bio-composites with novel characteristics are very much in demand. Enzymatic grafting is quite a new and attractive green chemistry technology. Therefore, the introduction of composite materials prepared from bio-polymers of microbial origin (P(3HB), bacterial cellulose) and other renewable resources in combination with enzymatic bio-catalytic method, is very timely. In this context, laccase is likely to remain the subject of investigations in production of green composites.

Chapter 4

In site development and characterisation of

keratin-EC-based novel bio-composites

4.0. Summary

This chapter focuses on the evaluation of raw keratin as a potential material to develop bio-composites with novel characteristics. Among the natural materials, keratin-associated proteins are interesting candidates for preparation of keratin-based composites with potential for utilisation in a variety of bio- and non-bio-sectors. In this context, consumption of feathers for the production of value-added products is an original concept providing extensive opportunities for experimentation and interdisciplinary scientific research. Considering this, a mild and eco-friendly fabrication of in-house extracted feather keratin based novel composites is reported in this Chapter. The composites consist of ethyl cellulose as a backbone, and laccase from *Trametes versicolor* as a grafting tool. A range of composites between keratin and EC with different keratin: EC ratios were prepared. Subsequently, the resulting composites were removed from the casting surfaces and characterised using various available techniques. Comparing untreated keratin to the composites, the FT-IR peak at 1,630 cm^{-1} shifted to a lower wavenumber of 1,610 cm^{-1} in the case of keratin-EC. This indicates the involvement of β-sheet structures of the keratin during the graft formation process. SEM analysis revealed that the uniform dispersion of the keratin increases the area of keratin-EC contact which further contributes to the efficient functionality of the resulting composites. In comparison to the untreated keratin and EC alone, a clear shift in the XRD peaks was also observed at the specific region of 2-Theta values of keratin-*g*-EC. The thermo- mechanical properties of the composites reached their highest levels in comparison to the keratin which was too fragile to be measured for its mechanical properties. Considerable improvement in the water contact angle and surface tension properties was also recorded.

4.1. Introduction

Green chemistry needs to overcome many challenges for successful implementation of innovative technologies to accomplish pollution prevention, reduction and/or elimination of harmful waste materials during the entire production process. In this regard, ever increasing environmental awareness and the demand for sustainable technology have gained substantial consideration by academia and industry to develop eco-friendly processing designs (Anastas *et al*., 2003; Iqbal *et al*., 2014a). To address the concerns of global dependence on petroleum-based polymers, attention has been directed to the engineering of bio-based composite materials for targeted applications in different industries (Anastas *et al*., 2003; Iqbal *et al*., 2014a, b; Roy *et al*., 2014). Research on several proteins, including collagen, fibroin, keratin, and others is in progress for the development of naturally-derived materials. Among the natural materials, keratin-associated proteins are interesting candidates for the preparation of keratin-based composites with potential for utilisation in a range of bio- and non-bio-sectors. A large variety of fibrous keratins are available in the form of feather, hair, nail, and horn as bio-waste. These keratin-rich sources are difficult to degrade as the polypeptide in their structure is tightly packed in α-helix (α-keratin) or β-sheet (β-keratin) into super coiled chains which are strongly stabilised by several hydrogen bonds and hydrophobic interactions, in addition to the di-sulphide bonds (Kreplak *et al*., 2004; Brandelli, 2008).

Keratin-based chicken feather from butchery account for more than 5 million tons per year worldwide in the form of waste material (Aluigi *et al*., 2011; Ghosh and Collie, 2014). Apart from its minor usage in low grade products such as glue, corrugated paper, cardboard, animal feed and fertilisers, the landfill disposal of poultry feather poses a significant ecological and environmental threat. On the other hand, from

107

economic and environmental point of view it is also desirable to establish an effective process for the application of such natural sources (Aluigi *et al*., 2008).

Keratin extracted from feather is a small protein, uniform in size, with a molecular weight between 11- 65 kDa (Aluigi *et al*., 2008; Ullah *et al*., 2011). The presence of multi-functional groups in keratin, such as di-sulphide, amino, thiol, phenolic and carboxylic, make it reactive under appropriate reaction conditions. Under reducing environment, the amino and other above mentioned groups in keratin make its surface positive, and thus solubilisation takes place (Khosa and Ullah, 2013). Keratin is among versatile biopolymers that can be modified and developed into various products of interests, owing to its unique properties and non-toxic nature. After modification, keratin composites may find potential applications in bio-medical, pharmaceutical, tissue engineering, and cosmetic industries (Khosa and Ullah, 2013).

In recent years, much effort has been made to fabricate keratin with other suitable materials. So far most of the reported work deals with blending or grafting of keratin with non-biodegradable synthetic polymers, such as polyethylene (PE), polypropylene (PP), polystyrene, and poly (vinyl chloride) (Djidjelli *et al*., 2002; Sombatsompop *et al*., 2003; Torres and Cubillas, 2005; Li and Mai, 2006; Ramakrishna *et al*., 2008; Singha *et al*., 2010). To date many researchers have proposed to valorise keratinous sources, either through surface grafting or by blending, to prepare innovative graft composites (Aluigi *et al*., 2008; Aluigi *et al*., 2011; Ullah *et al*., 2011; Khosa and Ullah, 2013). Grafting is preferred over other physiochemical techniques in order to obtain the requisite properties which individual materials fail to demonstrate on their own. Effective modifications should include changes in chemical group functionality, surface charge, biocompatibility and biodegradability (Khosa and Ullah, 2013; Iqbal *et al*., 2014a).

The use of enzyme in grafting of biopolymers is a recent technique where the enzyme, as an active component, offers mild and safe reaction conditions to the current practices in the grafting technology (Aljawish *et al.*, 2012; Iqbal *et al.*, 2014b). Enzymes offer the potential for eliminating the hazardous chemical reagents used in other chemical based grafting/blending processes. Moreover, there are several benefits for the use of enzymes in polymeric-based material synthesis and modification (Alves and Mano, 2008; Brandelli, 2008). Thus, a bank of information has become available on the characteristics and hydrolysis of keratin where recalcitrant keratinous wastes are converted into valuable products (Aluigi *et al.*, 2008, 2011; Khosa and Ullah, 2013). Consequently, keratin-rich wastes have been processed for use in cosmetics or in medicines to enhance drug delivery, and production of biodegradable films amongst other emerging biotechnological and biomedical applications (Brandelli, 2008; Brandelli *et al.*, 2010).

This study focuses on the evaluation of raw keratin as a potential material to develop composites with novel characteristics. To the best of our knowledge, there are no reports in recent literature on laccase-assisted grafting of keratin material onto EC backbone without addition of any plasticiser and/or compatibiliser. In this work we report that newly grafted composites of keratin and EC, with their unique structures under enzymatic environment, exhibit novel characteristics such as good thermal stability, tensile strength, and hydrophobic/hydrophilic balance.

4.2. Results and Discussion

4.2.1. Fourier transform infrared spectroscopy (FT-IR)

Figure 4.1 showed typical FT-IR spectra of the untreated keratin and keratin-EC based composites. The FT-IR spectra shows a peak at 1,630 cm^{-1} and 1,610 cm^{-1} for amide

I, 1,530 cm^{-1} with a shoulder at about 1,520 cm^{-1} for amide II, and 1,235 cm^{-1} for amide III, respectively. In particular, the FT-IR spectra (Figure 4.1) show predominant absorption bands at 1,630 cm^{-1} and 1,610 cm^{-1} in the case of untreated keratin and keratin-EC based composites. This typically indicates the involvement of β-sheet structures from the keratin. Based on the literature data, the peak at 1,650 cm^{-1} indicate α-helix structure and the range of 1,631-1,515 cm^{-1} is related to β-sheet structure (Aluigi *et al*., 2008; Zhang and Liu, 2013). Figure 4.1 illustrates an appearance of a new peak at 1,717 cm^{-1} in the grafted composites. It was observed that with the increase of cellulose content from 0 to 100% in the graft composites, the absorption peak of keratin at about 1,630 cm^{-1} shifted to a lower wave number of 1,610 cm^{-1}, and became much broader. This strongly suggests the formation of new link between keratin and cellulose molecules. From higher to lower keratin ratio in the graft composites, a decrease in the intensities of the keratin-associated absorption bands at 1,630 cm^{-1}, 1,530 cm^{-1}, and 1,235 cm^{-1} was recorded. An IR peak associated with C–O–C stretching, situated at 1,056 cm^{-1} region is due to the ethyl cellulose molecules (Mohammed-Ziegler *et al*., 2008). Furthermore, a high intensity peak at 3,358 cm^{-1} in the graft composite was observed which is linked to the hydrogen-bonded groups at that distinct band region (Aluigi *et al*., 2008). For untreated keratin, the peak at 3,240 cm^{-1} refers to hydroxyl end groups while the peak at 2,919 cm^{-1} is due to the stretching vibration of aliphatic C–H bond. The peaks present near to the 2,930 and 2,850 cm^{-1} represent characteristic infrared bands of aliphatic hydrocarbons of methylene asymmetric C–H stretching and symmetric C–H stretching, respectively. However, both signals for the methyl (CH$_3$) asymmetric and symmetric modes and the methylene (CH$_2$) asymmetric and symmetric modes originated from keratin and can be assigned to the aliphatic chain. In addition, the positions of these bands indicate the

conformations of the protein materials: 1650 cm^{-1} (α-helix) 1,630 cm^{-1} (β-sheet) for amide I, 1,544 cm^{-1} (α-helix), 1,530 cm^{-1} (random coil) and 1,520 cm^{-1} (β-sheet) for amide II, and 1,230 cm^{-1} (random coil) for amide III) (Jin *et al.*, 2011; Estévez-Martínez *et al.*, 2013). The amino acid chains of keratin present hanging groups such as: amino, hydroxyl, thiol and carboxyl that under a redox system can generate free radicals and thus they can easily react with functional groups of the cellulose (Rodriguez-Gonzalez *et al.*, 2013). There are several typical inter- and intramolecular interactions, such as hydrogen bond, dipole-actions, charge-charge, and hydrophobic interactions that are characteristics of natural proteins.
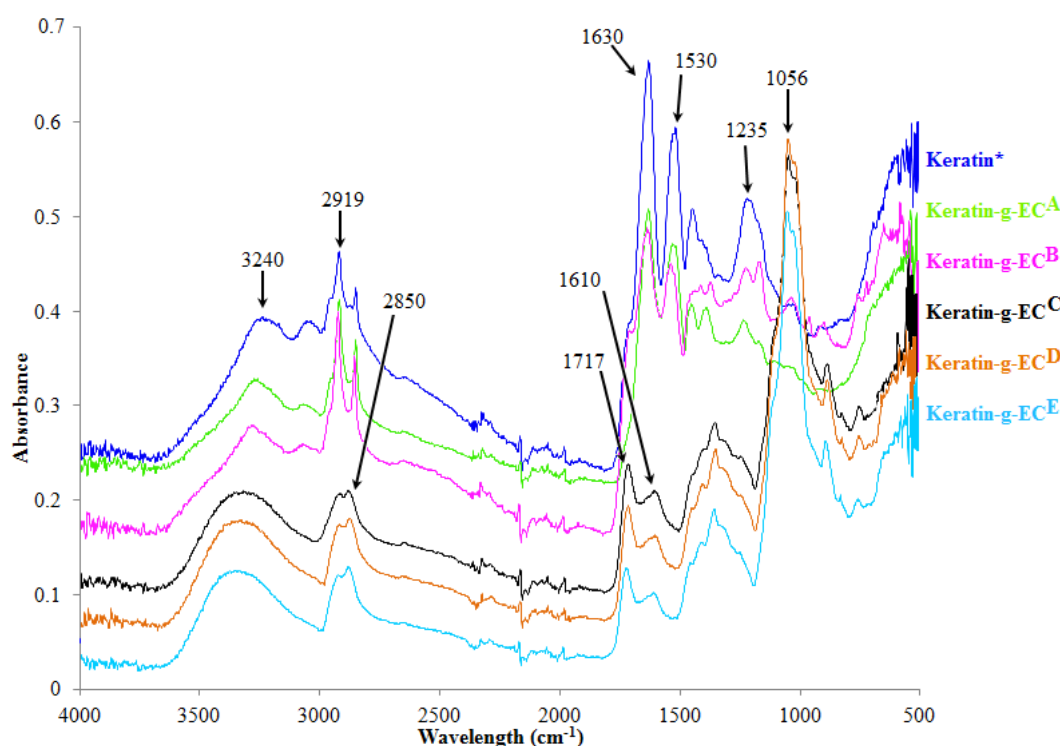
Figure 4.1 Typical FT-IR spectra of the untreated keratin and keratin-EC-based graft bio-composites *i.e.,* keratin-*g*-EC^A, keratin-*g*-EC^B, keratin-*g*-EC^C, keratin-*g*-EC^D, and keratin-*g*-EC^E prepared using laccase with different keratin to EC ratios.

Where, *: Untreated keratin film prepared without laccase treatment

^{A}: keratin: EC, 100:0; ^{B}: keratin: EC, 75:25; ^{C}: keratin: EC, 50:50; ^{D}: keratin: EC, 25:75 and ^{E}: keratin: EC, 0:100.

Based on the amino acid composition of feather keratin (Table 2.5), hydrogen bonding occurs among -NH$_2$ (in arginine and lysine), -NH- (in proline and histidine), -OH (in tyrosine, threonine, and serine), -COOH (in glutamic acid), and peptide bonds. Based on the availability of the functional groups there are different possibilities to propose a mechanism of graft formation between keratin and EC. However, figure 4.2 is only depicting one potential possibility as a tentative schematic mechanism of graft formation between keratin and EC under laccase-assisted process.
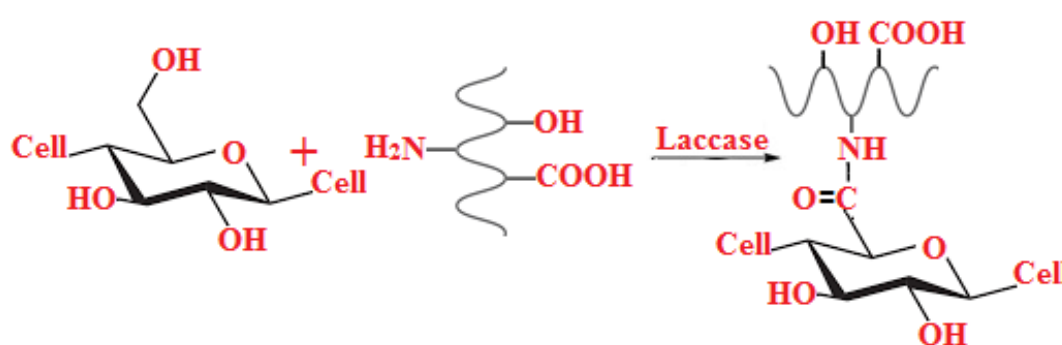
Figure 4.2 A schematic representation of proposed mechanism of graft formation between keratin and EC under laccase-assisted process (Iqbal *et al*., 2015).

4.2.2. Scanning electron microscopy (SEM)

The surface morphologies of the prepared composites were investigated by SEM, and the respective micrographs are shown in the Figure 4.3 (A-F). It can be observed that in case of the grafted composites, the keratin appears homogeneous within the cellulosic backbone during the graft formation process. Nevertheless, in case of the untreated keratin film the adhesion seems quite poor in comparison to the keratin film prepared in the presence of the laccase (Figure 4.3 A) and (Figure 4.2 B) respectively, where large number of pores were observed in the untreated keratin film. Similar results with porous appearance were observed by Selmin *et al*., (2012) during the membrane formation between regenerated keratin and ceramides (CERs).

Figure 4.3 SEM micrograph of the untreated keratin and keratin-EC-based bio-composites prepared using laccase with different keratin to EC ratios. The red arrows point to gaps and pores formed on the surface.

Where, (A): untreated keratin; (B): keratin: EC, 100:0; (C): keratin: EC, 75:25; (D): keratin: EC, 50:50; (E): keratin: EC, 25:75; (F): keratin: EC, 0:100 and (G): untreated EC

According to the Selmin and co-workers, the presence of these pores suggests poor adhesion between CERs and keratin (Selmin *et al*., 2012). It has also been reported in literature that the graft copolymerisation modifies the surface morphology; physical, chemical, and microstructural characteristics of grafted materials (Joshi and Sinha, 2006; Iqbal *et al*., 2014a, c). Better results were obtained in the grafted composites by increasing the cellulosic content ratio as testified by micrographs (Figure 4.3-D), and (Figure 4.3-E) where the keratin material appears more adherent to the cellulosic backbone with keratin to cellulose ratio, 50: 50 and 25: 75 wt. %. With the addition of cellulose, the distribution of pores was reduced on the surfaces of the grafted films and finally disappeared at 50: 50 and 25: 75 ratios as compared to untreated keratin film. On the other hand, the presence of aggregates is an evidence of the poor dispersion of the material of interests within the polymeric matrix and this behaviour is a consequence of the surface chemical modification that confers a non-polar character to the cellulose surfaces (Pasquini *et al*., 2006).

4.2.3. X-ray diffraction (XRD)

Figure 4.4 illustrates XRD patterns obtained for untreated keratin and keratin-*g*-EC (with keratin: EC, 100: 0; 75: 25; 50: 50; 25: 75 and 0: 100, respectively). The keratin powder showed a very broad peak at 20º (2θ), which is specifically corresponding to the β-sheet structure (Zembouai *et al*., 2013). Keratin gives characteristic X-ray diffraction pattern, either α-pattern or β-pattern. All keratins from mammals are of the α-type, but birds and reptiles can produce both α- and β- types. Feather keratins contain

β-sheets in some regions of their molecules, give an X-ray pattern of β-type and are capable of forming filaments (Zoccola *et al*., 2008).

XRD pattern showed crystallinity in the untreated keratin from the substantial 2θ peak values with sharp appearance at about 26°, 31°, 45° and 56°. In fact, the wider peaks appeared in the graft with keratin: EC 100: 0 in comparison to the peaks at 26°, 31° 45° and 56° obtained for untreated keratin which is possibly due to the laccase action. This notable shift in peaks specify clearly indicates the regeneration and breakdown of amorphous and some crystalline domains at that specific region of 2-Theta value. However, this phenomenon is more dominant in case of the graft with keratin: EC ratio 50: 50 as compare to the other grafts. The keratin-*g*-EC with keratin: EC ratio, 75: 25, 50: 50 and 25: 75 showed a notable peak shift between 20° to 25° (2-Theta). This is due to the occurrence of strong intermolecular and intramolecular bonding interactions which typically indicate the involvement of β-sheet structures from the keratin as evident by the FT-IR spectra. If there was no or weak interaction between keratin and cellulose molecules in the graft, each component would have its own individual region and the XRD patterns would be expressed as the simple mixture of keratin and cellulose. On the other hand, EC had broader diffraction with broad peak at 20° in the XRD-patterns that represents the highly amorphous nature of EC (Zhu *et al*., 2010).
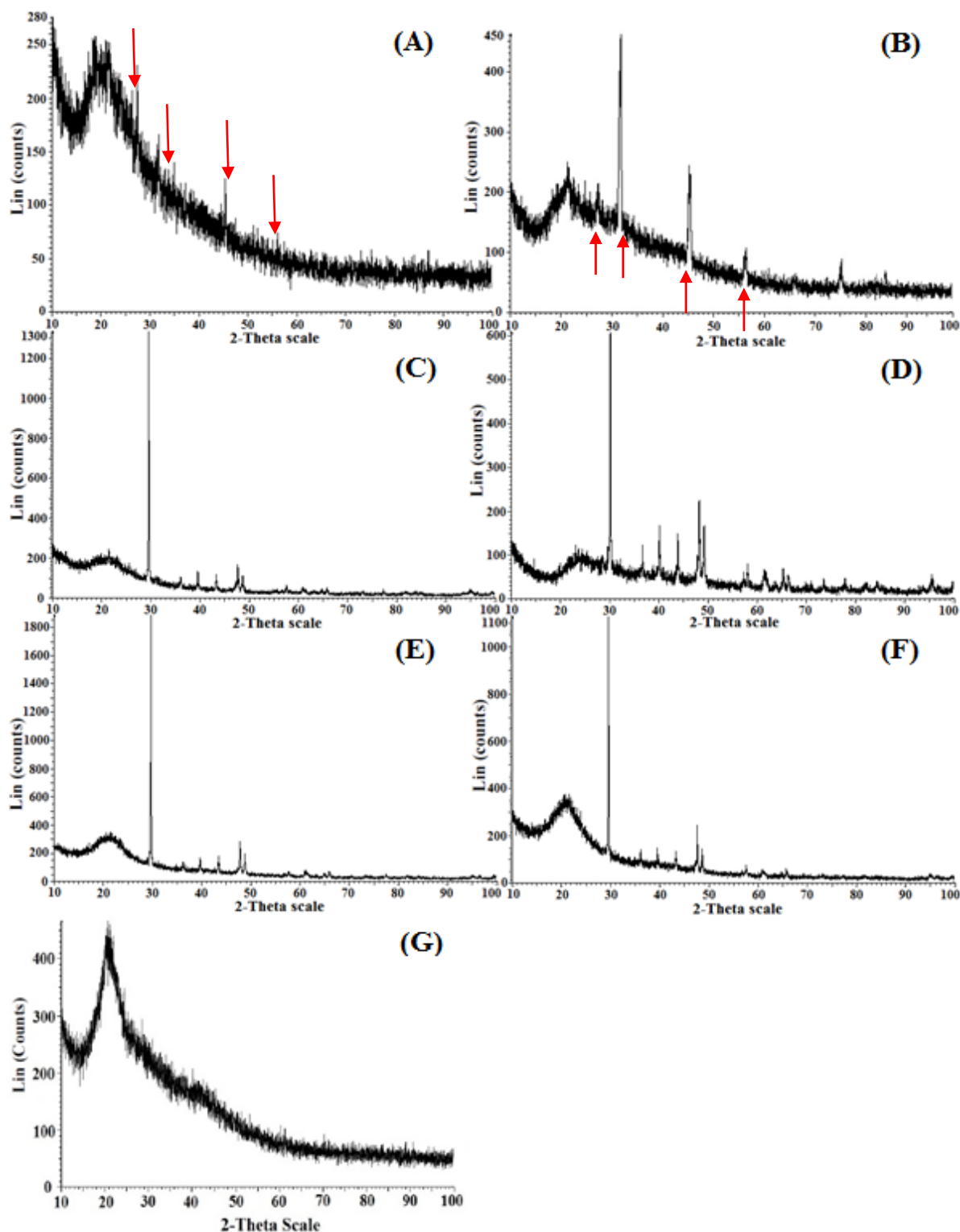
Figure 4.4 Typical X-ray diffractogram of untreated keratin, EC and keratin-EC-based bio-composites prepared using laccase with different keratin to EC ratios. The red arrows point to a change in the peaks.

Where, (A): Untreated keratin; (B): keratin: EC, 100:0; (C): keratin: EC, 75:25; (D): keratin: EC, 50:50; (E): keratin: EC, 25:75; (F): keratin: EC, 0:100 and (G): untreated EC.

4.2.4. Differential scanning calorimetry (DSC)

Thermal behaviour of the individual counterparts *i.e.,* keratin and EC along with their grafted composites prepared with different keratin: EC ratios *i.e.,* (100: 0; 75: 25; 50: 50; 25: 75; and 0: 100), respectively were compared to investigate their thermal properties. Thermal properties such as glass transition temperature (T_g), melting temperature (T_m), crystallisation temperature (T_c), and melting enthalpy (ΔH_m J/g) obtained from the DSC studies are summarised in Table 4.1. For each specimen an endothermal peak was observed during the temperature scan. The first endothermic peak for untreated keratin and keratin only (keratin: EC, 100: 0) composite was visible at low temperature of about 42 °C and 34 °C, respectively, which is in turn associated with the amount of hydrogen-bound molecules in the composite (sometimes referred to as the denaturation peak or glass transition temperature). The results showed a slight change in the glass transition temperature (T_g) from 42 °C to 34 °C and melting temperature (T_m) from 232 °C to 210 °C of the keratin only (keratin: EC, 100: 0) composite as compared to the untreated keratin. Based on the data reported in the literature T_m of the polymeric materials is linked to the size and/or are dependent on the crystalline domains of the polymers (Cheng *et al.*, 2009). This initial reduction in the T_m of the keratin only composite (keratin: EC, 100: 0) prepared in the presence of laccase is an indication of the clear change or disruption in the size of the crystalline domains during the reaction phase.

The DSC results are well in agreement with the observations recorded through XRD studies where the wider peaks appeared in the graft with keratin: EC (100: 0) as compared to the sharp peaks of the untreated keratin at 26°, 31° 45° and 56° which is possibly due to the laccase action. The introduction of the keratin into the cellulose systems determines a shift in the melting temperatures to higher values, indicating an

increase of the thermal stability. At high temperatures (more than 200 ℃), keratin can contribute to the formation of a protective barrier on the material surface. This layer delays the heat transfer to the system and diminishes the release of the gaseous products from the system (Fazilat *et al*., 2012). This communicates our current findings for keratin based composites in which the thermal stability seems to be directly proportional to the keratin ratio content in the systems (Table 4.1). From the T_g and T_m data of the individual polymers *i.e.,* keratin and cellulose and their grafted composites prepared in different keratin: EC ratios (keratin: EC, 100: 0; 75: 25; 50: 50; 25: 75; and 0: 100) respectively. It was noted that in the presence of laccase, the T_g and T_m becomes lower in case of individual polymers and higher in the grafted composites. Over the later phases of the graft formation process the re-joining of short segments of keratin-associated proteins would cause an increase in the T_g and T_m which is possibly due to the formation of new keratin-EC cross-linking. The endothermal peak occurring in the 200 °C to 250 °C range is related to α-helix denaturation, and the area under the curve is a measure of the α-helix content, whereas, smaller the T_c the greater the rate of crystallization is (Tanabe *et al*., 2002; Liu *et al*., 2009).

Table 4.1 DSC-thermal characteristics of keratin, EC and keratin-EC-based bio-composites prepared using laccase with different keratin to EC ratios.

Sample ID	T_g (°C)	T_m (°C)	T_c (°C)	ΔH_m (J/g)
Keratin*	42±0.35	232±2.22	112±1.50	31±1.25
Keratin-g-EC[A]	34±0.31	210±1.22	177±1.35	24±0.35
Keratin-g-EC[B]	74±0.20	228±2.65	165±2.10	16±0.08
Keratin-g-EC[C]	105±0.95	223±1.10	169±1.85	9.5±0.45
Keratin-g-EC[D]	88±1.10	212±2.20	155±2.21	12±0.12
Keratin-g-EC[E]	ND	199±1.65	120±1.32	92±1.11
EC*	ND	188±0.09	48±0.05	86±0.69

* Untreated

ND: Not detected

Where, [A]: keratin: EC, 100:0; [B]: keratin: EC, 75:25; [C]: keratin: EC, 50:50; [D]: keratin: EC, 25:75 and [E]: keratin: EC, 0:100.

4.2.5. Dynamic mechanical analyser (DMA)

Table 4.2 provides the results of mechanical profile of the grafted composites and their individual counterparts. The untreated keratin and keratin film prepared with laccase treatment were found to be too fragile to provide mechanical characteristics. However, the film prepared from keratin and cellulose with keratin: EC ratio 75: 25 was fairly flexible and strong judged from tensile strength (22 MPa), elongation at break (37 %) and Young's modulus (1.1 GPa) as compared to the untreated keratin

film. The further increase in the cellulose content ratio from 25 to 50 % gave little additional change on ultimate strength and elongation. However, the increase in Young's modulus, suggests that further increase of cellulose content up to 75% made the film stiffer. As it can be seen in Table 4.2, keratin film incorporated with 50 wt% of cellulose showed considerable improvements in the tensile strength (55 MPa), elongation (18 %) and Young's modulus (2.4 GPa) in comparison to the untreated keratin. From these results, EC was found to increase mainly the strength and the flexibility of keratin film. Based on the literature data an appropriate addition of polymers like cellulose, chitosan and glycerol could control the mechanical properties of keratin films and keratin containing composites (Tanabe *et al*., 2002). As shown in Table 4.2, the grafted composites with higher keratin (obtained from chicken feathers) content have lower tensile strength. This has also been reported by other researchers (Cheng *et al*., 2009), and can be ascribed based on the fact that the strength of hydrolysed chicken feather is inadequate to test for mechanical characteristics. Our tests showed that laccase-assisted grafting brings a slight increase in the tensile strength in the resulting composites relative to the untreated keratin. Recently, it has been reported that laccase treatments can significantly improve the existing properties of a material and/or impart new physicochemical characteristics including dry and wet tensile strength through various cross-linking reactions (Wong *et al*., 2000; Felby *et al*., 2002; Aluigi *et al*., 2008).

Table 4.2 DMA-mechanical characteristics of keratin, EC and keratin-EC-based bio-composites prepared using laccase with different keratin to EC ratios.

Sample ID	Tensile strength (MPa)	Young's modulus (GPa)	Elongation at break (%)
Keratin*	ND	ND	ND
Keratin-g-EC^A	ND	ND	ND
Keratin-g-EC^B	22±0.09	1.1±0.31	37±0.33
Keratin-g-EC^C	55±0.15	2.4±0.42	18±0.45
Keratin-g-EC^D	91±0.21	3.1±0.25	8±0.28
Keratin-g-EC^E	122±0.42	3.5±0.65	9±0.15
EC*	122 ± 9.85	3.38 ± 0.85	8.2 ± 1.25

* Untreated

ND: Not detected

Where, ^{A}: keratin: EC, 100:0; ^{B}: keratin: EC, 75:25; ^{C}: keratin: EC, 50:50; ^{D}: keratin: EC, 25:75 and ^{E}: keratin: EC, 0:100.

4.2.6. Water contact angle (WCA)

The hydrophobic/hydrophilic characteristics in terms of water contact angle and the surface tension properties of the newly synthesised graft bio-composites and their

individual counterparts *i.e.,* keratin and EC are presented in the Figure 4.5. The water contact angle and surface tension values for untreated keratin film prepared without laccase treatment were 61 $^{\circ}$ and 42 mN/m, respectively while, in comparison to this an increase in the water contact angle from 61° to 70 $^{\circ}$ and surface tension from 42 mN/m to 48 mN/m was observed for the keratin film prepared with laccase treatment (Figure 4.5). This initial reduction in the hydrophilicity of the untreated keratin film towards the hydrophobicity is perhaps because of the laccase action. On the other hand a similar kind of decreasing or increasing trend was observed in the hydrophilicity or hydrophobicity, respectively, in other cellulose and cellulose containing graft composites. The water contact angle values for untreated keratin and keratin-EC based laccase-assisted graft composites with different keratin to EC ratio, *i.e.,* keratin: EC; 100:0, 75:25, 50:50, 25:75 and 0:100, were 25°, 70°, 48°, 52°, 49° and 47° respectively. A substantial decrease in the surface tension value of untreated EC from 130 mN/m to 35mN/m was recorded. The increase in the EC content ratio indicates that the hydrophilic property of keratin-*g*-EC bio-composites is much better than that of the untreated keratin. Such a result is probably due to the high hydrophilicity of cellulose. It can be expected that the keratin-*g*-EC composites with high hydrophilicity are more suitable for cell adhesion and proliferation than untreated keratin film prepared directly from the keratin hydrolysate due to its hydrophobic nature. It has also been reported in literature that the hydrophilic/hydrophobic balance is among critical factors which affects the platelet adhesion potential and the cytocompatibility features of the materials, and these properties would endow these polymeric materials as a potential candidate for various biomedical type applications (Aluigi *et al*., 2008).

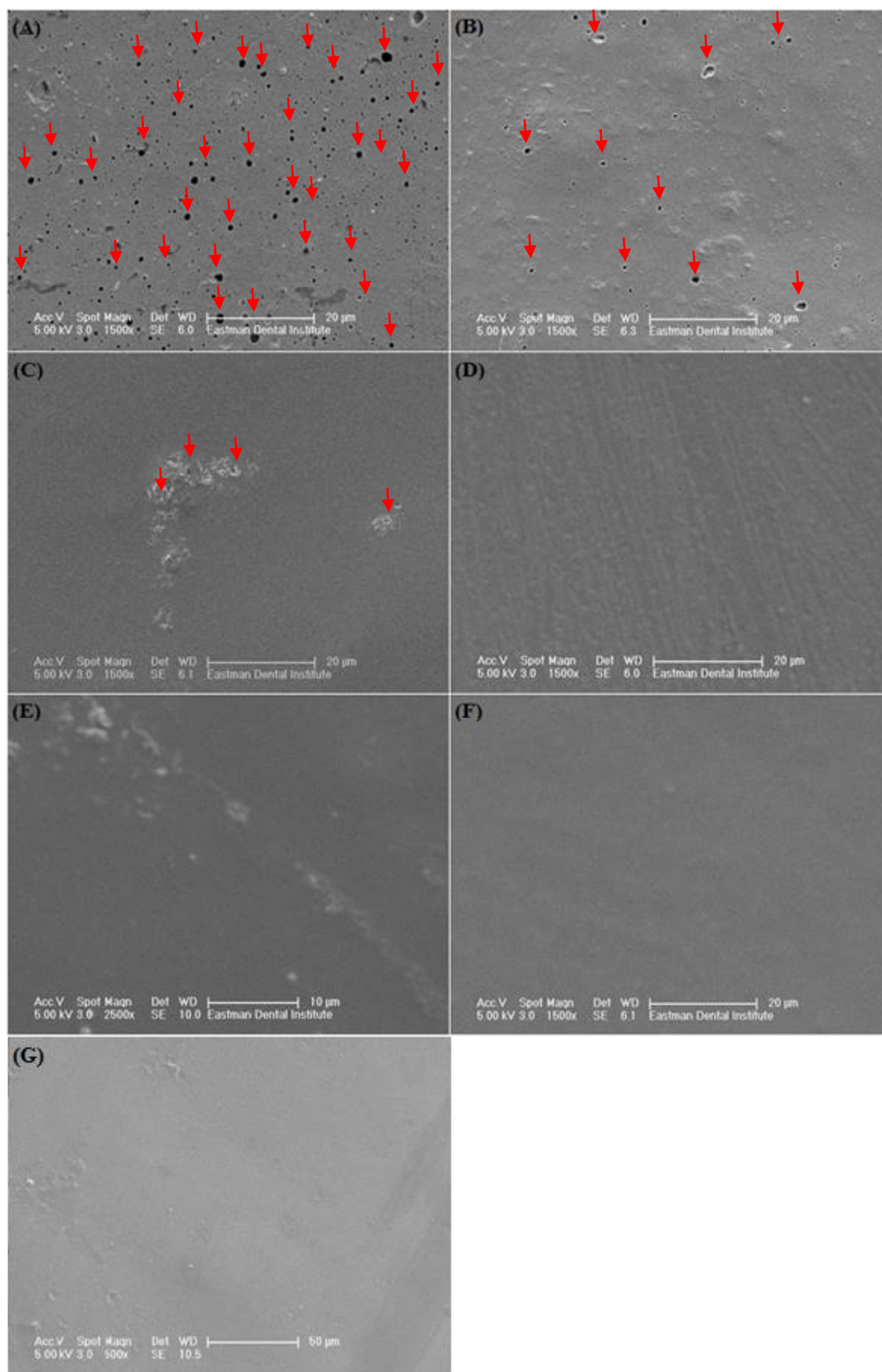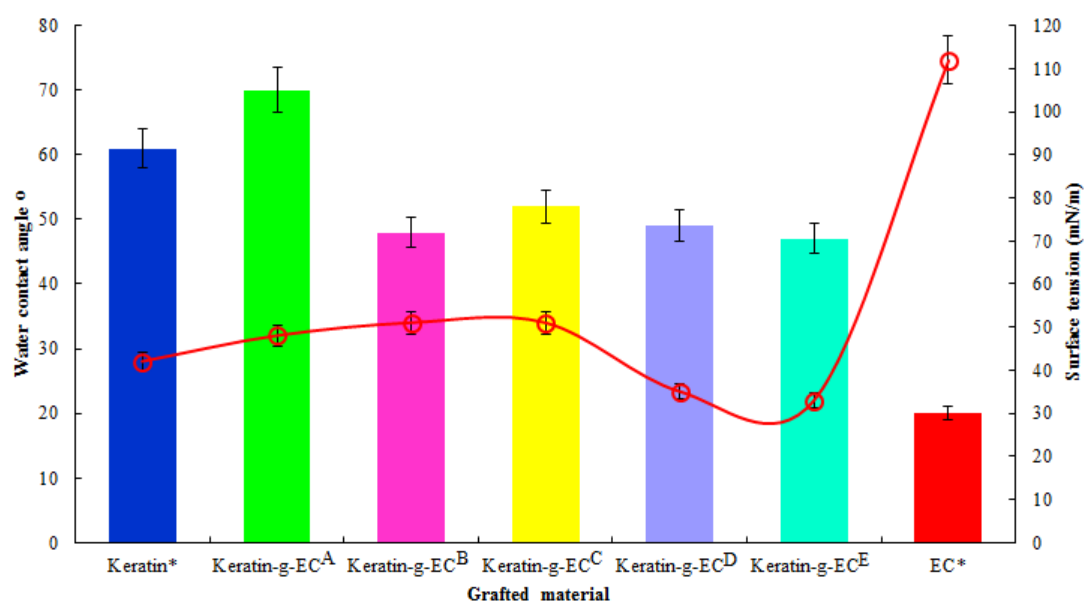**Figure 4.5** Water contact angle (bars in colour) and surface tension (red line) measurements of the untreated keratin and keratin-EC based bio-composites prepared using laccase with different keratin to EC ratios.

Where, *: Untreated keratin and EC films prepared without laccase treatment

Where, (A): keratin: EC, 100: 0; (B): keratin: EC, 75: 25; (C): keratin: EC, 50: 50; (D): keratin: EC, 25: 75 and (E): keratin: EC, 0: 100.

4.3. Concluding remarks

In this study, in-house extracted keratin from waste chicken feathers in combination with EC was used to develop novel composites using different keratin to EC ratios. The technology developed in this project enables the use of the chicken feather, a very troublesome waste of the poultry industry, which contributes in the current ecological and/or environmental pollution problems. As evidenced by the characterisation analyses, considerable improvement in the morphology, thermo-mechanical and wettability features was recorded in the newly synthesised composites that individual

material (keratin) fail to demonstrate on its own. In addition to non-toxic nature and other benefits of laccase, its use as a biocatalyst, for grafting purposes, offer a possibility to replace the hazardous solvent-based techniques. Moreover, to address the challenges of green chemistry, laccase-assisted grafting processes are simple, eco-friendly and provide energy saving reactions. Table 4.3 illustrates a comparative evaluation of various keratin based composites/blends and information is also given on their development, characterisation and potential applications in different sectors of the modern world.

Table 4.3 Comparative evaluation of various keratin-based biocomposites/blends: development, characterisation and potential/proposed applications.

Source of keratin	Co-material	Pre-treatment of keratin	Methodology used	Characterisation techniques	New/ improved functionality	Proposed applications	References
Feathers keratin	EC	Alkaline hydrolysis	Solution cast Enzyme based (laccase)	FTIR, SEM, XRD, DSC, DMA, WCA	Surface morphology, Thermo-mechanical, low crystallinity and hydrophilic characteristics	Coating materials, Packaging, Tissue engineering, and filtration membranes	Iqbal *et al.*, 2015b
Wool keratin	Chitosan	Mixture of urea, mercaptanol, and water at 40-60 ºC	Solution cast	DMA, SEM	Mechanical, Antibacterial, Biocompatible	Mammalian cell culture, Biomedical	Tanabe *et al.*, 2002
Wool keratin	-	Mixture of urea, SDS and $Na_2S_2O_5$ at 100 ºC	Compression moulded	SEM, DSC, DMA	Mechanical, Biocompatible	Mammalian cell culture, Biomedical	Katoh *et al.*, 2004
Chicken feathers	Glycerol	Alkaline hydrolysis	Oven dried at 30 ºC for 24 h	SEM, DMA, DSC	Mechanical and thermal properties	Packaging	Moore *et al.*, 2006
Wool keratin	Poly(ethylene oxide)	Sulphitolysis	Electrospinning	FTIR, DSC, SEM	Thermal, Morphological	Textile, Tissue engineering	Aluigi *et al.*, 2007
Chicken feathers	Poly(methyl methacrylate)	-	Air oven heated to 70 ºC for 24 h.	DMA, DSC, TGA,	Thermal properties	Thermoplastic	Martínez-Hernández *et al.*, 2007
Wool keratin	Poly(ethylene oxide)	Sulphitolysis	Solution cast	FTIR, DSC, POM, SDS-PAGE	Thermal and crystallisation properties	Drug delivery and filtration membranes	Tonin *et al.*, 2007
Wool keratin	Poly(ethylene oxide)	Sulphitolysis	Electro-spinning	SEM, FTIR, DSC, Electro-spun	Increased specific surface area	Filter for air cleaning	Aluigi *et al.*, 2008a
Wool fibre	Cellulose acetate	Ultrasonic treatment, Enzymatic (Serine protease)	Solution cast	SEM, FTIR, DSC, DMA, TGA	Fire resistance, moisture regain, dyeing performances	Packaging, films, textile fibres	Aluigi *et al.*, 2008b
Chicken quill	Polypropylene	-	Carver Press Compression moulder	FTIR, SEM, DMA	Mechanical and Sound absorption	Acoustic panels and headliner substrates	Huda and Yang, 2008
Wool fibre	Silk fibroin	Mixture of urea, SDS and $Na_2S_2O_5$ at 100 ºC	Solution cast	FTIR, DSC, SDS-PAGE, DMA	Mechanical and thermal properties	Biomedical	Vasconcelos *et al.*, 2009
Chicken feathers	Poly(L-lactic acid)	-	Extrusion and injection moulding	SEM, DMA, TMA, DSC	Mechanical and thermal	-	Cheng *et al.*, 2009
Chicken feathers	Methyl acrylate	Free radical	Solution cast	FTIR, DSC, DMA, NMR	Mechanical and thermal	Thermoplastic	Jin *et al.*, 2011
Human hair	-	Mixture of Tris, thiourea, urea, and mercapto-ethanol at 50 ºC for 72 h	Solution cast	Viscometer, SDS-PAGE, TEM, SEM, XRD	High seeding efficiency, Biomedical	Cell cultivation Biomedical, ocular surface reconstruction	Reichl *et al.*, 2011
Chicken feathers	Acrylonitrile and sodium carbonate	Alkaline hydrolysis	Oven dried at 50 °C for 12 h	FTIR, NMR, TGA, DMA, DSC, LC-MS	Mechanical and thermal	Thermoplastic products	Reddy *et al.*, 2011
Wool keratin	Biodegradable polyester	Washed in Soxhlet with acetone for 2 h and dried under vacuum at 105ºC for 4 h	Melt blending at 160ºC	SEM, POM, DSC, DMA, DTGA	Thermal, and mechanical	Polymer reinforcement	Conzatti *et al.*, 2012
Wool keratin	Polypropylene	Microwave irradiation (superheated water)	Melt-mixing at 190ºC for 10 min under nitrogen environment	Polarized optical microscopy (POM), DSC, DMA, GPC/SEC, TGA	Thermal and crystallization rate	Plastics and textile fibres	Bertini *et al.*, 2013

125

Wool keratin	Poly(vinyl alcohol)	Sulphitolysis	Electrospinning	SEM, FTIR, XRD, TGA, DMA	Mechanical and thermal	Thermoplastic	Li and Yang, 2014
Chicken feathers	Acrylates, Poly(lactic acid), glycerol	Alkaline hydrolysis	Compression moulded	NMR, DSC, DMA, Confocal microscope	Water stability and cyto-compatible	Tissue engineering	Reddy *et al.*, 2013a
Chicken feathers	Citric acid and glycerol	Alkaline hydrolysis	Compression moulded	DSC, DMA, SDS-PAGE	Mechanical and thermal, water instability	Thermoplastic products	Reddy *et al.*, 2013b
Chicken feathers	PLA, Chitosan	Mechanical	Compression moulded	FTIR, DMA, DTG, SEM, XRD	Mechanical and thermal	Thermoplastic	Spiridon *et al.*, 2013
Chicken feathers	Ethylene glycol, propylene glycol, glycerol	Alkaline hydrolysis	Compression moulded	FTIR, DSC, DMA, WCA	Mechanical and thermal	Thermoplastic	Ullah and Wu, 2013
Wool keratin	Poly(lactic-*co*-glycolic acid)	-	Electro-spinning	SEM, DMA, DSC, TGA	Improve cellular attraction, thermal and mechanical	Bone tissue engineering	Zhang and Liu, 2013
Chicken feathers	Polyhydroxyal kanoates	-	Melt compounding	SEM, DMA	Mechanical, improved barrier properties	Renewable packaging applications	Pardo-Ibáñez *et al.*, 2014

Chapter 5

In situ development of novel bio-composites through laccase-assisted grafting with natural phenols as functional entities

5.0. Summary

This chapter presents the results of *in-situ* green synthesis and evaluation of multi-characteristics, "as-prepared", novel bio-composites. A series of bio-composites were synthesised via laccase-assisted grafting of natural phenols *e.g.,* caffeic acid (CA), gallic acid (GA), *p*-4-hydroxybenzoic acid (HBA), and thymol (T) onto the previously developed P(3HB)-EC and kertain-EC-based bio-composites (presented and discussed in Chapter 3 and Chapter 4) without the use of additional initiators or crosslinking agents. In this part of the project, the focus is relatively wide - primarily on grafting natural phenols and evaluation of different characteristics of the grafted bio-composites. The chapter starts with an evaluation of structural groups through FT-IR followed by grafting parameters *i.e.* graft yield, %GY, grafting efficiency, %GE and swelling ratio, %SR of the bio-composites. An assessment is then made on their antibacterial potential against various Gram-positive bacteria *B. subtilis* NCTC 3610 and *S. aureus NCTC* 6571 as well as Gram-negative bacteria *E. coli NCTC* 10418 and *P. aeruginosa NCTC* 10662 strains. This was then followed by analyses of biocompatibility and biodegradability behaviours the composites provide under a controlled environment. Moreover, from the cytotoxicity point of view, at various phenolic concentrations up to 20 mM, 100% cell viability of human keratinocyte-like HaCaT cells was recorded after 5 days of incubation with the bio-composites. Towards the end of this chapter, an information is also given on the biodegradability features of these newly developed bio-composites.

5.1. Introduction

Since the late 1990s, enzyme-based techniques have evolved from the biotransformation of natural and synthetic polymers/materials into value-added

products. A new global thrust towards green chemistry and recent advancement in polymer synthesis and/or modifications via grafting of functional molecules have promoted interests due to the accrued understanding of enzyme reaction mechanisms (Anastas *et al*., 2003; Iqbal *et al*., 2014a, b; Yu *et al*., 2015). Moreover, enzymes, as green catalysts in polymeric-based materials synthesis and modifications, offer a potential for eliminating the hazards associated with reactive reagents and other health and safety issues linked with other chemical-based procedures (Alves and Mano, 2008; Brandelli *et al*., 2015). Recently laccases have gained particular attention owing to their versatile bio-catalytic potentials along with remarkable abilities to oxidise a wide variety of substrates such as phenols, diamines, benzenethiols, polyphenols, organic/inorganic compounds and many others. However, they do not require any additional initiators e.g. H_2O_2 (Riva, 2006; Iqbal *et al*., 2014b). The laccase-generated radicals provide ideal sites for cross-linking of various molecules of interest leading to grafting and/or formation of new biomaterials with novel characteristics. Therefore, laccase-assisted grafting has become a superior method to impart a wide spectrum of functional groups onto the backbone polymeric materials.

Over the last few years, many polymer researchers have directed their interests into the development of structured materials with multi-functional characteristics like anti-bacterial materials, for wider range of applications (Fillat *et al*., 2012; Iqbal *et al*., 2014a). In recent years, ever increasing consciousness and demands of legislative authorities to reduce the bacterial population in healthcare facilities and possibly to cut pathogenic infections, the development of novel antimicrobial active materials which are biocompatible and biodegradable are considered critically. The antibacterial effect of silver nanoparticles is already reported (Michl *et al*., 2014; Wang *et al*., 2014; Zou *et al*., 2014; Lu *et al*., 2015). However, excess release of silver nanoparticles

inhibits the growth of osteoblasts and can also cause severe side effects such as cytotoxicity (Wang *et al*., 2014). In this regard, green chemistry technology has considerable potential to provide a solution to reduce or even eliminate the risk of bacterial infection without adverse effects on human cells. Novel composites were developed earlier in this project through lipase and laccase-assisted grafting of P(3HB) and keratin onto the EC (*i.e.,* P(3HB)-*g*-EC and keratin-*g*-EC). The fabrication was under mild and eco-friendly environment, and improved thermo-mechanical characteristics and hydrophobic/hydrophilic balance were achieved and the results were analysed (as discussed in Chapter 3 and Chapter 4). Among the tested phenolic structures, the well-known polyphenolic compounds used caffeic acid, gallic acid, *p*-4-hydroxybenzoic acid and thymol have pronounced antibacterial characteristics against various bacterial strains (Rukmani and Sundrarajan, 2012; Shahidi *et al*., 2014). This project hypothesised that the aforementioned natural phenols are a very efficient choice for inhibiting bacterial infections. Most phenols, as natural antimicrobial agents, can be grafted onto cellulose surface to impart antimicrobial properties. The cross-linking behaviours of various phenolic molecules to different fibres was evidenced after treatment with laccase from *Pycnoporus cinnabarinus* and others (Aracri *et al*., 2010; Cadena *et al*., 2011).

In continuation of our previous investigation described in Chapter 3 and Chapter 4, this Chapter reports on the development of antibacterial bio-composites which are biocompatible and biodegradable. In this study, firstly, natural phenols were grafted onto the P(3HB)-EC and keratin-EC-base grafted material where laccase from *Trametes versicolor* was used as a grafting tool. Secondly, the newly synthesised composites were characterised by Fourier-transform infrared (FT-IR) spectroscopy, and various grafting parameters were also analysed. Thirdly, *in-vitro* evaluation of

their antibacterial potential against Gram-positive and Gram-negative bacterial strains, their biocompatibility against human keratinocyte-like (HaCaT) cell line and their biodegradability features were also investigated.

5.2. Results and Discussion

5.2.0 PART – 1

5.2.1. Fourier transform infrared spectroscopy (FT-IR)

FT-IR spectroscopy was used to examine the structural and functional elements of the phenol grafted composites *i.e.,* CA-*g*-P(3HB)-EC, GA-*g*-P(3HB)-EC, HBA-*g*-P(3HB)-EC and T-*g*-P(3HB)-EC along with their individual counterparts *i.e.,* CA, GA, HBA, T and P(3HB)-EC, respectively. In Figure 5.1, CA-*g*-P(3HB)-EC composites show a band at 3,345 cm^{-1} corresponding to phenolic -OH stretching involving hydrogen bonding, and a peak at 1,360 cm^{-1} corresponds to -OH bending of the phenolic group (Rukmani and Sundrarajan, 2012). In comparison to the untreated CA and P(3HB)-EC, an increase in absorbance at 1,351 cm^{-1}, and 1,056 cm^{-1} was noticed in the CA-*g*-P(3HB)-EC composites as shown in Figure 5.1. The peaks at 3,345 cm^{-1} and in a broad region of 3,100-3,470 cm^{-1} can be attributed to the stretching vibrations from -OH, groups. Interestingly, some of the distinct peaks from untreated CA disappeared when it was grafted with P(3HB)-EC in the presence of laccase as a model catalyst. Figure 5.2 illustrates a schematic mechanism of graft formation through laccase-assisted grafting of natural phenols onto the P(3HB)-EC based material.
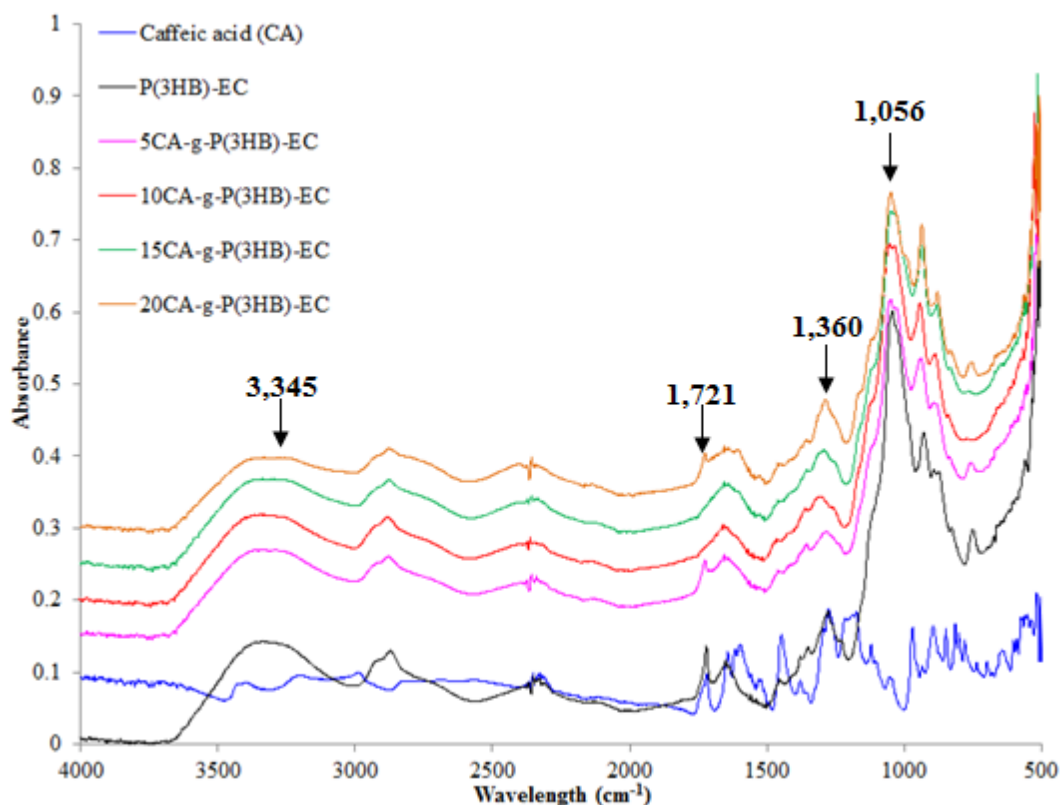
Figure 5.1 Typical FT-IR spectra of caffeic acid and caffeic acid grafted P(3HB)-EC based bio-composites.

Figure 5.3 illustrates an FT-IR spectra of GA-*g*-P(3HB)-EC composites, and the absorption peaks at 3,491 cm^{-1}, 3,265 cm^{-1}, 1,605 cm^{-1}, 1,540 cm^{-1}, 1,421 cm^{-1}, 1,380 cm^{-1}, and 1,022 cm^{-1} in the spectrum are typical indications of GA. An increase in the band range from 3,200 cm^{-1} to 3,400 cm^{-1} corresponds to the appearance of inter- and intramolecular hydrogen bond between untreated GA and P(3HB)-EC during graft formation process. The region between 1,260 cm^{-1} and 1,056 cm^{-1} relates to the C–H and C–O–C bond stretching frequencies respectively, whereas, a band at 2,985 cm^{-1} is assigned to C–H vibration mode in the graft composites. A peak at 1,000-1,150 cm^{-1}, corresponding mainly to ethers (C–O–C), was increased in comparison to the GA monomers used in this study, indicating extended polymerisation (Yamada *et al.*, 2007; Božič *et al.*, 2012). It has typical polyphenol characteristics, showing a broad peaks centred at 3,345 cm^{-1} and 1,375 cm^{-1} due to the vibration of O–H linkage of

132

phenolic and hydroxyl groups, at 1,450–1,600 cm^{-1} due to the aromatic ring C=C stretching, and C=O stretching vibration at 1,200–1,300 cm^{-1}, respectively.
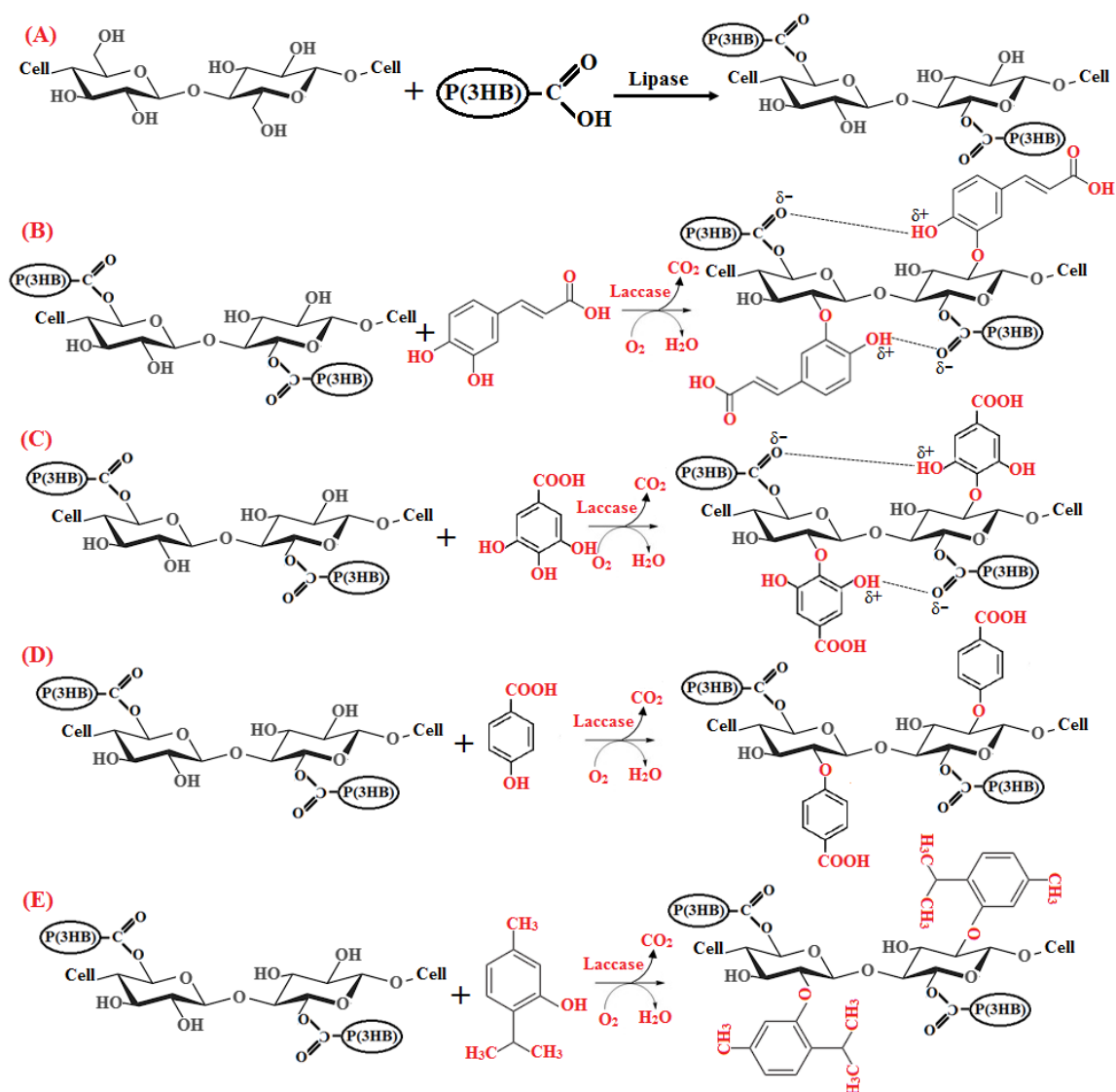
Figure 5.2 A schematic representation of proposed mechanism of graft formation; (**A**) between P(3HB) and EC, (**B**) between P(3HB)-EC and caffeic acid, (**C**) between P(3HB)-EC and gallic acid, (**D**) between P(3HB)-EC and p-4-hydroxybenzoic acid, and (**E**) between P(3HB)-EC and thymol.

The FT-IR spectra of the HBA, P(3HB)-EC and their laccase-assisted HBA-*g*-P(3HB)-EC composites are shown in Figure 5.4. The HBA-*g*-P(3HB)-EC spectra exhibit a different profile compared to the HBA monomers. The strong bands at 1,689 cm^{-1} and 1,607 cm^{-1} are attributed to the C=O and COO$^-$ vibrations of HBA and HBA-

g-P(3HB)-EC moieties, respectively. The bands at 1,446 cm^{-1} and 1,240 cm^{-1} are due to the in-plane -OH modes (-OH) of two hydrogen bonds, which are shifted to 1,360cm^{-1} and 1,056 cm^{-1} in the spectrum of the HBA-*g*-P(3HB)-EC samples. The typical bands in the 3,070–2,860 cm^{-1} region are due to the C–H, CH$_2$ and CH$_3$ vibrations. In the fingerprint region (1,500–500 cm^{-1}), the bands are assigned to the aromatic and hetero aliphatic rings as well as to the CH$_2$ and CH$_3$ modes (Smith and Dent, 2005). The most probable explanation is that the structure of the -OH band arises from overtones or a combination of modes of internal vibrations of HBA-*g*-P(3HB)-EC and HBA, which overlap the -OH broad band and the Fermi resonance between the -OH fundamental of hydrogen bonds and overtone of its deformation modes (Dega-Szafran *et al.*, 2008).
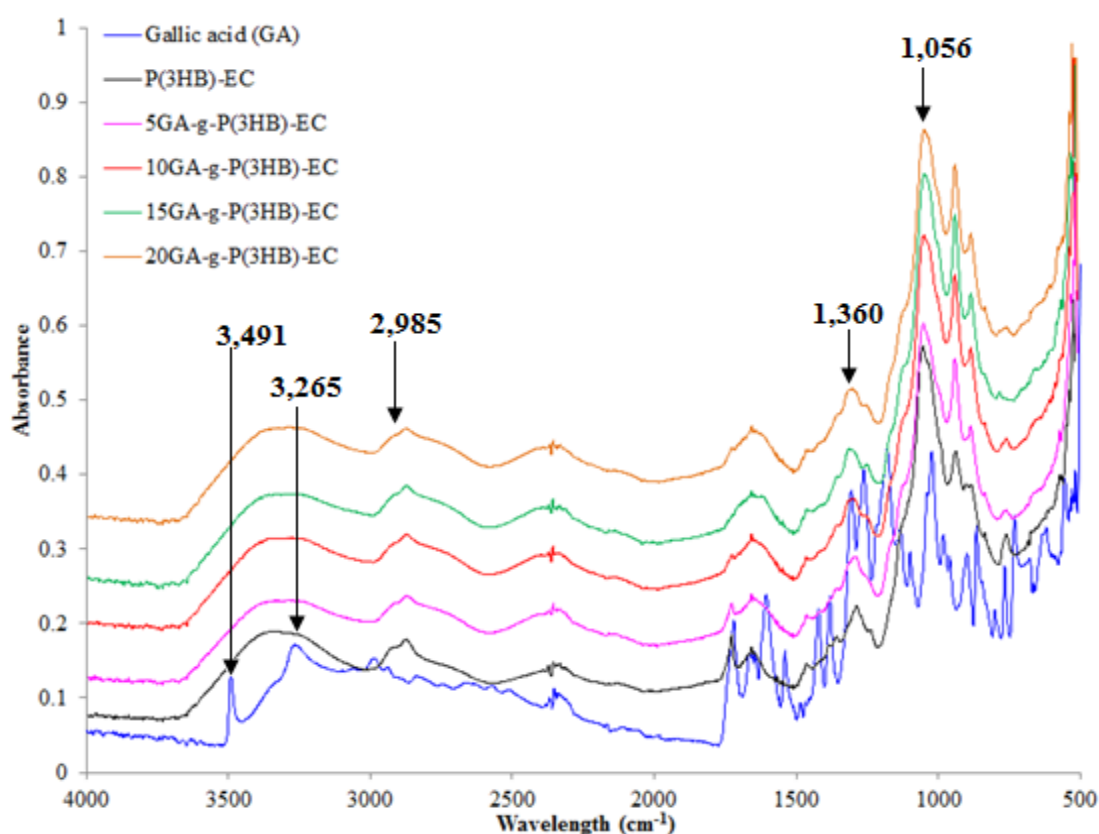
Figure 5.3 Typical FT-IR spectra of gallic acid and gallic acid grafted P(3HB)-EC based bio-composites.

The FT-IR spectra of T and T grafted P(3HB)-EC composites (T-g-P(3HB)-EC) is presented in Figure 5.5. The peaks around 3,300-3,400 cm^{-1} are assigned to hydrogen bonds and can be seen at the wavelength 3,360 cm^{-1}. Figure 5.5 depict an increase in the peak at 3,360 cm^{-1} as a result of thymol affinity to the baseline material P(3HB)-EC, this peak was not found in the spectra of T monomers. The bands at 1,446 cm^{-1} and 1,240 cm^{-1} are due to the in-plane -OH modes (-OH) of two hydrogen bonds, which are shifted to 1,360 cm^{-1} and 1,056 cm^{-1} in the spectrum of the T-g-P(3HB)-EC composites. The bands in the 3,070–2,860 cm^{-1} region are assigned to the C–H, CH$_2$ and CH$_3$ vibrations. It has typical polyphenol characteristics, showing broad peaks centred at 3,360 cm^{-1} and 1,446 cm^{-1} due to the vibration of O-H linkage of phenolic and hydroxyl groups. Furthermore, the vibration band of carbonyl stretching appeared in the region 1,720 cm^{-1} for the T-g-P(3HB)-EC spectra while in the T monomer spectra it is missing. By comparison between this and the T-g-P(3HB)-EC spectra, it can be seen that some bands changed intensity and/or shape during the graft formation process. Laccase treatment can lead to an increased reactivity of the respective surface and this is possible because of the breaking of the different bonds and further formation of free radicals (Chandra et al., 2004). Due to the laccase action, the reaction of the oxygen and nitrogen in the atmosphere with the free radicals takes place and thus surface functionalisation occurs. In particular, the major spectral change of thymol can be observed in the bands at 3,360 cm^{-1}, 2,957 cm^{-1}, 1,446cm^{-1}, 1,360cm^{-1}, 1,240 cm^{-1}, and 807 cm^{-1}. Whereas, the most intense peaks at 738 cm^{-1} and 807cm^{-1} are assigned to ring vibrations of the thymol chemistry (Schulz et al., 2003; Torres-Giner et al., 2014).
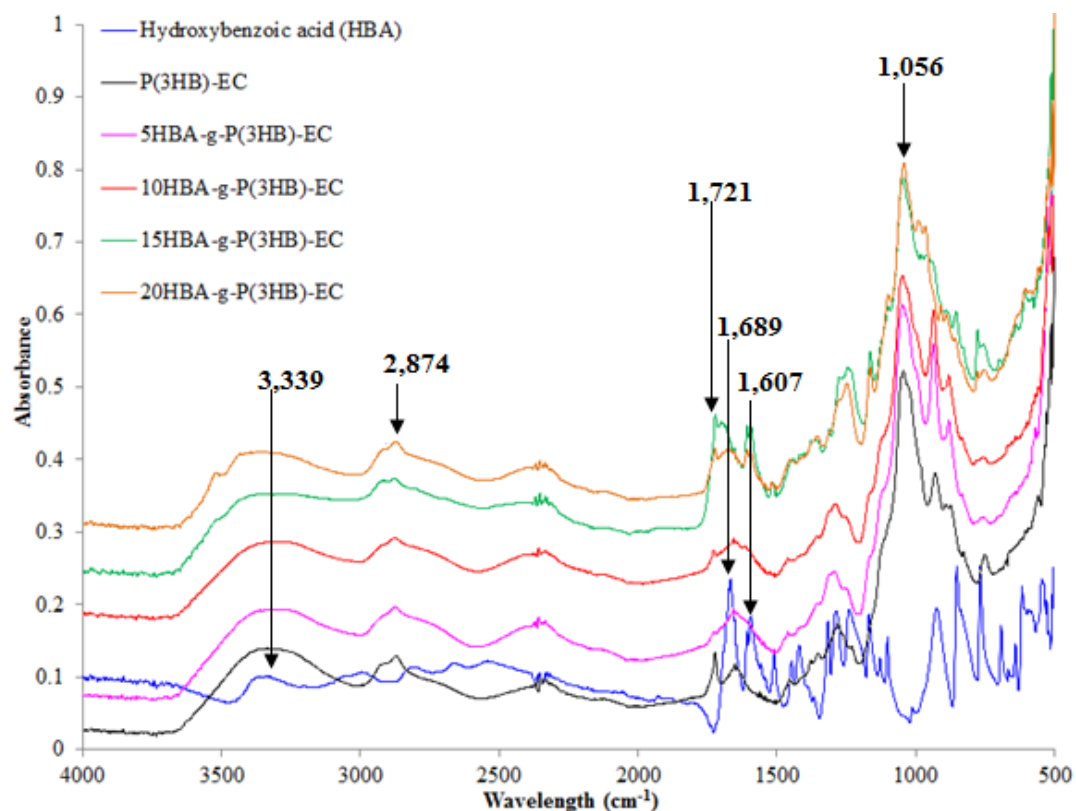
Figure 5.4 Typical FT-IR spectra of *p*-4-hydroxybenzoic acid and *p*-4-hydroxybenzoic acid grafted P(3HB)-EC based bio-composites.
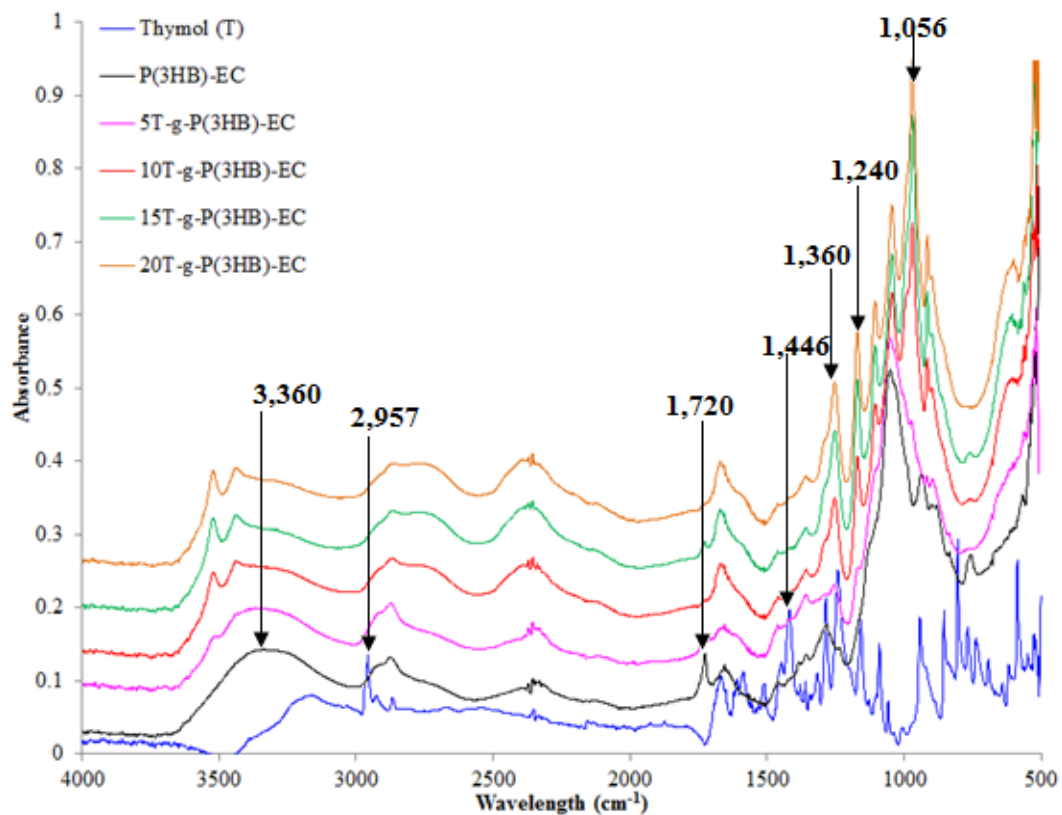
Figure 5.5 Typical FT-IR spectra of thymol and thymol grafted P(3HB)-EC bio-composites.

136

5.2.2. Grafting parameters

Figs. 5.6 to 5.9 shows the grafting parameters (GP) (*i.e.,* graft yield (GY %), grafting efficiency (GE %) and swelling ratio (SR %) profiles of CA-*g*-P(3HB)-EC, GA-*g*-P(3HB)-EC, HBA-*g*-P(3HB)-EC and T-*g*-P(3HB)-EC composites, respectively prepared by SDI method. In particular, as shown in Figure 5.6, a consistent increase was recorded in the grafting efficiency and swelling ratio behaviour in case of the 20CA-*g*-P(3HB)-EC composite, whereas in case of gallic acid, *p*-4-hydroxybenzoic acid and thymol, the composites prepared with their respective 15mM concentrations *i.e.,* 15GA-*g*-P(3HB)-EC, 15HBA-*g*-P(3HB)-EC and 15T-*g*-P(3HB)-EC were proved best under the same reaction environment. However, a further increase in their mM concentration showed decreasing trend in the aforementioned parameters. This decreasing trend in the graft parameters could be due to the steric hindrance at higher concentration of these phenolic structures. Furthermore, one possible reason for the observed behaviour could be the substantial amount of phenolic components grafted onto the baseline P(3HB)-EC material at their optimal level which can hinders further grafting at higher concentrations due to the unavailability of the reactive sites, thus, unreacted phenols were washed out in later stage of the SDI technique used in this study.

The increase in the monomer concentration would be expected to increase the grafting percentage which in turn increases the molecular weight of the graft composite (Aggour, 2001; Constantin *et al*., 2011). Indeed, the results presented in Figure 5.7 to 5.9 illustrate that as the concentrations of GA, HBA and T increased from 0 to 15 mM, the percentage of GP was remained optimal with an increase in the swelling ratio and grafting efficiency, respectively. It has also been reported that the reaction time is an

important parameter which can increase or decrease the grafting parameters like graft yield, grafting efficiency and swelling behaviour (Sun *et al*., 2003).
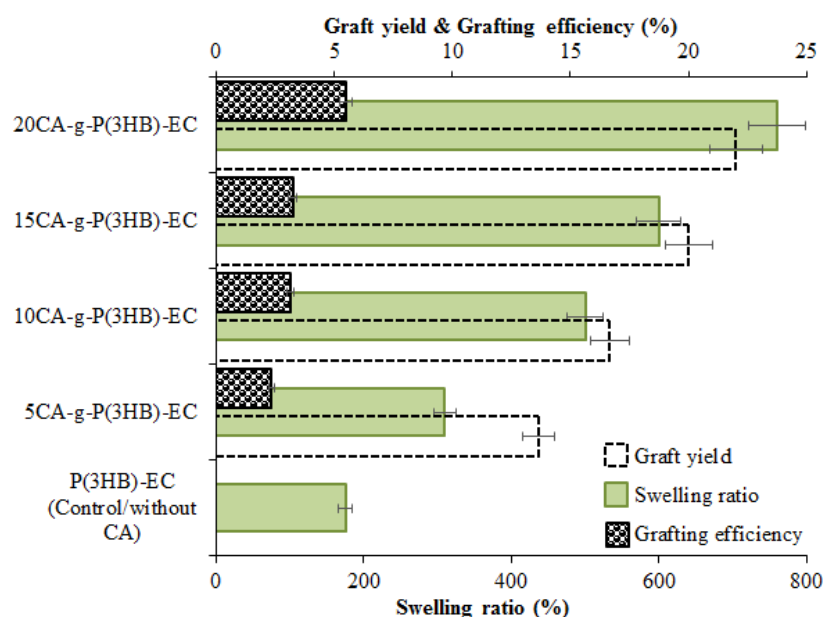
Figure 5.6 Evaluation of grafting parameters *i.e.,* graft yield (%GY), grafting efficiency (%GE) and swelling ratio (%SR) behaviours of CA-*g*-P(3HB)-EC bio-composites prepared using laccase as a model catalyst (mean ± SD, n = 3).
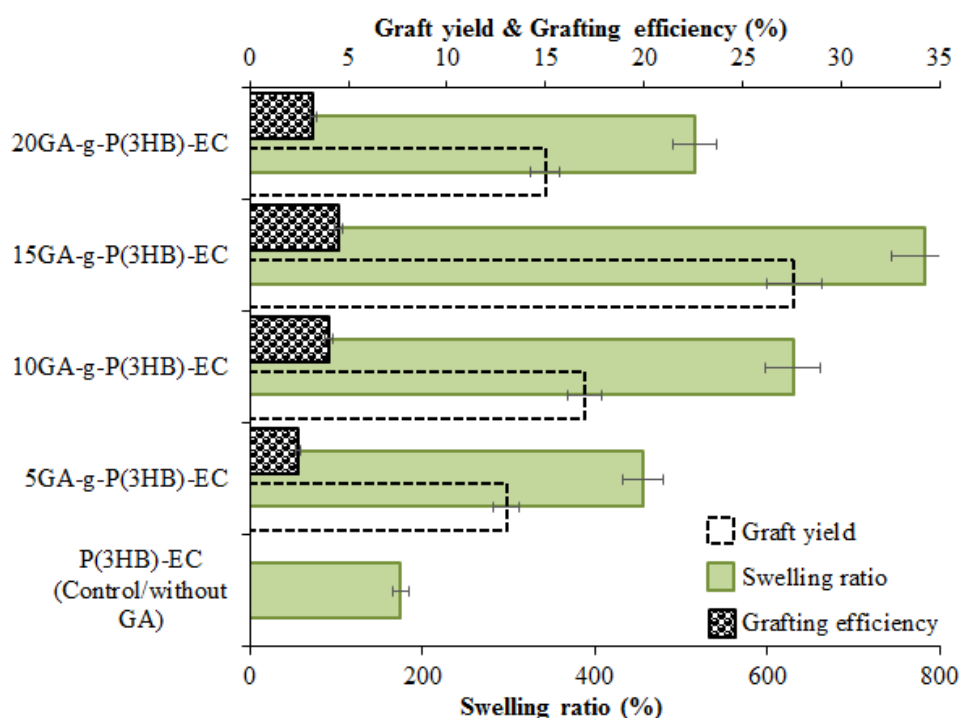
Figure 5.7 Evaluation of grafting parameters *i.e.,* graft yield (%GY), grafting efficiency (%GE) and swelling ratio (%SR) behaviours of GA-*g*-P(3HB)-EC bio-composites prepared using laccase as a model catalyst (mean ± SD, n = 3).
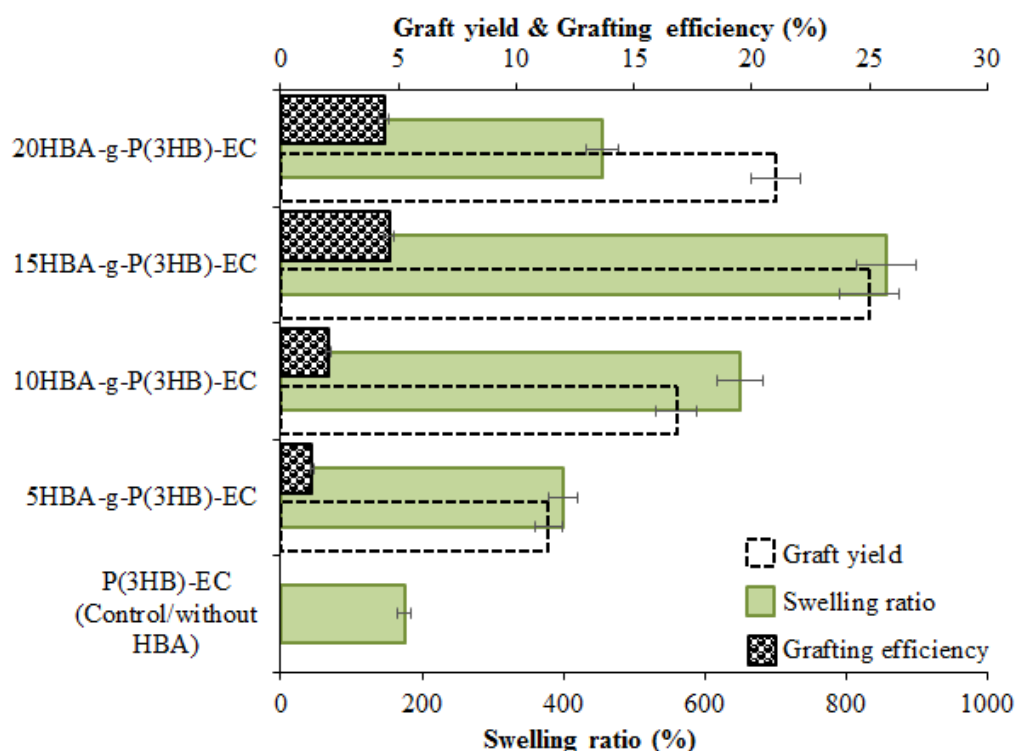
Figure 5.8 Evaluation of grafting parameters *i.e.,* graft yield (%GY), grafting efficiency (%GE) and swelling ratio (%SR) behaviours of HBA-*g*-P(3HB)-EC biocomposites prepared using laccase as a model catalyst (mean ± SD, n = 3).
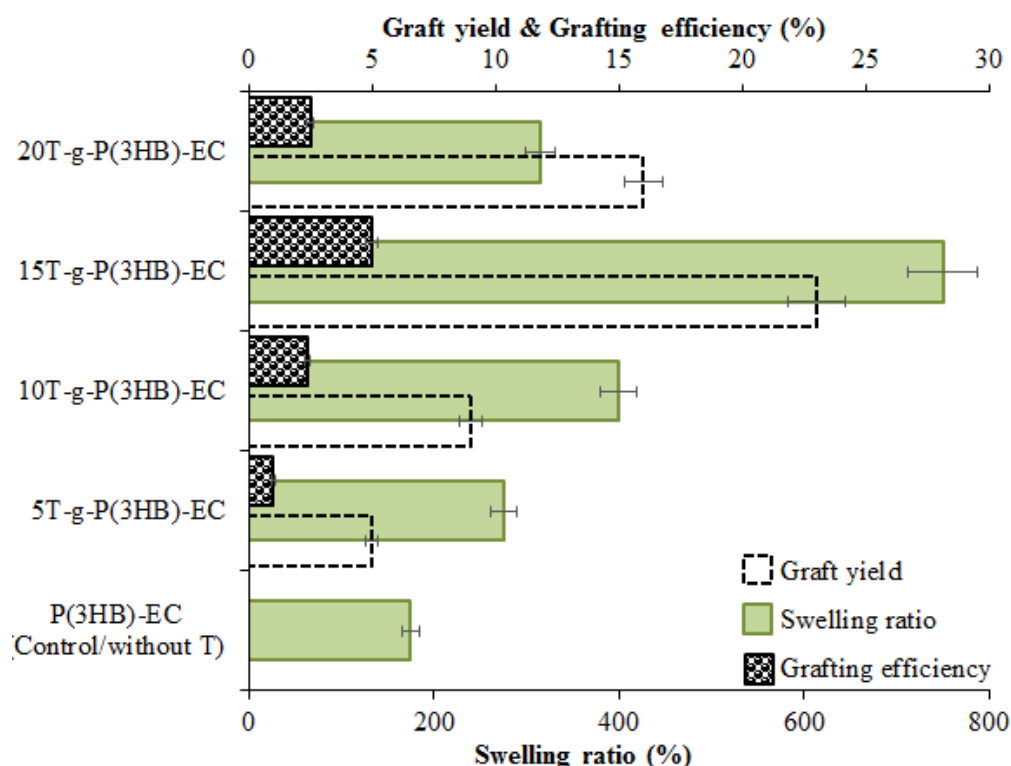
Figure 5.9 Evaluation of grafting parameters *i.e.,* graft yield (%GY), grafting efficiency (%GE) and swelling ratio (%SR) behaviours of T-*g*-P(3HB)-EC biocomposites prepared using laccase as a model catalyst (mean ± SD, n = 3).

139

5.2.3. Antibacterial activity

The results of the spread-plate method are given in Figs. 5.10 to 5.13. The bacterial growth on untreated P(3HB)-EC showed an increase in the log values for *B. subtilis* NCTC 3610, *S. aureus* NCTC 6571, *E. coli NCTC* 10418 and *P. aeruginosa* NCTC 10662, in comparison to the initial bacterial count (control value *i.e.,* 1×10^5 CFU/mL) thus showing that the untreated P(3HB)-EC is a good support media for the growth of bacteria. It was observed that 5CA-*g*-P(3HB)-EC and 10CA-*g*-P(3HB)-EC did not show any potential to inhibit the bacterial count especially against Gram-positive strains, however 10CA-*g*-P(3HB)-EC and 15CA-*g*-P(3HB)-EC showed limited bacteriostatic activities. Whereas, in comparison to the control, 20CA-*g*-P(3HB)-EC displayed significant log reduction value from 5 to 2 and 1 against *E. coli NCTC* 10418 and *P. aeruginosa* NCTC 10662, respectively (Fig. 5.10).

The anti-bacterial activity of test composites (GA-*g*-P(3HB)-EC) versus *B. subtilis* NCTC 3610, *S. aureus* NCTC 6571, *E. coli NCTC* 10418 and *P. aeruginosa* NCTC 10662 strains, as a function of GA concentration is reported in Figure 5.11. The results obtained after 24 h incubation with 10GA-*g*-P(3HB)-EC and 20GA-*g*-P(3HB)-EC exhibit only a slight bacteriostatic effect against all of the tested strains. Whereas, 15GA-*g*-P(3HB)-EC showed a significant bactericidal effect against *S. aureus* NCTC 6571, *E. coli* NTCT 10418 and *P. aeruginosa* NCTC 10662 strains.
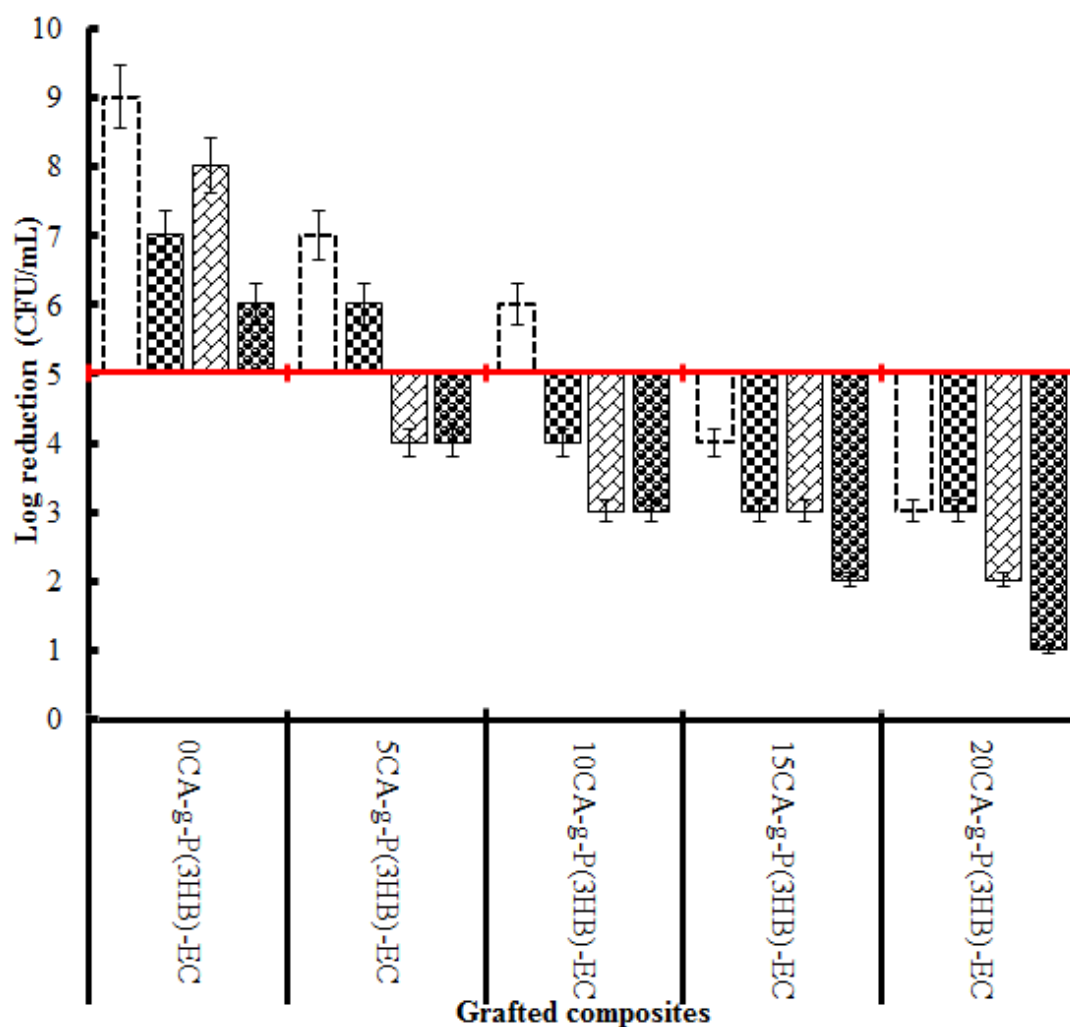
Figure 5.10 Evaluation of antimicrobial potential of caffeic acid grafted P(3HB)-EC based bio-composites against various Gram-positive and Gram-negative bacterial strains *i.e., B. subtilis* NCTC 3610 (▢); *S. aureus NCTC* 6571 (▨); *E. coli NCTC* 10418 (▨) and *P. aeruginosa NCTC* 10662 (▨). Red line indicates an initial bacterial count *i.e.,* 1×10^5 CFU/mL. An increase in this count (as compared to the initial bacterial count) showed susceptibility whereas, reduction in the initial bacterial count showed bacteriostatic and bactericidal activities of the respective composites. A 2 log reduction was considered to claim an antibacterial activity.
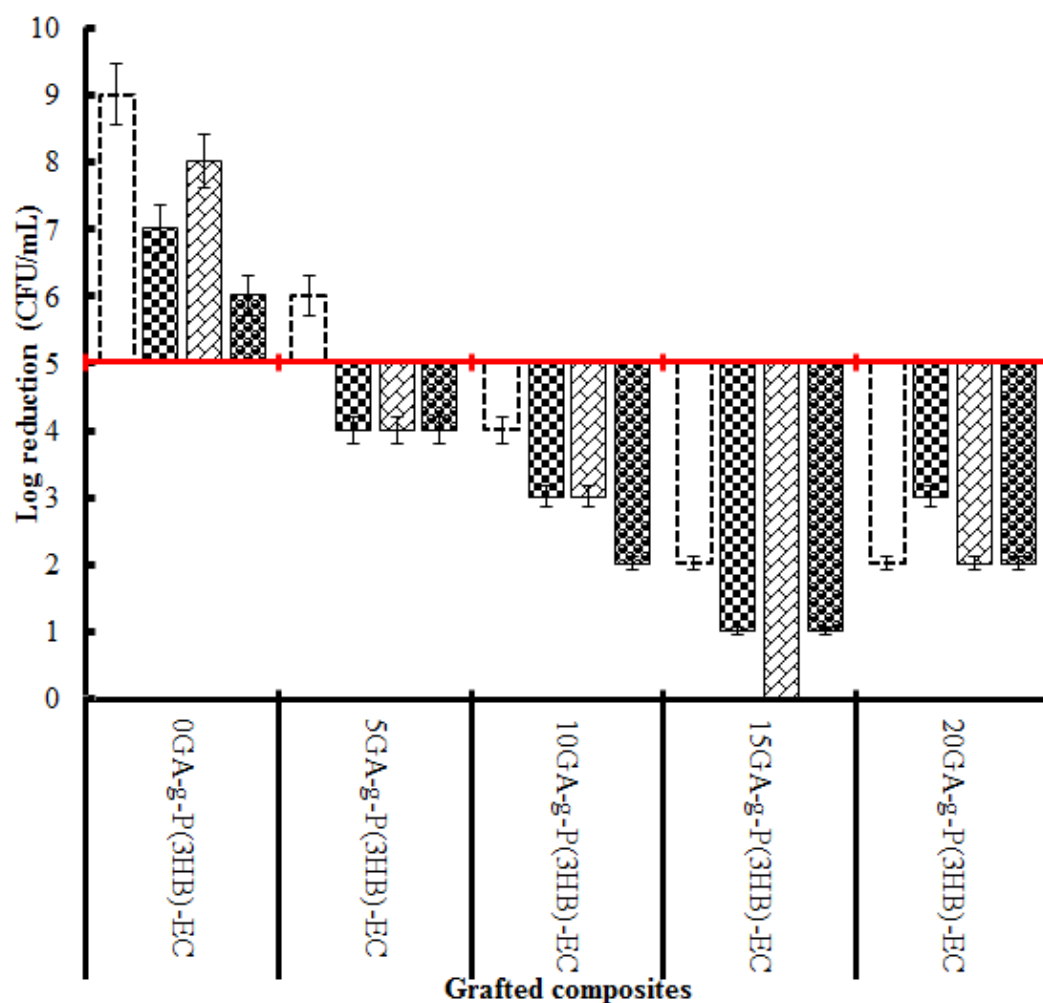
Figure 5.11 Evaluation of antimicrobial potential of gallic acid grafted P(3HB)-EC based bio-composites against various Gram-positive and Gram-negative bacterial strains *i.e., B. subtilis* NCTC 3610 (▱); *S. aureus NCTC* 6571 (▨); *E. coli NCTC* 10418 (▨) and *P. aeruginosa NCTC* 10662 (▨). Red line indicates an initial bacterial count *i.e.,* 1×10^5 CFU/mL. An increase in this count (as compared to the initial bacterial count) showed susceptibility whereas, reduction in the initial bacterial count showed bacteriostatic and bactericidal activities of the respective composites. A 2 log reduction was considered to claim an antibacterial activity.

Figure 5.12 illustrates the anti-bacterial analyses profile of HBA-*g*-P(3HB)-EC composites tested against Gram-positive and -negative strains. The HBA containing composites, 10HBA-*g*-P(3HB)-EC and 15HBA-*g*-P(3HB)-EC showed clear bacteriostatic and bactericidal activities against all of the Gram-positive and Gram-negative strains, resulting in complete eradication of the strains used in this study. However, 5HBA-*g*-P(3HB)-EC and 20HBA-*g*-P(3HB)-EC composites were not as effective against any of the cultured strains and showed only a slight bacteriostatic activity. The results of the counting test for T-*g*-P(3HB)-EC are shown in Fig. 5.13. Likewise, GA and HBA, 15T-*g*-P(3HB)-EC also showed a complete bactericidal effect (bacterial count of zero) with a log value reduction from 5 to 0 against *S. aureus* NCTC 6571, *E. coli NCTC* 10418 and *P. aeruginosa* NCTC 10662. However, only 10T-*g*-P(3HB)-EC composite showed a significant bacteriostatic potential against all of the tested strains.

The interaction between natural phenols grafted onto the P(3HB)-EC and bacteria can change the metabolic activity of the bacterial cell which in turn lead to their eventual death. Based on an earlier published data, thymol has an ability to disrupt the lipid structure of the bacterial cell wall, further leading to a destruction of the cell membrane, cytoplasmic leakage, and cell lysis culminating in cell death (Veras *et al*., 2012; Milovanovic *et al*., 2013; Shahidi *et al*., 2014). It is well-known that the anti-bacterial, bacteriostatic and/or bactericidal potential of natural phenols is due to the presence of phenolic hydroxyl groups in their structures, an important feature of the anti-bacterial potential (Koech *et al*., 2013). Nance *et al*., (2006), concluded in their study that antimicrobial activity of catechins (a type of natural phenol) is predominantly a result of the gallic moiety and hydroxyl group member. Furthermore, the delocalisation of the electrons in phenolic structures have been reported to

contribute to their activity as well. (Ultee *et al*., 2002; Elegir *et al*., 2008). Our investigations are consistent with the earlier published literature where the highest activity of natural phenols against Gram-negative bacteria is often reported although many exceptions suggest that it cannot be taken as a general rule. (Elegir *et al*., 2008). Based on the optimal grafting parameters and anti-bacterial activities, the composites *i.e.,* 20CA-*g*-P(3HB)-EC, 15GA-*g*-P(3HB)-EC, 15HBA-*g*-P(3HB)-EC and 15T-*g*-P(3HB)-EC were selected to investigate for their HaCaT biocompatibility and biodegradability analyses.
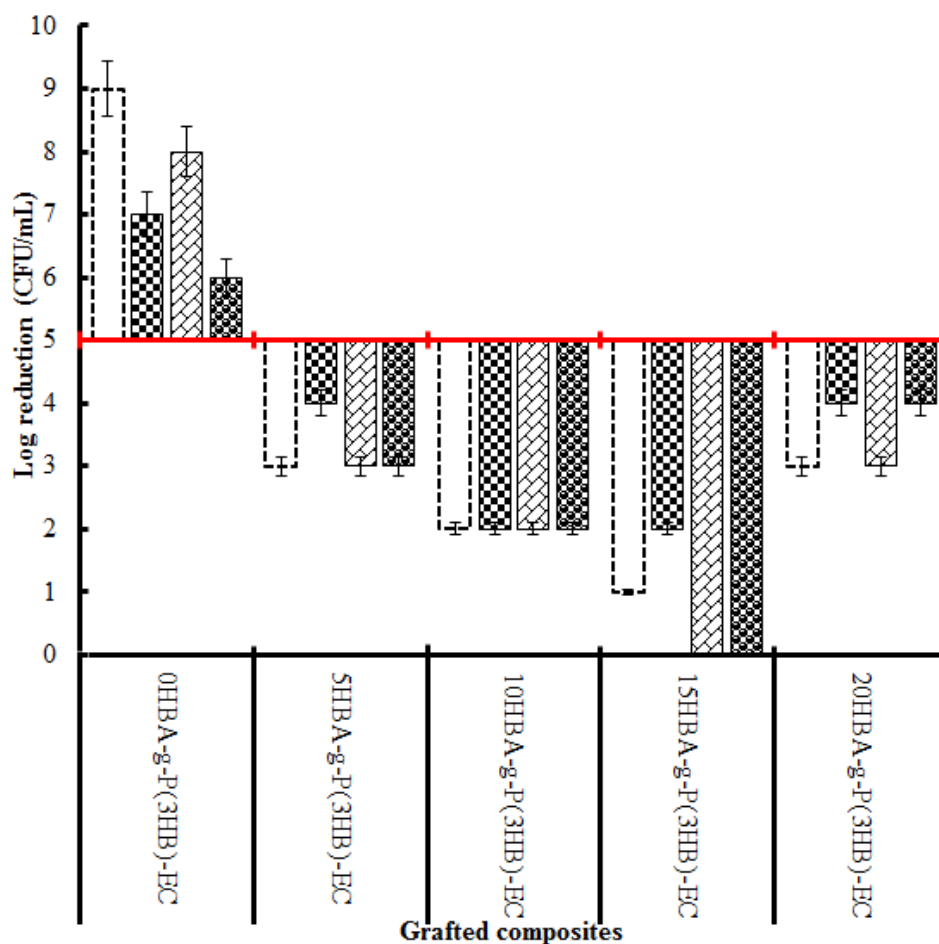
Figure 5.12 Evaluation of antimicrobial potential of *p*-4-hydroxybenzoic acid grafted P(3HB)-EC based bio-composites against various Gram-positive and Gram-negative bacterial strains *i.e., B. subtilis* NCTC 3610 (▢); *S. aureus NCTC* 6571 (▧); *E. coli NCTC* 10418 (▨) and *P. aeruginosa NCTC* 10662 (▩). Red line indicates an initial bacterial count *i.e.,* 1×10^5 CFU/mL. An increase in this count (as compared to the initial bacterial count) showed susceptibility whereas, reduction in the initial bacterial count showed bacteriostatic and bactericidal activities of the respective composites. A 2 log reduction was considered to claim an antibacterial activity.
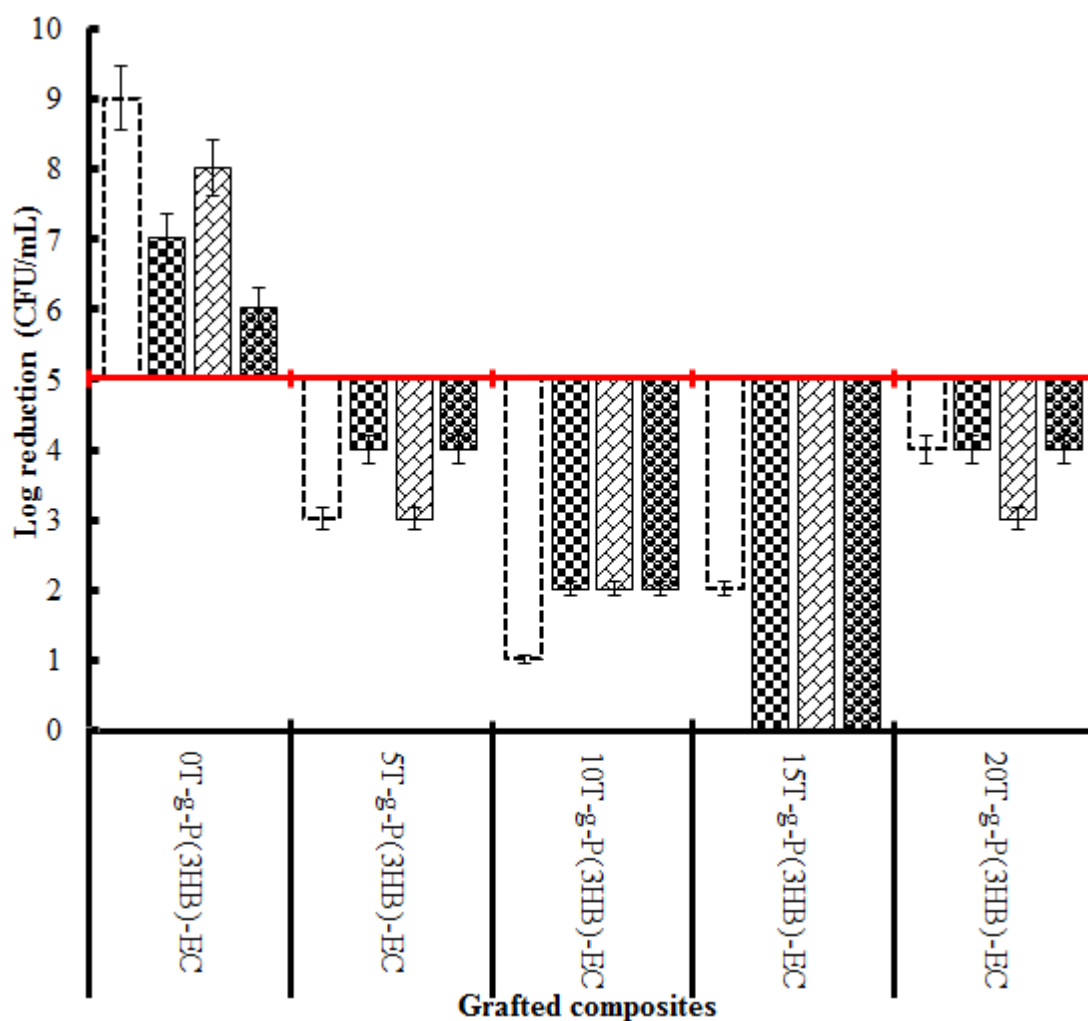
Figure 5.13 Evaluation of antimicrobial potential of thymol grafted P(3HB)-EC based bio-composites against various Gram-positive and Gram-negative bacterial strains *i.e., B. subtilis* NCTC 3610 (▢); *S. aureus NCTC* 6571 (▨); *E. coli NCTC* 10418 (▧) and *P. aeruginosa NCTC* 10662 (▨). Red line indicates an initial bacterial count *i.e.,* 1×10^5 CFU/mL. An increase in this count (as compared to the initial bacterial count) showed susceptibility whereas, reduction in the initial bacterial count showed bacteriostatic and bactericidal activities of the respective composites. A 2 log reduction was considered to claim an antibacterial activity.

5.2.4. *In-vitro* bio-compatibility

In recent years, cellulosic-based composites have been widely employed in various sectors particularly in bio-medical fields and medical devices in the areas of wound

healing, tissue engineering and/or implants applications. In this perspective, the newly synthesised bio-composites, are anticipated to exhibit excellent HaCaT compatibility, potentially favourable for cell proliferation. It is generally believed that the behaviour of cells on a biomaterial is related to their biocompatibility with that material. Once the cells are brought to contact with the biomaterial, they will undergo their morphological changes to stabilize the cell–material interface. Therefore, the whole process of cell adhesion and consequently their spreading consists of cell attachment, filopodial growth, cytoplasmic webbing, and the ruffling of peripheral cytoplasm progressing (Ma *et al*., 2002; Wang *et al*., 2014).

The cell viability and adherent morphology of the human keratinocyte-like HaCaT skin cells on as-prepared and selected composites *i.e.,* 20CA-*g*-P(3HB)-EC, 15GA-*g*-P(3HB)-EC, 15HBA-*g*-P(3HB)-EC and 15T-*g*-P(3HB)-EC were evaluated in this study. Initially, it was observed that after 1 and 3 days of incubation all of the composites supported the percent viability of HaCaT cells to different extent. More specifically, after 3 days of incubation 20CA-*g*-P(3HB)-EC was found with highest HaCaT percent viability (78%) followed by 15T-*g*-P(3HB)-EC, 15GA-*g*-P(3HB)-EC and 15HBA-*g*-P(3HB)-EC with 69%, 65% and 55% HaCaT viability, respectively, under the same environment. This was also supported qualitatively by the light microscope images shown in Figure 5.15, where the extent of cell adhesion on the phenol grafted bio-composites *i.e*., CA-*g*-P(3HB)-EC, 5GA-*g*-P(3HB)-EC, 15HBA-*g*-P(3HB)-EC and 15T-*g*-P(3HB)-EC can be compared to a P(3HB)-EC (control) specimen. However, it was interesting to note that all of the aforementioned composites displayed 100% cell viability after 5 days of incubation (Fig. 5.14), indicating that the test composites were non-cytotoxic under *in-vitro* cell culture conditions, thus could promote the adhesion of HaCaT cells. Additionally, the

morphologies of cell cultured from all of the test composites displayed oval/round, flat and scale-like ('squamous') shape at day 5 (Figure 5.15), However, after incubating for 5 days the viability rate revealed no differences among all groups, because the cells became saturated on the surface of the tested composites, and no cytotoxicity was observed in all of the test specimens.
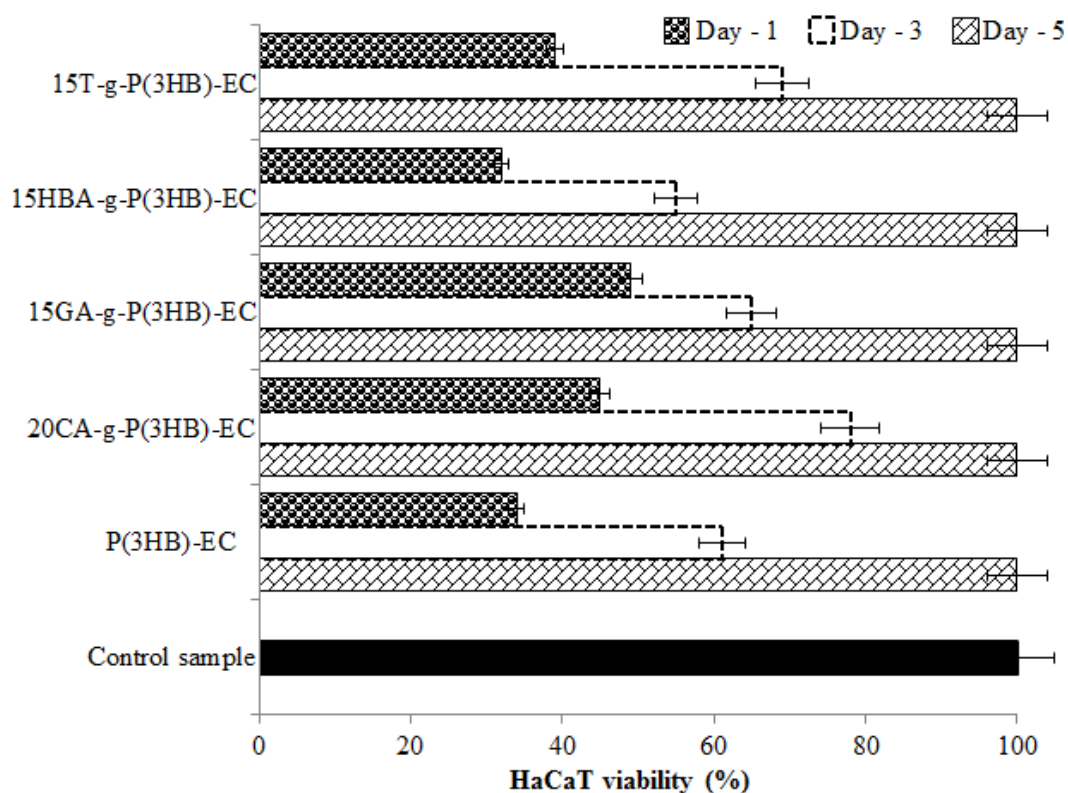
Figure 5.14 Neutral red dye concentration dependent percentage cell viability of human keratinocyte-like HaCaT cells seeded onto the selected bio-composites *i.e.,* 20CA-*g*-P(3HB)-EC, 15GA-*g*-P(3HB)-EC, 15HBA-*g*-P(3HB)-EC and 15T-*g*-P(3HB)-EC surfaces for prescribed periods (mean ± SD, n = 3).

The HaCaT cells responded to the test composites by exhibiting good attachment and spreading (Fig. 6.15). The number of cells attached to each sample surface increased with the extension of culture incubation from day 1 to day 5 using DMEM. Moreover, the growing HaCaT cells demonstrated normal cell morphology with their typical shape. Furthermore, after long-term culture (5 days), no visual differences could be found among all of the test specimens; HaCaT cells covered almost the whole surfaces to form cell layers on the surfaces at 5 days. The whole process of cell adhesion after contact with the test materials, and consequently their spread, consists of cell attachment, filopodial growth, cytoplasmic webbing, and the ruffling of peripheral cytoplasm progressing (Ma *et al*., 2002; Wang *et al*., 2014). It is well known that roughness and porosity of the composite materials greatly influence the cell adhesion and proliferation. Besides, surface polar entities content is also an important factor because HaCaT cells are mainly attached by carbonyl and carboxyl groups, thus their cell growth tends to be favoured in hydrophilic surfaces (Lehocký *et al*., 2006; Peschel *et al*., 2007; Lehocký *et al*., 2009; García *et al*., 2010).
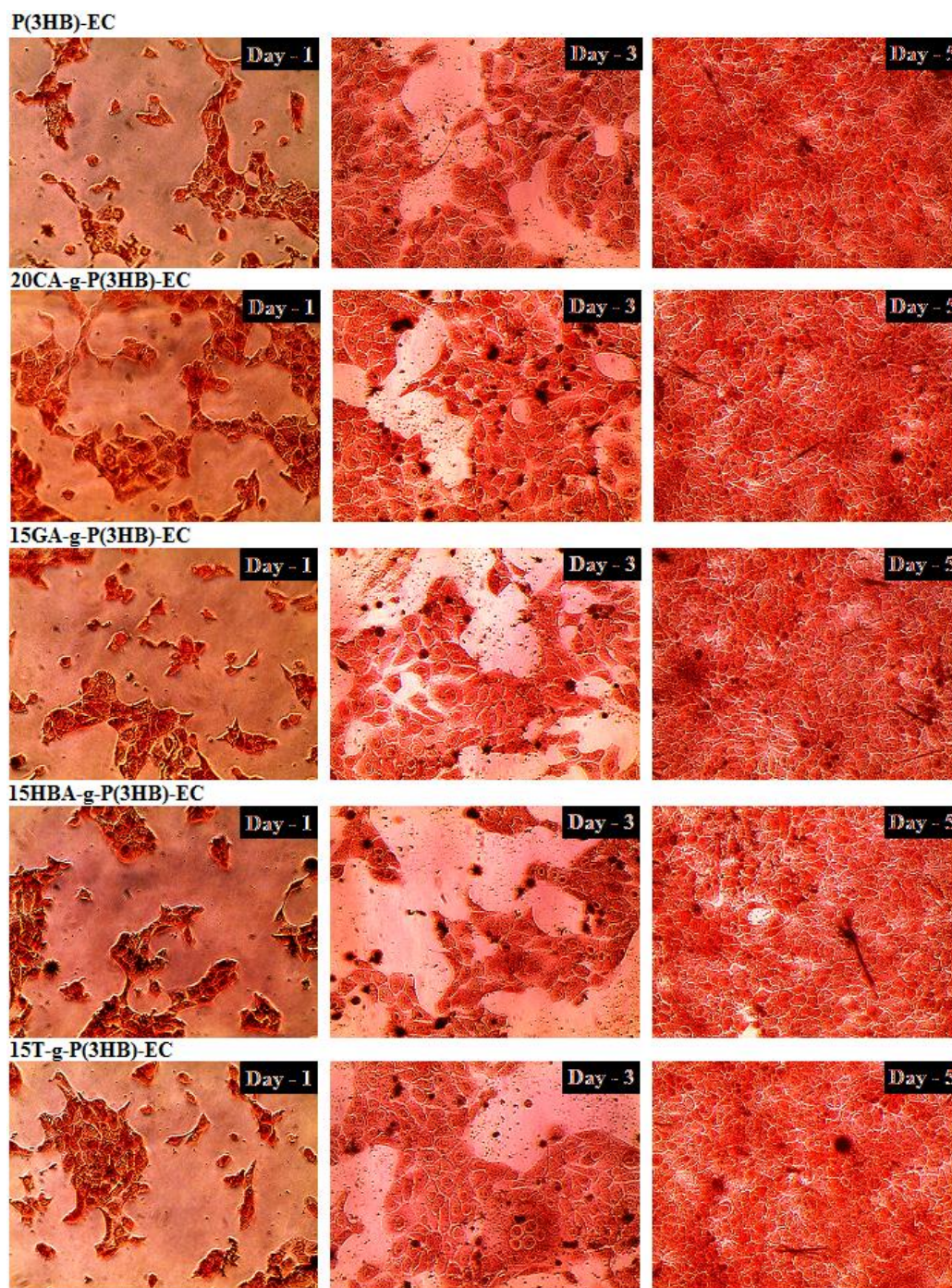
Figure 5.15 Adherent morphology of stained images of human keratinocyte-like HaCaT cells seeded onto the selected bio-composites *i.e.,* 20CA-*g*-P(3HB)-EC, 15GA-*g*-P(3HB)-EC, 15HBA-*g*-P(3HB)-EC and 15T-*g*-P(3HB)-EC for prescribed periods (1, 3 and 5 Days). All of the test samples were stained using neutral red dye (5 mg/mL) for 1 h followed by three consecutive washings with PBS at an ambient temperature. All images were taken at 100× magnification.

5.2.5. Soil burial degradation

Figure 5.16 (A-F) shows the soil burial degradation profiles of the untreated P(3HB)-EC, 20CA-*g*-P(3HB)-EC, 15GA-*g*-P(3HB)-EC, 15HBA-*g*-P(3HB)-EC and 15T-*g*-P(3HB)-EC composites buried in soil up to 6 weeks. A significant difference was recorded in the degradation rate of the untreated P(3HB)-EC as compared to the phenol incorporated composites. More specifically, over a 4-week burial period, all of the test composites degraded faster than the control (untreated P(3HB)-EC). The faster degradation rate of the test composites can be explained through swelling ratio, one of the grafting parameters. It is evident that the swelling capability is linked to the water absorption capacity of the polymers and plays a crucial role in degradability by causing the hydrolysis of surfaces and interfaces (Vieira *et al*., 2011; Tham *et al*., 2014). A lower swelling ratio or lower water absorption capacity results in a decrease in the soil burial degradation rate of the composites (Alvarez *et al*., 2006; Cocca *et al*., 2015). In the nature, cellulosic-based materials can be degraded by a wide spectrum of microorganisms harbouring cellulolytic or ligninolytic enzymes. Brown rot fungi are more effective in decomposing cellulose and hemicellulose, whereas, white rot fungi are capable of degrading phenol containing structures. Several processes in the degradation of the polymers may be proposed. These include hydrolysis, cracking, de-bonding, and degradation by microorganisms (Alam *et al*., 2014). After 42 days of incubation the order of degradation was as follows: 15GA-*g*-P(3HB)-EC > 20CA-*g*-P(3HB)-EC > 15HBA-*g*-P(3HB)-EC > 15T-*g*-P(3HB)-EC > P(3HB)-EC.
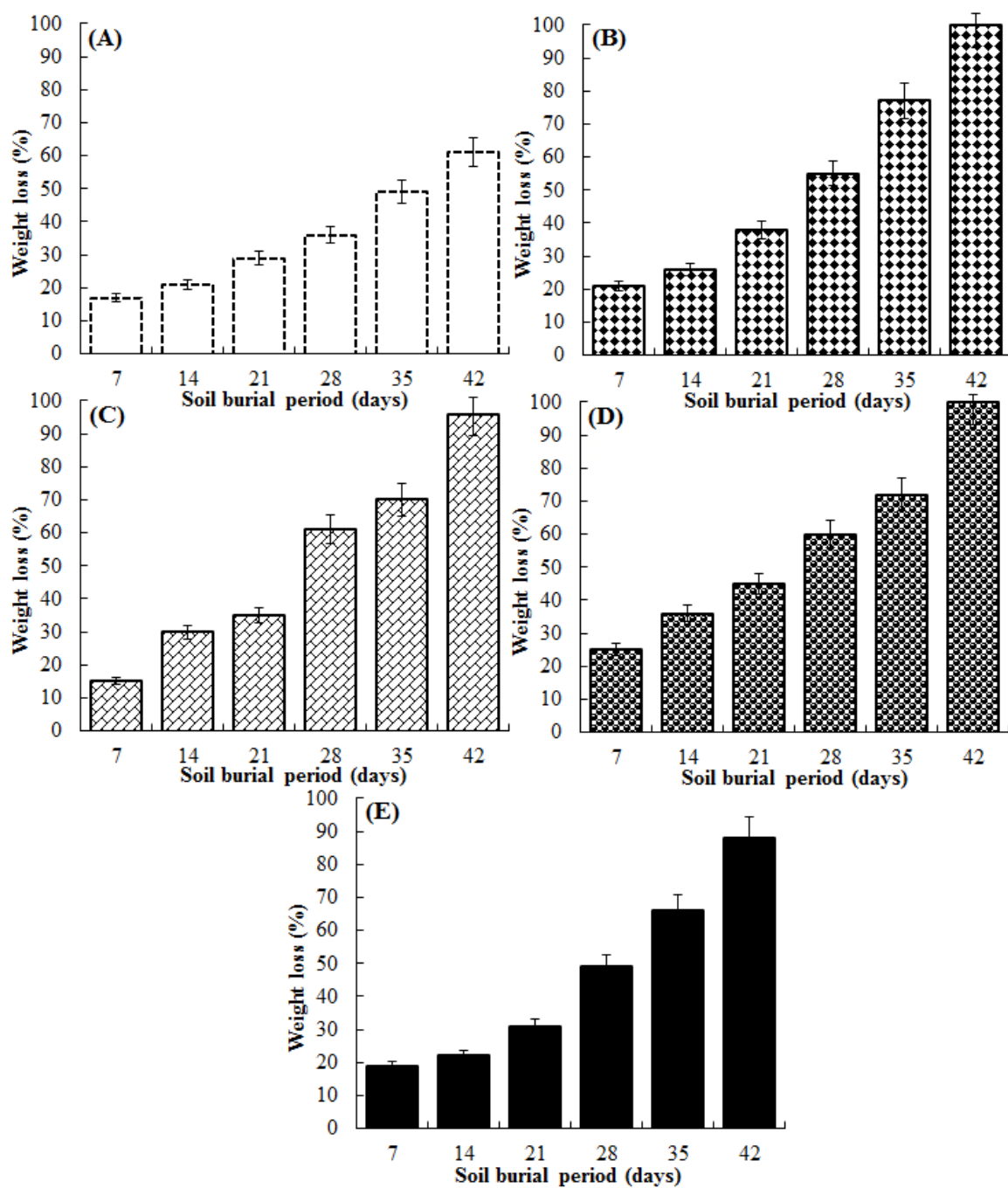
Figure 5.16 Effect of soil burial period on the biodegradability in terms of percentage weight loss; (A) P(3HB)-EC, (B) 20CA-*g*-P(3HB)-EC, (C) 15GA-*g*-P(3HB)-EC, (D) 15HBA-*g*-P(3HB)-EC and (E) 15T-*g*-P(3HB)-EC composites buried for prescribed periods (mean ± SD, n = 3).

5.3. Concluding remarks

In conclusion, this project has provided a series of novel composites with natural phenols as functional entities which display excellent antibacterial activity against Gram-positive and Gram-negative bacterial strains. Cell viability of the tested composites against HaCaT cells was 100% after 5 days of control incubation using DMEM media. Furthermore, soil burial profile demonstrated that these composites were biodegradable to a different extent and thus do not cause any deleterious ecological impact on the natural ecosystem. The improved resistance against a wide spectrum of microbes as well as the biodegradability and biocompatibility with HaCaT cell line indicate that the newly developed composites have great potential to be used in biomedical applications.

5.4.1. Fourier Transform Infrared spectroscopy (FT-IR)

An FT-IR spectroscopy was used to examine the functional and elemental groups of the control and enzymatically treated samples after grafting four different concentrations of the phenolic compound ranging from 5 to 20 mM. The phenolic compound used in this study was caffeic acid (CA), and it was grafted onto the baseline material P(3HB)-g-EC (presented and discussed in Chapter 3). The results are shown below in Figure 5.17. In comparison to the untreated caffeic acid, an increase in absorbance at the 1,720 cm^{-1} (C=O) band, and 1,050-1,300 cm^{-1} (C–O) group was noticed after treatment. The peaks at 3,396 cm^{-1} and in a broad 3,100-3,470 cm^{-1} region can be attributed to -OH stretch. In Figure 5.17, CA-loaded composites show a band at 3,345 cm^{-1} corresponding to phenolic -OH stretching involving hydrogen bonding, and a peak at 1,360 cm^{-1} corresponding to -OH bending of the phenolic group (Rukmani and Sundrarajan, 2012).
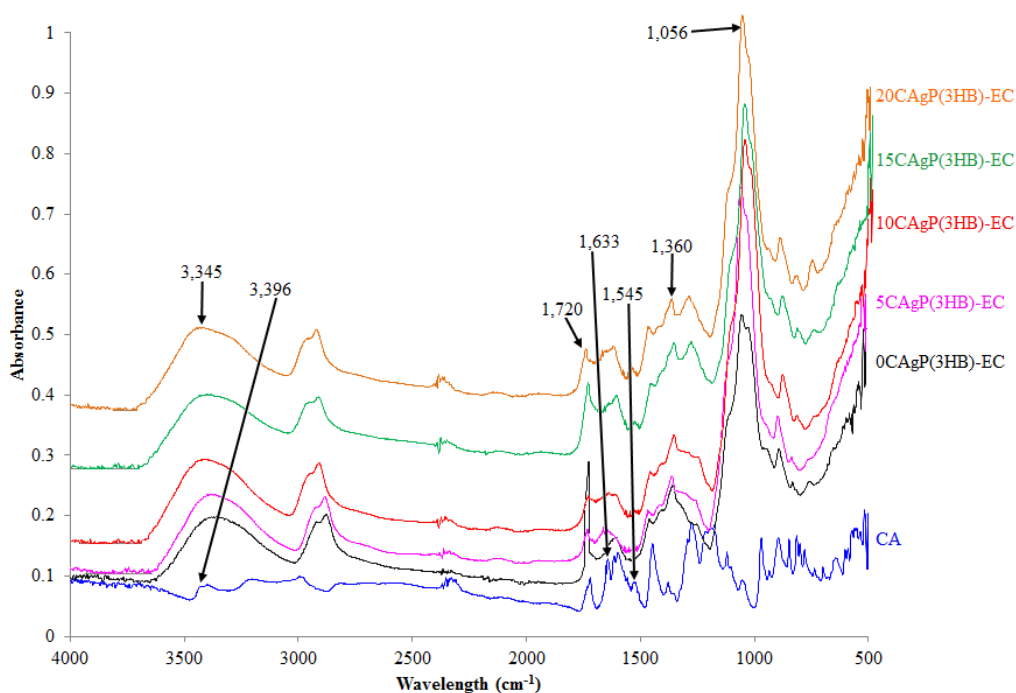
Figure 5.17 Typical FT-IR spectra of caffeic acid (CA) and CA-*g*-P(3HB)-EC composites prepared using laccase as a model catalyst.

The FT-IR spectra were used to characterise the structural element of the individual gallic acid (GA) and GA-*g*-P(3HB)-EC composite (shown in Figure 5.18). For GA-*g*-P(3HB)-EC, the absorptions at 3,345 cm^{-1}, 1,720 cm^{-1}, 1,360 cm^{-1}, and 1,056 cm^{-1} in the spectrum are indications of GA presence. The region between 1,260 cm^{-1} and 1,056cm^{-1} relates to the C–H and C–O–C bond stretching frequencies; a band at 2,985cm^{-1} is assigned to C–H vibration; the band range from 3,200 cm^{-1} to 3,400cm^{-1} corresponds to the vibration stretching of inter- and intramolecular hydrogen bonds of GA-*g*-P(3HB)-EC. The peak at 1000–1150 cm^{-1}, corresponding mainly to ethers (C–O–C), increased compared to phenolics monomers spectra, indicating extended polymerisation (Yamada *et al*., 2007). It has typical polyphenol characteristics showing a broad peak centred at 3,345 cm^{-1} which is due to the vibration of O–H linkages of phenolic OH groups. The characteristic peaks between 1,200-1,300 cm^{-1} and 1,450–1,600 cm^{-1} regions are due to the aromatic ring C=C stretching, and C=O stretching vibration, respectively.
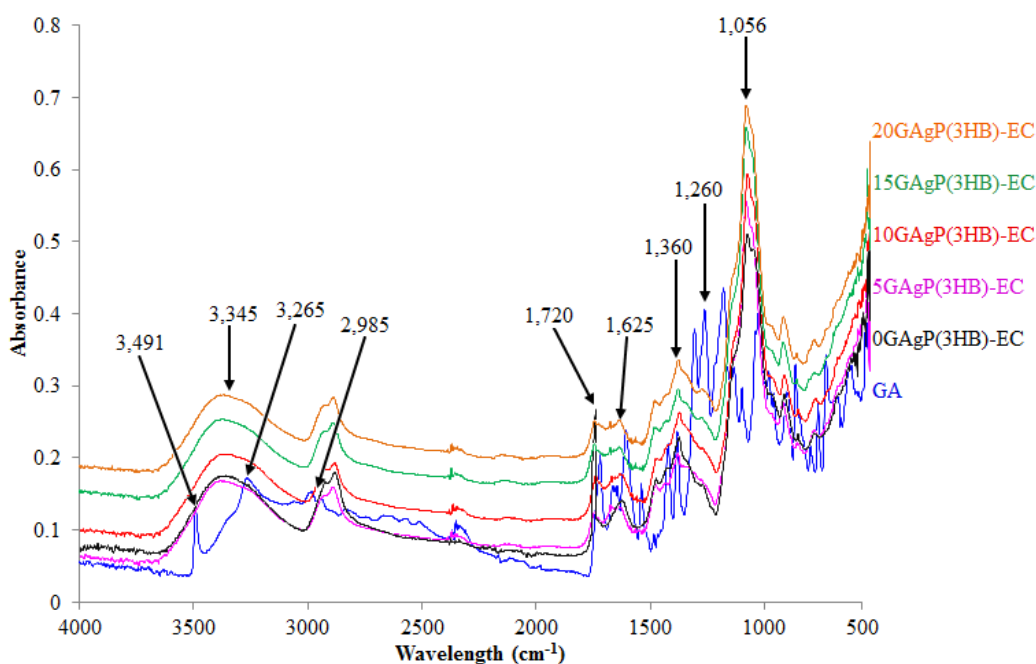
Figure 5.18 Typical FT-IR spectra of gallic acid (GA) and GA-*g*-P(3HB)-*g*-EC composites prepared using laccase as a model catalyst.

Typical IR spectra of the individual HBA, P(3HB)-*g*-EC and their laccase assisted HBA-*g*-P(3HB)-*g*-EC composites is shown in Figure 5.19. Evidently, the FT-IR spectral profile of the HBA-*g*-P(3HB)-EC was different in comparison to that of the pristine HBA profile. The appearance of strong peaks at 1,689 cm^{-1} and 1,607 cm^{-1} regions are accredited to C=O and COO$^-$ vibrations of HBA and HBA-*g*-P(3HB)-EC moieties, respectively. The bands at 1,446 cm^{-1} and 1,240 cm^{-1} wavelength regions are accredited to in-plane hydrogen bonding, which shifted to 1,360cm^{-1} and 1,056 cm^{-1} in the spectrum of the HBA-*g*-P(3HB)-EC composites. Whereas, the bands in the region 3,070-2,860 cm^{-1} are due to the aromatic and hetero aliphatic rings as well as accredited to C–H, CH$_2$ and CH$_3$ vibrational modes (Smith and Dent, 2005). The grafted composites have typical polyphenol attributes, due to the appearance of broad peaks cantered at 3,346 cm^{-1} and 1,446 cm^{-1} which are assigned to the vibrational mode of O-H linkages of phenolic and -OH groups.
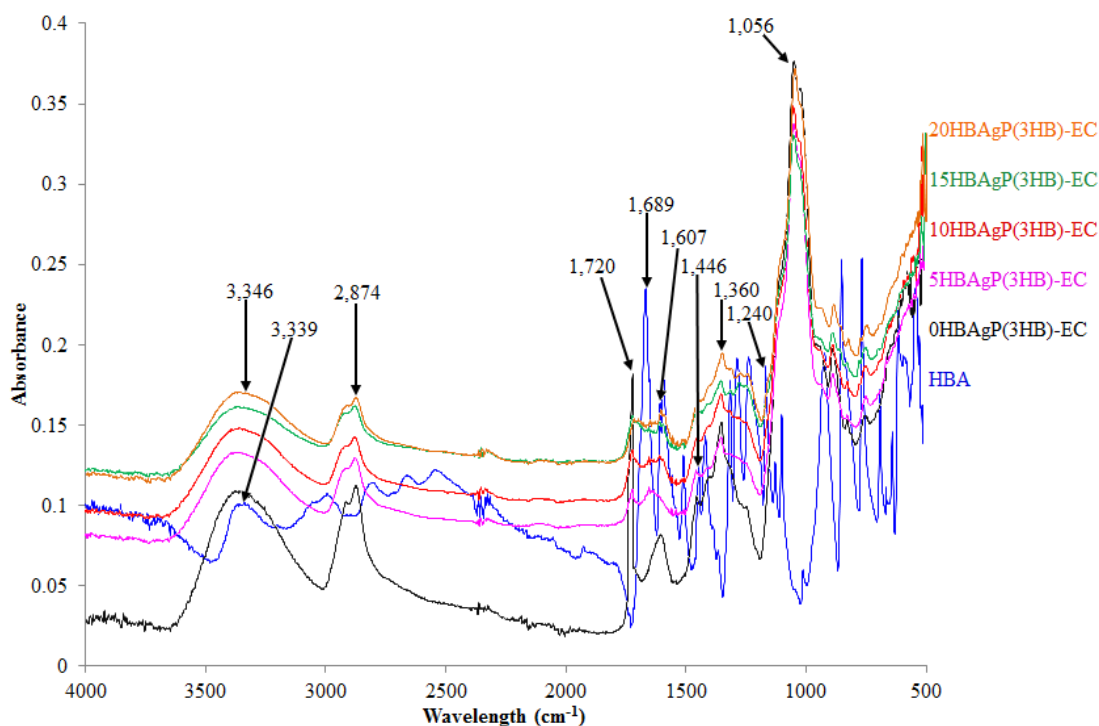
Figure 5.19 Typical FT-IR spectra of *p*-4-hydroxybenzoic acid (HBA) and HBA-*g*-P(3HB)-EC bio-composites prepared using laccase as a model catalyst.

The FT-IR spectra of T and T-*g*-P(3HB)-EC composites is presented in Figure 5.20. The most peaks at 738 cm^{-1} and 807 cm^{-1} are assigned to ring vibrations of the thymol (Schulz *et al*., 2003; Torres-Giner *et al*., 2014). The peaks around 3,300-3,400 cm^{-1} are assigned to hydrogen bonds and can be seen at the wavelength 3,360 cm^{-1}. The T-*g*-P(3HB)-EC spectra exhibit a different profile compared to the T monomers. The bands at 1,446 and 1,240 cm^{-1} are due to the in-plane -OH modes of two hydrogen bonds, which are shifted to 1,360 cm^{-1} and 1,056 cm^{-1} in the spectrum of the T-*g*-P(3HB)-EC samples. The bands in the 3,070–2,860 cm^{-1} region are assigned to the C–H, CH$_2$ and CH$_3$ vibrations. In the fingerprint region, there are the bands assigned to the aromatic and hetero aliphatic rings as well as to the CH$_2$ and CH$_3$ modes. By comparison between this and the T-*g*-P(3HB)-EC spectra, it can be seen that some bands changed intensity and/or shape during the graft formation process.
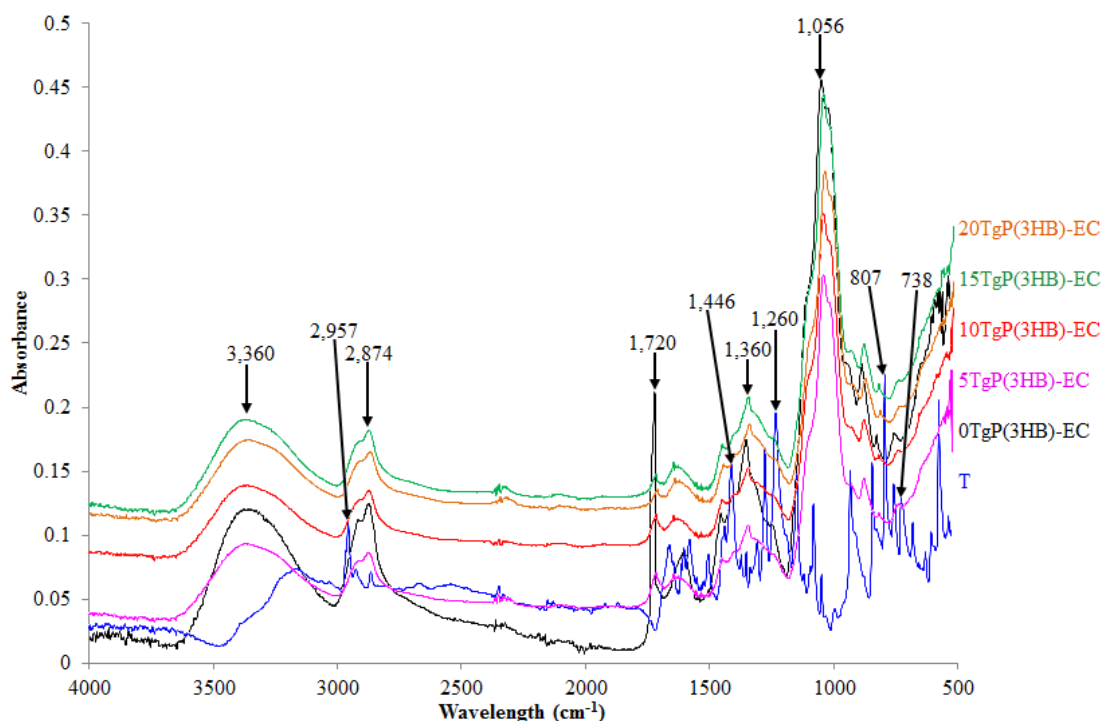
Figure 5.20 Typical FT-IR spectra of thymol (T) and T-*g*-P(3HB)-EC bio-composites prepared using laccase as a model catalyst.

Figure 5.21 illustrates a proposed mechanism of graft formation through laccase-assisted grafting of HBA (as a model phenolic structure) onto the P(3HB)-EC based material.
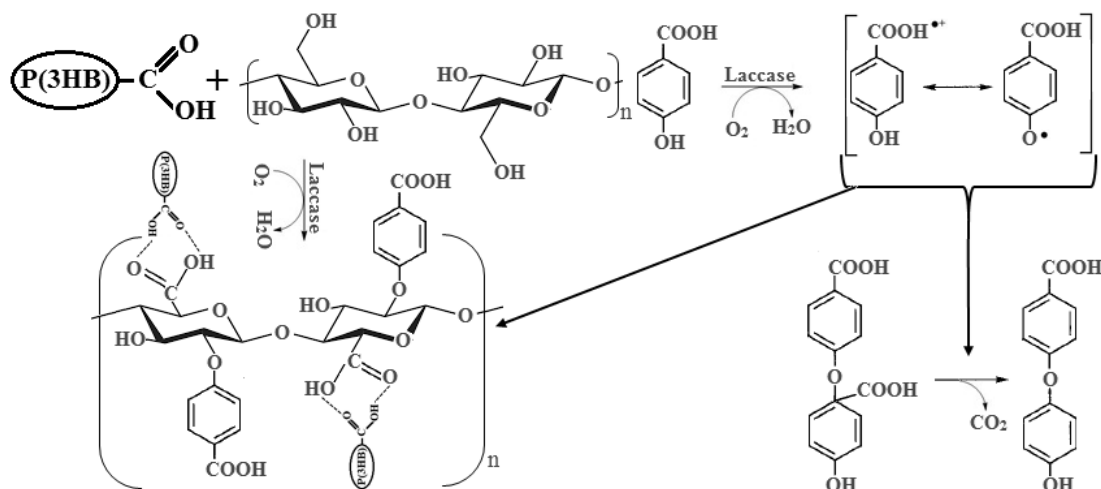
Figure 5.21 A proposed mechanism of graft formation through laccase-assisted grafting of *p*-4-hydroxybenzoic acid (as a model phenolic structure) onto the P(3HB)-*g*-EC based material.

5.4.2. Grafting parameters

The grafting parameters *i.e.,* graft yield (%GY), grafting efficiency (%GE) and swelling ratio (%SR) were evaluated as a result of surface dipping and incorporation (SDI) technique under an ambient environment. The results obtained are illustrated as mean values of three replicates in Figure 5.22, whereas, the standard error of means are shown as Y-error bars in Figure 5.22. The data revealed the increase in both the graft yield (%GY) and graft efficiency (%GE) reaching its maximum value at 15 mM CA concentration, then starts to decrease showing that higher concentrations do not promote further grafting (Figure 5.22). One possible reason for the observed behaviour could be the substantial amount of CA grafted onto the baseline composite, which creates steric hindrance for further grafting. The increase in monomer concentration

would be expected to increase both the grafting percentage which in turn increase the molecular weight of the graft composite (Aggour 2001; Constantin *et al*., 2011). Indeed, the results presented in Figure 8.6 indicate that as the concentration of CA increases from 0 to 15 mM both the %GY and %GE were optimal with an increase in the swelling ratio. The order of %SR observed was: 20CA-*g*-P(3HB)-EC > 15CA-*g*-P(3HB)-EC > 10CA-*g*-P(3HB)-EC > 5CA-*g*-P(3HB)-EC > 0CA-*g*-P(3HB)-EC. It has also been reported in literature that the reaction time is an important parameter which can increase or decrease the grafting parameters like graft yield, grafting efficiency and swelling behaviour (Sun *et al*., 2003; Constantin *et al*., 2011). This may be due to the decrease in the monomer concentrations, the retardation of diffusion after some polymer forms on the surface and/or the homo- polymerisation of phenolic monomers. It could also be due to a decrease in the number of available sites from the backbone material for further grafting (Lutfor *et al*., 2000).
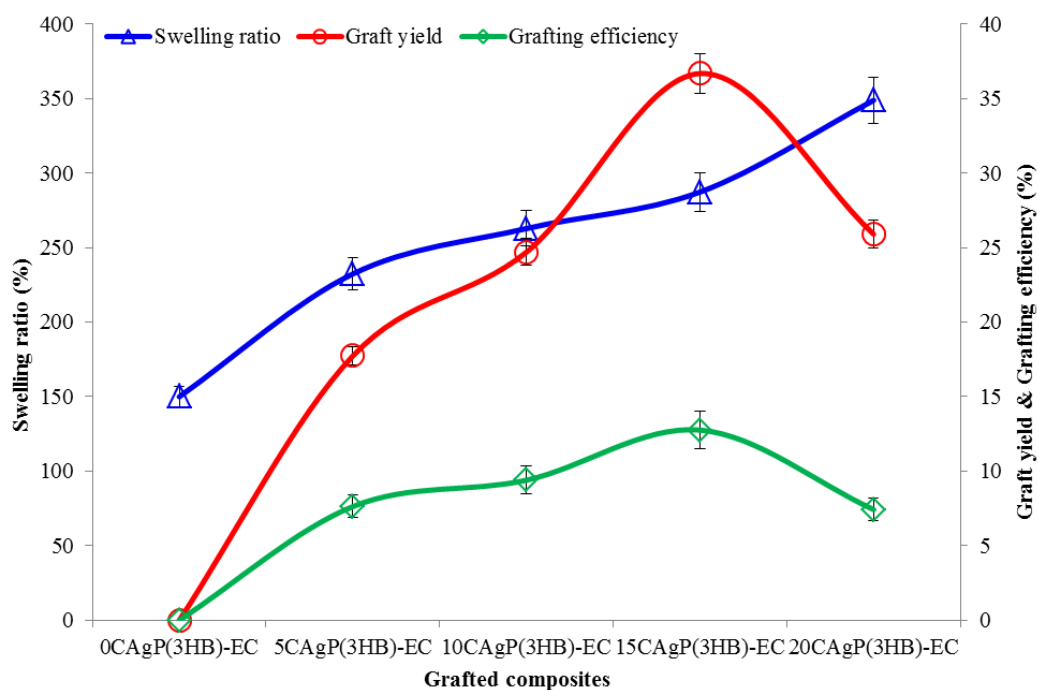
Figure 5.22 Evaluation of grafting parameters: graft yield (%GY), grafting efficiency (%GE) and swelling ratio (%SR) behaviours of CA-*g*-P(3HB)-EC bio-composites prepared using laccase as a model catalyst (mean ± SD, n = 3).

Figs. 5.23 and 5.24 show the grafting parameters (GP) *i.e.,* graft yield (%GY), grafting efficiency (%GE) and swelling ratio (%SR) profiles of GA-*g*-P(3HB)-EC *i.e.,* 0GA-*g*-P(3HB)-EC, 5GA-*g*-P(3HB)-EC, 10GA-*g*-P(3HB)-EC, 15GA-*g*-P(3HB)-EC and 20GA-*g*-P(3HB)-EC and T-*g*-P(3HB)-EC *i.e.,* 0T-*g*-P(3HB)-EC, 5T-*g*-P(3HB)-EC, 10T-*g*-P(3HB)-EC, 15T-*g*-P(3HB)-EC and 20T-*g*-P(3HB)-EC composites, respectively. A consistent increase in all of the grafting parameters, %GY, %GE and %SR was recorded up to the concentration of 15 mM GA, whereas, in the case of T 20 mM concentration was proved best under the same environment. However, further increase up to 20 mM GA concentration showed decreasing trend in aforementioned parameters. One possible reason for the observed behaviour could be the substantial amount of GA grafted onto the P(3HB)-EC composite, which creates steric hindrance for further grafting. The increase in monomer concentration would be expected to increase both the grafting percentage which in turn increase the molecular weight of the graft composite (Aggour, 2001; Constantin *et al*., 2011).
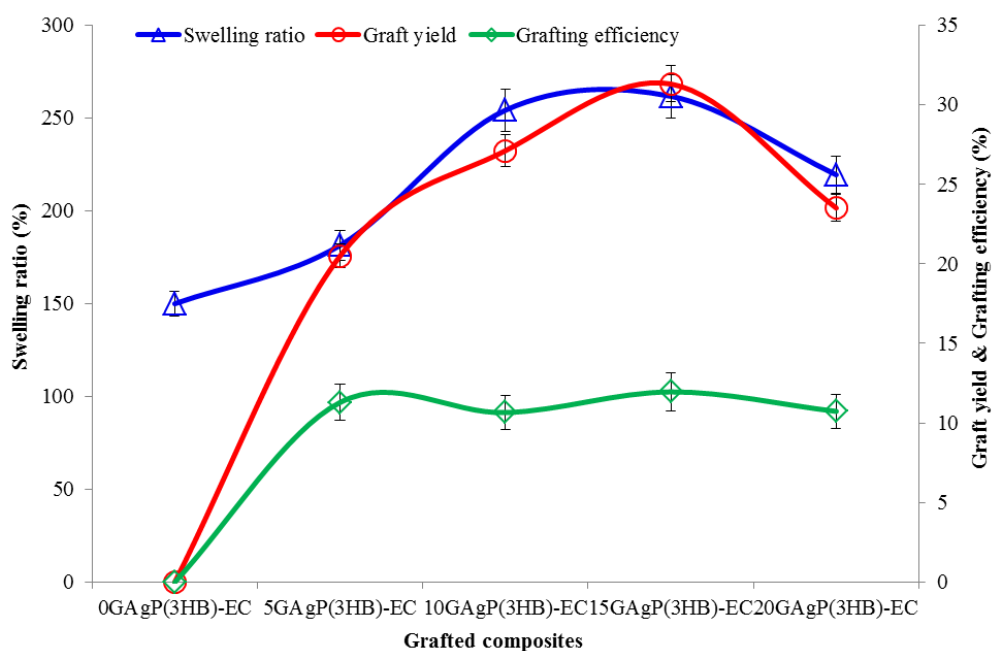
Figure 5.23 Evaluation of grafting parameters *i.e.,* graft yield (%GY), grafting efficiency (%GE) and swelling ratio (%SR) behaviours of GA-*g*-P(3HB)-EC bio-composites prepared using laccase as a model catalyst (mean ± SD, n = 3).

Indeed, the results presented in Figure 5.23 indicate that as the concentration of GA increases from 0 to 15 mM both the %GY and %GE were optimal with an increase in the swelling ratio. The orders of %GP observed for GA-*g*-P(3HB)-EC and T-*g*-P(3HB)-EC composites were: 15GA-*g*-P(3HB)-EC > 10GA-*g*-P(3HB)-EC > 20GA-*g*-P(3HB)-EC > 5GA-*g*-P(3HB)-EC > 0GA-*g*-P(3HB)-EC and 20T-*g*-P(3HB)-EC > 15T-*g*-P(3HB)-EC > 10T-*g*-P(3HB)-EC > 5T-*g*-P(3HB)-EC > 0T-*g*-P(3HB)-EC, respectively. Figure 5.25 shows the effect of HBA concentration on the grafting parameters of the HBA-*g*-P(3HB)-EC *i.e.,* 0HBA-*g*-P(3HB)-EC, 5HBA-*g*-P(3HB)-EC, 10HBA-*g*-P(3HB)-EC, 15HBA-*g*-P(3HB)-EC and 20HBA-*g*-P(3HB)-EC composites. An increase in all of the grafting parameters *i.e.,* GY%, GE% and SR% was recorded up to 20 mM HBA concentration. Indeed, the grafting parameters profile presented in Figure 5.25 indicates that as the concentration of HBA increases from 0 to 20 mM both the %GY and %GE were optimal with an increase in the swelling ratio. The order of grafting parameters observed was as follows: 20HBA-*g*-P(3HB)-EC > 15HBA-*g*-P(3HB)-EC > 10HBA-*g*-P(3HB)-EC > 5HBA-*g*-P(3HB)-EC > 0HBA-*g*-P(3HB)-EC composites. Aggour, 2001, observed similar phenomenon with an increase in the grafting percentage due to the increase in monomer concentration, which in turn intensifies the molecular weight of the grafted composite (Aggour, 2001; Constantin *et al*. 2011).
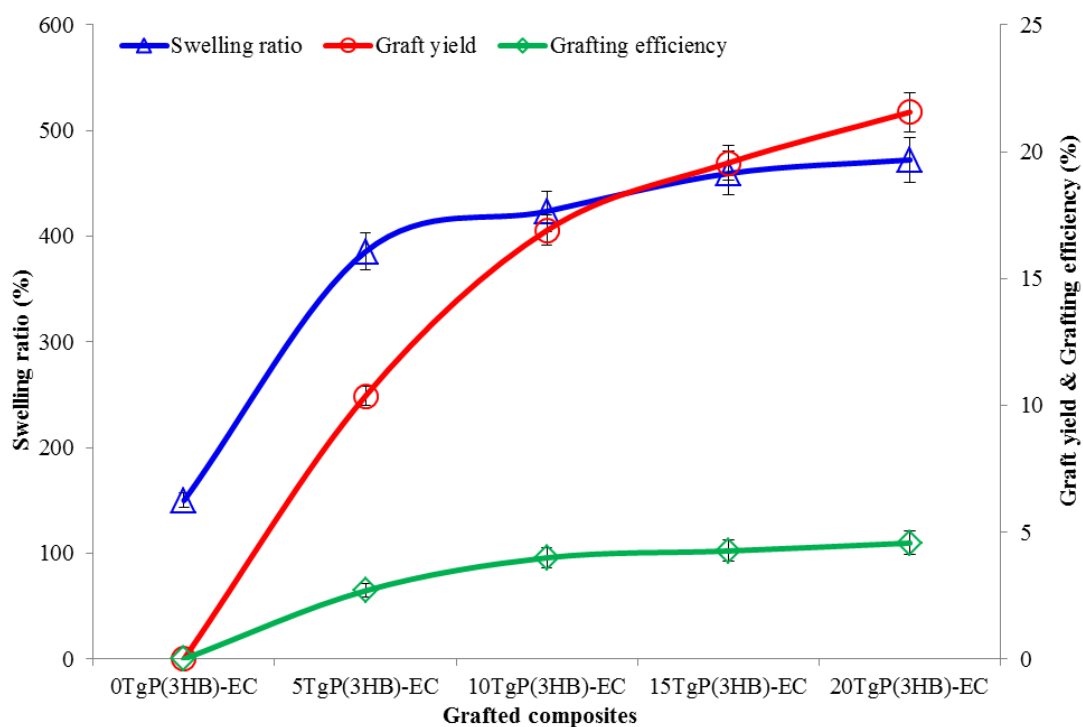
Figure 5.24 Evaluation of grafting parameters *i.e.,* graft yield (%GY), grafting efficiency (%GE) and swelling ratio (%SR) behaviours of T-*g*-P(3HB)-EC bio-composites prepared using laccase as a model catalyst (mean ± SD, n = 3).
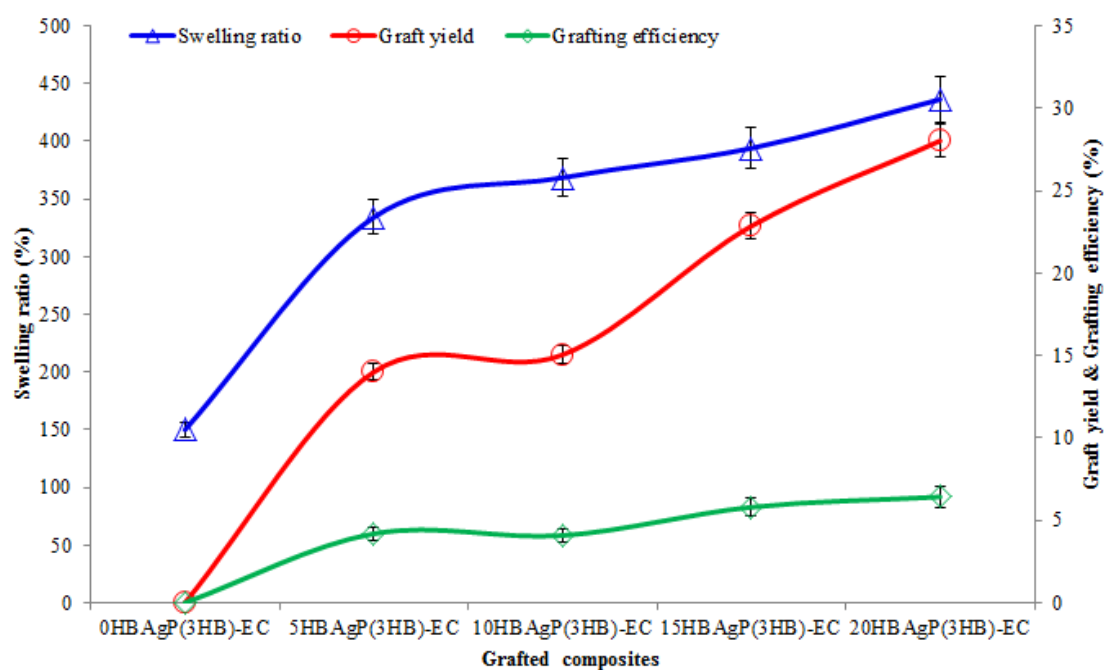
Figure 5.25 Evaluation of grafting parameters *i.e.,* graft yield (%GY), grafting efficiency (%GE) and swelling ratio (%SR) behaviours of HBA-*g*-P(3HB)-EC bio-composites prepared using laccase as a model catalyst (mean ± SD, n = 3).

161

5.4.3. Anti-bacterial activity

The anti-bacterial potential of CA-*g*-P(3HB)-EC composites were tested against Gram-positive and Gram-negative strains. As shown in Figure 5.26, after 24 h incubation the remaining bacterial counts decreased with increasing CA content on the surface of P(3HB)-EC, and this trend was maximum at the concentration of 15mM CA. As can be observed in (Figure 5.26), a significant antibacterial potential was detected for sample (15CA-*g*-P(3HB)-EC) against *E. coli NCTC* 10418 and *P. aeruginosa* NCTC 10662 in comparison to the control sample and relative to other concentrations. However, the grafted sample without any CA was found ineffective against all of the tested microorganisms. A strong antibacterial activity from 15CA-*g*-P(3HB)-EC composite was recorded against Gram-negative bacteria as compare to the Gram-positive, which is, probably because of the difference between Gram-negative and Gram-positive bacteria in terms of cell structures and antimicrobial mechanism (Li *et al*., 2011; Dong *et al*., 2014).
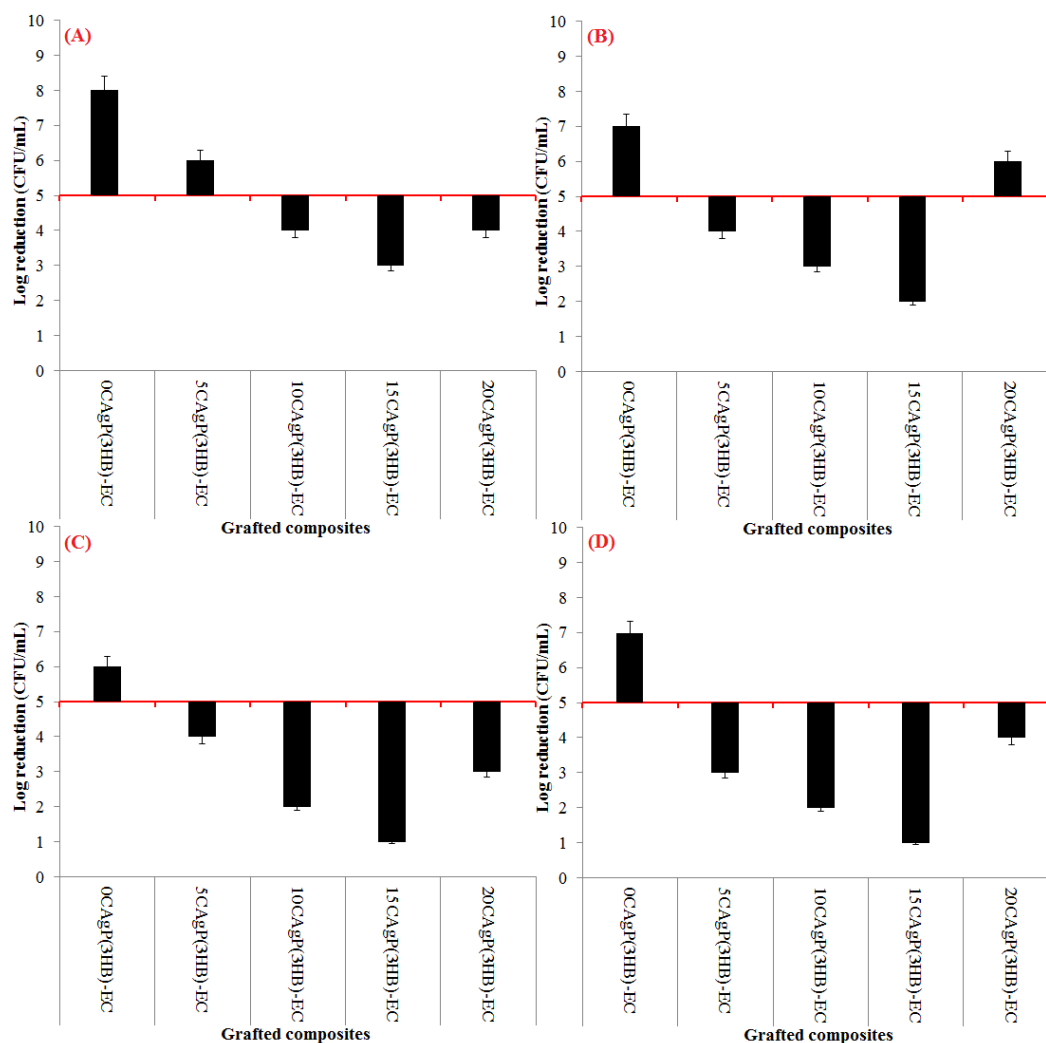
Figure 5.26 Evaluation of anti-bacterial potential of CA-*g*-P(3HB)-EC bio-composites against *B. subtilis* NCTC 3610 (A); *P. aeruginosa NCTC* 10662 (B); *E. coli NCTC* 10418 (C) and *S. aureus NCTC* 6571 (D) (mean ± SD, n = 3).

The results of the spread-plate method for GA-*g*-P(3HB)-EC composites against each bacterial strain are given in the Figure 5.27. 0GA-*g*-P(3HB)-EC used as a control, did not show any log reduction (CFU/mL) against *B. subtilis* NCTC 3610, *S. aureus* NCTC 6571, *E. coli NCTC* 10418 and *P. aeruginosa* NCTC 10662, thus showing no antibacterial activity. Whereas, 5GA-*g*-P(3HB)-EC and 20GA-*g*-P(3HB)-EC composites prepared with 5 and 20 mM GA concentration, respectively, did not show any activity to inhibit bacterial count against each of the above mentioned bacterial

species. However, the composite prepared by the incorporation of 10 and 15 mM GA onto P(3HB)-EC backbone material displayed excellent anti-bacterial activities against all of the tested species.
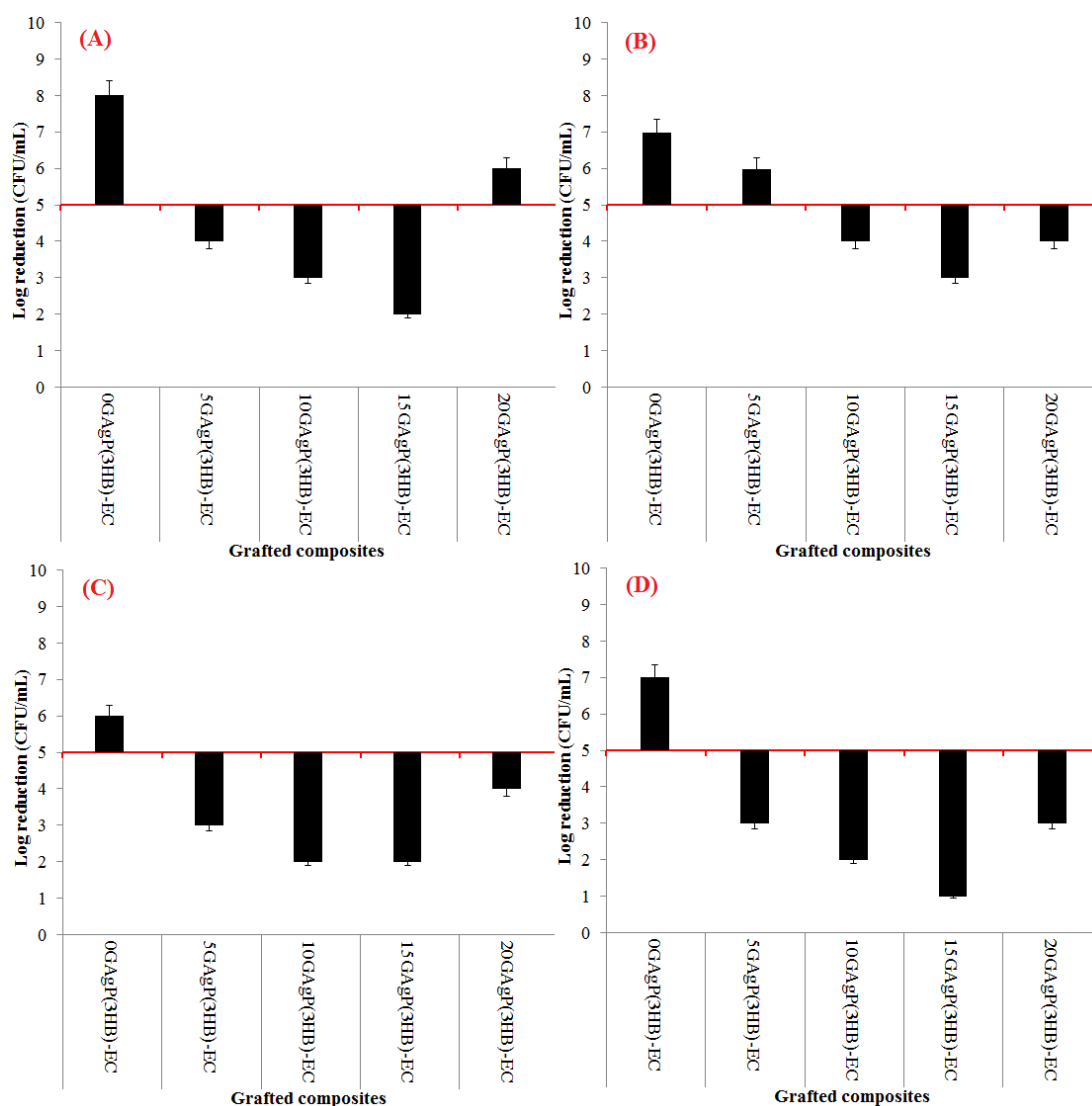
Figure 5.27 Evaluation of anti-bacterial potential of GA-*g*-P(3HB)-EC bio-composites against *B. subtilis* NCTC 3610 (A); *P. aeruginosa NCTC* 10662 (B); *E. coli NCTC* 10418 (C) and *S. aureus NCTC* 6571 (D) (mean ± SD, n = 3).

The anti-bacterial activity of the test composites versus *B. subtilis* NCTC 3610, *S. aureus* NCTC 6571, *E. coli* NTCT 10418 and *P. aeruginosa* NCTC 10662 strains, as

a function of thymol concentration is reported in Figure 5.28. For the samples prepared in the presence of laccase, the results clearly show that increasing the concentration of thymol enhanced the antibacterial activity, reaching a complete bactericidal effect at 20 mM concentration against the test microorganisms. As already seen in Figure 5.28, composites prepared with varying thymol concentrations (0 to 20 mM) in the presence of laccase produced a slight bacteriostatic effect on *B. subtilis* NCTC 3610 and *P. aeruginosa* NCTC 10662, but only under 15 and 20 mM concentrations.
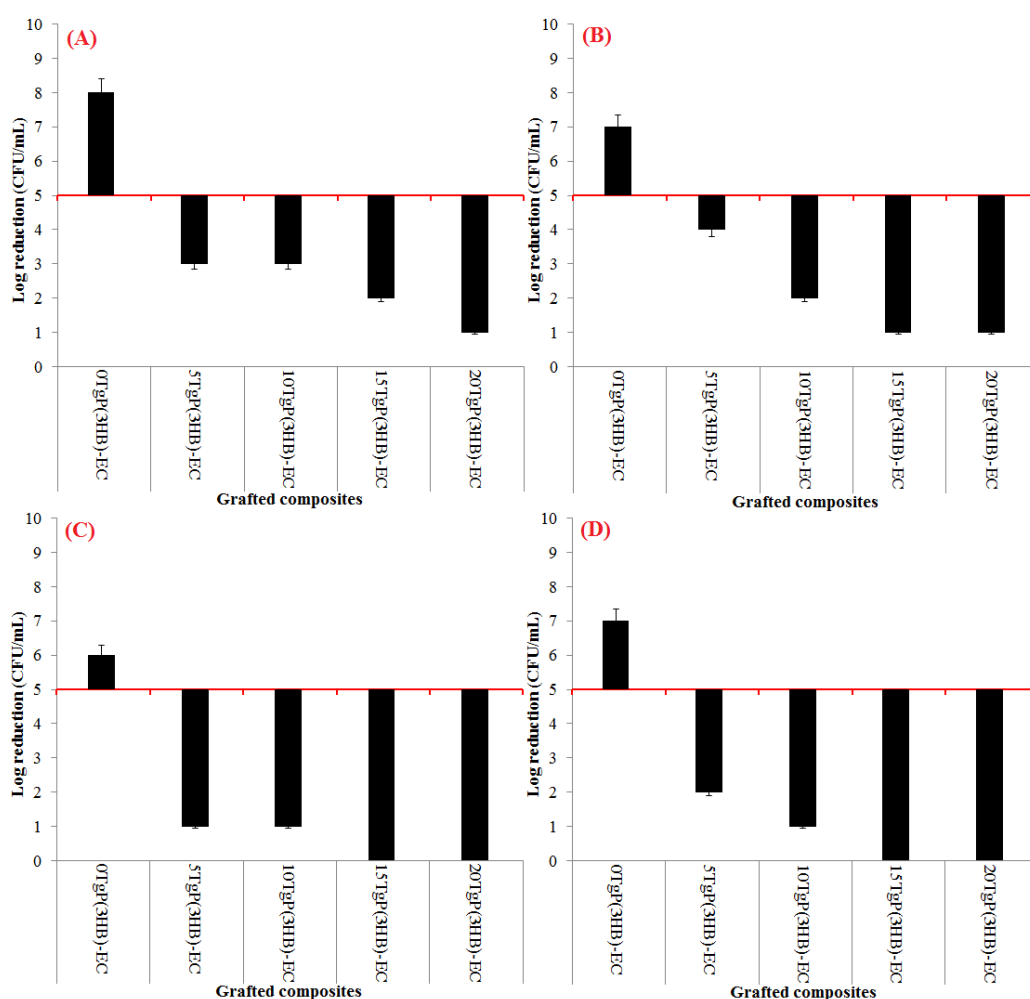
Figure 5.28 Evaluation of anti-bacterial potential of T-*g*-P(3HB)-EC bio-composites against *B. subtilis* NCTC 3610 (A); *P. aeruginosa NCTC* 10662 (B); *E. coli NCTC* 10418 (C) and *S. aureus NCTC* 6571 (D) (mean ± SD, n = 3).

The same composites showed a complete bactericidal effect on *E. coli NCTC* 10418 and *P. aeruginosa* NCTC 10662. The results of the counting test showed a complete bactericidal effect (100 % reduction of bacterial count) on *E. coli NCTC* 10418 and *S. aureus* NCTC 6571, from the graft composites prepared with 15 mM and 20 mM thymol concentrations. This is because the interaction between thymol and bacteria can change the metabolic activity of bacteria and eventually cause their death, however, the exact mechanism of the antimicrobial action of thymol is not established yet. Based on an earlier published data, thymol has the ability to disrupt the lipid structure of the bacterial cell wall, further leading to a destruction of the cell membrane, cytoplasmic leakage, and cell lysis which ultimately lead to cell death (Veras *et al*. 2012; Milovanovic *et al*. 2013; Shahidi *et al*., 2014).

The anti-bacterial activities of HBA-*g*-P(3HB)-EC composites were initially tested against *B. subtilis* NCTC 3610 and *E. coli NCTC* 10418 and the results obtained are shown in Fig. 5.29. For the control samples, after 24 h of incubation, a significant bacterial proliferation with an increase in the log value from 5 to 8 and 6 for *B. subtilis* NCTC 3610 and *E. coli NCTC* 10418, was recorded respectively. In contrast, for 15HBA-*g*-P(3HB)-EC and 20HBA-*g*-P(3HB)-EC composites, samples prepared with 15mM and 20mM HBA concentrations respectively, showed a clear bacteriostatic and bactericidal effects on *B. subtilis* NCTC 3610 and *E. coli NCTC* 10418, respectively, as for other composites, 5HBA-*g*-P(3HB)-EC and 10HBA-*g*-P(3HB)-EC were not as effective particularly against *B. subtilis* NCTC 3610. However, both composites showed a significant bacteriostatic activity against *E. coli NCTC* 10418 with a log reduction value from 5 to 2 and 1, respectively. The total log reduction value caused by 20HBA-*g*-P(3HB)-EC composite for *E. coli NCTC* 10418 and *B. subtilis* NCTC

3610 was 0 and 2, respectively in comparison to the control log value of 5 (Figure 5.29).
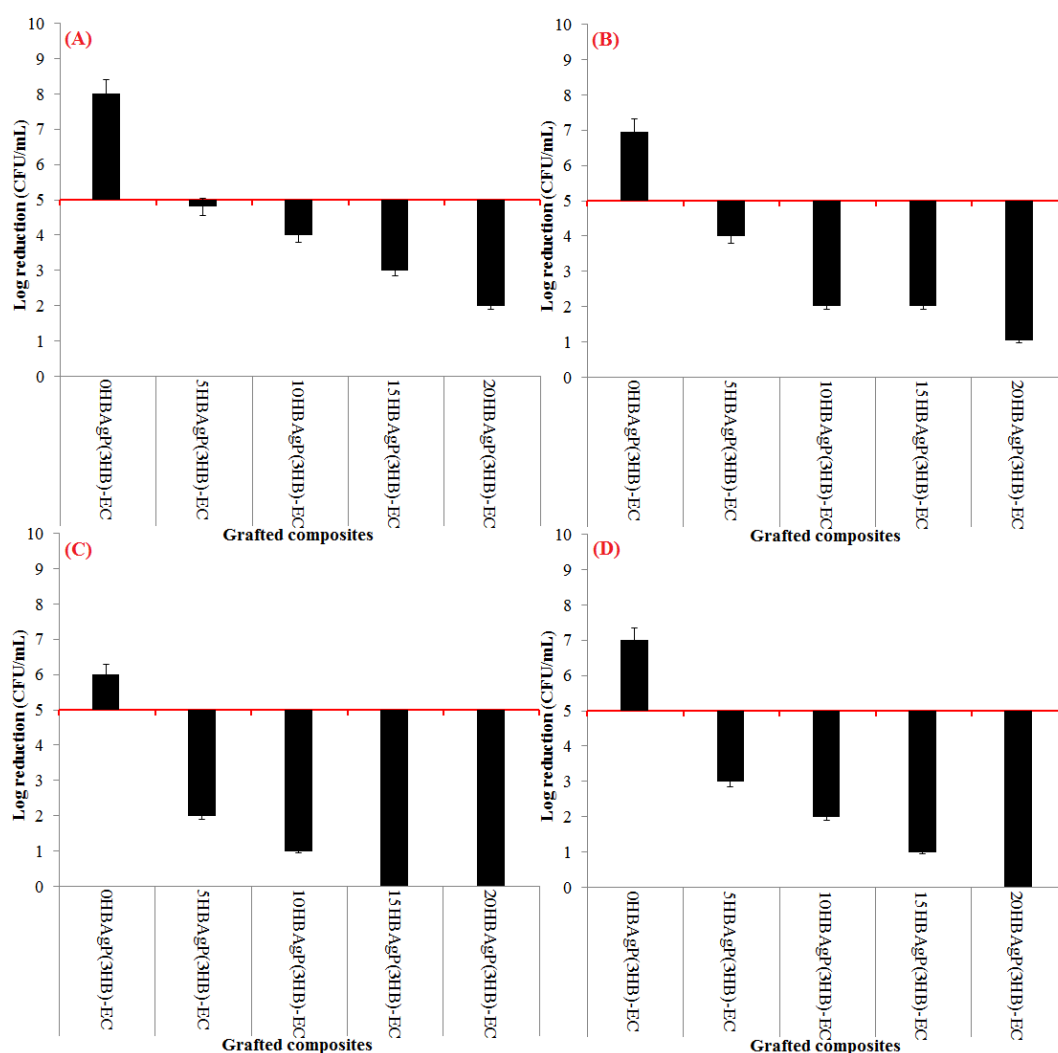
Figure 5.29 Evaluation of anti-bacterial potential of HBA-*g*-P(3HB)-EC bio-composites against *B. subtilis* NCTC 3610 (A); *P. aeruginosa NCTC* 10662 (B); *E. coli NCTC* 10418 (C) and *S. aureus NCTC* 6571 (D) (mean ± SD, n = 3).

5.4.4. *In-vitro* bio-compatibility

The cell viability of the grafted composites was determined quantitatively using neutral red assay. The non-toxicity of as-prepared and selected composites *i.e.* 15CA-

g-P(3HB)-EC, 15GA-*g*-P(3HB)-EC, 20HBA-*g*-P(3HB)-EC, and 20T-*g*-P(3HB)-EC was depicted by the % viability of the HaCaT cells and the results obtained are shown in Figure 5.30.
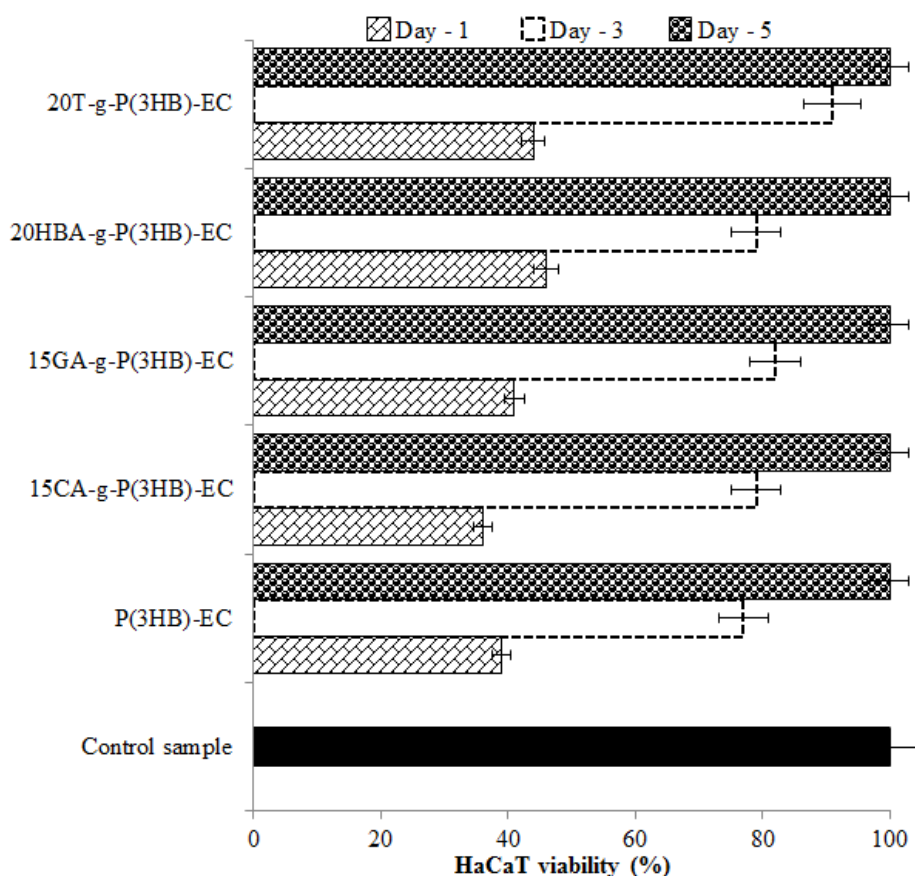
Figure 5.30 Neutral red dye concentration dependent percentage cell viability of human keratinocyte-like HaCaT cells seeded onto selected composites *i.e.,* 15CA-*g*-P(3HB)-EC, 15GA-*g*-P(3HB)-EC, 20HBA-*g*-P(3HB)-EC and 20T-*g*-P(3HB)-EC surfaces for prescribed periods (mean ± SD, n = 3).

The adherent morphologies of the HaCaT cells cultured on all of the test composites displayed irregular shapes after 5 days of incubation in 24-well tissue culture plates at a density of 1×10^5 cells per well, using culture media (DMEM). Previous reports have stated that the keratinocytes are irregular-shaped, enlarged and flattened, with

clear vacuoles in perinuclear cytoplasm (Rheinwald *et al*., 2002; Kang *et al*., 2003). Notably, irrespective of the type of phenol and its concentration, all of the tested composites displayed increasing cell viability up to 100% after 5 days of incubation (Figure 5.31), indicating that these composites were non-cytotoxic under *in-vitro* cell culture conditions, thus could be used to promote the adhesion of HaCaT cells. The morphology of HaCaT cells grafted onto the composites after 1, 3 and 5 days seeding is shown in Figure 5.31. HaCaT cells exhibited good attachment and spread. Moreover, the growing HaCaT cells demonstrated normal cell morphology with their typical shape, and spread covering the material surface. Furthermore, after long-term culture (5 days), HaCaT cells were distributed uniformly on the surfaces of the test composites and a confluent monolayer was formed on the fifth day as shown in Figure 8.15.
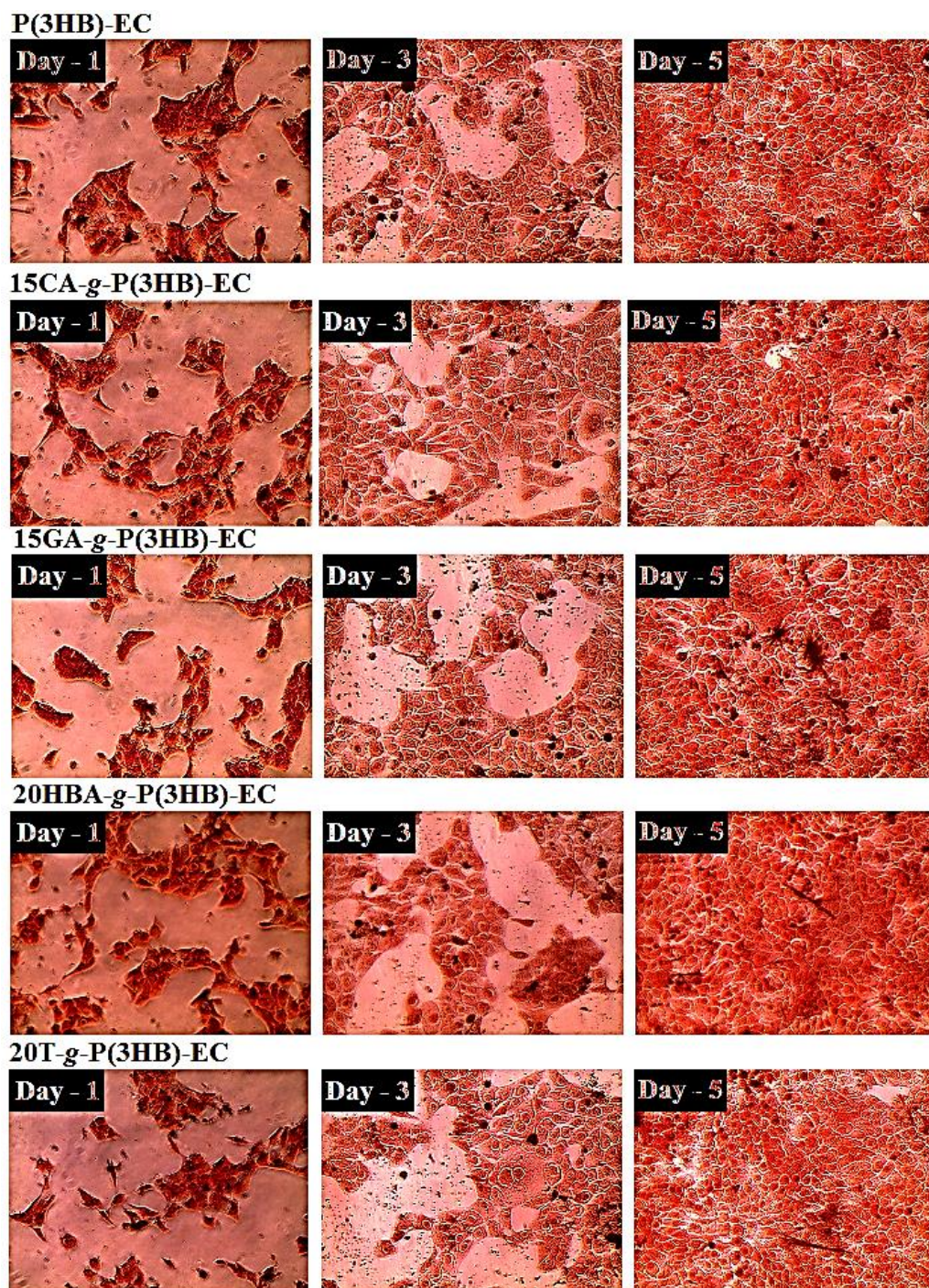
Figure 5.31 Adherent morphology of stained images of human keratinocytes-like HaCaT cells seeded onto the selected composites *i.e.,* 15CA-*g*-P(3HB)-EC, 15GA-*g*-P(3HB)-EC, 20HBA-*g*-P(3HB)-EC and 20T-*g*-P(3HB)-EC for prescribed periods (1, 3 and 5 Days). All of the test samples were stained using neutral red dye (5 mg/mL) for 1 h followed by three consecutive washings with PBS at an ambient temperature. All images were taken at 100× magnification.

5.4.5. Soil burial degradation

A soil burial degradation test was carried out to evaluate the biodegradation profile of the aforementioned composites. The degradation behaviour of P(3HB)-EC and all of the selected composites *i.e.,* 15CA-*g*-P(3HB)-EC, 15GA-*g*-P(3HB)-EC, 20HBA-*g*-P(3HB)-EC, and 20T-*g*-P(3HB)-EC was investigated by measuring the % weight loss of the test composites subjected to soil burial for 42 days. Figure 5.32 illustrates the % weight loss of the pristine base material in addition to the test composites as a function of degradation time. All of the composites showed an increased degradation rate to different extents during the burial process. According to the ASTM D6400-99 and ISO 14855 procedure, this is likely a result of the penetration of moisture (water) into the composites, causing the hydrolysis of surfaces and interfaces (Vieira *et al.*, 2011; Tham *et al.*, 2014).

As shown in Figure 5.32, after 42-days consecutive exposure, the weight loss of composites reaches 59% (w/w) for the pristine P(3HB)-EC base, 89% (w/w) for 15CA-*g*-P(3HB)-EC, 80% (w/w) for 15GA-*g*-P(3HB)-EC, 100% (w/w) for 20HBA-*g*-P(3HB)-EC and 100% (w/w) for 20T-*g*-P(3HB)-EC. The degradation profile revealed that the degradability of the phenol grafted composites is slightly higher than that of bare P(3HB)-EC base, which is possibly due to the higher hydrophobicity and lower surface tension properties of the P(3HB)-EC base composite (Iqbal *et al.*, 2014b). It has been reported already in literature that during soil burial the polymers' molecular chains degrade followed by their transformation into water and CO_2 after a long term degradation. Thus, it seems that the soil burial degradation mechanism involves a recyclable, green, and environment-friendly process to fully degrade the biodegradable polymeric composites (Alam *et al.*, 2014).

As it can be seen from Figure 5.32, a progressive increase in the degradation rate is recorded with the passage of time. More specifically, after 4 week of burial all of the test composites undergo a faster degradation. This behaviour can be well explained taking into account the results of the swelling ratio of the test composites demonstrating the high swelling linked to the water absorption capacity of the composites. Therefore, it seems evident that the swelling capability linked to the water absorption capacity plays a crucial role by causing the hydrolysis of surfaces and interfaces to determine the degradation kinetics of the composites (Vieira *et al*., 2011; Tham *et al*., 2014). On the contrary, a lower swelling ratio or lower water absorption capacity of the test composites induces a decrease in the soil burial degradation rate (Alvarez *et al*., 2006; Cocca *et al*., 2015). Finally, the appearance of grooves on the composites' surfaces was also observed, these grooves are attributed in the literature to the degradation, indicating that the degradation of the materials started not only from the cellulose fraction of the composite, but also from the phenolic and P(3HB) phase of the composite materials. It has already been well documented in literature that the degradation capability of various cellulolytic organisms, in the soil, to degrade cellulose or cellulose-based composites varies greatly with the physicochemical characteristics of the composites (Amano *et al*. 2001; Wan *et al*. 2009).
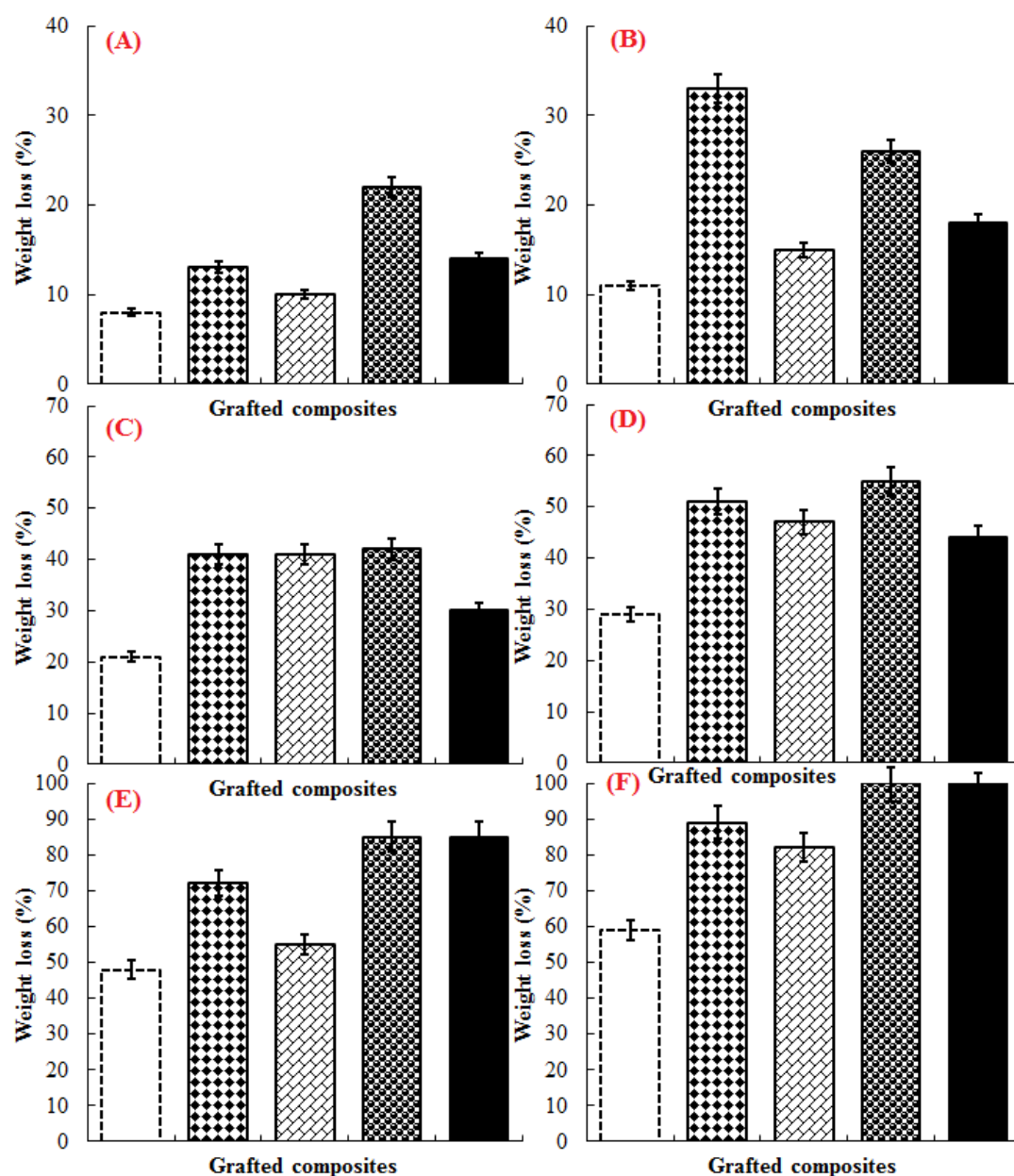
Figure 5.32 Effect of soil burial period on the bio-degradability in terms of percentage weight loss of P(3HB)-EC (⬚), 15CA-*g*-P(3HB)-EC (▨), 15GA-*g*-P(3HB)-EC (▨), 20HBA-*g*-P(3HB)-EC (▨) and 20T-*g*-P(3HB)-EC (■) buried for prescribed periods *i.e.,* (A) 7 days; (B) 14 days; (C) 21 days; (D) 28 days; (E) 35 days and (F) 42 days (mean ± SD, n = 3).

5.5. Concluding remarks

In conclusion, the newly synthesised laccase-assisted graft composites illustrated noteworthy antibacterial activity against various Gram-positive and Gram-negative strains together with compatibility with human keratinocyte-like HaCaT cell line. So, 15CA-*g*-P(3HB)-EC, 15GA-*g*-P(3HB)-EC, 20HBA-*g*-P(3HB)-EC, and 20T-*g*-P(3HB)-EC composites have considerable potential to be used for bio-medical type applications particularly in infection-free wound healing, tissue engineering or implant devices. However, further studies, both *in-vivo* and *ex-vivo*, are required for definite verification. Extended investigation is needed to reveal other suitable applications such as biomedical implants of these newly developed novel bio-composites. Undoubtedly, the results obtained after soil burial degradation revealed that the newly synthesised composites will not contribute and/or cause any deleterious impact on the natural ecosystem.

5.6.0. PART – 3

5.6.1. Fourier transform infrared spectroscopy (FT-IR)

Infrared absorption spectra of caffeic acid (CA), gallic acid (GA), 4-*p*-hydroxybenzoic acid (HBA), thymol (T), CA-*g*-keratin-EC, GA-*g*-keratin-EC, HBA-*g*-keratin-EC and T-*g*-keratin-EC composites show characteristic absorption bands assigned to the peptide bonds (-CONH-) that originate bands known as amide I, amide II, and amide III. In IR spectral analysis, amide I is mainly related with the C=O stretching, and it occurs in the range of 1,700-1,600cm^{-1}, whereas, amide II is mainly related to N-H bending and C-H stretching vibration, and it occurs in the range of 1,540-1,520cm^{-1}. Finally, amide III mainly originates from in-phase combination of C-N stretching and C=O bending vibration, and it occurs in the range of 1,220-1,300 cm^{-1} (Tanabe *et al*., 2002; Vasconcelos *et al*., 2008).

Moreover, as can be seen from the Figures 5.33 to 5.36, the positions of the aforementioned bands indicate the conformations of the grafted materials: 1,630 cm^{-1} for amide I, 1,545 cm^{-1} for amide II, and 1,270 cm^{-1} for amide III (Ha *et al*., 2005; Vasconcelos *et al*., 2008). Evidently, a typical peak at 1,056 cm^{-1} region was observed with sharp appearance which is due to the C–O–C stretching and specifically linked with the cellulose molecules (Mohammed-Ziegler *et al*., 2008). The peaks present near to the 2,930 and 2,850 cm^{-1} are characteristic infrared bands of aliphatic hydrocarbons of methylene asymmetric C–H stretching and symmetric C–H stretching, respectively. However, both signals for the methyl (CH$_3$) asymmetric and symmetric modes and the methylene (CH$_2$) asymmetric and symmetric modes originated from keratin, and can be assigned to the aliphatic chain. In comparison to the pristine caffeic acid and *p*-4-hydroxybenzoic acid, a broad peak appeared in the spectra of CA-*g*-keratin-EC and

HBA-*g*-keratin-EC at 3,345 cm^{-1} region which typically corresponds to the phenolic -OH stretching and involvement of hydrogen bonding type interactions between those -OH groups (Rukmani and Sundrarajan, 2012).

On the other hand, GA-*g*-keratin-EC and T-*g*-keratin-EC composites have typical polyphenol characteristics, showing broad peaks cantered at 3,360 cm^{-1} which are due to the vibrational mode of -OH linkage of phenolic and hydroxyl groups. Furthermore, phenol grafted keratin-EC composites showed a broad peak between the regions of 3,200-3,400 cm^{-1} which is linked to the hydrogen-bonded groups at that distinct band region (Aluigi *et al.*, 2008). The higher wavenumber of amide I can be explained by the protein extraction procedure suggesting again the presence of R-helix structure. Nevertheless, an increase in the peak area of the amide I band in the grafted composites spectra with respect to the same band in the spectra of the individual counterparts indicates the stabilisation of R-helix conformation and destabilisation and/or the involvement of the *β*-sheet structure during the graft formation process.
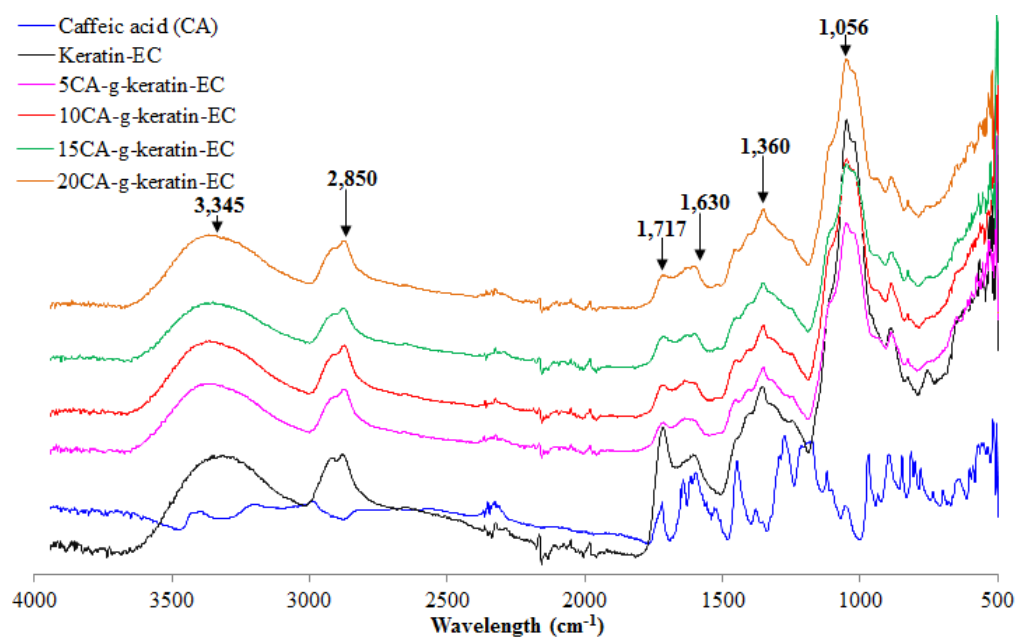
Figure 5.33 Typical FT-IR spectra of pristine caffeic acid, keratin-EC and caffeic acid grafted keratin-EC based bio-composites prepared using laccase as a model catalyst.
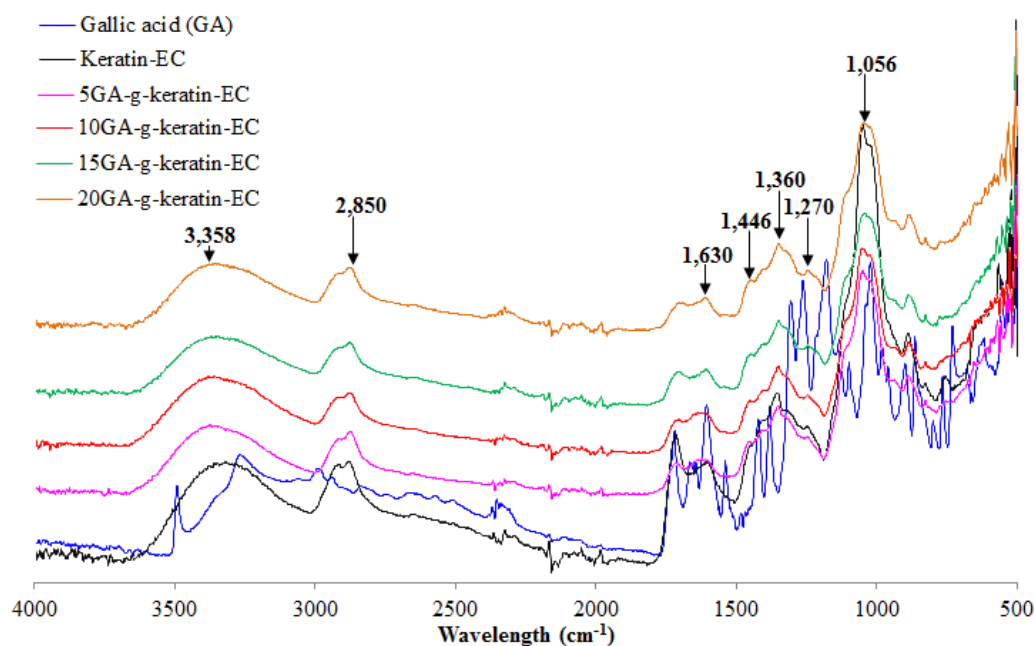
Figure 5.34 Typical FT-IR spectra of pristine gallic acid, keratin-EC and gallic acid grafted keratin-EC based bio-composites prepared using laccase as a model catalyst.
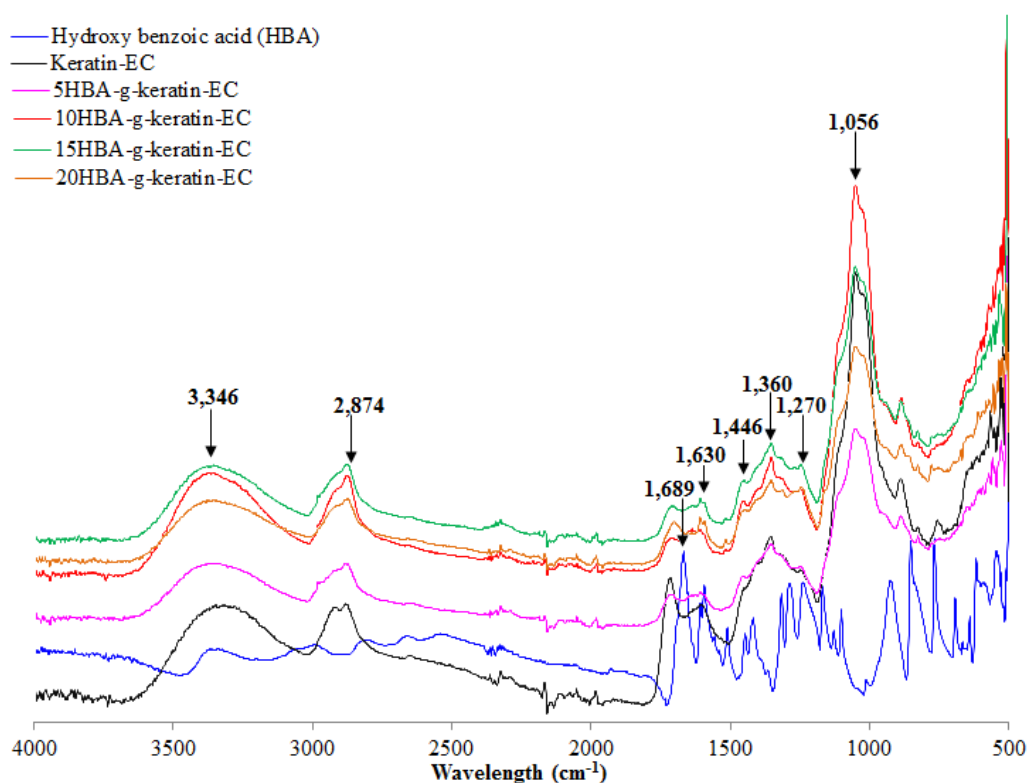
Figure 5.35 Typical FT-IR spectra of pristine *p*-4-hydroxybenzoic acid, keratin-EC and *p*-4-hydroxybenzoic acid grafted keratin-EC based bio-composites prepared using laccase as a model catalyst.
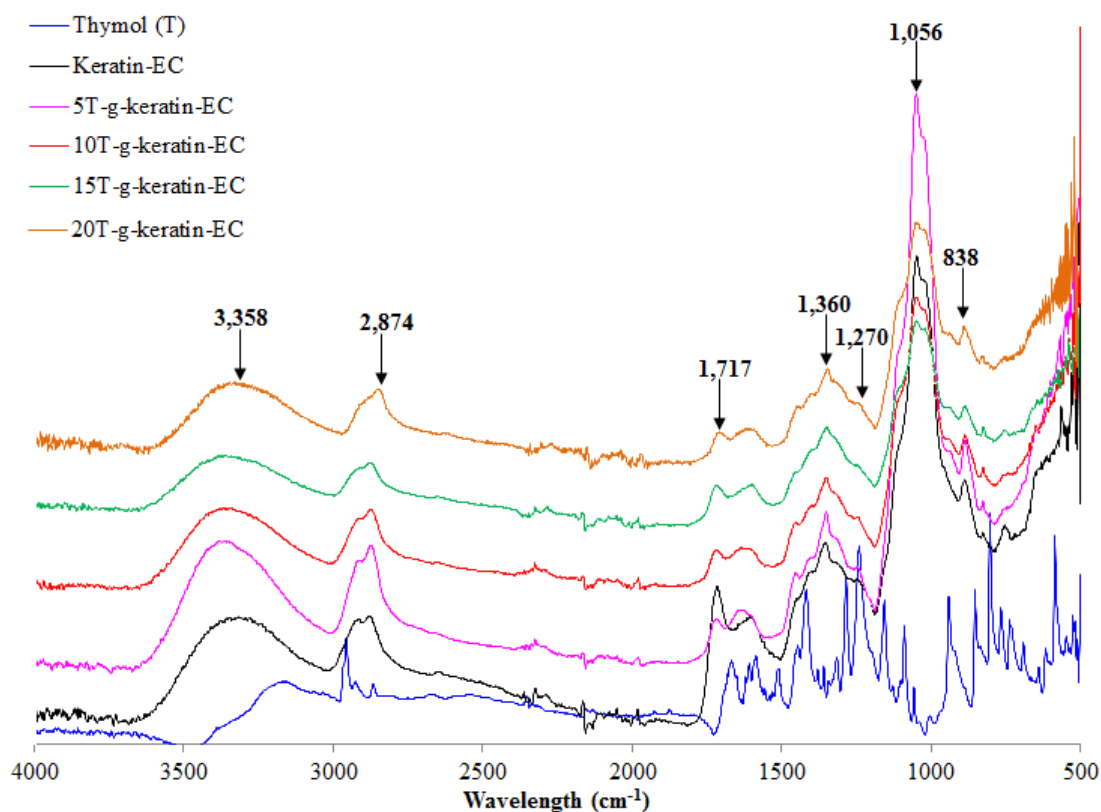
Figure 5.36 Typical FT-IR spectra of pristine thymol, keratin-EC and thymol grafted keratin-EC based bio-composites prepared using laccase as a model catalyst.

Figure 5.37 illustrates a schematic mechanism of laccase-assisted grafting of natural phenols onto the keratin-EC-based material.
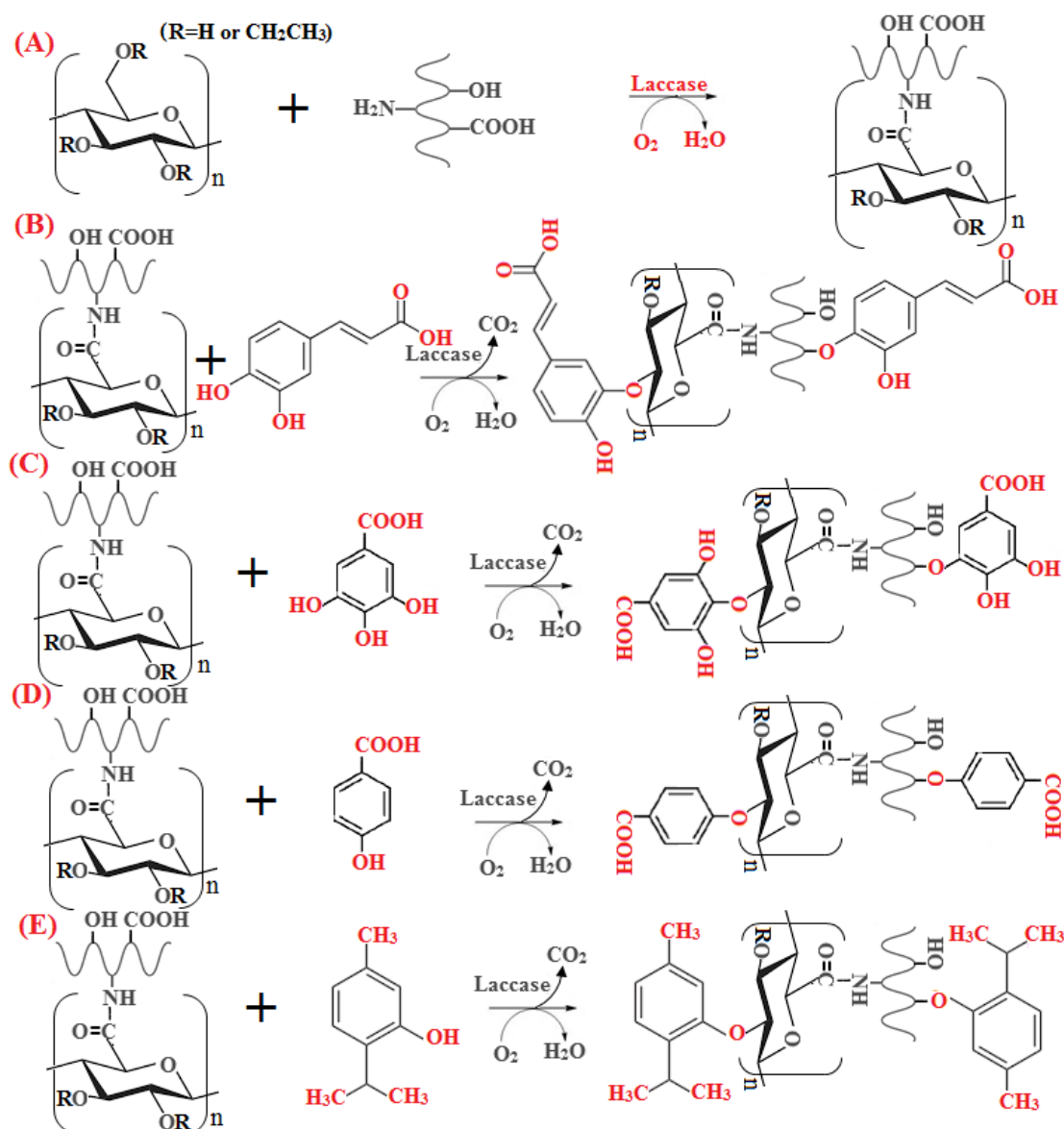
Figure 5.37 A schematic representation of the proposed mechanism of graft formation; (A) between keratin and EC, (B) between keratin-EC and caffeic acid, (C) between keratin-EC and gallic acid, (D) between keratin-EC and *p*-4-hydroxybenzoic acid, and (E) between keratin-EC and thymol.

5.6.2. Grafting parameters

To evaluate the grafting behaviour of the newly synthesised phenol-*g*-keratin-EC based bio-composites, the grafting parameters that includes graft yield (%GY),

grafting efficiency (%GE) and swelling ratio (%SR) were investigated. Figure 5.38 illustrates the aforementioned grafting parameter profiles of CA-*g*-keratin-EC composites. The data revealed that the ultimate graft yield, grafting efficiency and swelling ratio values were highest in case of 15CA-g-keratin-EC composite with an overall CA concentration of 15 mM. On the other hand, these parameters decreased in case of other composites. One possible reason for the observed behaviour could be the substantial amount of CA grafted onto the baseline (keratin-EC) composite, which creates steric hindrance for further grafting, increasing beyond the optimal point. The order of GP % observed for CA-*g*-keratin-EC composites was: 15CA-g-keratin-EC > 20CA-g-keratin-EC > 10CA-g-keratin-EC > 5CA-g-keratin-EC.
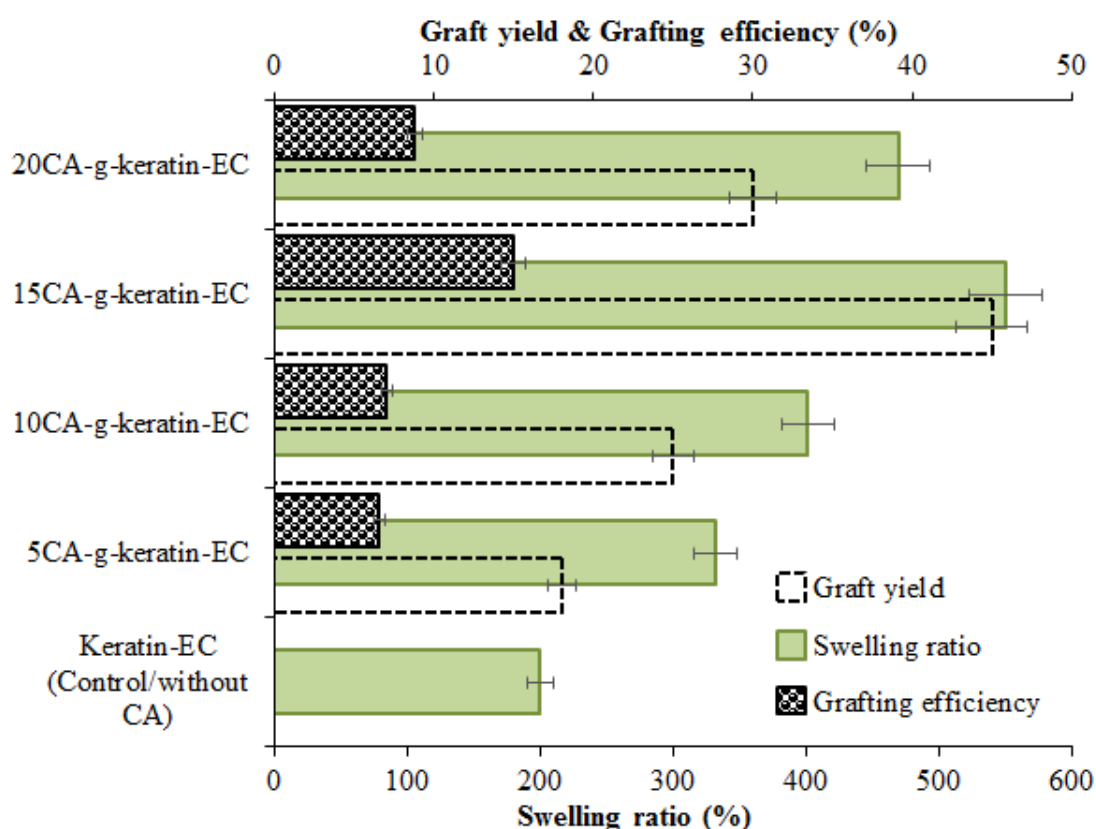
Figure 5.38 Evaluation of grafting parameters *i.e.* graft yield (%GY), grafting efficiency (%GE) and swelling ratio (%SR) behaviours of pristine caffeic acid, keratin-EC and caffeic acid grafted keratin-EC based bio-composites prepared using laccase as a model catalyst.

The results of the grafting parameters (graft yield, %GY, grafting efficiency, %GE and swelling ratio, %SR) of GA-*g*-keratin-EC composites as a function of GA are shown in Figure 5.39. In comparison to the control sample a consistent increase in the swelling ratio in addition to the graft yield and grafting efficiency was recorded from 5 mM to 15 mM GA concentration for the bio-composites, where 15GA-*g*-keratin-EC was proved best under the same conditions. However, further increase up to 20 mM GA concentration showed decreasing trend in the aforementioned parameters. The order of %GP observed for GA-*g*-keratin-EC composites was: 15GA-g-keratin-EC > 10GA-g-keratin-EC > 20GA-g-keratin-EC > 5GA-g-keratin-EC.
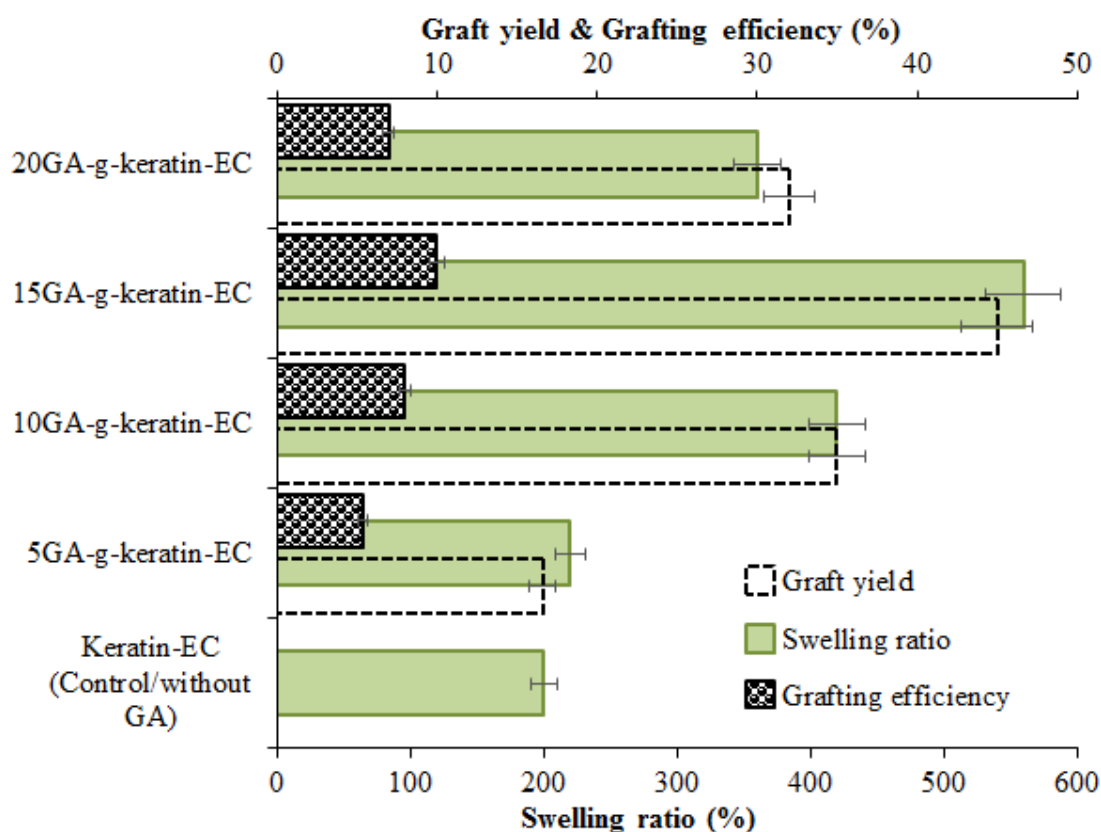
Figure 5.39 Evaluation of grafting parameters *i.e.,* graft yield (%GY), grafting efficiency (%GE) and swelling ratio (%SR) behaviours of pristine gallic acid, keratin-EC and gallic acid grafted keratin-EC based bio-composites prepared using laccase as a model catalyst.

In Figure 5.40, the grafting profile of the HBA-*g*-keratin-EC composites *i.e.* 5HBA-*g*-keratin-EC, 10HBA-*g*-keratin-EC, 15HBA-*g*-keratin-EC and 20HBA-*g*-keratin-EC in terms of graft yield, grafting efficiency and swelling ratio is shown. The grafting between HBA and keratin-EC was maximum when the composite was prepared using 10 mM HBA followed by 15 mM HBA under the same reaction conditions and the difference between the grafting behaviour was insignificant in both of the composites *i.e.* 10HBA-*g*-keratin-EC and 15HBA-*g*-keratin-EC. However, in comparison to the other two composites *i.e.* 5HBA-*g*-keratin-EC and 20HBA-*g*-keratin-EC the grafting behaviour was much higher and significant in the 10HBA-*g*-keratin-EC and 15HBA-*g*-keratin-EC composites. The order of %GP observed for HBA-*g*-keratin-EC composites was: 10HBA-g-keratin-EC > 15HBA-g-keratin-EC > 5HBA-g-keratin-EC > 20HBA-g-keratin-EC.
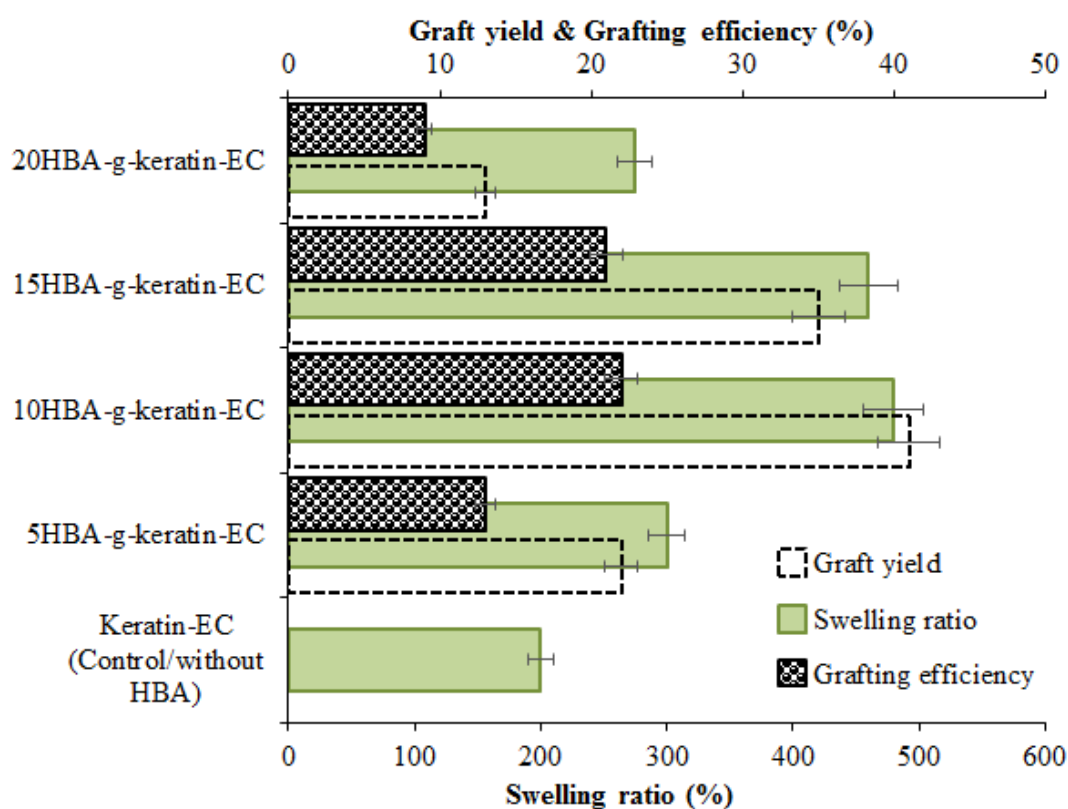
Figure 5.40 Evaluation of grafting parameters of HBA, keratin-EC and HBA grafted keratin-EC-based bio-composites prepared using laccase as a model catalyst.

The grafting parameter profiles of the composites prepared using thymol as a functional entity is shown in Figure 5.41. Indeed, the grafting parameter profiles presented in Fig. 5.41 indicates a gradual increase in the %GP as the concentration of T increases from 0 to 20 mM. The order of grafting parameters observed was as follows: 20T-g-keratin-EC > 15T-g-keratin-EC > 10T-g-keratin-EC > 5T-g-keratin-EC composites. One possible reason for such a consistent increase in the %GP could be the availability of lower number of functional groups, hence more active sites were available in the baseline keratin-EC to accommodate higher ratio of thymol as compared to other tested phenols.
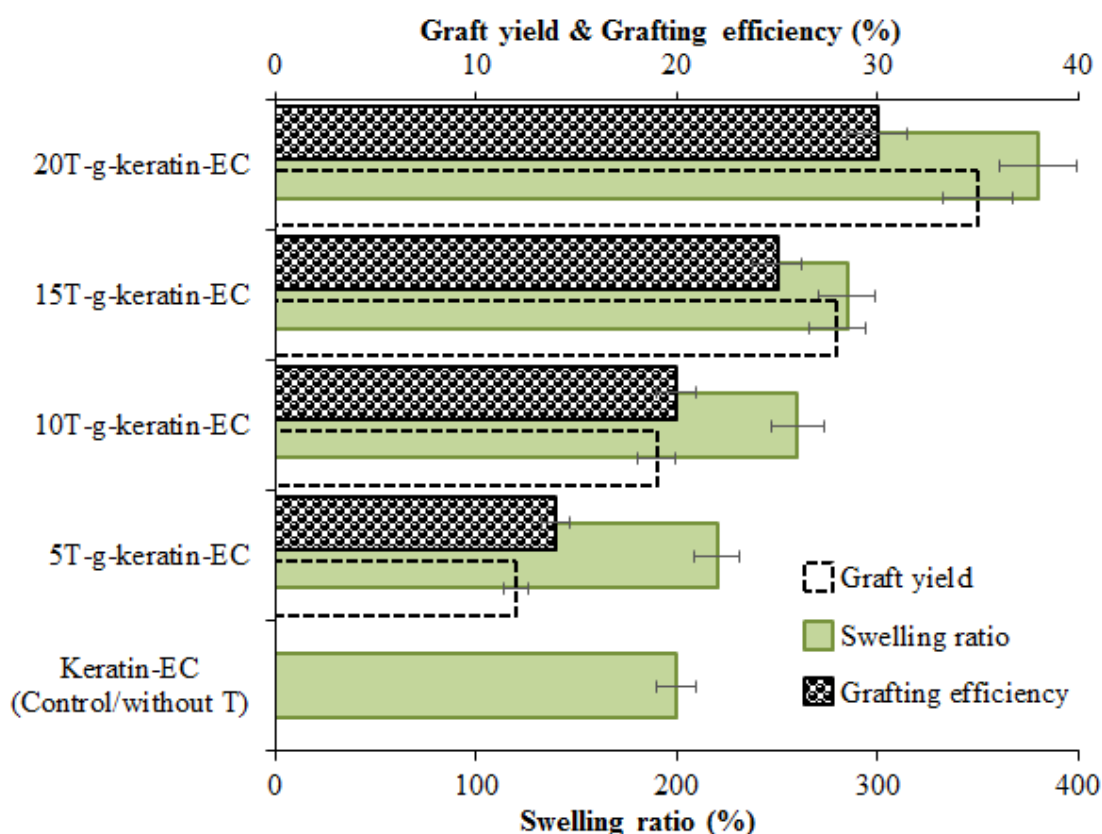
Figure 5.41 Evaluation of grafting parameters *i.e.* graft yield (%GY), grafting efficiency (%GE) and swelling ratio (%SR) behaviours of pristine thymol, keratin-EC and thymol grafted keratin-EC.

5.6.3. Antibacterial activity

Antibacterial activity analyses were performed using the CFU/mL counting method. Figure 5.42 reports the antibacterial activities of CA-*g*-keratin-EC composites against *B. subtilis* NCTC 3610 (Gram+), *S. aureus* NCTC 6571 (Gram+), *E. coli* NCTC 10418 (Gram-) and *P. aeruginosa* NCTC 10662 (Gram-) strains. In comparison to the initial bacterial count against each strain, after 24 h of control incubation, the bacterial counts increased to 1×10^7 CFU/mL on the pristine keratin-EC composite. However, a different behaviour was observed for the composites prepared with different mM concentrations of CA: 15CA-*g*-keratin-EC showed excellent bactericidal and bacteriostatic potential with a log value decreased from 5 to 0 for Gram-negative (*E. coli* NCTC 10418 and *P. aeruginosa* NCTC 10662) and 5 to 1 and 2 for Gram-positive strains i.e., *S. aureus* NCTC 6571 and *B. subtilis* NCTC 3610, respectively (Figure 5.42). The antibacterial activity of 15CA-*g*-keratin-EC was more than that of the 10CA-*g*-keratin-EC, which only showed bacteriostatic activity against Gram-negative strains. Whereas, 5CA-*g*-keratin-EC and 20CA-*g*-keratin-EC both showed a negligible reduction in the bacterial count verses all of the tested strains.

The anti-bacterial profile of the composites, using gallic acid as a functional entity, is shown in the Figure 5.43. Compared to the keratin-EC composite, 15GA-*g*-keratin-EC showed more prominent (complete killing of bacteria) properties against *E. coli* NCTC 10418 and *P. aeruginosa* NCTC 10662. The bacteriostatic behaviour of 10GA-*g*-keratin-EC was slightly stronger against *E. coli* NCTC 10418 and *P. aeruginosa* NCTC 10662 than *B. subtilis* NCTC 3610 and *S. aureus* NCTC 6571. However, 5GA-*g*-keratin-EC only showed bacteriostatic potential against Gram-negative strains, whereas, among Gram-positive strains *B. subtilis* NCTC 3610 was found able to withstand against the concentration range of gallic acid used in this study.
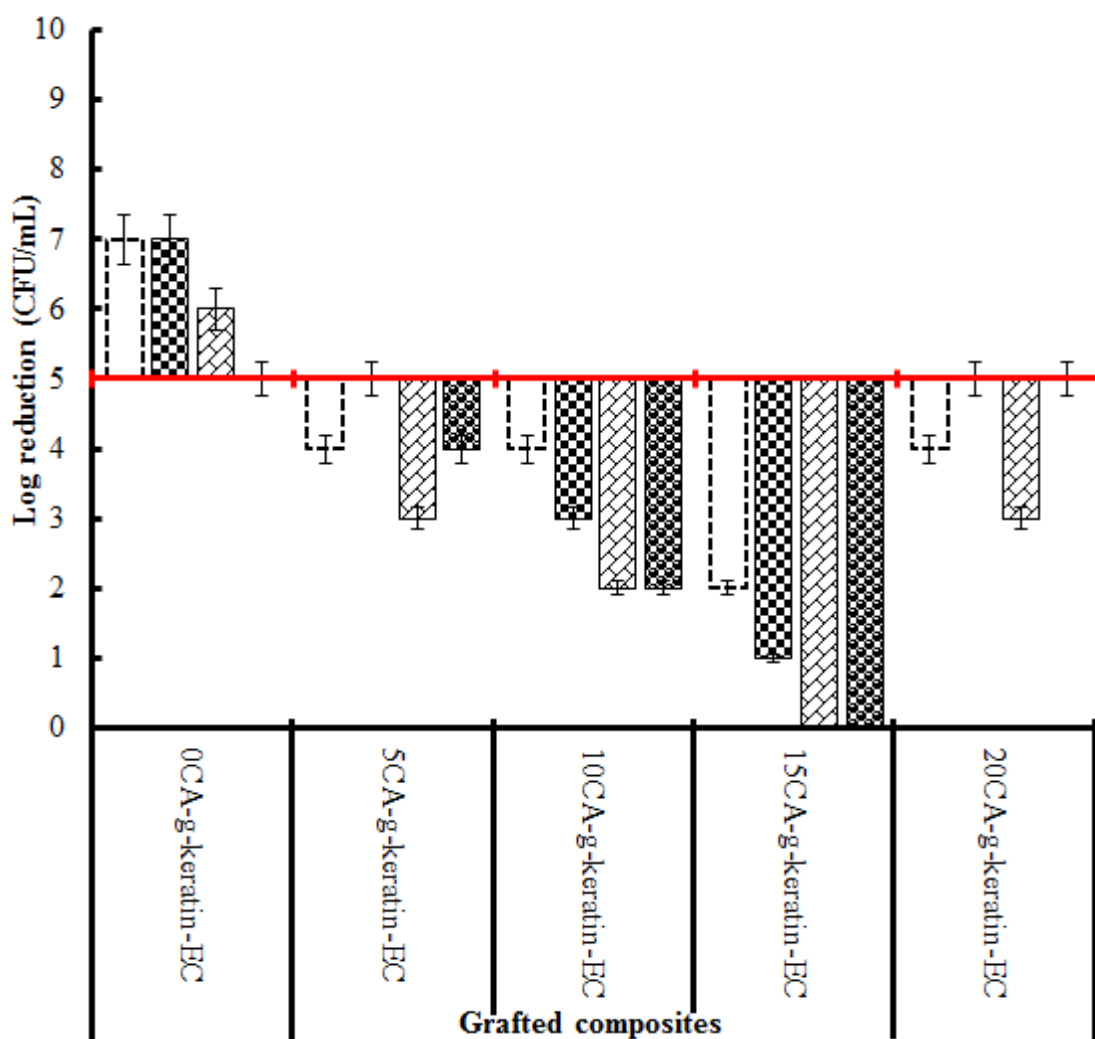
Figure 5.42 Evaluation of antimicrobial potential of caffeic acid grafted keratin-EC based bio-composites against various Gram-positive and Gram-negative bacterial strains *i.e. B. subtilis* NCTC 3610 (▢); *S. aureus NCTC* 6571 (▨); *E. coli* NCTC 10418 (▨) and *P. aeruginosa NCTC* 10662 (▨). Red line indicates an initial bacterial count of 1×10^5 CFU/mL. An increase in this count (as compared to the initial bacterial count) showed susceptibility whereas, reduction in the initial bacterial count showed bacteriostatic and bactericidal activities of the respective composites. A 2 log reduction was considered to claim an antibacterial activity.
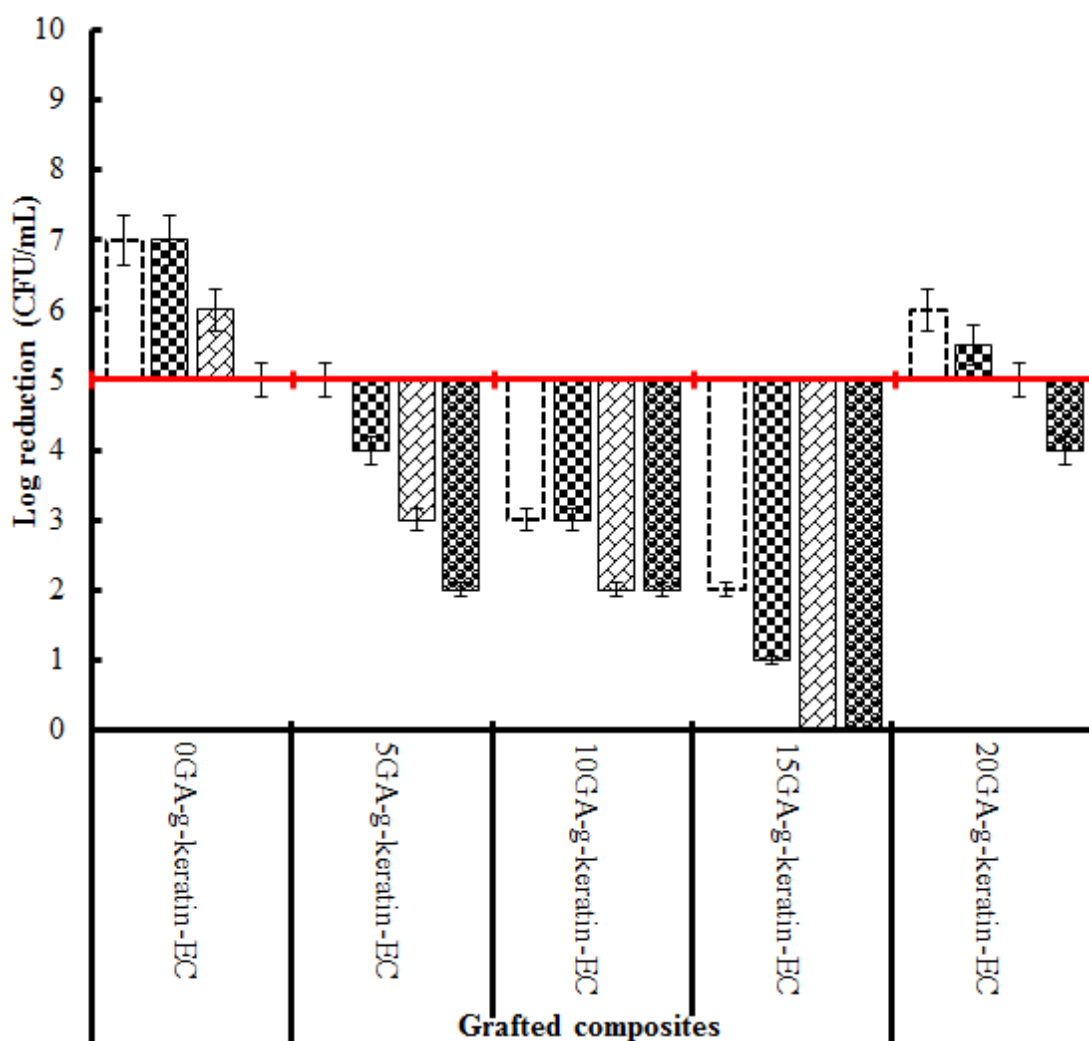
Figure 5.43 Evaluation of antimicrobial potential of gallic acid grafted keratin-EC based bio-composites against various Gram-positive and Gram-negative bacterial strains *B. subtilis* NCTC 3610 (▢); *S. aureus NCTC* 6571 (▨); *E. coli* NCTC 10418 (▨) and *P. aeruginosa NCTC* 10662 (▨). Red line indicates an initial bacterial count of 1×10^5 CFU/mL. An increase in this count (as compared to the initial bacterial count) showed susceptibility whereas, reduction in the initial bacterial count showed bacteriostatic and bactericidal activities of the respective composites. A 2 log reduction was considered to claim an antibacterial activity.

In Figure 5.44, the anti-bacterial activities of the HBA-*g*-keratin-EC composites against the aforementioned bacterial strains are shown. An excellent level of anti-bacterial (bactericidal) and bacteriostatic properties was observed against each of the test bacterial species. In the case of 10HBA-*g*-keratin-EC, a maximum of five log reduction in bacterial counts (100% bactericidal) was observed as compared to the plain keratin-EC control samples. In tests of 15HBA-*g*-keratin-EC, the log value decreased from 5 to 0 and 1 against Gram-negative (*E. coli* NCTC 10418 and *P. aeruginosa* NCTC 10662) and Gram-positive (*B. subtilis* NCTC 3610 and *S. aureus* NCTC 6571) strains, respectively. Among other composites, only 5HBA-*g*-keratin-EC showed slight bacteriostatic activity whereas, the remaining bacterial count was negligible in the case of 20HBA-*g*-keratin-EC composite.

The anti-bacterial efficacy levels of the T-*g*-keratin-EC composites against various Gram-positive and Gram-negative bacterial strains is shown in Figure 5.45. The levels of anti-bacterial activity observed were maximum with 20T-*g*-keratin-EC and 15T-*g*-keratin-EC composites with a greater than 4 log reduction in the initial bacterial count verses all of the test organisms. Although the reduction in the bacterial count with 10T-*g*-keratin-EC was less than the initial bacterial count of 1×10^5 CFU/mL, the level was still well above the minimum acceptable anti-bacterial (bacteriostatic) activity level of 2 and it was particularly against the *E. coli* NCTC 10418 and *P. aeruginosa NCTC* 10662 strains.
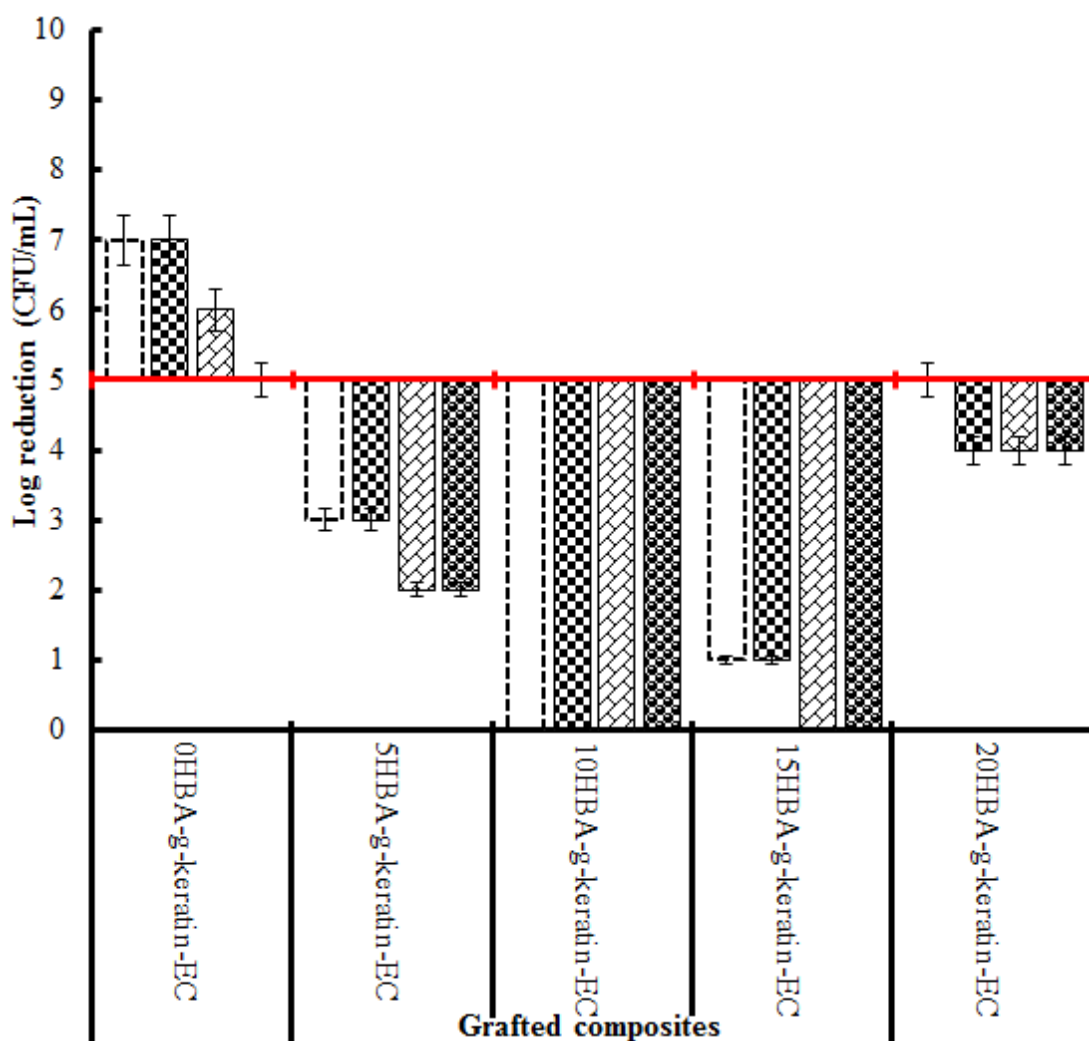
Figure 5.44 Evaluation of antimicrobial potential of *p*-4-hydroxybenzoic acid grafted keratin-EC based bio-composites against various Gram-positive and Gram-negative bacterial strains *B. subtilis* NCTC 3610 (▯); *S. aureus NCTC* 6571 (▨); *E. coli* NCTC 10418 (▨) and *P. aeruginosa NCTC* 10662 (▨). Red line indicates an initial bacterial count of 1×10^5 CFU/mL. An increase in this count (as compared to the initial bacterial count) showed susceptibility whereas, reduction in the initial bacterial count showed bacteriostatic and bactericidal activities of the respective composites. A 2 log reduction was considered to claim an antibacterial activity.
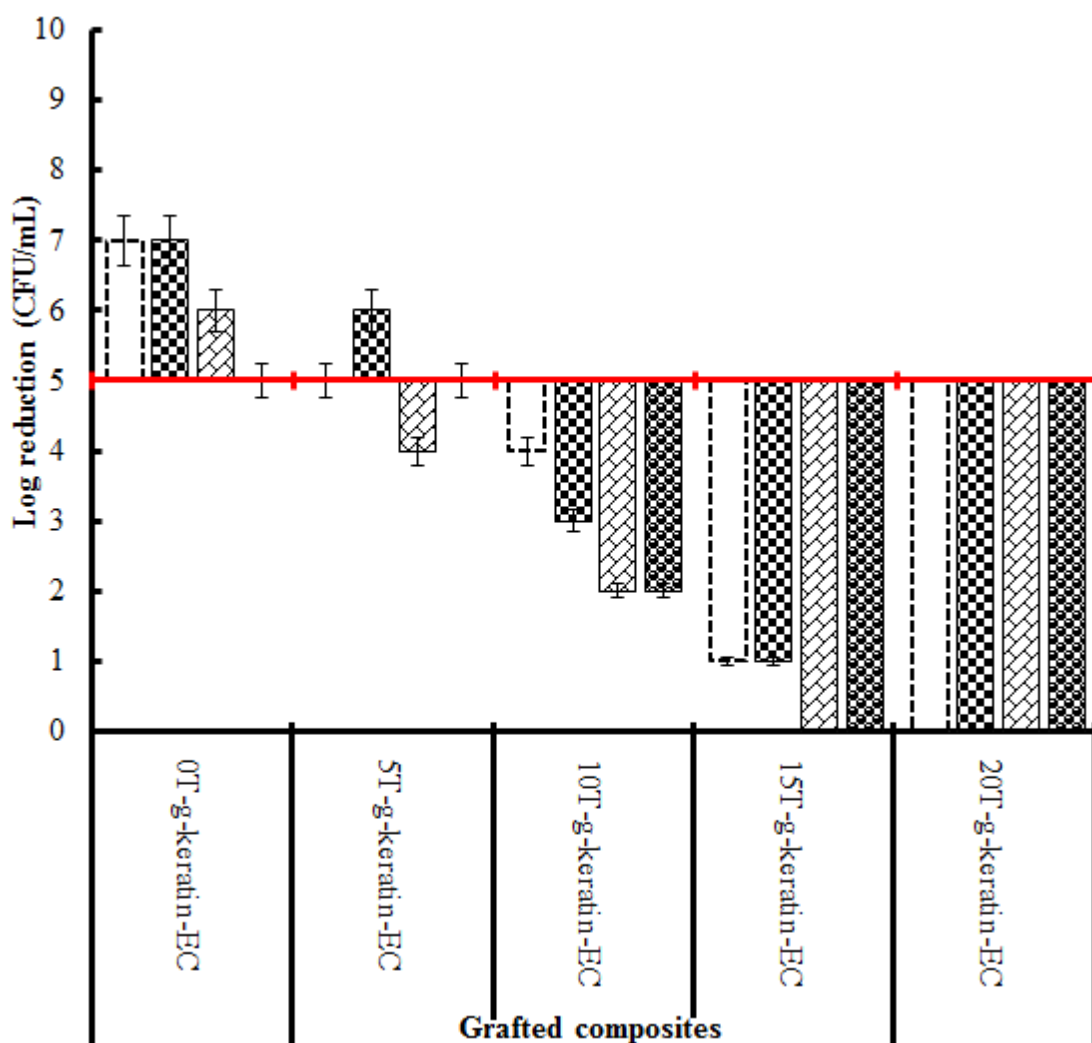
Figure 5.45 Evaluation of antimicrobial potential of thymol grafted keratin-EC based bio-composites against various Gram-positive and Gram-negative bacterial strains *i.e.,* *B. subtilis* NCTC 3610 (□); *S. aureus NCTC* 6571 (▨); *E. coli* NCTC 10418 (▧) and *P. aeruginosa NCTC* 10662 (▨). Red line indicates an initial bacterial count of 1×10^5 CFU/mL. An increase in this count (as compared to the initial bacterial count) showed susceptibility whereas, reduction in the initial bacterial count showed bacteriostatic and bactericidal activities of the respective composites. A 2 log reduction was considered to claim an antibacterial activity.

5.6.4. *In-vitro* bio-compatibility

The % cell viability and adherent morphology of the human keratinocyte-like HaCaT skin cells on "as-prepared", and "selected" composites were determined quantitatively using neutral red assay uptake and staining procedures, respectively. The percent viability was recorded against each sample seeded for 1, 3 and 5 days in 24-well tissue culture plates containing test specimens (1 cm^2 in area) at a density of 1×10^5 cells per well using culture media (DMEM). Notably, all of the aforementioned composites displayed up to 100% cell viability after 5 days of incubation (Figure 5.46), indicating that the test composites were non-cytotoxic in nature thus promote the viability of HaCaT cells. However, the growth-rate after 1 and 3 days of incubation was found different as shown in Figure 5.46, which could be due to the nature of each phenolic component used.
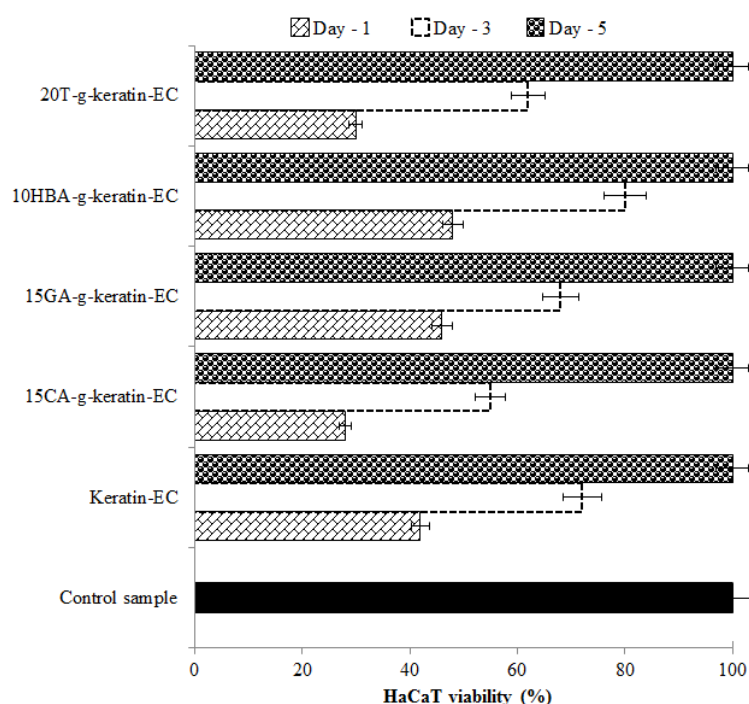
Figure 5.46 Neutral red dye concentration dependent percentage cell viability of human keratinocytes-like HaCaT cells seeded onto selected bio-composites surfaces for prescribed periods (mean ± SD, n = 3).

Keratin-EC
Day – 1   Day – 3   Day – 5

15CA-*g*-keratin-EC
Day – 1   Day – 3   Day – 5

15GA-*g*-keratin-EC
Day – 1   Day – 3   Day – 5

10HBA-*g*-keratin-EC
Day – 1   Day – 3   Day – 5

20T-*g*-keratin-EC
Day – 1   Day – 3   Day – 5
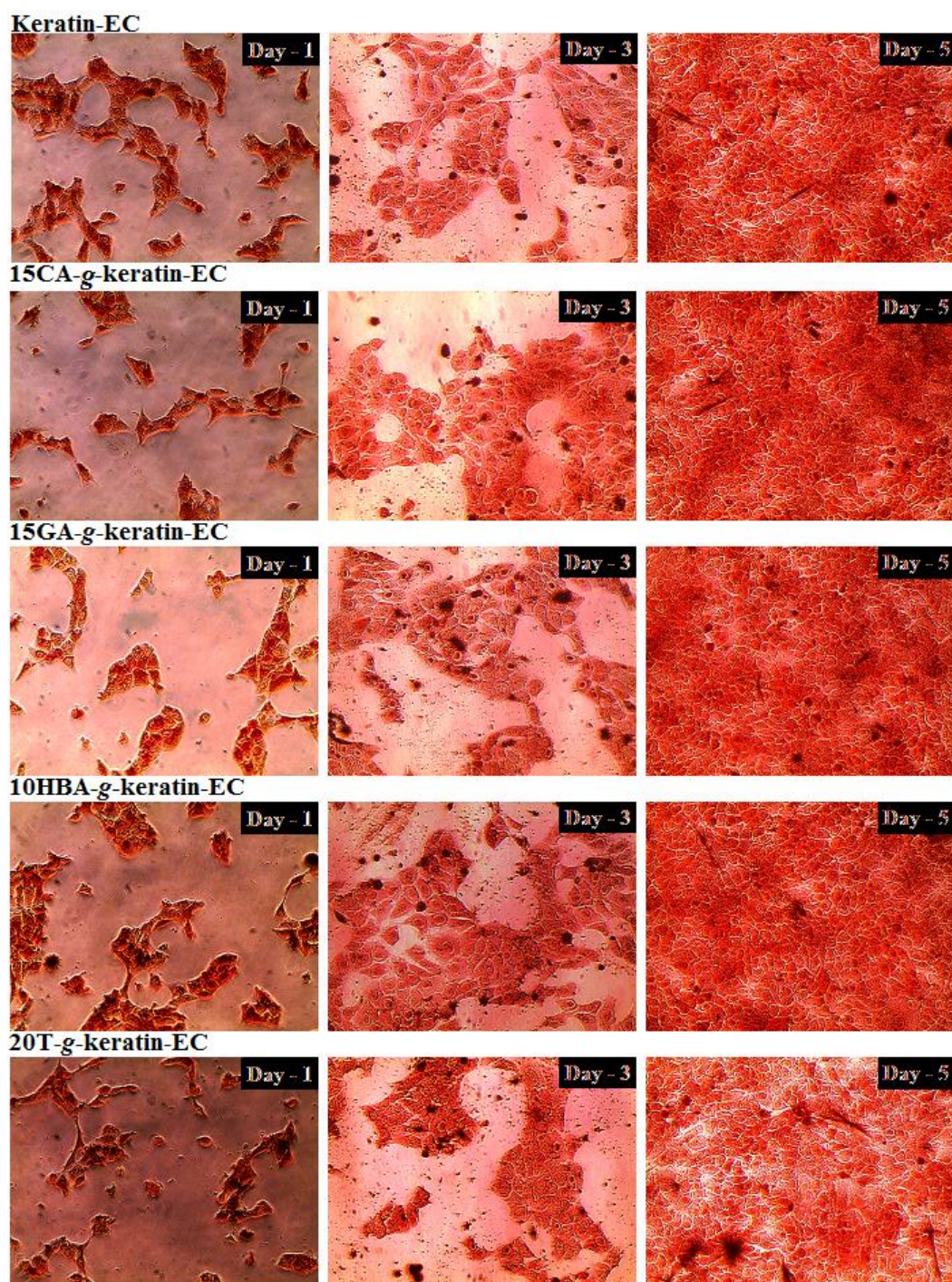
Figure 5.47 Adherent morphology of stained images of human keratinocytes-like HaCaT cells seeded onto the selected bio-composites: 15CA-*g*-keratin-EC, 15GA-*g*-keratin-EC, 10HBA-*g*-keratin-EC and 20T-*g*-keratin-EC surfaces for prescribed periods (1, 3 and 5 Days). All of the test samples were stained using neutral red dye (5 mg/mL) for 1 h followed by three consecutive washings with PBS at an ambient temperature. All images were taken at 100× magnification.

5.6.5. Soil burial degradation

The effect of the soil burial degradation, as observable by the weight loss (%) of the keratin-EC, 15CA-*g*-keratin-EC, 15GA-*g*-keratin-EC, 10HBA-*g*-keratin-EC and 20T-*g*-keratin-EC composites buried for prescribed periods up to 42 days, is reported in the Figure 5.48. The percent weight loss of the grafted composites was significantly affected by their formulation using different phenols while a negligible change was observed from day 7 to day 21 of degradation be more specific, mention which composites. In particular, the weight loss increased from 23 ± 0.9 % to $29 \pm 1.1\%$ for the keratin-EC composite, this difference remained almost constant in all of the tested composites up to day 21 (Figure 5.48 A-C). The observed degradation behaviour is directly dependent on the multi-phase and keratin-associated protein nature of the composites. Notably, after increasing the burial period from 21 days to 42 days, an increase in the weight loss from $43 \pm 2.2\%$ to $99 \pm 3.5\%$ was recorded for the keratin-EC composite (Figure 5.48 C-F). On the other hand, in the case of 15CA-*g*-keratin-EC, 15GA-*g*-keratin-EC and 10HBA-*g*-keratin-EC composites a 100% degradation was observed after 42 days of controlled incubation. The degrading behaviour was least in 20T-*g*-keratin-EC with an overall weight loss of $85 \pm 2.2\%$ (Figure 5.48 F).
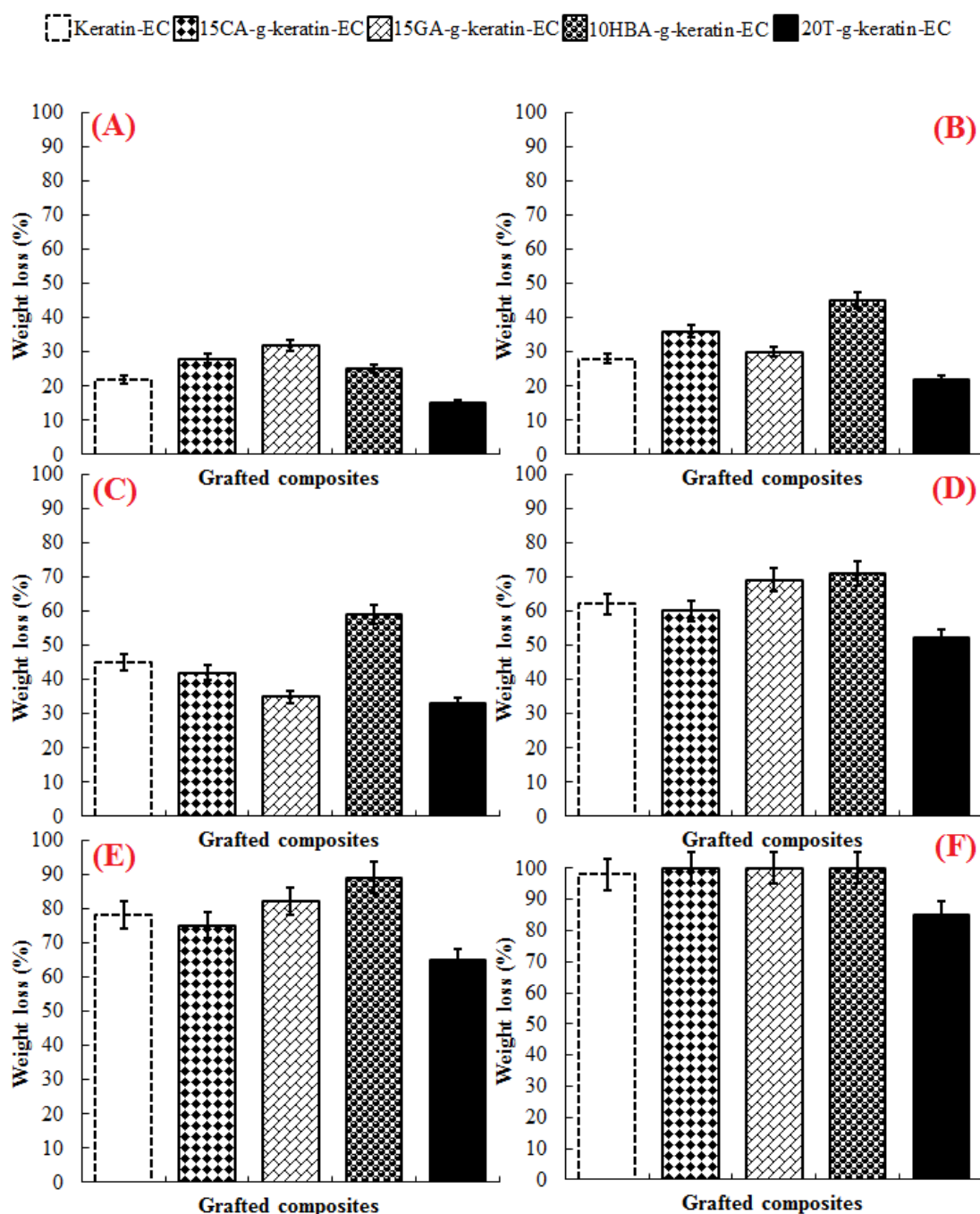
Figure 5.48 Effect of soil burial period on the biodegradability in terms of percentage weight loss of keratin-EC, 15CA-*g*-keratin-EC, 15GA-*g*-keratin-EC, 10HBA-*g*-keratin-EC and 20T-*g*-keratin-EC composites buried for prescribed periods: (A) 7 days; (B) 14 days; (C) 21 days; (D) 28 days; (E) 35 days and (F) 42 days (mean ± SD, n = 3).

5.7. Concluding remarks

Green chemistry approach to synthesise bio-composites with novel characteristics through enzymatic grafting has several advantages including: (i) high added-value; (ii) eco-friendly processing; (iii) convenient preparation methods; (iv) minimum use of water and energy, and finally (v) no or little use of harsh chemicals.

In this study, we have developed a self-defensive concept for bacteria-responsive keratin-EC based natural materials that cannot cope with bacterial attacks under their separate native forms. Therefore, natural phenols were used as functional entities for the preparation of fully bio-based composites. Since reactive reagents are not required for laccase-catalysed modification, the safety concerns are considerably lessened, and simpler manufacturing facilities could be envisioned. This thesis suggests that laccase-catalysed grafting of natural phenols onto the previously developed keratin-EC material provide a "green" alternative for developing bio-composites with novel characteristics.

Chapter 6

Conclusions
&
Future work

6.1. Conclusions

This chapter concludes the thesis by presenting the overall contribution of the research carried out on the development of bio-composites with novel characteristics. In addition, this chapter highlights the limitations and potential future research directions.

The prime focus of this thesis was the design and production of bio-composites with novel characteristics through enzymatic grafting. In this context, FDA approved biopolymers were used to synthesise a series of novel bio-composite materials. This comprised of lipase-assisted P(3HB)-*g*-EC, laccase-assisted P(3HB)-*g*-EC/BC, laccase-assisted keratin-*g*-EC, laccase-assisted phenol-*g*-P(3HB)-*g*-EC and laccase-assisted phenol-*g*-keratin-*g*-EC-based bio-composites. The development of these bio-composites was in-line-with the principles of green chemistry, aimed at the design and commercialising of products that reduce or eliminate the generation of persistent, often toxic wastes, generally associated with the chemical-based processes. The enzyme-based grafting method, presented in this thesis, has several advantages including: (i) high added-value; (ii) eco-friendly processing; (iii) convenient preparation methods; (iv) minimum use of water and energy, and finally (v) no or little use of harsh chemicals.

According to the results presented and discussed in Chapter 3, and Chapter 4, the following conclusions can be drawn:

1) Lipase-catalysed esterification reactions are versatile to synthesise graft bio-composites using multifunctional materials of interests such as P(3HB) and cellulose (EC) with potential applications in bio-medical, tissue engineering and/or medical implants.

2) Lipase-assisted synthesis appears to be an alternative to the green chemistry technologies as compared to the pre-existing bulk chemical routes.

3) XRD analyses revealed micro-structural changes happened during the graft formation process between P(3HB) and EC in the presence of lipase. As shown in Figure 3.4, wider peaks were observed in the graft bio-composites prepared with P(3HB): EC 100:0, 75:25 and 50:50 in the presence of lipase as a grafting catalyst, as compared to the sharp peaks of the untreated P(3HB) at some specific region of 2-Theta. This shift from sharp to the wider peaks clearly indicates the breakdown of some crystalline domains at 2-Theta values.

4) DSC analyses revealed that the lipase treatment has accelerated the cold crystallisation of P(3HB) and the crystallisation temperature (T_c) decreased from 135 ^{o}C to 58 ^{o}C. Whereas, as compared to the P(3HB)-g-EC^A (P(3HB): EC, 100: 0), this was boost up from 58 ^{o}C to 92 ^{o}C when the EC content ratio increased from 0 to 50 (wt. %) *i.e.*, P(3HB)-g-EC^C (P(3HB): EC, 50: 50).

5) It was also observed that the inclusion of EC, with a content ratio (P(3HB): EC, 50: 50), in the presence of laccase from *Trametes versicolor* has also accelerated the cold crystallisation and the crystallisation temperature (T_c) decreased from 135 ^{o}C to 78 ^{o}C and 88 ^{o}C for P(3HB)-g-EC and P(3HB)-g-BC, respectively.

6) In comparison to the untreated P(3HB), the grafts prepared with P(3HB): EC *e.g.* 50:50 and 25:75 were proved best amongst P(3HB): EC *e.g.* 100:0, 75:25 and 0:100 with their thermo- mechanical and morphological characteristics. There was significant improvement in Young's modulus of the composites with increasing EC content ratio and these results were found to fit the Halpin Tsai model. The Young's modulus increased from 0.22 to 2.35 (GPa) when the EC content ratio increased from 0 to 50 (wt. %).

7) WCA study confirmed an improvement in the hydrophobic/hydrophilic characteristics of the P(3HB)-EC-based bio-composites. Interestingly, the bio-composites prepared with different P(3HB): EC ratio using lipase exhibited a more than two-fold decrease in the water contact angle in comparison to the untreated P(3HB). This could be due to hydrolysis caused by lipase during the graft formation process. Such characteristics are sought after for successful tissue development and/or implantation in a host.

8) The P(3HB)-*g*-EC bio-composites prepared using lipase were more hydrophilic in nature as compare to the P(3HB)-*g*-EC prepared using laccase.

9) A novel laccase-assisted method was developed to manufacture keratin-EC-based bio-composites. The main benefits of laccase-assisted grafting process were the simple synthesis in the absence of harmful solvents and chemicals, the mild eco-friendly and energy saving reaction conditions.

10) The technology developed in this particular research project (presented in Chapter 4) enables the use of the chicken feather, the bio-waste of the poultry industry, to develop bio-composites with novel characteristics.

11) As evidenced by the characterisation analyses, considerable improvement in the morphology, thermo-mechanical and wettability features was recorded in the newly synthesised composites compared to the individual material (untreated keratin).

12) Morphological analysis via SEM for keratin-EC-based bio-composites showed a uniform dispersion of the keratin which further contributes to the efficient functionality of the resulting bio-composites like higher thermo- mechanical and hydrophobic/hydrophilic properties. It was also observed that keratin material appears more adherent to the EC with keratin to EC ratio, 50: 50 and 25: 75

wt. % where the distribution of pores was reduced on the surfaces and finally disappeared at keratin: EC, 50: 50 and 25: 75 ratios as compared to untreated keratin.

13) There was significant improvement in the mechanical characteristics of laccase-assisted keratin-EC bio-composites prepared with keratin to EC ratio, 25: 75 and 50: 50 wt. %. The elongation at break was maximally improved up to 37% in case of Keratin-*g*-EC[B]. Moreover, the keratin film incorporated with 50 wt. % of EC showed a considerable improvements in the tensile strength (55 MPa), elongation at break (18 %) and Young's modulus (2.4 GPa) in comparison to the untreated keratin film and Keratin-*g*-EC[A] which were too fragile to be measured for their mechanical properties. This also indicates better interaction between the keratin and EC with improved mechanical characteristics.

In the study (presented and discussed in Chapter 5), laccase was used for the *in situ* activation of the natural phenols including caffeic acid, gallic acid, *p*-4-hydroxybenzoic acid and thymol for grafting onto the previously developed P(3HB)-*g*-EC (from Chapter 3) and keratin-*g*-EC (from Chapter 4) based bio-composites. Since reactive reagents were not required for laccase-assisted grafting technique, therefore, the safety concerns are considerably lessened, and simpler manufacturing facilities could be envisioned. Thus, laccase-catalysed grafting of natural phenols onto the newly developed P(3HB)-*g*-EC and keratin-*g*-EC provide a "green" alternative to develop bio-composites with novel characteristics including antibacterial activity, biocompatibility and biodegradability. According to the results presented and discussed in Chapter 5, the following conclusions can be drawn:

1) A novel laccase-assisted method was developed to manufacture bacteria-responsive bio-composites that cannot cope with bacterial attacks under their instinctive forms.

2) Laccase-assisted development of bio-composites provides the opportunity to develop antimicrobial bio-composites *i.e.,* phenol-*g*-P(3HB)-*g*-EC and phenol-*g*-keratin-*g*-EC.

3) The newly developed phenol-*g*-P(3HB)-*g*-EC and phenol-*g*-keratin-*g*-EC bio-composites were bactericidal and bacteriostatic against various bacterial strains including *B. subtilis* NCTC 3610, *S. aureus* NCTC 6571, *E. coli* NCTC 10418 and *P. aeruginosa* NCTC 10662. The current findings suggest that these bio-composites have great potential for use in the wound healing; covering the affected skin area and prove to be more effective for contaminated wounds.

4) The soil burial experiment revealed that the developed composites were degradable and would not be a burden for the natural ecosystem.

5) In conclusion, the improved bacterial resistance, HaCaT biocompatibility, and biodegradability all indicate that the newly synthesised phenol-*g*-P(3HB)-EC and phenol-*g*-keratin-EC based bio-composites could be potential candidates for biomedical applications. However further studies, both *in vivo* and *ex vivo*, are required for in-depth investigation to find other suitable applications such as biomedical implants.

6.2. Future work

As stated previously, finally, this section of Chapter 7 highlights some avenues for possible future research based on the limitations of this study.

The concluding remarks of this thesis highlights possible directions for future research to enhance the opportunities for exploitation of such bio-composites. The proposed future work could include in-depth analyses, structural confirmation, controlled optimisation and improvement of the bio-composites for multipurpose applications.

The primary limitation of this study, is a lack of proper statistical analyses to reveal a significance of differences within the same or between the various materials and their bio-composites. However, due to time constrain, this will be considered more carefully in designing further future research work. To further enhance the reliability and generate statistically evaluated results, the use of statistical models like one-wat and two-way analysis of variance (ANOVA) and linear regression is recommended.

When characterisation techniques are considered, this study also lacks with the GPC and H NMR which are robust methods for deep insight into the structural aspects of the composites. Although the tentative mechanisms of graft formation have been proposed and factor analyses indicate acceptable degrees of construct validity and reliability of the data presented in this study, however, to further enhance the reliability and generate more detailed information, the use of the aforementioned techniques is recommended.

Theoretical aspects of *rheology* are the relation of the deformation behaviour of material that cannot be described by elasticity and its internal structure. It is also concerned with establishing predictions for mechanical behaviour based on the micro- or nanostructure of the material. There are different categories of stress and materials-based composites can respond differently for different stresses. In this context, one of the major tasks of *rheology* is to establish a relationships between deformations and stresses behaviours of the individual and grafted bio-composites. The inclusion of a

suitable plasticiser or compatibiliser, within the system developed in this study, can also be a potential route, for further consideration in future work, to limit the mechanical constrains of the untreated P(3HB) and keratin-based materials.

Grafting of natural phenols as functional entities onto the P(3HB)-EC and keratin-EC bio-composites using laccase showed encouraging results. However, many of the possible applications are still at laboratory scale. Further reaction engineering studies of the reaction conditions would bring about faster industrial implementation. In the case of cellulose, intensive efforts have to be directed towards increasing the reactivity of the enzymatic modification in order to gain insight into bottlenecks.

Other future directions could include synthesis bio-composites into a wider range of geometries such as 3-D scaffolds, rods, tablets and/or nanospheres for other potential applications e.g. medical implants. Medical implants or implantable medical devices are among the best known to the general public for saving lives or, at least, for improving the quality of life. However, how these devices work, and their risks and benefits, are not fully investigated yet. Apart from medical implants, another interesting area for future research would be the encapsulation of multiple drugs or drug loaded composites and their critical evaluation for controlled drug delivery features.

Bio-functionalisation of biopolymers with improved properties or the introduction of functional entities is an active research area aimed at developing biopolymer-based materials that interact with the infected/injured skin at molecular level, thereby accelerating the healing process. Such investigations would allow going beyond the traditional approaches for treatments of dermal injuries (wound healing, skin burn or regeneration, etc.). In this context, intense research is aimed at developing

temperature-responsive, pH-sensitive, and controllable hydrolysable hydrogels as injectable drug delivery system for sustained and controlled drug release.

In this study, the biocompatibility analyses with human keratinocyte-like HaCaT skin cells showed encouraging results. In future, co-culturing of several other cell lines, for example fibroblasts, macrophages and neutrophils, on the newly developed bio-composites, should be performed in order to detect occurrence of cell – cell interactions.

Chapter 7

References

7.1. Referenecs

Abe, H., & Doi, Y. (1999). Structural effects on enzymatic degradabilities for poly [(R)-3-hydroxybutyric acid] and its copolymers. *International Journal of Biological Macromolecules*, *25*(1), 185-192.

Aggour, Y. A. (2001). Reaction kinetics of graft copolymerization and thermochemical studies of the degradation of poly (vinyl alcohol) graft copolymer. *Polymer international*, *50*(3), 347-353.

Akaraonye, E., Keshavarz, T., & Roy, I. (2010). Production of polyhydroxyalkanoates: the future green materials of choice. *Journal of Chemical Technology and Biotechnology*, *85*(6), 732-743.

Akmal, D., Azizan, M. N., & Majid, M. I. A. (2003). Biodegradation of microbial polyesters P (3HB) and P (3HB-co-3HV) under the tropical climate environment. *Polymer degradation and stability*, *80*(3), 513-518.

Alam, A. M., Beg, M. D. H., Mina, M. F., Mamun, A. A., & Bledzki, A. K. (2014). Degradation and stability of green composites fabricated from oil palm empty fruit bunch fiber and polylactic acid: Effect of fiber length. *Journal of Composite Materials*, 0021998314560219.

Alcalde, M. (2007). Laccase: biological functions, molecular structure and industrial applications. In: Polaina J, Maccabe AP (eds.) Industrial enzymes: structure, function and applications. Netherlands: Springer.

Alejandra, R. C., Margarita, C. M., & Soledad, M. C. M. (2012). Enzymatic degradation of poly (3-hydroxybutyrate) by a commercial lipase. *Polymer Degradation and Stability*, *97*(11), 2473-2476.

Aljawish, A., Chevalot, I., Piffaut, B., Rondeau-Mouro, C., Girardin, M., Jasniewski, J., & Muniglia, L. (2012). Functionalization of chitosan by laccase-catalyzed oxidation of ferulic acid and ethyl ferulate under heterogeneous reaction conditions. *Carbohydrate Polymers*, *87*(1), 537-544.

Aluigi, A., Tonetti, C., Vineis, C., Tonin, C., & Mazzuchetti, G. (2011). Adsorption of copper (II) ions by keratin/PA6 blend nanofibres. *European Polymer Journal*, *47*(9), 1756-1764.

Aluigi, A., Vineis, C., Ceria, A., & Tonin, C. (2008b). Composite biomaterials from fibre wastes: Characterization of wool–cellulose acetate blends. *Composites Part A: Applied Science and Manufacturing*, *39*(1), 126-132.

Aluigi, A., Vineis, C., Varesano, A., Mazzuchetti, G., Ferrero, F., & Tonin, C. (2008a). Structure and properties of keratin/PEO blend nanofibres. *European Polymer Journal*, *44*(8), 2465-2475.

Aluigi, A., Zoccola, M., Vineis, C., Tonin, C., Ferrero, F., & Canetti, M. (2007). Study on the structure and properties of wool keratin regenerated from formic acid. *International journal of biological macromolecules*, *41*(3), 266-273.

Alvarez, V. A., Ruseckaite, R. A., & Vazquez, A. (2006). Degradation of sisal fibre/Mater Bi-Y biocomposites buried in soil. *Polymer Degradation and Stability*, *91*(12), 3156-3162.

Alves, C., Ferrão, P. M. C., Silva, A. J., Reis, L. G., Freitas, M., Rodrigues, L. B., & Alves, D. E. (2010). Ecodesign of automotive components making use of natural jute fiber composites. *Journal of Cleaner Production*, *18*(4), 313-327.

Alves, N. M., & Mano, J. F. (2008). Chitosan derivatives obtained by chemical modifications for biomedical and environmental applications. *International journal of biological Macromolecules*, *43*(5), 401-414.

Amass, W., Amass, A., & Tighe, B. (1998). A review of biodegradable polymers: uses, current developments in the synthesis and characterization of biodegradable polyesters, blends of biodegradable polymers and recent advances in biodegradation studies. *Polymer International*, *47*(2), 89-144.

Anastas, P. T., & Zimmerman, J. B. (2003). Peer reviewed: design through the 12 principles of green engineering. *Environmental Science & Technology*, *37*(5), 94A-101A.

Andrady, A. L., Torikai, A., Redhwi, H. H., Pandey, K. K., & Gies, P. (2015). Consequences of stratospheric ozone depletion and climate change on the use of materials. *Photochemical & Photobiological Sciences*, *14*(1), 170-184.

Andualema, B., & Gessesse, A. (2012). Microbial lipases and their industrial applications: review. *Biotechnology*, *11*(3), 100.

Anobom, C. D., Pinheiro, A. S., De-Andrade, R. A., Aguieiras, E. C., Andrade, G. C., Moura, M. V., ... & Freire, D. M. (2014). From structure to catalysis: recent developments in the biotechnological applications of lipases. *BioMed Research International*, *2014*, Article ID 684506, 11 pages.

Aracri, E., Fillat, A., Colom, J. F., Gutiérrez, A., José, C., Martínez, Á. T., & Vidal, T. (2010). Enzymatic grafting of simple phenols on flax and sisal pulp fibres using laccases. *Bioresource Technology*, *101*(21), 8211-8216.

Araujo, R., Casal, M., & Cavaco-Paulo, A. (2008). Application of enzymes for textile fibres processing. *Biocatalysis and Biotransformation*, *26*(5), 332-349.

Aravindan, R., Anbumathi, P., & Viruthagiri, T. (2007). Lipase applications in food industry. *Indian Journal of Biotechnology*, *6*(2), 141.

Archana, P. R., Rao, B. N., & Rao, B. S. (2011). Modulation of gamma ray–induced genotoxic effect by thymol, a monoterpene phenol derivative of cymene. *Integrative Cancer Therapies*, *10*(4), 374-383.

Ashby, M. F. (2000). Multi-objective optimization in material design and selection. *Acta Materialia*, *48*(1), 359-369.

Ashori, A. (2008). Wood–plastic composites as promising green-composites for automotive industries!. *Bioresource Technology*, *99*(11), 4661-4667.

Atadashi, I. M., Aroua, M. K., Aziz, A. A., & Sulaiman, N. M. N. (2013). The effects of catalysts in biodiesel production: a review. *Journal of Industrial and Engineering Chemistry*, *19*(1), 14-26.

Auras, R. A., Lim, L. T., Selke, S. E., & Tsuji, H. (Eds.). (2011). *Poly (lactic acid): synthesis, structures, properties, processing, and applications* (Vol. 10). John Wiley & Sons.

Austin, R. (2003). The art of sucking spaghetti. *Nature materials*, *2*, 567-568.

Awal, A., Rana, M., & Sain, M. (2015). Thermorheological and mechanical properties of cellulose reinforced PLA bio-composites. *Mechanics of Materials*, *80*, 87-95.

Babu, R., O'Connor, K., & Seeram, R. (2013). Current progress on bio-based polymers and their future trends. *Progress in Biomaterials*, *2*(8), doi:10.1186/2194-0517-2-8.

Bae, S., Sugano, Y., & Shoda, M. (2004). Improvement of bacterial cellulose production by addition of agar in a jar fermentor. *Journal of bioscience and bioengineering*, *97*(1), 33-38.

Bajpai, P. K., Singh, I., & Madaan, J. (2013). Tribological behavior of natural fiber reinforced PLA composites. *Wear*, *297*(1), 829-840.

Baldrian, P. (2006). Fungal laccases–occurrence and properties. *FEMS Microbiology Reviews*, *30*(2), 215-242.

Baltieri, R.C., Mei, L.H.I., Bartoli, J. 2003. Study of the influence of plasticizers on the thermal and mechanical properties of poly(3- hydroxybutyrate) compounds. *Macromolecular Symposia*, *197*, 33-44.

209

Barham, P. J., Keller, A., Otun, E. L., & Holmes, P. A. (1984). Crystallization and morphology of a bacterial thermoplastic: poly-3-hydroxybutyrate. *Journal of Materials Science*, *19*(9), 2781-2794.

Barker, P. A., Mason, F., & Barham, P. J. (1990). Density and crystallinity of poly (3-hydroxybutyrate/3-hydroxyvalerate) copolymers. *Journal of Materials Science*, *25*(4), 1952-1956.

Bartels, T. (2003). Variations in the morphology, distribution, and arrangement of feathers in domesticated birds. *Journal of Experimental Zoology Part B: Molecular and Developmental Evolution*, *298*(1), 91-108.

Basnett, P., Ching, K. Y., Stolz, M., Knowles, J. C., Boccaccini, A. R., Smith, C., & Roy, I. (2013). Novel Poly (3-hydroxyoctanoate)/Poly (3-hydroxybutyrate) blends for medical applications. *Reactive and Functional Polymers*, *73*(10), 1340-1348.

Bayram, C., Denkbaş, E. B., Kiliçay, E., Hazer, B., Çakmak, H. B., & Noda, I. (2008). Preparation and characterization of triamcinolone acetonide-loaded poly (3-hydroxybutyrate-co-3-hydroxyhexanoate)(PHBHx) microspheres. *Journal of Bioactive and Compatible Polymers*, *23*(4), 334-347.

Beltrami, L. V., Bandeira, J. A., Scienza, L. C., & Zattera, A. J. (2014). Biodegradable composites: Morphological, chemical, thermal, and mechanical properties of composites of poly (hydroxybutyrate-co-hydroxyvalerate) with curaua fibers after exposure to simulated soil. *Journal of Applied Polymer Science*, *131*(17), 40712.

Bertero, M., de la Puente, G., & Sedran, U. (2012). Fuels from bio-oils: Bio-oil production from different residual sources, characterization and thermal conditioning. *Fuel*, *95*, 263-271.

Bertini, F., Canetti, M., Patrucco, A., & Zoccola, M. (2013). Wool keratin-polypropylene composites: Properties and thermal degradation. *Polymer Degradation and Stability*, *98*(5), 980-987.

Bertrand, G. (1894). Sur le latex de l'arbre à laque. *CR Hebd. Acad. Sci. (Paris)*, *118*, 1215-1218.

Bettinger, C.J. 2011. Biodegradable elastomers for tissue engineering and cell-biomaterial interactions. *Macromolecular Bioscience*, *11*, 467-482.

Bhardwaj, R., Mohanty, A. K., Drzal, L. T., Pourboghrat, F., & Misra, M. (2006). Renewable resource-based green composites from recycled cellulose fiber and poly (3-hydroxybutyrate-co-3-hydroxyvalerate) bioplastic. *Biomacromolecules*, *7*(6), 2044-2051.

Bhat, M. K. (2000). Cellulases and related enzymes in biotechnology. *Biotechnology Advances*, *18*(5), 355-383.

Billingham, R. E., & Reynolds, J. (1952). Transplantation studies on sheets of pure epidermal epithelium and on epidermal cell suspensions. *British Journal of Plastic Surgery*, *5*(1), 25-36.

Bledzki, A. K., & Jaszkiewicz, A. (2010). Mechanical performance of biocomposites based on PLA and PHBV reinforced with natural fibres–A comparative study to PP. *Composites science and technology*, *70*(12), 1687-1696.

Bourbonnais, R., & Paice, M. G. (1990). Oxidation of non-phenolic substrates: an expanded role for laccase in lignin biodegradation. *FEBS Letters*, *267*(1), 99-102.

Bourbonnais, R., Paice, M. G., Freiermuth, B., Bodie, E., & Borneman, S. (1997). Reactivities of various mediators and laccases with kraft pulp and lignin model compounds. *Applied and Environmental Microbiology*, *63*(12), 4627-4632.

Boyandin, A. N., Prudnikova, S. V., Filipenko, M. L., Khrapov, E. A., Vasil'ev, A. D., & Volova, T. G. (2012). Biodegradation of polyhydroxyalkanoates by soil microbial communities of different structures and detection of PHA degrading microorganisms. *Applied Biochemistry and Microbiology*, *48*(1), 28-36.

Božič, M., Gorgieva, S., & Kokol, V. (2012). Homogeneous and heterogeneous methods for laccase-mediated functionalization of chitosan by tannic acid and quercetin. *Carbohydrate polymers*, *89*(3), 854-864.

Brady, L., Brzozowski, A. M., Derewenda, Z. S., Dodson, E., Dodson, G., Tolley, S., & Menge, U. (1990). A serine protease triad forms the catalytic centre of a triacylglycerol lipase. *Nature*, *343*, 767-70.

Brandelli, A. (2008). Bacterial keratinases: useful enzymes for bioprocessing agroindustrial wastes and beyond. *Food and Bioprocess Technology*, *1*(2), 105-116.

Brandelli, A., Daroit, D. J., & Riffel, A. (2010). Biochemical features of microbial keratinases and their production and applications. *Applied Microbiology and Biotechnology*, *85*(6), 1735-1750.

Brandelli, A., Sala, L., & Kalil, S. J. (2015). Microbial enzymes for bioconversion of poultry waste into added-value products. *Food Research International*, *73*, 3-12.

Braybrook, J. E. (1997). (Eds.); Biocompatibility Assessment of Medical Devices and Materials. 1st Edition. Chichester: John Wiley & Sons.

Briand, D., Dubreucq, E., & Galzy, P. (1994). Enzymatic fatty esters synthesis in aqueous medium with lipase from Candida parapsilosis (Ashford) Langeron and Talice. *Biotechnology Letters*, *16*(8), 813-818.

Brown, R. A., Prajapati, R., McGrouther, D. A., Yannas, I. V., & Eastwood, M. (1998). Tensional homeostasis in dermal fibroblasts: mechanical responses to mechanical loading in three-dimensional substrates. *Journal of Cellular Physiology*, *175*(3), 323-332.

Burlein, G. A., & Rocha, M. C. (2014). LDPE/PHB blends filled with castor oil pressed cake. *Materials Research*, *17*(1), 203-212.

Buttafoco, L., Kolkman, N. G., Engbers-Buijtenhuijs, P., Poot, A. A., Dijkstra, P. J., Vermes, I., & Feijen, J. (2006). Electrospinning of collagen and elastin for tissue engineering applications. *Biomaterials*, *27*(5), 724-734.

Cadena, E. M., Du, X., Gellerstedt, G., Li, J., Fillat, A., García-Ubasart, J., & Colom, J. F. (2011). On hexenuronic acid (HexA) removal and mediator coupling to pulp

fiber in the laccase/mediator treatment. *Bioresource Technology*, *102*(4), 3911-
3917.

Campos, R., Kandelbauer, A., Robra, K. H., Cavaco-Paulo, A., & Gübitz, G. M. (2001).
Indigo degradation with purified laccases from Trametes hirsuta and Sclerotium
rolfsii. *Journal of Biotechnology*, *89*(2), 131-139.

Canejo, J. P., Borges, J. P., Godinho, M. H., Brogueira, P., Teixeira, P. I., & Terentjev,
E. M. (2008). Helical twisting of electrospun liquid crystalline cellulose micro-and
nanofibers. *Adv. Mater*, *20*(24), 4821-4825.

Cao, H., Wool, R. P., Bonanno, P., Dan, Q., Kramer, J., & Lipschitz, S. (2014).
Development and evaluation of apparel and footwear made from renewable bio-
based materials. *International Journal of Fashion Design, Technology and
Education*, *7*(1), 21-30.

Carlsson, L., Malmström, E., & Carlmark, A. (2012). Surface-initiated ring-opening
metathesis polymerisation from cellulose fibres. *Polymer Chemistry*, *3*(3), 727-
733.

Casas-Godoy, L., Duquesne, S., Bordes, F., Sandoval, G., & Marty, A. (2012). Lipases:
an overview. In: Sandoval G, editor. Lipases and phospholipases: methods and
protocols. N.Y.: Springer. p 3–30.

Chandra, R. P., Lehtonen, L. K., & Ragauskas, A. J. (2004). Modification of high lignin
content kraft pulps with laccase to improve paper strength properties. 1. Laccase
treatment in the presence of gallic acid. *Biotechnology progress*, *20*(1), 255-261.

Chen, G. Q., & Wu, Q. (2005). The application of polyhydroxyalkanoates as tissue engineering materials. *Biomaterials*, *26*(33), 6565-6578.

Chen, N., Tong, Z., Yang, W., & Brennan, A. B. (2015). Biocomposites with tunable properties from poly (lactic acid)-based copolymers and carboxymethyl cellulose via ionic assembly. *Carbohydrate polymers*, *128*, 122-129.

Chen, Q. Z., Harding, S. E., Ali, N. N., Lyon, A. R., & Boccaccini, A. R. (2008). Biomaterials in cardiac tissue engineering: ten years of research survey. *Materials Science and Engineering: R: Reports*, *59*(1), 1-37.

Chen, Q., Liang, S., & Thouas, G. A. (2013). Elastomeric biomaterials for tissue engineering. *Progress in Polymer Science*, *38*(3), 584-671.

Chen, T., Kumar, G., Harris, M. T., Smith, P. J., & Payne, G. F. (2000). Enzymatic grafting of hexyloxyphenol onto chitosan to alter surface and rheological properties. *Biotechnology and Bioengineering*, *70*(5), 564-573.

Cheng, S. Z. (Ed.). (2002). *Handbook of thermal analysis and calorimetry: applications to polymers and plastics* (Vol. 3). Elsevier.

Cheng, S., Lau, K. T., Liu, T., Zhao, Y., Lam, P. M., & Yin, Y. (2009). Mechanical and thermal properties of chicken feather fiber/PLA green composites. *Composites Part B: Engineering*, *40*(7), 650-654.

Chou, K. S., Chang-Ho, H. W. R., & Goodrich, P. R. (1997). Poly (hydroxybutyrate-co-hydroxy-valerate) from swine waste liquor by Azotobacter vinelandii UWD. *Biotechnology Letters*, *19*(1), 7-10.

215

Christophe, J., & Coszach, P. (2000). *PLA: A potential solution to plastic waste dilemma. Macromolecular Symposia*, *153*, 287-303.

Church, J. S., Voda, A. S., Sutti, A., George, J., Fox, B. L., & Magniez, K. (2015). A simple and effective method to ameliorate the interfacial properties of cellulosic fibre based bio-composites using poly (ethylene glycol) based amphiphiles. *European Polymer Journal*, *64*, 70-78.

Clarinval, A. M., & Halleux, J. (2005). Classification of biodegradable polymers. In: Smith R (ed.) Biodegradable polymers for industrial applications. Woodhead, Cambridge.

Claus, H. (2004). Laccases: structure, reactions, distribution. *Micron*, *35*(1), 93-96.

Cocca, M., Avolio, R., Gentile, G., Di Pace, E., Errico, M. E., & Avella, M. (2015). Amorphized cellulose as filler in biocomposites based on poly (ε-caprolactone). *Carbohydrate polymers*, *118*, 170-182.

Coffee, R. A. (1998). A Dispensing Device and Method for Forming Material, PCT International Application No: PCT/GB97/01968.

Constantin, M., Mihalcea, I., Oanea, I., Harabagiu, V., & Fundueanu, G. (2011). Studies on graft copolymerization of 3-acrylamidopropyl trimethylammonium chloride on pullulan. *Carbohydrate Polymers*, *84*(3), 926-932.

Conzatti, L., Giunco, F., Stagnaro, P., Capobianco, M., Castellano, M., & Marsano, E. (2012). Polyester-based biocomposites containing wool fibres. *Composites Part A: Applied Science and Manufacturing*, *43*(7), 1113-1119.

216

Conzatti, L., Giunco, F., Stagnaro, P., Patrucco, A., Tonin, C., Marano, C., & Marsano, E. (2014). Wool fibres functionalised with a silane-based coupling agent for reinforced polypropylene composites. *Composites Part A: Applied Science and Manufacturing*, *61*, 51-59.

Cyras, V. P., Soledad, C. M., & Analía, V. (2009). Biocomposites based on renewable resource: Acetylated and non-acetylated cellulose cardboard coated with polyhydroxybutyrate. *Polymer*, *50*, 6274-6280.

Czaja, W. K., Young, D. J., Kawecki, M., & Brown, R. M. (2007). The future prospects of microbial cellulose in biomedical applications. *Biomacromolecules*, *8*(1), 1-12.

Czaja, W., Krystynowicz, A., Bielecki, S., Brown Jr, R.M. (2006). Microbial cellulose-the natural power to heal wounds. *Biomaterials*, *27*(2), 145-151.

Dai, Y., Lambert, L., Yuan, Z., & Keller, J. (2008). Characterisation of polyhydroxyalkanoate copolymers with controllable four-monomer composition. *Journal of Biotechnology*, *134*(1), 137-145.

Dawes, E. A. & Senior, P. J. 1973. The role and regulation of energy reserve polymers in micro-organisms. *Advances in Microbial Physiology, 10*, 135-266.

de Roo, G., Kellerhals, M. B., Ren, Q., Witholt, B., & Kessler, B. (2002). Production of chiral R-3-hydroxyalkanoic acids and R-3-hydroxyalkanoic acid methylesters via hydrolytic degradation of polyhydroxyalkanoate synthesized by pseudomonads. *Biotechnology and Bioengineering*, *77*(6), 717-722.

De Smet, M. J., Eggink, G., Witholt, B., Kingma, J., & Wynberg, H. (1983). Characterization of intracellular inclusions formed by Pseudomonas oleovorans during growth on octane. *Journal of Bacteriology*, *154*(2), 870-878.

Deamer, D. W., & Akeson, M. (2000). Nanopores and nucleic acids: prospects for ultrarapid sequencing. *Trends in Biotechnology*, *18*(4), 147-151.

Dega-Szafran, Z., Dutkiewicz, G., Kosturkiewicz, Z., & Szafran, M. (2008). Structure of complex of N-methylpiperidine betaine with p-hydroxybenzoic acid studied by X-ray, FT-IR and DFT methods. *Journal of Molecular Structure*, *875*(1), 346-353.

Deng, Y., Lin, X. S., Zheng, Z., Deng, J. G., Chen, J. C., Ma, H., & Chen, G. Q. (2003). Poly (hydroxybutyrate-co-hydroxyhexanoate) promoted production of extracellular matrix of articular cartilage chondrocytes in vitro. *Biomaterials*, *24*(23), 4273-4281.

Deng, Y., Zhao, K., Zhang, X. F., Hu, P., & Chen, G. Q. (2002). Study on the three-dimensional proliferation of rabbit articular cartilage-derived chondrocytes on polyhydroxyalkanoate scaffolds. *Biomaterials*, *23*(20), 4049-4056.

Desai, S. S., & Nityanand, C. (2011). Microbial laccases and their applications: a review. *Asian Journal of Biotechnol*, *3*(2), 98-124.

Desmet, G., Takács, E., Wojnárovits, L., & Borsa, J. (2011). Cellulose functionalization via high-energy irradiation-initiated grafting of glycidyl methacrylate and cyclodextrin immobilization. *Radiation Physics and Chemistry*, *80*(12), 1358-1362.

Dhake, K. P., Thakare, D. D., & Bhanage, B. M. (2013). Lipase: A potential biocatalyst for the synthesis of valuable flavour and fragrance ester compounds. *Flavour and Fragrance Journal*, *28*(2), 71-83.

Djidjelli, H., Martinez-Vega, J. J., Farenc, J., & Benachour, D. (2002). Effect of wood flour content on the thermal, mechanical and dielectric properties of poly (vinyl chloride). *Macromolecular Materials and Engineering*, *287*(9), 611-618.

Doi, Y. (1990). Microbial polyesters. *VCH Publishers*.

Doi, Y., Kitamura, S., & Abe, H. (1995). Microbial synthesis and characterization of poly (3-hydroxybutyrate-co-3-hydroxyhexanoate). *Macromolecules*, *28*(14), 4822-4828.

Dong, C., Ye, Y., Qian, L., Zhao, G., He, B., & Xiao, H. (2014). Antibacterial modification of cellulose fibers by grafting β-cyclodextrin and inclusion with ciprofloxacin. *Cellulose*, *21*(3), 1921-1932.

Doyle, C., Tanner, E. T. & Bonfield, W. 1991. *In vitro* and i*n vivo* evaluation of polyhydroxybutyrate and of polyhydroxybutyrate reinforced with hydroxyapatite. *Biomaterials, 12*, 841-847.

Dufresne, A., & Vincendon, M. (2000). Poly (3-hydroxybutyrate) and poly (3-hydroxyoctanoate) blends: morphology and mechanical behavior. *Macromolecules*, *33*(8), 2998-3008.

Duvernoy, O., Malm, T., Ramström, J., & Bowald, S. (1995). A biodegradable patch used as a pericardial substitute after cardiac surgery: 6-and 24-month evaluation with CT. *The Thoracic and Cardiovascular Surgeon*, *43*(5), 271-274.

Dwivedi, U. N., Singh, P., Pandey, V. P., & Kumar, A. (2011). Structure–function relationship among bacterial, fungal and plant laccases. *Journal of Molecular Catalysis B: Enzymatic*, *68*(2), 117-128.

Elegir, G., Kindl, A., Sadocco, P., & Orlandi, M. (2008). Development of antimicrobial cellulose packaging through laccase-mediated grafting of phenolic compounds. *Enzyme and Microbial Technology*, *43*(2), 84-92.

Engelberg, I. & Kohn, J. 1991. Physico-mechanical properties of degradable polymers used in medical applications: A comparative study. *Biomaterials, 12*, 292-304.

Enguita, F. J., Martins, L. O., Henriques, A. O., & Carrondo, M. A. (2003). Crystal structure of a bacterial endospore coat component a laccase with enhanced thermostability properties. *Journal of Biological Chemistry*, *278*(21), 19416-19425.

Espert, A., Vilaplana, F., & Karlsson, S. (2004). Comparison of water absorption in natural cellulosic fibres from wood and one-year crops in polypropylene composites and its influence on their mechanical properties. *Composites Part A: Applied Science and Manufacturing*, *35*(11), 1267-1276.

Estévez-Martínez, Y., Velasco-Santos, C., Martínez-Hernández, A. L., Delgado, G., Cuevas-Yáñez, E., Alaníz-Lumbreras, D., & Castaño, V. M. (2013). Grafting of

multiwalled carbon nanotubes with chicken feather keratin. *Journal of Nanomaterials*, *2013*, 38.

Fazilat, H., Akhlaghi, S., Shiri, M. E., & Sharif, A. (2012). Predicting thermal degradation kinetics of nylon6/feather keratin blends using artificial intelligence techniques. *Polymer*, *53*(11), 2255-2264.

Felby, C., Hassingboe, J., & Lund, M. (2002). Pilot-scale production of fiberboards made by laccase oxidized wood fibers: board properties and evidence for cross-linking of lignin. *Enzyme and Microbial Technology*, *31*(6), 736-741.

Fillat, A., Gallardo, O., Vidal, T., Pastor, F. I. J., Díaz, P., & Roncero, M. B. (2012). Enzymatic grafting of natural phenols to flax fibres: Development of antimicrobial properties. *Carbohydrate Polymers*, *87*(1), 146-152.

Fowler, P. A., Hughes, J. M., & Elias, R. M. (2006). Biocomposites: technology, environmental credentials and market forces. *Journal of the Science of Food and Agriculture*, *86*(12), 1781-1789.

Freier, T., Kunze, C., Nischan, C., Kramer, S., Sternberg, K., Saß, M., & Schmitz, K. P. (2002). In vitro and in vivo degradation studies for development of a biodegradable patch based on poly (3-hydroxybutyrate). *Biomaterials*, *23*(13), 2649-2657.

Freire, R.S., Duran, N., & Kubota, L.T. (2001). Effects of fungal laccase immobilization procedures for the development of a biosensor for phenol compounds. *Talanta*, *54*, 681-686.

García, J. L., Asadinezhad, A., Pacherník, J., Lehocký, M., Junkar, I., Humpolíček, P., & Valášek, P. (2010). Cell proliferation of HaCaT keratinocytes on collagen films modified by argon plasma treatment. *Molecules*, *15*(4), 2845-2856.

Garcia, Y., Collighan, R., Griffin, M., & Pandit, A. (2007). Assessment of cell viability in a three-dimensional enzymatically cross-linked collagen scaffold. *Journal of Materials Science: Materials in Medicine*, *18*(10), 1991-2001.

Gassner, F., & Owen, A. J. (1996). Some properties of poly (3-hydroxybutyrate)–poly (3-hydroxyvalerate) blends. *Polymer international*, *39*(3), 215-219.

Gerits, L. R., Pareyt, B., Decamps, K., & Delcour, J. A. (2014). Lipases and Their Functionality in the Production of Wheat-Based Food Systems. *Comprehensive Reviews in Food Science and Food Safety*, *13*(5), 978-989.

Ghanbarzadeh, B., & Almasi, H. (2013). Biodegradable polymers. *Biodegradation—Life of Science. R. Chamy and F. Rosenkranz, ed. InTech, Rijeka, Croatia*, 141-186.

Ghosh, A., & Collie, S. R. (2014). Keratinous materials as novel absorbent systems for toxic Pollutants. *Defence Science Journal*, *64*(3), 209-221.

Giardina, P., & Sannia, G. (2015). Laccases: old enzymes with a promising future. *Cellular and Molecular Life Sciences*, *72*(5), 855-856.

Gindl, W., Keckes, J. (2004). Tensile properties of cellulose acetate butyrate composites reinforced with bacterial cellulose. *Composites Science and Technology*, *64*(15), 2407-2413.

Gohil, G. S., Nagarale, R. K., Binsu, V. V., & Shahi, V. K. (2006). Preparation and characterization of monovalent cation selective sulfonated poly (ether ether ketone) and poly (ether sulfone) composite membranes. *Journal of Colloid and Interface Science*, *298*(2), 845-853.

Green, H., Kehinde, O., & Thomas, J. (1979). Growth of cultured human epidermal cells into multiple epithelia suitable for grafting. *Proceedings of the National Academy of Sciences*, *76*(11), 5665-5668.

Grochulski, P., Li, Y., Schrag, J. D., Bouthillier, F., Smith, P., Harrison, D., & Cygler, M. (1993). Insights into interfacial activation from an open structure of Candida rugosa lipase. *Journal of Biological Chemistry*, *268*(17), 12843-12847.

Grøndahl, L., Chandler-Temple, A., & Trau, M. (2005). Polymeric grafting of acrylic acid onto poly (3-hydroxybutyrate-co-3-hydroxyvalerate): Surface functionalization for tissue engineering applications. *Biomacromolecules*, *6*(4), 2197-2203.

Grunert, M., Winter, W.T. 2002. Nanocomposite of cellulose acetate butyrate reinforced with cellulose nanocrystals. *Journal of Polymers and the Environment*, *10*, 28-30.

Gupta, R., Gupta, N., & Rathi, P. (2004). Bacterial lipases: an overview of production, purification and biochemical properties. *Applied Microbiology and Biotechnology*, *64*(6), 763-781.

Guzmán, D., Kirsebom, H., Solano, C., Quillaguamán, J., & Hatti-Kaul, R. (2011). Preparation of hydrophilic poly (3-hydroxybutyrate) macroporous scaffolds

through enzyme-mediated modifications. *Journal of Bioactive and Compatible Polymers*, *26*(5), 452-463.

Ha, C. S., & Cho, W. J. (2002). Miscibility, properties, and biodegradability of microbial polyester containing blends. *Progress in Polymer Science*, *27*(4), 759-809.

Ha, S. W., Tonelli, A. E., & Hudson, S. M. (2005). Structural Studies of Bombyx m ori Silk Fibroin during Regeneration from Solutions and Wet Fiber Spinning. *Biomacromolecules*, *6*(3), 1722-1731.

Hameed, N., Guo, Q., Tay, F. H., & Kazarian, S. G. (2011). Blends of cellulose and poly (3-hydroxybutyrate-co-3-hydroxyvalerate) prepared from the ionic liquid 1-butyl-3-methylimidazolium chloride. *Carbohydrate Polymers*, *86*(1), 94-104.

Hancox, L. (2001). Thermoplastic composite manufacture: Opportunities and Challenges. *J. Macromol. Sci. Dev. Macromol. Chem. Phys*. C19, 418.

Hanefeld, U., Gardossi, L., & Magner, E. (2009). Understanding enzyme immobilisation. *Chemical Society Reviews*, *38*(2), 453-468.

Hatcher, L. Q., & Karlin, K. D. (2004). Oxidant types in copper–dioxygen chemistry: the ligand coordination defines the Cu n-O2 structure and subsequent reactivity. *JBIC Journal of Biological Inorganic Chemistry*, *9*(6), 669-683.

Hazari, A., Wiberg, M., Johansson-Ruden, G., Green, C., & Terenghi, G. (1999). A resorbable nerve conduit as an alternative to nerve autograft in nerve gap repair. *British Journal of Plastic Surgery*, *52*(8), 653-657.

Henriksson, M., Berglund, L. A., Isaksson, P., Lindstrom, T., & Nishino, T. (2008). Cellulose nanopaper structures of high toughness. *Biomacromolecules*, *9*(6), 1579-1585.

Herrmann, A. S., Nickel, J., & Riedel, U. (1998). Construction materials based upon biologically renewable resources—from components to finished parts. *Polymer Degradation and Stability*, *59*(1), 251-261.

Hinterstoisser, B., Åkerholm, M., Salmén, L. 2003. Load distribution in native cellulose. *Biomacromolecules*, *4*(5), 1232-1237.

Hiriart-Ramírez, E., Contreras-García, A., Garcia-Fernandez, M. J., Concheiro, A., Alvarez-Lorenzo, C., & Bucio, E. (2012). Radiation grafting of glycidyl methacrylate onto cotton gauzes for functionalization with cyclodextrins and elution of antimicrobial agents. *Cellulose*, *19*(6), 2165-2177.

Hoegger, P. J., Kilaru, S., James, T. Y., Thacker, J. R., & Kües, U. (2006). Phylogenetic comparison and classification of laccase and related multicopper oxidase protein sequences. *Febs Journal*, *273*(10), 2308-2326.

Hooshmand, S., Aitomäki, Y., Skrifvars, M., Mathew, A. P., & Oksman, K. (2014). All-cellulose nanocomposite fibers produced by melt spinning cellulose acetate butyrate and cellulose nanocrystals. *Cellulose*, *21*(4), 2665-2678.

Hossain, K. M. G., González, M. D., Lozano, G. R., & Tzanov, T. (2009). Multifunctional modification of wool using an enzymatic process in aqueous–organic media. *Journal of Biotechnology*, *141*(1), 58-63.

Houde, A., Kademi, A., & Leblanc, D. (2004). Lipases and their industrial applications. *Applied Biochemistry and Biotechnology*, *118*(1-3), 155-170.

Huang, L. P., Zhou, X. P., Cui, W., Xie, X. L., & Tong, S. Y. (2009). Maleic anhydride-grafted linear low-density polyethylene with low gel content. *Polymer Engineering and Science*, *49*(4), 673.

Huda, M. S., Drzal, L. T., Misra, M., Mohanty, A. K., Williams, K., & Mielewski, D. F. (2005). A study on biocomposites from recycled newspaper fiber and poly (lactic acid). *Industrial & engineering chemistry research*, *44*(15), 5593-5601.

Huda, S., & Yang, Y. (2008). Composites from ground chicken quill and polypropylene. *Composites Science and Technology*, *68*(3), 790-798.

Ikada, Y. (2006). Challenges in tissue engineering. *Journal of the Royal Society Interface*, *3*(10), 589-601.

Iqbal, H. M. N., Kyazze, G., & Keshavarz, T. (2013). Advances in the valorization of lignocellulosic materials by biotechnology: an overview. *BioResources*, *8*(2), 3157-3176.

Iqbal, H. M. N., Kyazze, G., Locke, I. C., Tron, T., & Keshavarz, T. (2015). In-situ development of self-defensive antibacterial biomaterials: phenol-g-keratin-EC based bio-composites with characteristics for biomedical applications. *Green Chemistry*, *17*, 3858-3869.

Iqbal, H. M. N., Kyazze, G., Tron, T., & Keshavarz, T. (2014a). "One-pot" synthesis and characterisation of novel P (3HB)–ethyl cellulose based graft composites through lipase catalysed esterification. *Polymer Chemistry*, *5*(24), 7004-7012.

Iqbal, H. M. N., Kyazze, G., Tron, T., & Keshavarz, T. (2014b). A preliminary study on the development and characterisation of enzymatically grafted P (3HB)-ethyl cellulose based novel composites. *Cellulose*, *21*(5), 3613-3621.

Iqbal, H. M. N., Kyazze, G., Tron, T., & Keshavarz, T. (2014c). Laccase-assisted grafting of poly (3-hydroxybutyrate) onto the bacterial cellulose as backbone polymer: Development and characterisation. *Carbohydrate Polymers*, *113*, 131-137.

Iqbal, H. M. N., Kyazze, G., Tron, T., & Keshavarz, T. (2015). Laccase-assisted approach to graft multifunctional materials of interest: keratin-EC based novel composites and their characterisation. *Macromolecular Materials and Engineering*, *300*, 712-720.

Jaeger, K. E., Dijkstra, B. W., & Reetz, M. T. (1999). Bacterial biocatalysts: molecular biology, three-dimensional structures, and biotechnological applications of lipases. *Annual Reviews in Microbiology*, *53*(1), 315-351.

Jaeger, K. E., Dijkstra, B. W., & Reetz, M. T. (1999). Bacterial biocatalysts: molecular biology, three-dimensional structures, and biotechnological applications of lipases. *Annual Reviews in Microbiology*, *53*(1), 315-351.

Jeon, J. R., Kim, E. J., Murugesan, K., Park, H. K., Kim, Y. M., Kwon, J. H., & Chang, Y. S. (2010). Laccase-catalysed polymeric dye synthesis from plant-derived phenols for potential application in hair dyeing: Enzymatic colourations driven by homo-or hetero-polymer synthesis. *Microbial Biotechnology*, *3*(3), 324-335.

Jillian, G. R. M., & Van Dyke, M. E. (2010) A review of keratin-based biomaterials for biomedical applications. *Materials*, *3*, 999-1014.

Jin, E., Reddy, N., Zhu, Z., & Yang, Y. (2011). Graft polymerization of native chicken feathers for thermoplastic applications. *Journal of Agricultural and Food Chemistry*, *59*(5), 1729-1738.

John, M. J., & Thomas, S. (2008). Biofibres and biocomposites. *Carbohydrate Polymers*, *71*(3), 343-364.

Jonas, R., Farah L.F. 1998. Production and application of microbial cellulose. *Polymer Degradation and Stability*, *59*, 101-106.

Jonathan, A., 2009. How Scanning Electron Microscopes Work. HowStuffWorks.com.

Joshi, J. M., & Sinha, V. K. (2006). Graft copolymerization of 2-hydroxyethylmethacrylate onto carboxymethyl chitosan using CAN as an initiator. *Polymer*, *47*(6), 2198-2204.

Kai, Z., Ying, D., & Guo-Qiang, C. (2003). Effects of surface morphology on the biocompatibility of polyhydroxyalkanoates. *Biochemical Engineering Journal*, *16*(2), 115-123.

Kai, Z., Ying, D., & Guo-Qiang, C. (2003). Effects of surface morphology on the biocompatibility of polyhydroxyalkanoates. *Biochemical Engineering Journal*, *16*(2), 115-123.

Kalangos, A., & Faidutti, B. (1996). Preliminary clinical results of implantation of biodegradable pericardial substitute in pediatric open heart operations. *The Journal of Thoracic and Cardiovascular Surgery*, *112*(5), 1401-1402.

Kalia, S., Dufresne, A., Cherian, B. M., Kaith, B. S., Avérous, L., Njuguna, J., & Nassiopoulos, E. (2011). Cellulose-based bio-and nanocomposites: a review. *International Journal of Polymer Science*, *2011*. Article ID 837875, 35 pages.

Kang, M. K., Kameta, A., Shin, K. H., Baluda, M. A., Kim, H. R., & Park, N. H. (2003). Senescence-associated genes in normal human oral keratinocytes. *Experimental Cell Research*, *287*(2), 272-281.

Kanwar, S. S., Srivastava, M., Chimni, S. S., Ghazi, I. A., Kaushal, R. K., & Joshi, G. K. (2004). Properties of an immobilized lipase of Bacillus coagulans BTS-1. *Acta Microbiologica et Immunologica Hungarica*, *51*(1-2), 57-73.

Katoh, K., Shibayama, M., Tanabe, T., & Yamauchi, K. (2004). Preparation and physicochemical properties of compression-molded keratin films. *Biomaterials*, *25*(12), 2265-2272.

Kawaguchi, Y. & Doi, Y. 1992. Kinetics and mechanism of synthesis and degradation of poly(3-hydroxybutyrate) in *Alcaligenes eutrophus*. *Macromolecules, 25*, 2324-2329.

Kenawy, E. R., Layman, J. M., Watkins, J. R., Bowlin, G. L., Matthews, J. A., Simpson, D. G., & Wnek, G. E. (2003). Electrospinning of poly (ethylene-co-vinyl alcohol) fibers. *Biomaterials*, *24*(6), 907-913.

Keshavarz, T., & Roy, I. (2010). Polyhydroxyalkanoates: bioplastics with a green agenda. *Current Opinion in Microbiology*, *13*(3), 321-326.

Khosa, M. A., & Ullah, A. (2013). A sustainable role of keratin biopolymer in green chemistry: a review. *J Food Processing & Beverages*, *1*(1), 8.

Kim, C. W., Kim, D. S., Kang, S. Y., Marquez, M., & Joo, Y. L. (2006). Structural studies of electrospun cellulose nanofibers. *Polymer*, *47*(14), 5097-5107.

Kim, H. S., Waksman, R., Cottin, Y., Kollum, M., Bhargava, B., Mehran, R., & Mintz, G. S. (2001). Edge stenosis and geographical miss following intracoronary gamma radiation therapy for in-stent restenosis. *Journal of the American College of Cardiology*, *37*(4), 1026-1030.

Kim, H. W., Chung, C. W., Kim, S. S., Kim, Y. B., & Rhee, Y. H. (2002). Preparation and cell compatibility of acrylamide-grafted poly (3-hydroxyoctanoate). *International Journal of Biological Macromolecules*, *30*(2), 129-135.

Klemm, D., Schumann, D., Udhardt, U., & Marsch, S. (2001). Bacterial synthesized cellulose—artificial blood vessels for microsurgery. *Progress in Polymer Science*, *26*(9), 1561-1603.

Kobayashi, S. (2009). Recent developments in lipase-catalyzed synthesis of polyesters. *Macromolecular Rapid Communications*, *30*(4-5), 237-266.

Kobayashi, S., & Makino, A. (2009). Enzymatic polymer synthesis: an opportunity for green polymer chemistry. *Chemical Reviews*, *109*(11), 5288-5353.

Koech, K. R., Wachira, F. N., Ngure, R. M., Wanyoko, J. K., Bii, C. C., Karori, S. M., & Kerio, L. C. (2013). Antimicrobial, synergistic and antioxidant activities of tea polyphenols. *Microbial Pathogens and Strategies for Combating Them: Science, Technology and Education, Formatex Research Center, Badajoz*, 971-981.

Köse, G. T., Korkusuz, F., Özkul, A., Soysal, Y., Özdemir, T., Yildiz, C., & Hasirci, V. (2005). Tissue engineered cartilage on collagen and PHBV matrices. *Biomaterials*, *26*(25), 5187-5197.

Kreplak, L., Doucet, J., Dumas, P., & Briki, F. (2004). New aspects of the α-helix to β-sheet transition in stretched hard α-keratin fibers. *Biophysical Journal*, *87*(1), 640-647.

Krivoguz, Y. M., Guliyev, A. M., & Pesetskii, S. S. (2013). Free-radical grafting of trans-ethylene-1, 2-dicarboxylic acid onto molten ethylene-vinyl acetate copolymer. *Journal of Applied Polymer Science*, *127*(4), 3104-3113.

Kubik, T., Bogunia-Kubik, K., & Sugisaka, M. (2005). Nanotechnology on duty in medical applications. *Current Pharmaceutical Biotechnology*, *6*(1), 17-33.

Kubota, H., Suka, I. G., Kuroda, S. I., & Kondo, T. (2001). Introduction of stimuli-responsive polymers into regenerated cellulose film by means of photografting. *European Polymer Journal*, *37*(7), 1367-1372.

Kudanga, T., Nyanhongo, G. S., Guebitz, G. M., & Burton, S. (2011). Potential applications of laccase-mediated coupling and grafting reactions: a review. *Enzyme and Microbial Technology*, *48*(3), 195-208.

Kudelski, A. (2002). Raman study on the structure of 3-mercaptopropionic acid monolayers on silver. *Surface Science*, *502*, 219-223.

Kull, K. R., Steen, M. L., & Fisher, E. R. (2005). Surface modification with nitrogen-containing plasmas to produce hydrophilic, low-fouling membranes. *Journal of Membrane Science*, *246*(2), 203-215.

Kumar, P., Barrett, D. M., Delwiche, M. J., & Stroeve, P. (2009). Methods for pretreatment of lignocellulosic biomass for efficient hydrolysis and biofuel production. *Industrial & Engineering Chemistry Research*, *48*(8), 3713-3729.

Kumari, T. V., Vasudev, U., Kumar, A., & Menon, B. (2001). Cell surface interactions in the study of biocompatibility. *Trends in Biomaterials and Artificial Organs*, *15*, 37-41.

Kunamneni, A., Camarero, S., García-Burgos, C., Plou, F. J., Ballesteros, A., & Alcalde, M. (2008). Engineering and applications of fungal laccases for organic synthesis. *Microbial Cell Factories*, *7*(1), 32.

Kunze, C., Bernd, H. E., Androsch, R., Nischan, C., Freier, T., Kramer, S., ... & Schmitz, K. P. (2006). In vitro and in vivo studies on blends of isotactic and atactic poly (3-hydroxybutyrate) for development of a dura substitute material. *Biomaterials*, *27*(2), 192-201.

Langer, R., & Vacanti, J. P. (1993). "Tissue engineering". Science, 260, 920-6.

Lao, H. K., Renard, E., Langlois, V., Vallée-Rehel, K., & Linossier, I. (2010). Surface functionalization of PHBV by HEMA grafting via UV treatment: Comparison with thermal free radical polymerization. *Journal of applied polymer science*, *116*(1), 288-297.

Lao, H. K., Renard, E., Linossier, I., Langlois, V., & Vallée-Rehel, K. (2007). Modification of poly (3-hydroxybutyrate-co-3-hydroxyvalerate) film by chemical graft copolymerization. *Biomacromolecules*, *8*(2), 416-423.

Lecointe, C., Dubreucq, E., & Galzy, P. (1996). Ester synthesis in aqueous media in the presence of various lipases. *Biotechnology Letters*, *18*(8), 869-874.

Lee, S. Y. (1996). Bacterial polyhydroxyalkanoates. *Biotechnology and Bioengineering*, *49*(1), 1-14.

Lehocký, M., Amaral, P. F. F., Coelho, M. A. Z., Sťahel, P., Barros-Timmons, A. M., & Coutinho, J. A. P. (2006). Attachment/detachment of Saccharomyces cerevisiae on plasma deposited organosilicon thin films. *Czechoslovak Journal of Physics*, *56*(2), B1256-B1262.

Lehocký, M., Sťahel, P., Koutný, M., Čech, J., Institoris, J., & Mráček, A. (2009). Adhesion of Rhodococcus sp. S3E2 and Rhodococcus sp. S3E3 to plasma prepared Teflon-like and organosilicon surfaces. *journal of Materials Processing Technology*, *209*(6), 2871-2875.

Lemoigne, M. (1926). Products of dehydration and of polymerization of ß-hydroxybutyric acid. *Bull Soc Chem Biol*, *8*, 770-782.

Lenz, R. W., & Marchessault, R. H. (2005). Bacterial polyesters: biosynthesis, biodegradable plastics and biotechnology. *Biomacromolecules*, *6*(1), 1-8.

Li, J., Gershow, M., Stein, D., Brandin, E., & Golovchenko, J. A. (2003). DNA molecules and configurations in a solid-state nanopore microscope. *Nature Materials*, *2*(9), 611-615.

Li, S. M., Jia, N., Ma, M. G., Zhang, Z., Liu, Q. H., & Sun, R. C. (2011). Cellulose–silver nanocomposites: Microwave-assisted synthesis, characterization, their thermal stability, and antimicrobial property. *Carbohydrate Polymers*, *86*(2), 441-447.

Li, S., & Yang, X. H. (2014). Fabrication and Characterization of Electrospun Wool Keratin/Poly (vinyl alcohol) Blend Nanofibers. *Advances in Materials Science and Engineering*, *2014*, 163678.

Li, Y., & Mai, Y. W. (2006). Interfacial characteristics of sisal fiber and polymeric matrices. *The Journal of Adhesion*, *82*(5), 527-554.

Li, Z., & Loh, X. J. (2015). Water soluble polyhydroxyalkanoates: future materials for therapeutic applications. *Chemical Society Reviews*, *44*(10), 2865-2879.

Lin, N., Huang, J., Chang, P. R., Feng, J., & Yu, J. (2011). Surface acetylation of cellulose nanocrystal and its reinforcing function in poly (lactic acid). *Carbohydrate Polymers*, *83*(4), 1834-1842.

Liu, Q. S., Zhu, M. F., Wu, W. H., & Qin, Z. Y. (2009). Reducing the formation of six-membered ring ester during thermal degradation of biodegradable PHBV to enhance its thermal stability. *Polymer Degradation and Stability*, *94*(1), 18-24.

Liu, Q., Zhang, H., Deng, B., & Zhao, X. (2014). Poly (3-hydroxybutyrate) and Poly (3-hydroxybutyrate-co-3-hydroxyvalerate): Structure, Property, and Fiber. *International Journal of Polymer Science*, *2014*. Article ID 374368, 11 pages.

Liu, R., & Saunders, B. R. (2009). Thermoresponsive surfaces prepared using adsorption of a cationic graft copolymer: A versatile method for triggered particle capture. *Journal of Colloid and Interface Science*, *338*(1), 40-47.

Lu, Z., Zhang, X., Li, Z., Wu, Z., Song, J., & Li, C. (2015). Composite copolymer hybrid silver nanoparticles: preparation and characterization of antibacterial activity and cytotoxicity. *Polymer Chemistry*, *6*(5), 772-779.

Luklinska, Z. B., & Bonfield, W. (1997). Morphology and ultrastructure of the interface between hydroxyapatite-polyhydroxybutyrate composite implant and bone. *Journal of Materials Science: Materials in Medicine*, *8*(6), 379-383.

Luo, L., Wei, X., & Chen, G. Q. (2009). Physical properties and biocompatibility of poly (3-hydroxybutyrate-co-3-hydroxyhexanoate) blended with poly (3-hydroxybutyrate-co-4-hydroxybutyrate). *Journal of Biomaterials Science, Polymer Edition*, *20*(11), 1537-1553.

Luzuriaga, S., Kovářová, J., & Fortelný, I. (2006). Degradation of pre-aged polymers exposed to simulated recycling: properties and thermal stability. *Polymer Degradation and Stability*, *91*(6), 1226-1232.

Lv, X., Song, W., Ti, Y., Qu, L., Zhao, Z., & Zheng, H. (2013). Gamma radiation-induced grafting of acrylamide and dimethyl diallyl ammonium chloride onto starch. *Carbohydrate Polymers*, *92*(1), 388-393.

Ma, Z., Gao, C., Ji, J., & Shen, J. (2002). Protein immobilization on the surface of poly-L-lactic acid films for improvement of cellular interactions. *European Polymer Journal*, *38*(11), 2279-2284.

MacArthur, B. D. & Oreffo, R. O. (2005). Bridging the gap. Nature, 433, 19. doi:10.1038/433019a.

Macrae, A. R., & Hammond, R. C. (1985). Present and future applications of lipases. *Biotechnology and Genetic Engineering Reviews*, *3*(1), 193-218.

MacVicar, R., Matuana, L. M., & Balatinecz, J. J. (1999). Aging mechanisms in cellulose fiber reinforced cement composites. *Cement and Concrete Composites*, *21*(3), 189-196.

Mani, R., & Bhattacharya, M. (2001). Properties of injection moulded blends of starch and modified biodegradable polyesters. *European Polymer Journal*, *37*(3), 515-526.

Mansur, H. S., Sadahira, C. M., Souza, A. N., & Mansur, A. A. (2008). FTIR spectroscopy characterization of poly (vinyl alcohol) hydrogel with different hydrolysis degree and chemically crosslinked with glutaraldehyde. *Materials Science and Engineering: C*, *28*(4), 539-548.

Markarian, J. (2008). Biopolymers present new market opportunities for additives in packaging. *Plastics, Additives and Compounding*, *10*(3), 22-25.

Martínez-Hernández, A. L., Velasco-Santos, C., de Icaza, M., & Castaño, V. M. (2005). Microstructural characterization of keratin fibers from chicken feathers. *International Journal Environmental and Pollution*, *23*, 162-178.

Mathew, A. P., Oksman, K., Pierron, D., & Harmand, M. F. (2012). Fibrous cellulose nanocomposite scaffolds prepared by partial dissolution for potential use as ligament or tendon substitutes. *Carbohydrate Polymers*, *87*(3), 2291-2298.

Menczel, J. D., & Prime, R. B. (Eds.). (2014). *Thermal analysis of polymers: fundamentals and applications*. John Wiley & Sons.

Mergaert, J., Anderson, C., Wouters, A., Swings, J., Kersters, K., (1992). Biodegradation of polyhydoxyalkanoates. *FEMS Microbiology Reviews*, *103*, 317–322.

Messner, K., Koller, K., Wall, M. B., Akther, M., and Scott, G. M. (1998). "Fungal treatment of wood chips for chemical pulping," In: Young, R. A., and Akther, M. (eds) John Wiley and Sons, Inc., pp. 385-398.

Metcalfe, A. D., & Ferguson, M. W. (2007). Tissue engineering of replacement skin: the crossroads of biomaterials, wound healing, embryonic development, stem cells and regeneration. *Journal of the Royal Society Interface*, *4*(14), 413-437.

Miao, C., & Hamad, W. Y. (2013). Cellulose reinforced polymer composites and nanocomposites: a critical review. *Cellulose*, *20*(5), 2221-2262.

Miao, J., Pangule, R. C., Paskaleva, E. E., Hwang, E. E., Kane, R. S., Linhardt, R. J., & Dordick, J. S. (2011). Lysostaphin-functionalized cellulose fibers with antistaphylococcal activity for wound healing applications. *Biomaterials*, *32*(36), 9557-9567.

Michl, T. D., Locock, K. E., Stevens, N. E., Hayball, J. D., Vasilev, K., Postma, A., ... & Griesser, H. J. (2014). RAFT-derived antimicrobial polymethacrylates: elucidating the impact of end-groups on activity and cytotoxicity. *Polymer Chemistry*, *5*(19), 5813-5822.

Mikolasch, A., & Schauer, F. (2009). Fungal laccases as tools for the synthesis of new hybrid molecules and biomaterials. *Applied Microbiology and Biotechnology*, *82*(4), 605-624.

Milovanovic, S., Stamenic, M., Markovic, D., Radetic, M., & Zizovic, I. (2013). Solubility of thymol in supercritical carbon dioxide and its impregnation on cotton gauze. *The Journal of Supercritical Fluids*, *84*, 173-181.

Min, B. M., Lee, G., Kim, S. H., Nam, Y. S., Lee, T. S., & Park, W. H. (2004). Electrospinning of silk fibroin nanofibers and its effect on the adhesion and spreading of normal human keratinocytes and fibroblasts in vitro. *Biomaterials*, *25*(7), 1289-1297.

Misra, S. K., Valappil, S. P., Roy, I. & Boccaccini, A. R. 2006. Polyhydroxyalkanoate (PHA)/Inorganic Phase Composites for Tissue Engineering Applications. *Biomacromolecules, 7*, 2249-2258.

Mitomo, H., Watanabe, Y., Yoshii, F., Makuuchi, K. (1995). Radiation effect on polyesters. *Radiation Physics and Chemistry*, *46*(2), 233-238.

Mohammed-Ziegler, I., Tánczos, I., Hórvölgyi, Z., & Agoston, B. (2008). Water-repellent acylated and silylated wood samples and their surface analytical characterization. *Colloids and Surfaces A: Physicochemical and Engineering Aspects*, *319*(1), 204-212.

Mohanty, A. K., Misra, M., & Drzal, L. T. (2002). Sustainable bio-composites from renewable resources: opportunities and challenges in the green materials world. *Journal of Polymers and the Environment*, *10*(1-2), 19-26.

Mohanty, A. K., Misra, M., & Hinrichsen, G. (2000). Biofibres, biodegradable polymers and biocomposites: an overview. *Macromolecular Materials and Engineering*, *276*(1), 1-24.

Moore, G. R. P., Martelli, S. M., Gandolfo, C., do Amaral Sobral, P. J., & Laurindo, J. B. (2006). Influence of the glycerol concentration on some physical properties of feather keratin films. *Food Hydrocolloids*, *20*(7), 975-982.

Morozova, O. V., Shumakovich, G. P., Shleev, S. V., & Yaropolov, Y. I. (2007). Laccase-mediator systems and their applications: a review. *Applied Biochemistry and Microbiology*, *43*(5), 523-535.

Mustafa, R., Muniglia, L., Rovel, B., & Girardin, M. (2005). Phenolic colorants obtained by enzymatic synthesis using a fungal laccase in a hydro-organic biphasic system. *Food Research International*, *38*(8), 995-1000.

Nady, N., Franssen, M. C., Zuilhof, H., Eldin, M. S. M., Boom, R., & Schroën, K. (2011). Modification methods for poly (arylsulfone) membranes: a mini-review focusing on surface modification. *Desalination*, *275*(1), 1-9.

Nair, L. S., & Laurencin, C. T. (2007). Biodegradable polymers as biomaterials. *Progress in Polymer Science*, *32*(8), 762-798.

Nance, C. L., Williamson, M. P., McCormick, T. G., Paulson, S. M., & Shearer, W. T. (2006). Epigallocatechin gallate, green tea catechin, binds to the T cell receptor, CD4. *Journal of Allergy and Clinical Immunology*, *117*(2), S325.

Nasef, M. M. (2014). Radiation-Grafted Membranes for Polymer Electrolyte Fuel Cells: Current Trends and Future Directions. *Chemical Reviews*, *114*(24), 12278-12329.

Ng, C. P., & Swartz, M. A. (2003). Fibroblast alignment under interstitial fluid flow using a novel 3-D tissue culture model. *American Journal of Physiology-Heart and Circulatory Physiology*, *284*(5), H1771-H1777.

Nigmatullin, R., Thomas, P., Lukasiewicz, B., Puthussery, H., & Roy, I. (2015). Polyhydroxyalkanoates, a family of natural polymers, and their applications in drug delivery. *Journal of Chemical Technology and Biotechnology*. *90*, 1209-1221.

Nishizawa, M., Menon, V. P., Martin, C. R. (1995). Metal Nanotubule Membranes with Electrochemically Switchable Ion-Transport Selectivity, *Science*, *268*, 700-702.

Ojumu, T. V., Yu, J., & Solomon, B. O. (2004). Production of polyhydroxyalkanoates, a bacterial biodegradable polymer. *African Journal of Biotechnology*, *3*(1), 18-24.

Ottosson, J., Rotticci-Mulder, J. C., Rotticci, D., & Hult, K. (2001). Rational design of enantioselective enzymes requires considerations of entropy. *Protein Science*, *10*(9), 1769-1774.

Pandey, J. K., Ahn, S. H., Lee, C. S., Mohanty, A. K., & Misra, M. (2010). Recent advances in the application of natural fiber based composites. *Macromolecular Materials and Engineering*, *295*(11), 975-989.

Pardo-Ibáñez, P., Lopez-Rubio, A., Martínez-Sanz, M., Cabedo, L., & Lagaron, J. M. (2014). Keratin–polyhydroxyalkanoate melt-compounded composites with

improved barrier properties of interest in food packaging applications. *Journal of Applied Polymer Science*, *131*(4), DOI: 10.1002/APP.39947.

Park, M., Kim, B. S., Shin, H. K., Park, S. J., & Kim, H. Y. (2013). Preparation and characterization of keratin-based biocomposite hydrogels prepared by electron beam irradiation. *Materials Science and Engineering: C*, *33*(8), 5051-5057.

Pasquini, D., Belgacem, M. N., Gandini, A., & da Silva Curvelo, A. A. (2006). Surface esterification of cellulose fibers: Characterization by DRIFT and contact angle measurements. *Journal of Colloid and Interface Science*, *295*(1), 79-83.

Patel, N. R. (2007). Biocatalysis in the pharmaceutical and biotechnology industries, CRC Press, Boca Raton.

Pei, Y., Sugita, O. R., Quek, J. Y., Roth, P. J., & Lowe, A. B. (2015). pH-, thermo-and electrolyte-responsive polymer gels derived from a well-defined, RAFT-synthesized, poly (2-vinyl-4, 4-dimethylazlactone) homopolymer via one-pot post-polymerization modification. *European Polymer Journal*, *62*, 204-213.

Peng, T., & Cheng, Y. L. (2001). PNIPAAm and PMAA co-grafted porous PE membranes: living radical co-grafting mechanism and multi-stimuli responsive permeability. *Polymer*, *42*(5), 2091-2100.

Pereira, L., Bastos, C., Tzanov, T., Cavaco-Paulo, A., & Gübitz, G. M. (2005). Environmentally friendly bleaching of cotton using laccases. *Environmental Chemistry Letters*, *3*(2), 66-69.

Peschel, G., Dahse, H. M., Konrad, A., Wieland, G. D., Mueller, P. J., Martin, D. P., & Roth, M. (2008). Growth of keratinocytes on porous films of poly (3-hydroxybutyrate) and poly (4-hydroxybutyrate) blended with hyaluronic acid and chitosan. *Journal of Biomedical Materials Research Part A*, *85*(4), 1072-1081.

Philip, S., Keshavarz, T., & Roy, I. (2007). Polyhydroxyalkanoates: biodegradable polymers with a range of applications. *Journal of Chemical Technology and Biotechnology*, *82*(3), 233-247.

Piao, H. (2006). Microbial-derived Cellulose-reinforced Biocomposites: A Thesis Submitted in Partial Fulfilment of the Requirements for the Degree of Master of Engineering in the Department of Mechanical Engineering, Engineering School. University of Canterbury, Christchurch, New Zealand.

Plackett, D. (ed) (2011) Front Matter, in Biopolymers - New Materials for Sustainable Films and Coatings, John Wiley & Sons, Ltd, Chichester, UK. doi: 10.1002/9781119994312.fmatter.

Plackett, D., Andersen, T. L., Pedersen, W. B., & Nielsen, L. (2003). Biodegradable composites based on L-polylactide and jute fibres. *Composites Science and Technology*, *63*(9), 1287-1296.

Rahman, L., Silong, S., Zin, W. M., Rahman, M. Z. A. B., Ahmad, M., & Haron, J. (2000). Graft copolymerization of methyl acrylate onto sago starch using ceric

ammonium nitrate as an initiator. *Journal of Applied Polymer Science*, *76*(4), 516-523.

Rai, R., Yunos, D. M., Boccaccini, A. R., Knowles, J. C., Barker, I. A., Howdle, S. M., Keshavarz, T., & Roy, I. (2011). Poly-3-hydroxyoctanoate P (3HO), a medium chain length polyhydroxyalkanoate homopolymer from Pseudomonas mendocina. *Biomacromolecules*, *12*(6), 2126-2136.

Ramakrishna, M., Vivek, K., & Yuvraj, S. N. (2009). Recent development in natural fiber reinforced polypropylene composites. *Journal of Reinforced Plastics and Composites*, *28*, 1169-1189.

Ratner, B. D., Hoffman, A. S., Schoen, F. J., & Lemons, J. E. (2004). *Biomaterials science: an introduction to materials in medicine*. Academic press.

Reddy, N., Chen, L., & Yang, Y. (2013b). Biothermoplastics from hydrolyzed and citric acid Crosslinked chicken feathers. *Materials Science and Engineering: C*, *33*(3), 1203-1208.

Reddy, N., Hu, C., Yan, K., & Yang, Y. (2011). Thermoplastic films from cyanoethylated chicken feathers. *Materials Science and Engineering: C*, *31*(8), 1706-1710.

Reddy, N., Jiang, Q., Jin, E., Shi, Z., Hou, X., & Yang, Y. (2013a). Bio-thermoplastics from grafted chicken feathers for potential biomedical applications. *Colloids and Surfaces B: Biointerfaces*, *110*, 51-58.

Rehm, B. H. (2015). Microbial Synthesis of Biodegradable Polyesters: Processes, Products, Applications. *Biodegradable Polyesters*, 47-72.

Reichl, S., Borrelli, M., & Geerling, G. (2011). Keratin films for ocular surface reconstruction. *Biomaterials*, *32*(13), 3375-3386.

Rhee, S., & Grinnell, F. (2007). Fibroblast mechanics in 3D collagen matrices. *Advanced Drug Delivery Reviews*, *59*(13), 1299-1305.

Rheinwald, J. G., Hahn, W. C., Ramsey, M. R., Wu, J. Y., Guo, Z., Tsao, H., & O'Toole, K. M. (2002). A two-stage, p16INK4A-and p53-dependent keratinocyte senescence mechanism that limits replicative potential independent of telomere status. *Molecular and cellular biology*, *22*(14), 5157-5172.

Riva, S. (2006). Laccases: blue enzymes for green chemistry. *TRENDS in Biotechnology*, *24*(5), 219-226.

Rizzarelli, P., Puglisi, C., & Montaudo, G. (2004). Soil burial and enzymatic degradation in solution of aliphatic co-polyesters. *Polymer Degradation and Stability*, *85*(2), 855-863.

Roach, P., Eglin, D., Rohde, K., & Perry, C. C. (2007). Modern biomaterials: a review—bulk properties and implications of surface modifications. *Journal of Materials Science: Materials in Medicine*, *18*(7), 1263-1277.

Robles, A., Lucas, R., de Cienfuegos, G. A., & Gálvez, A. (2000). Phenol-oxidase (laccase) activity in strains of the hyphomycete Chalara paradoxa isolated from

olive mill wastewater disposal ponds. *Enzyme and Microbial Technology*, *26*(7), 484-490.

Rodríguez-Couto, S., & Sanromán, M.A. (2006). Application of solid-state fermentation to food industry-a review. *Journal of Food Engineering*, *76*(3), 291-302.

Rodriguez-Gonzalez, C., Kharissova, O. V., MARTÍNEZ-HERNÁNDEZ, A. N. A. L., Castano, V. M., & Velasco-Santos, C. (2013). Graphene oxide sheets covalently grafted with keratin obtained from chicken feathers. *Digest Journal of Nanomaterials and Biostructures*, *8*(1), 127-38.

Rosenzweig, A. C., & Sazinsky, M. H. (2006). Structural insights into dioxygen-activating copper enzymes. *Current Opinion in Structural Biology*, *16*(6), 729-735.

Roy, S. G., & De, P. (2014). Facile RAFT synthesis of side-chain amino acids containing pH-responsive hyperbranched and star architectures. *Polymer Chemistry*, *5*(21), 6365-6378.

Roy, S. G., Acharya, R., Chatterji, U., & De, P. (2013). RAFT polymerization of methacrylates containing a tryptophan moiety: controlled synthesis of biocompatible fluorescent cationic chiral polymers with smart pH-responsiveness. *Polymer Chemistry*, *4*(4), 1141-1152.

Ruka, D. R., Simon, G. P., & Dean, K. (2014). Harvesting fibrils from bacterial cellulose pellicles and subsequent formation of biodegradable poly-3-hydroxybutyrate nanocomposites. *Cellulose*, *21*(6), 4299-4308.

Rukmani, A., & Sundrarajan, M. (2012). Inclusion of antibacterial agent thymol on β-cyclodextrin-grafted organic cotton. *Journal of Industrial Textiles*, *42*(2), 132-144.

Ruth, K., Grubelnik, A., Hartmann, R., Egli, T., Zinn, M., & Ren, Q. (2007). Efficient production of (R)-3-hydroxycarboxylic acids by biotechnological conversion of polyhydroxyalkanoates and their purification. *Biomacromolecules*, *8*(1), 279-286.

Sabaa, M. W., Mohamed, N. A., Mohamed, R. R., Khalil, N. M., & El Latif, S. M. A. (2010). Synthesis, characterization and antimicrobial activity of poly (N-vinyl imidazole) grafted carboxymethyl chitosan. *Carbohydrate Polymers*, *79*(4), 998-1005.

Saleh, O. A., & Sohn, L. L. (2003). An artificial nanopore for molecular sensing. *Nano Letters*, *3*(1), 37-38.

Sánchez, C. (2009). Lignocellulosic residues: biodegradation and bioconversion by fungi. *Biotechnology Advances*, *27*(2), 185-194.

Sanchez-Garcia, M. D., Ocio, M. J., Gimenez, E., & Lagaron, J. M. (2008). Novel polycaprolactone nanocomposites containing thymol of interest in antimicrobial film and coating applications. *Journal of Plastic Film and Sheeting*, *24*(3-4), 239-251.

Sato, H., Nakamura, M., Padermshoke, A., Yamaguchi, H., Terauchi, H., Ekgasit, S., & Ozaki, Y. (2004). Thermal behavior and molecular interaction of poly (3-hydroxybutyrate-co-3-hydroxyhexanoate) studied by wide-angle X-ray diffraction. *Macromolecules*, *37*(10), 3763-3769.

Satoh, H., Yoshie, N., & Inoue, Y. (1994). Hydrolytic degradation of blends of poly (3-hydroxybutyrate) with poly (3-hydroxybutyrate-co-3-hydroxyvalerate). *Polymer*, *35*(2), 286-290.

Saxena, R. K., Sheoran, A., Giri, B., & Davidson, W. S. (2003). Purification strategies for microbial lipases. *Journal of Microbiological Methods*, *52*(1), 1-18.

Schawe, J. E. K., Hütter, T., Heitz, C., Alig, I., & Lellinger, D. (2006). Stochastic temperature modulation: a new technique in temperature-modulated DSC. *Thermochimica Acta*, *446*(1), 147-155.

Schmidt, W.F., (1998), Innovative feather utilization strategies. Proceedings of National Poultry Waste Management conference, pp 276-282, Springdale, Ar., October 19-22, 1998.

Schulz, H., Özkan, G., Baranska, M., Krüger, H., & Özcan, M. (2005). Characterisation of essential oil plants from Turkey by IR and Raman spectroscopy. *Vibrational Spectroscopy*, *39*(2), 249-256.

Schulz, H., Quilitzsch, R., & Krüger, H. (2003). Rapid evaluation and quantitative analysis of thyme, origano and chamomile essential oils by ATR-IR and NIR spectroscopy. *Journal of Molecular Structure*, *661*, 299-306.

Selmin, F., Cilurzo, F., Aluigi, A., Franzè, S., & Minghetti, P. (2012). Regenerated keratin membrane to match the in vitro drug diffusion through human epidermis. *Results in Pharma Sciences*, *2*, 72-78.

Serafim, L.S., Lemos, P.C., Torres, C., Reis, M.A., Ramos, A.M. 2008. The influence of process parameters on the characteristics of polyhydroxyalkanoates produced by mixed cultures. *Macromolecular Bioscience*, *8*(4), 355-366.

Sevastianov, V. I., Perova, N. V., Shishatskaya, E. I., Kalacheva, G. S., & Volova, T. G. (2003). Production of purified polyhydroxyalkanoates (PHAs) for applications in contact with blood. *Journal of Biomaterials Science, Polymer Edition*, *14*(10), 1029-1042.

Shahidi, S., Aslan, N., Ghoranneviss, M., & Korachi, M. (2014). Effect of thymol on the antibacterial efficiency of plasma-treated cotton fabric. *Cellulose*,*21*(3), 1933-1943.

Shahidi, S., Rashidi, A., Ghoranneviss, M., Anvari, A., Rahimi, M. K., Moghaddam, M. B., & Wiener, J. (2010). Investigation of metal absorption and antibacterial activity on cotton fabric modified by low temperature plasma. *Cellulose*, *17*(3), 627-634.

Sharma, R., Chisti, Y., & Banerjee, U. C. (2001). Production, purification, characterization, and applications of lipases. *Biotechnology Advances*, *19*(8), 627-662.

Shaw, J. (2002). Cellulose derivatives. *Adv. Polym. Sci*, *105*, 224-231.

Silva, N. C., Miranda, J. S., Bolina, I. C., Silva, W. C., Hirata, D. B., de Castro, H. F., & Mendes, A. A. (2014). Immobilization of porcine pancreatic lipase on poly-

hydroxybutyrate particles for the production of ethyl esters from macaw palm oils and pineapple flavor. *Biochemical Engineering Journal*, *82*, 139-149.

Singha, A. S., Rana, R. K., & Rana, A. (2010). Natural fiber reinforced polystyrene matrix based composites. In *Advanced Materials Research*, *123*, 1175-1178.

Skelton, P., (2006). *Biopolymer packaging in UK grocery market*, Materials change for a better environment.

Smith, D., Reneker, D., Mcmanus, A., Schreuder-gibson, H., Mello, C., Sennett, M., & Gibson, P. (2001). Electrospun Fibers and an Apparatus Therefore, PCT International Application No: PCT/US00/27776.

Smith, E., & Dent, G. (2005) Modern Raman Spectroscopy. A Practical Approach, J. Wiley & Sons, Ltd, Chinchester.

Smith, E., & Dent, G. (2013). *Modern Raman spectroscopy: a practical approach*. John Wiley & Sons.

Sodian, R., Hoerstrup, S. P., Sperling, J. S., Daebritz, S., Martin, D. P., Moran, A. M., Kim, B.S., Schoen, F.J., Vacanti, J.P., & Mayer, J. E. (2000). Early in vivo experience with tissue-engineered trileaflet heart valves. *Circulation*, *102*, 22-29.

Sombatsompop, N., Chaochanchaikul, K., Phromchirasuk, C., & Thongsang, S. (2003). Effect of wood sawdust content on rheological and structural changes, and thermo-mechanical properties of PVC/sawdust composites. *Polymer International*, *52*(12), 1847-1855.

Son, H.J., Heo, M.S., Kim, Y.G., & Lee, S.J. (2001). Optimization of fermentation conditions for the production of bacterial cellulose by a newly isolated *Acetobacter. Biotechnology and Applied Biochemistry*, *33*(1), 1-5.

Son, W. K., Youk, J. H., & Park, W. H. (2006). Antimicrobial cellulose acetate nanofibers containing silver nanoparticles. *Carbohydrate Polymers*, *65*(4), 430-434.

Spiridon, I., Paduraru, O. M., Zaltariov, M. F., & Darie, R. N. (2013). Influence of keratin on polylactic acid/chitosan composite properties. Behavior upon accelerated weathering. *Industrial & Engineering Chemistry Research*, *52*(29), 9822-9833.

Srubar, W. V., Pilla, S., Wright, Z. C., Ryan, C. A., Greene, J. P., Frank, C. W., & Billington, S. L. (2012). Mechanisms and impact of fiber–matrix compatibilization techniques on the material characterization of PHBV/oak wood flour engineered biobased composites. *Composites Science and Technology*, *72*(6), 708-715.

Steinmann, W., Seide, G., Beckers, M., Walter, S., & Gries, T. (2013). *Thermal Analysis of Phase Transitions and Crystallization in Polymeric Fibers*. INTECH Open Access Publisher.

Stevens, M. M. (2008). Biomaterials for bone tissue engineering. *Materials Today*, *11*(5), 18-25.

Subhash, D., Mandal, C., & Mandal, M. (2010). Current status and future prospects of new drug delivery system. *Pharma Times, 42*, 13-6.

Sudesh, K., Abe, H. & Doi, Y. 2000. Synthesis, structure and properties of polyhydroxyalkanoates: Biological polyesters. *Progress in Polymer Science, 25*, 1503-1555.

Sun, J., & Liu, S. Q. (2015). Ester Synthesis in Aqueous Media by Lipase: Alcoholysis, Esterification and Substrate Hydrophobicity. *Journal of Food Biochemistry*, *39*(1), 11-18.

Sun, J., Wu, J., Li, H., & Chang, J. (2005). Macroporous poly (3-hydroxybutyrate-co-3-hydroxyvalerate) matrices for cartilage tissue engineering. *European Polymer Journal*, *41*(10), 2443-2449.

Sun, T., Xu, P., Liu, Q., Xue, J., & Xie, W. (2003). Graft copolymerization of methacrylic acid onto carboxymethyl chitosan. *European Polymer Journal*, *39*(1), 189-192.

Suthar, V., Pratap, A., Raval, H. 2000. Studies on poly (hydroxy alkanoates)/ (ethylcellulose) blends. *Bulletin of Materials Science*, *23*(3), 215-219.

Svensson, A., Nicklasson, E., Harrah, T., Panilaitis, B., Kaplan, D. L., Brittberg, M., Gatenholm, P. (2005). Bacterial cellulose as a potential scaffold for tissue engineering of cartilage. *Biomaterials*, *26*(4), 419-431.

Tanabe, T., Okitsu, N., Tachibana, A., & Yamauchi, K. (2002). Preparation and characterization of keratin–chitosan composite film. *Biomaterials*, *23*(3), 817-825.

Terabe, K., Hasegawa, T., Nakayama, T., & Aono, M. (2005). Quantized conductance atomic switch. *Nature*, *433*(7021), 47-50.

Tham, W. L., Ishak, Z. M., & Chow, W. S. (2014). Water absorption and hygrothermal aging behaviors of SEBS-g-MAH toughened poly (lactic acid)/halloysite nanocomposites. *Polymer-Plastics Technology and Engineering*, *53*(5), 472-480.

Thévenot, D. R., Toth, K., Durst, R. A., & Wilson, G. S. (2001). Electrochemical biosensors: recommended definitions and classification. *Biosensors and Bioelectronics*, *16*(1), 121-131.

Thomas, S. (1990). *Wound management and dressings*. Pharmaceutical Press.

Tokiwa, Y., & Calabia, B. P. (2004). Review degradation of microbial polyesters. *Biotechnology Letters*, *26*(15), 1181-1189.

Tokoh, C., Takabe, K., Fujita, M., & Saiki, H. (1998). Cellulose synthesized by Acetobacter xylinum in the presence of acetyl glucomannan. *Cellulose*, *5*(4), 249-261.

Tonin, C., Aluigi, A., Vineis, C., Varesano, A., Montarsolo, A., & Ferrero, F. (2006). Thermal and structural characterization of poly (ethylene-oxide)/keratin blend films. *Journal of Thermal Analysis and Calorimetry*, *89*(2), 601-608.

Torres, F. G., & Cubillas, M. L. (2005). Study of the interfacial properties of natural fibre reinforced polyethylene. *Polymer Testing*, *24*(6), 694-698.

Torres-Giner, S., Martinez-Abad, A., & Lagaron, J. M. (2014). Zein-based ultrathin fibers containing ceramic nanofillers obtained by electrospinning. II. Mechanical

properties, gas barrier, and sustained release capacity of biocide thymol in multilayer polylactide films. *Journal of Applied Polymer Science*, *131*(18).

Tserki, V., Matzinos, P., Kokkou, S., & Panayiotou, C. (2005). Novel biodegradable composites based on treated lignocellulosic waste flour as filler. Part I. Surface chemical modification and characterization of waste flour. *Composites Part A: Applied Science and Manufacturing*, *36*(7), 965-974.

Tsujii, Y., Ohno, K., Yamamoto, S., Goto, A., & Fukuda, T. (2006). Structure and properties of high-density polymer brushes prepared by surface-initiated living radical polymerization. In *Surface-initiated polymerization I* (pp. 1-45). Springer Berlin Heidelberg.

Türesin, F., Gürsel, I., & Hasirci, V. (2001). Biodegradable polyhydroxyalkanoate implants for osteomyelitis therapy: in vitro antibiotic release. *Journal of Biomaterials Science, Polymer Edition*, *12*(2), 195-207.

Tyagi, R. (Ed.). (2015). *Processing Techniques and Tribological Behavior of Composite Materials*. IGI Global.

Ul-Islam, M., Khan, T., & Park, J. K. (2012). Nanoreinforced bacterial cellulose–montmorillonite composites for biomedical applications. *Carbohydrate Polymers*, *89*(4), 1189-1197.

Ullah, A., & Wu, J. (2013). Feather Fiber-Based Thermoplastics: Effects of Different Plasticizers on Material Properties. *Macromolecular Materials and Engineering*, *298*(2), 153-162.

254

Ullah, A., Vasanthan, T., Bressler, D., Elias, A. L., & Wu, J. (2011). Bioplastics from feather quill. *Biomacromolecules*, *12*(10), 3826-3832.

Ultee, A., Bennik, M. H. J., & Moezelaar, R. (2002). The phenolic hydroxyl group of carvacrol is essential for action against the food-borne pathogen Bacillus cereus. *Applied and Environmental Microbiology*, *68*(4), 1561-1568.

Unelius, C. R., Sandell, J., & Orrenius, C. (1998). Enantioselective Preparation of the Stereoisomersof 4-Methylheptan-3-ol Using *Candida antarctica* Lipase B. *Collection of Czechoslovak chemical communications*, *63*(4), 525-533.

Valappil, S. P., Misra, S. K., Boccaccini, A. R., & Roy, I. (2006). Biomedical applications of polyhydroxyalkanoates, an overview of animal testing and in vivo responses. *Expert Review of Medical Devices*, *3*(6), 853-868.

Valappil, S. P., Misra, S. K., Boccaccini, A. R., Keshavarz, T., Bucke, C., & Roy, I. (2007). Large-scale production and efficient recovery of PHB with desirable material properties, from the newly characterised Bacillus cereus SPV. *Journal of Biotechnology*, *132*(3), 251-258.

Vandamme, E. J., De Baets, S., Vanbaelen, A., Joris, K., De Wulf, P. 1998. Improved production of bacterial cellulose and its application potential. *Polymer Degradation and Stability*, *59*(1), 93-99.

Varma, I. K., Albertsson, A. C., Rajkhowa, R., & Srivastava, R. K. (2005). Enzyme catalyzed synthesis of polyesters. *Progress in Polymer Science*, *30*(10), 949-981.

Vasconcelos, A., Freddi, G., & Cavaco-Paulo, A. (2008). Biodegradable materials based on silk fibroin and keratin. *Biomacromolecules*, *9*(4), 1299-1305.

Vasconcelos, A., Freddi, G., & Cavaco-Paulo, A. (2009). Biodegradable materials based on silk fibroin and keratin. *Biomacromolecules*, *10*(4), 1019-1019.

Veras, H. N., Rodrigues, F. F., Colares, A. V., Menezes, I. R., Coutinho, H. D., Botelho, M. A., & Costa, J. G. (2012). Synergistic antibiotic activity of volatile compounds from the essential oil of Lippia sidoides and thymol. *Fitoterapia*, *83*(3), 508-512.

Verma, M., Azmi, W., & Kanwar, S. (2008). Microbial lipases: at the interface of aqueous and non-aqueous media: a review. *Acta microbiologica et immunologica Hungarica*, *55*(3), 265-294.

Vicente, G., Aguado, J., Serrano, D. P., & Sánchez, N. (2009). HDPE chemical recycling promoted by phenol solvent. *Journal of Analytical and Applied Pyrolysis*, *85*(1), 366-371.

Vieira, A. C., Vieira, J. C., Ferra, J. M., Magalhães, F. D., Guedes, R. M., & Marques, A. T. (2011). Mechanical study of PLA–PCL fibers during in vitro degradation. *Journal of the Mechanical Behavior of Biomedical Materials*, *4*(3), 451-460.

Viola, J., Lal, B., & Grad, O. (2003). The emergence of tissue engineering as a research field. *National Science Foundation, Arlington, VA*.

Vo-Dinh, T., & Cullum, B. (2000). Biosensors and biochips: advances in biological and medical diagnostics. *Fresenius' Journal of Analytical Ahemistry*, *366*, 540-551.

Vo-Dinh, T., Cullum, B. M., & Stokes, D. L. (2001). Nanosensors and biochips: frontiers in biomolecular diagnostics. *Sensors and Actuators B: Chemical*, *74*(1), 2-11.

Volova, T. G., Boyandin, A. N., Vasiliev, A. D., Karpov, V. A., Prudnikova, S. V., Mishukova, O. V., & Gitelson, I. I. (2010). Biodegradation of polyhydroxyalkanoates (PHAs) in tropical coastal waters and identification of PHA-degrading bacteria. *Polymer Degradation and Stability*, *95*(12), 2350-2359.

Volova, T., Shishatskaya, E., Sevastianov, V., Efremov, S., & Mogilnaya, O. (2003). Results of biomedical investigations of PHB and PHB/PHV fibers. *Biochemical Engineering Journal*, *16*(2), 125-133.

Vrlinic, T., Vesel, A., Cvelbar, U., Krajnc, M., & Mozetič, M. (2007). Rapid surface functionalization of poly (ethersulphone) foils using a highly reactive oxygen-plasma treatment. *Surface and Interface Analysis*, *39*(6), 476-481.

Walle, G. A. M., de Koning, G. J. M., Weusthuis, R. A., & Eggink, G. (2001) Properties, modifications and applications of biopolyesters. *Biopolyesters,* 71, 264–291.

Wan, Y. Z., Huang, Y., Yuan, C. D., Raman, S., Zhu, Y., Jiang, H. J., & Gao, C. (2007). Biomimetic synthesis of hydroxyapatite/bacterial cellulose nanocomposites for biomedical applications. *Materials Science and Engineering: C*, *27*(4), 855-864.

Wang, L., He, S., Wu, X., Liang, S., Mu, Z., Wei, J., & Wei, S. (2014). Polyetheretherketone/nano-fluorohydroxyapatite composite with antimicrobial activity and osseointegration properties. *Biomaterials*, *35*(25), 6758-6775.

Wang, Y. W., Wu, Q., & Chen, G. Q. (2003). Reduced mouse fibroblast cell growth by increased hydrophilicity of microbial polyhydroxyalkanoates via hyaluronan coating. *Biomaterials*, *24*(25), 4621-4629.

Wang, Y. W., Yang, F., Wu, Q., Cheng, Y. C., Peter, H. F., Chen, J., & Chen, G. Q. (2005). Effect of composition of poly (3-hydroxybutyrate-co-3-hydroxyhexanoate) on growth of fibroblast and osteoblast. *Biomaterials*, *26*(7), 755-761.

Wang, Y. X., & Cao, X. J. (2012). Extracting keratin from chicken feathers by using a hydrophobic ionic liquid. *Process Biochemistry*, *47*(5), 896-899.

Wang, Y., & Chen, L. (2011). Impacts of nanowhisker on formation kinetics and properties of all-cellulose composite gels. *Carbohydrate Polymers*, *83*, 1937-1946.

Wang, Z., Itoh, Y., Hosaka, Y., Kobayashi, I., Nakano, Y., Maeda, I., Umeda, F., Yamakawa, J., Kawase, M., & Yag, K. (2003). Novel transdermal drug delivery system with polyhydroxyalkanoate and starburst polyamidoamine dendrimer. *Journal of Bioscience and Bioengineering*, *95*(5), 541-543.

Wattanakornsiri, A., Pachana, K., Kaewpirom, S., Traina, M., & Migliaresi, C. (2012). Preparation and properties of green composites based on tapioca starch and differently recycled paper cellulose fibers. *Journal of Polymers and the Environment*, *20*(3), 801-809.

Wavhal, D. S., & Fisher, E. R. (2002). Hydrophilic modification of polyethersulfone membranes by low temperature plasma-induced graft polymerization. *Journal of Membrane Science*, *209*(1), 255-269.

Weng, Y. X., Wang, X. L., & Wang, Y. Z. (2011). Biodegradation behavior of PHAs with different chemical structures under controlled composting conditions. *Polymer Testing*, *30*(4), 372-380.

Whitesides, G. M. (2005). Nanoscience, nanotechnology, and chemistry. *Small*, *1*(2), 172-179.

Widsten, P., Kandelbauer, A. 2008. Laccase applications in the forest products industry: a review. *Enzyme and Microbial Technology*, *42*(4), 293-307.

Williams, D. F. (Ed.). (1987). Definitions in biomaterials: proceedings of a consensus conference of the European Society for Biomaterials, Chester*, England, March 3-5, 1986* (Vol. 4). Elsevier Science Limited.

Williams, S. F., Martin, D. P., Horowitz, D. M., & Peoples, O. P. (1999). PHA applications: addressing the price performance issue: I. Tissue engineering. *International Journal of Biological Macromolecules*, *25*(1), 111-121.

Wnek, G. E., Carr, M. E., Simpson, D. G., & Bowlin, G. L. (2003). Electrospinning of nanofiber fibrinogen structures. *Nano Letters*, *3*(2), 213-216.

Wollerdorfer, M., & Bader, H. (1998). Influence of natural fibres on the mechanical properties of biodegradable polymers. *Industrial Crops and Products*, *8*(2), 105-112.

Wong, K. K., Richardson, J. D., & Mansfield, S. D. (2000). Enzymatic treatment of mechanical pulp fibers for improving papermaking properties. *Biotechnology progress*, *16*(6), 1025-1029.

Xiao, P., Dumur, F., Zhang, J., Gigmes, D., Fouassier, J. P., & Lalevée, J. (2014). Copper complexes: the effect of ligands on their photoinitiation efficiencies in radical polymerization reactions under visible light. *Polymer Chemistry*, *5*(21), 6350-6357.

Xu, F. (1996). Oxidation of phenols, anilines, and benzenethiols by fungal laccases: correlation between activity and redox potentials as well as halide inhibition. *Biochemistry*, *35*(23), 7608-7614.

Xu, F., Kulys, J. J., Duke, K., Li, K., Krikstopaitis, K., Deussen, H. J. W., & Schneider, P. (2000). Redox chemistry in laccase-catalyzed oxidation of N-hydroxy compounds. *Applied and Environmental Microbiology*, *66*(5), 2052-2056.

Yamada, K., Abe, T., & Tanizawa, Y. (2007). Black tea stain formed on the surface of teacups and pots. Part 2–Study of the structure change caused by aging and calcium addition. *Food chemistry*, *103*(1), 8-14.

Yamada, K., Chen, T., Kumar, G., Vesnovsky, O., Topoleski, L. T., & Payne, G. F. (2000). Chitosan based water-resistant adhesive. Analogy to mussel glue. *Biomacromolecules*, *1*(2), 252-258.

Yan, Q., Yuan, J., Zhang, F., Sui, X., Xie, X., Yin, Y., Wei, Y. 2009. Cellulose-based dual graft molecular brushes as potential drug nanocarriers: stimulus-responsive

micelles, self-assembled phase transition behavior, and tunable crystalline morphologies. *Biomacromolecules*, *10*(8), 2033-2042.

Yang, F., Murugan, R., Wang, S., & Ramakrishna, S. (2005). Electrospinning of nano/micro scale poly (L-lactic acid) aligned fibers and their potential in neural tissue engineering. *Biomaterials*, *26*(15), 2603-2610.

Yang, H. S., Kim, H. J., Son, J., Park, H. J., Lee, B. J., & Hwang, T. S. (2004). Rice-husk flour filled polypropylene composites; mechanical and morphological study. *Composite Structures*, *63*(3), 305-312.

Yang, X., Zhao, K., & Chen, G. Q. (2002). Effect of surface treatment on the biocompatibility of microbial polyhydroxyalkanoates. *Biomaterials*, *23*(5), 1391-1397.

Yao, C., Li, X., & Song, T. (2007). Fabrication of zein/hyaluronic acid fibrous membranes by electrospinning. *Journal of Biomaterials Science, Polymer Edition*, *18*(6), 731-742.

Yeniad, B., Naik, H., & Heise, A. (2011). Lipases in polymer chemistry. In*Biofunctionalization of Polymers and their Applications* (pp. 69-95). Springer Berlin Heidelberg.

Ying, T. H., Ishii, D., Mahara, A., Murakami, S., Yamaoka, T., Sudesh, K., & Iwata, T. (2008). Scaffolds from electrospun polyhydroxyalkanoate copolymers: fabrication, characterization, bioabsorption and tissue response. *Biomaterials*, *29*(10), 1307-1317.

Yokouchi, M., Chatani, Y., Tadokoro, H., Teranishi, K., & Tani, H. (1973). Structural studies of polyesters: 5. Molecular and crystal structures of optically active and racemic poly (β-hydroxybutyrate). *Polymer*, *14*(6), 267-272.

Yoshida, H. (1883). LXIII.—chemistry of lacquer (Urushi). Part I. communication from the chemical society of Tokio. *Journal of the Chemical Society, Transactions*, *43*, 472-486.

Young, R. C., Terenghi, G., & Wiberg, M. (2002). Poly-3-hydroxybutyrate (PHB): a resorbable conduit for long-gap repair in peripheral nerves. *British Journal of Plastic Surgery*, *55*(3), 235-240.

Yu, H. Y., Qin, Z. Y., Wang, L. F., & Zhou, Z. (2012). Crystallization behavior and hydrophobic properties of biodegradable ethyl cellulose-g-poly (3-hydroxybutyrate-co-3-hydroxyvalerate): The influence of the side-chain length and grafting density. *Carbohydrate Polymers*, *87*(4), 2447-2454.

Yu, L., Dean, K., & Li, L. (2006). Polymer blends and composites from renewable resources. *Progress in Polymer Science*, *31*(6), 576-602.

Yu, Q., Wu, Z., & Chen, H. (2015). Dual-function antibacterial surfaces for biomedical applications. *Acta Biomaterialia*, *16*, 1-13.

Yuan, W., Yuan, J., Zhang, F., & Xie, X. (2007). Syntheses, characterization, and in vitro degradation of ethyl cellulose-graft-poly (ε-caprolactone)-block-poly (l-lactide) copolymers by sequential ring-opening polymerization. *Biomacromolecules*, *8*(4), 1101-1108.

Yuan, Y., & Lee, T. R. (2013). Contact angle and wetting properties. In *Surface science techniques* (pp. 3-34). Springer Berlin Heidelberg.

Zembouai, I., Kaci, M., Bruzaud, S., Benhamida, A., Corre, Y. M., & Grohens, Y. (2013). A study of morphological, thermal, rheological and barrier properties of Poly (3-hydroxybutyrate-Co-3-Hydroxyvalerate)/polylactide blends prepared by melt mixing. *Polymer Testing*, *32*(5), 842-851.

Zhang, B., Carlson, R., Srienc, F. 2006. Engineering the monomer composition of polyhydroxyalkanoates synthesized in *Saccharomyces cerevisiae*. *Applied and Environmental Microbiology*, *72*(1), 536-543.

Zhang, H., & Liu, J. (2013). Electrospun poly (lactic-co-glycolic acid)/wool keratin fibrous composite scaffolds potential for bone tissue engineering applications. *Journal of Bioactive and Compatible Polymers*, *28*(2), 141-153.

Zhang, L., Deng, X., & Huang, Z. (1997). Miscibility, thermal behaviour and morphological structure of poly (3-hydroxybutyrate) and ethyl cellulose binary blends. *Polymer*, *38*(21), 5379-5387.

Zhao, J., Mountrichas, G., Zhang, G., & Pispas, S. (2010). Thermoresponsive Core−Shell Brush Copolymers with Poly (propylene oxide)-block-poly (ethylene oxide) Side Chains via a "Grafting from" Technique. *Macromolecules*, *43*(4), 1771-1777.

Zhao, K., Tian, G., Zheng, Z., Chen, J. C., & Chen, G. Q. (2003). Production of D-(−)-3-hydroxyalkanoic acid by recombinant *Escherichia coli*. *FEMS Microbiology Letters*, *218*(1), 59-64.

Zhao, K., Yang, X., Chen, G. Q., & Chen, J. C. (2002). Effect of lipase treatment on the biocompatibility of microbial polyhydroxyalkanoates. *Journal of Materials Science: Materials in Medicine*, *13*(9), 849-854.

Zheng, Z., Bei, F. F., Tian, H. L., & Chen, G. Q. (2005). Effects of crystallization of polyhydroxyalkanoate blend on surface physicochemical properties and interactions with rabbit articular cartilage chondrocytes. *Biomaterials*, *26*(17), 3537-3548.

Zhijiang, C., Chengwei, H., & Guang, Y. (2012). Characteristics and bending performance of electroactive polymer blend made with cellulose and poly (3-hydroxybutyrate). *Carbohydrate Polymers*, *87*(1), 650-657.

Zhijiang, C., Guang, Y., & Kim, J. (2011). Biocompatible nanocomposites prepared by impregnating bacterial cellulose nanofibrils into poly (3-hydroxybutyrate). *Current Applied Physics*, *11*(2), 247-249.

Zhu, J., Dong, X. T., Wang, X. L., & Wang, Y. Z. (2010). Preparation and properties of a novel biodegradable ethyl cellulose grafting copolymer with poly (p-dioxanone) side-chains. *Carbohydrate Polymers*, *80*(2), 350-359.

Zhuo, H., Hu, J., Chen, S., & Yeung, L. (2008). Preparation of polyurethane nanofibers by electrospinning. *Journal of Applied Polymer Science*, *109*(1), 406-411.

Zille, A. (2005). Laccase reactions for textile applications. PhD Thesis. Universidade de Minho, Portugal.

Zini, E., Focarete, M. L., Noda, I., & Scandola, M. (2007). Bio-composite of bacterial poly (3-hydroxybutyrate-co-3-hydroxyhexanoate) reinforced with vegetable fibers. *Composites Science and Technology*, *67*(10), 2085-2094.

Zinn, M., Witholt, B., & Egli, T. (2001). Occurrence, synthesis and medical application of bacterial polyhydroxyalkanoate. *Advanced Drug Delivery Reviews*, *53*(1), 5-21.

Zoccola, M., Aluigi, A., Vineis, C., Tonin, C., Ferrero, F., & Piacentino, M. G. (2008). Study on cast membranes and electrospun nanofibers made from keratin/fibroin blends. *Biomacromolecules*, *9*(10), 2819-2825.

Zou, K., Liu, Q., Chen, J., & Du, J. (2014). Silver-decorated biodegradable polymer vesicles with excellent antibacterial efficacy. *Polymer Chemistry*, *5*(2), 405-411.

Characterisation techniques

A1. Characterisation of graft composites

Characterisation of graft composites is one among the various critical parameters which needs to be access carefully using appropriate techniques. To date various techniques have been reported and used for the characterisation of biopolymers or polymeric based bio-composite materials In scientific era many researchers have obtained different results with methods based on different principles therefore, it is important to indicate the method of characterisation with comprehensive design and tool.

A1.1. Fourier transform infrared spectroscopy (FT-IR)

Fourier transform infrared spectroscopy (FT-IR) is a most commonly used IR measurement technique which is used to obtain an infrared spectrum of absorption, emission, or Raman scattering of a solid, liquid or gas. The wavelength of the absorption peak is determined by the transition energy, which corresponds to the vibrating wavelength of a bond or group of molecules. The intensity of absorption peaks is a direct measure of the amount of material. Through the molecules' characteristic absorption of IR radiation, the types of chemical bonds (functional groups) and possible elements can be identified. The application of FT-IR allows a simultaneous collection of spectra data in a wide spectral range within a few seconds with improved sensitivity. The commonly used region for IR spectroscopy is in the range of 4000-400 cm^{-1} because the absorption frequency of most organic compounds and inorganic ions is within this region. Figure A1.1 illustrate a layout of the Fourier Transform Infrared Spectroscopy (FT-IR) experimental system.
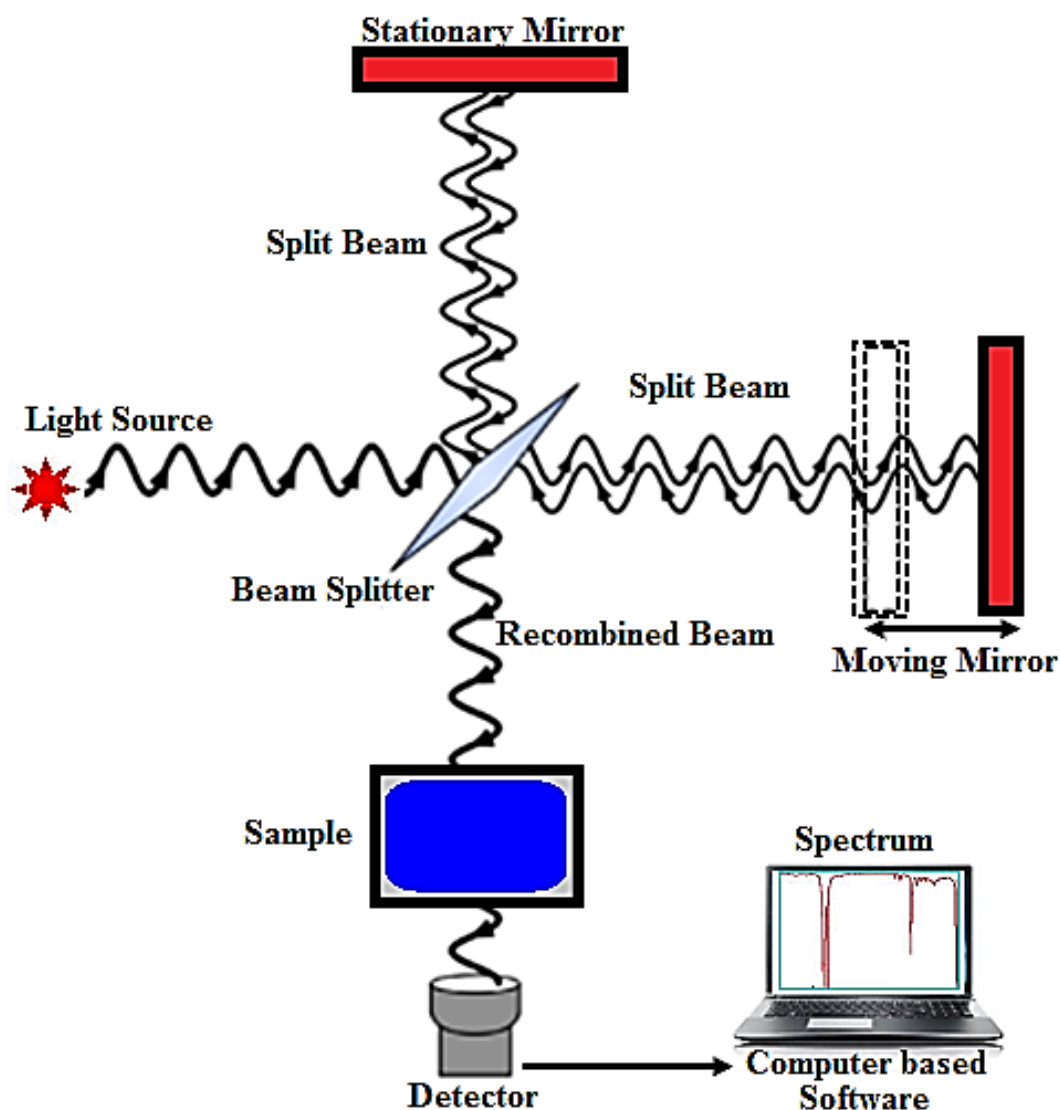
Figure A1.1 The layout of the Fourier Transform Infrared Spectroscopy (FT-IR) experimental system. FT-IR directs infrared light through a sample, ideally 50% of the light is refracted towards the fixed mirror and 50% is transmitted towards the moving mirror. Light is reflected from the two mirrors back to the beam splitter and (ideally) 50% of the original light passes into the sample compartment, which absorbs a portion of the light based on the sample's chemical composition. On leaving the sample compartment the light is refocused on to the detector.

A1.2. Scanning electron microscopy (SEM)

Scanning electron microscopy (SEM) was invented by Ernst Ruska and Max Knoll in 1931, and first commercialised in 1965. The SEM produces 2-D images of surface structures, which provide detailed morphological information that are easily interpretable. For imaging purposes, a sharp electron beam is produced and the emitted

electrons are then accelerated and focused by magnetic lenses, before the beam interacts with the sample. When the electron beam interacts with the sample, low energy secondary electrons are emitted from the sample surface, which are then collected by a secondary detector before they are further amplified electronically. The electron beam scans across the sample surface and the variations in the emission of secondary electrons generate an image of the sample external morphology. Figure A1.2 illustrate a schematic layout of the Scanning Electron Microscope (SEM) experimental system.
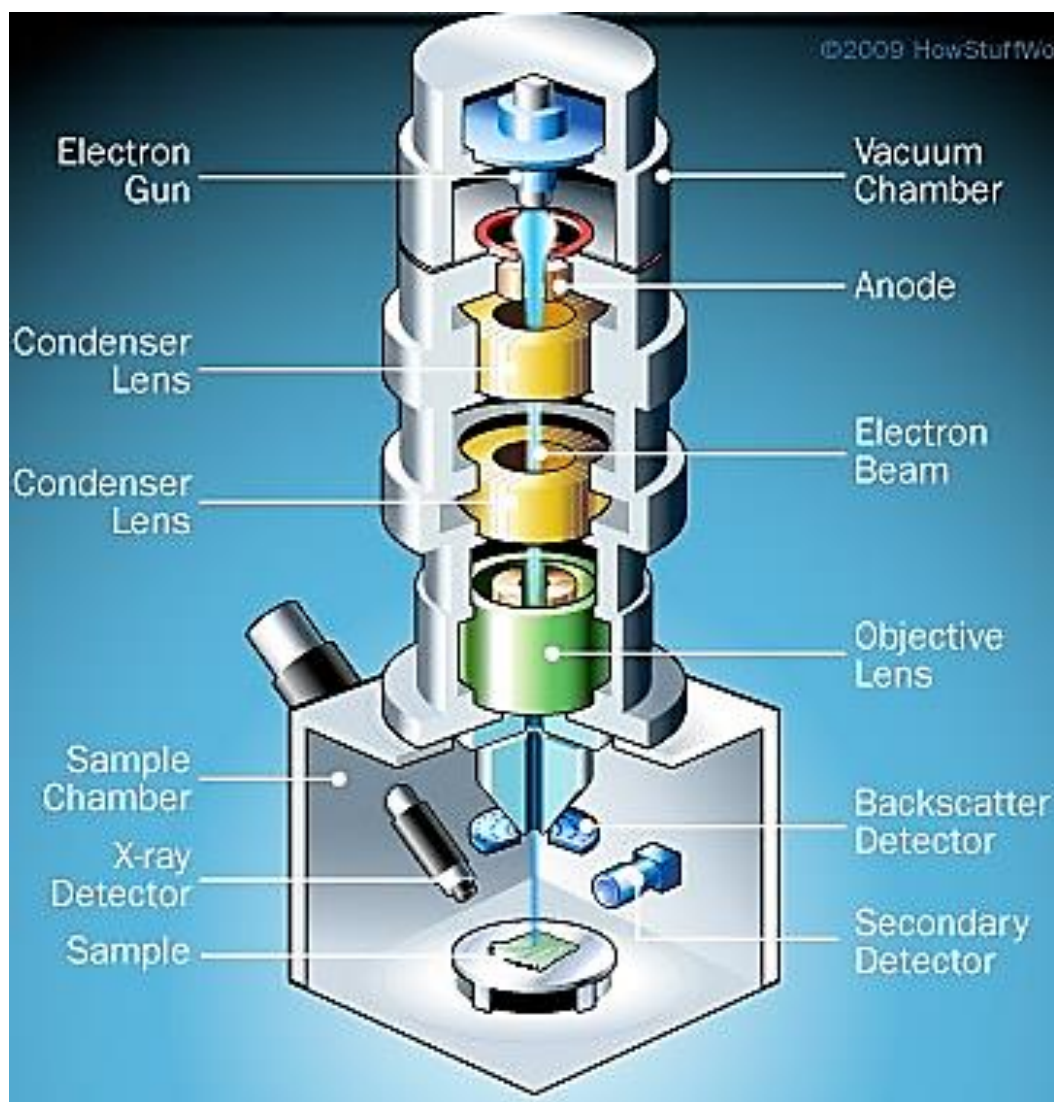

Figure A1.2 A schematic layout of the Scanning Electron Microscope (SEM) experimental system (Jonathan, 2009).

A1.3. X-ray diffraction (XRD)

XRD is most commonly used to investigate the structural features of the individual materials or composites to evaluate the crystalline structure, the ratio of crystalline to non-crystalline (amorphous) regions, crystal size, the arrangement pattern of crystals and the distance between the planes of the crystal (Ul-Islam *et al*., 2012). This means that structural changes induced in a crystalline material by grafting/blending with other materials can be monitored using the XRD technique. Figure A1.3 illustrate a schematic layout of the X-ray diffraction (XRD) experimental system.
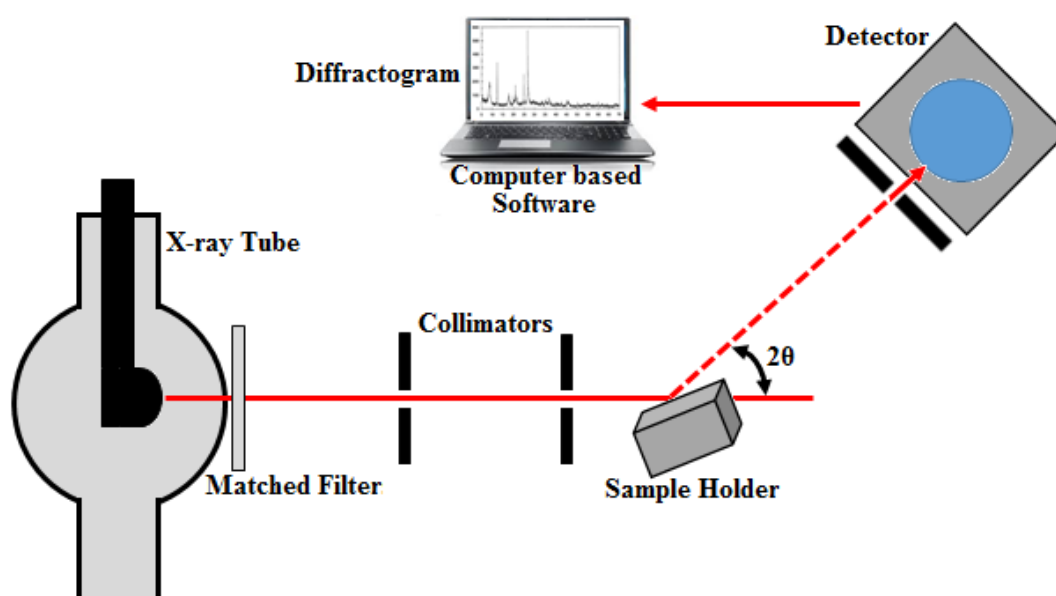

Figure A1.3 A schematic layout of the X-ray diffraction (XRD) experimental system.

A1.4. Differential scanning calorimetry (DSC)

Differential scanning calorimetry (DSC) follows a principle of the measurement of heat flow differences between a test sample and control reference. By performing DSC a sample whose temperature is increased gradually and then subsequently cooled down is investigated and finally compared to a reference probe. Therefore, it is

possible to determine enthalpies and melting points of an arbitrary polymeric material and/or polymer based composites. In order to perform DSC a furnace which can be heated up and cooled down homogenously is required. Inside this oven there are two mountings for the samples and each mounting is equipped with a high-sensitive temperature sensor (Cheng, 2002; Menczel and Prime, 2014). A general experimental layout of DSC set up is depicted in Figure A1.4 (Steinmann et al., 2013). The lid of the crucible has at least one hole to allow an exchange with the surrounding atmosphere. Furthermore, pressure build-up in the crucibles is prevented if parts of the sample vaporise. Due to the usage of a reference only effects caused by the sample itself are observable in the final thermo-gram. The oven is purged with a gas (sample gas), so that transitions and chemical reactions in different atmospheres can be examined. To avoid oxidation processes a protective gas (e.g. N_2) can be used to create an atmosphere around the sample during the process of DSC. Furthermore, the space around the oven is purged with a N_2 gas to avoid ice formation at low temperatures (Cheng, 2002; Schawe et al., 2006; Menczel and Prime, 2014).
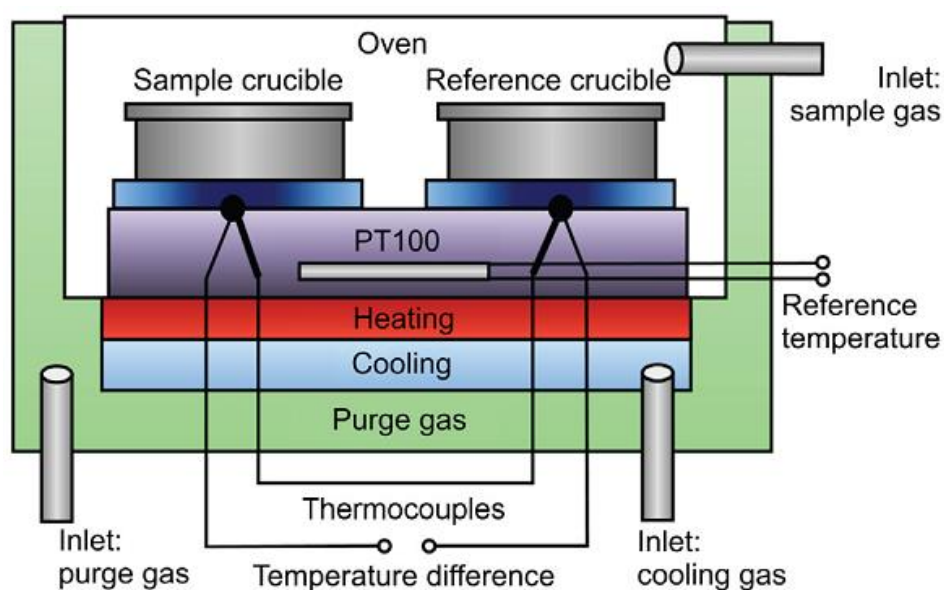

Figure A1.4 Schematic set up of differential scanning calorimetry (DSC) (Steinmann et al., 2013).

A1.5. Dynamic Mechanical Analysis (DMA)

Dynamic Mechanical Analysis (DMA) is a versatile technique that is widely used to characterise a range of polymeric materials as a function of stress, temperature, frequency or a combination of these characteristics. In principal, DMA works by applying a small deformation to a sample of known geometry in a cyclic manner. This allows the materials response to stress, and other values to be studied. A general schematic of the primary components of a DMA instrument is shown in Figure A1.5.
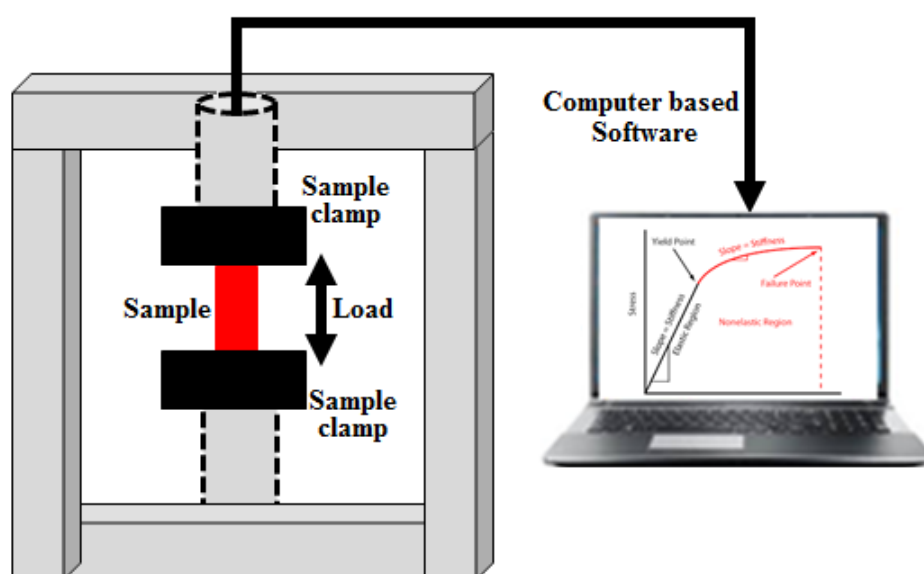

Figure A1.5 Schematic set up of Dynamic Mechanical Analyser (DMA).

A1.6. Water contact angle (WCA)

The contact angle, Theta value, is defined as the angle between the surface of the liquid and the outline of the contact surface when an interface exists between a liquid and a solid material. It was first described by Thomas Young in 1805. Figure A1.6 shows that a small contact angle can be observed when the liquid spreads on the surface, while a large contact angle can be observed when the liquid beads on the surface.

272

Whereas, an intermolecular force to contract the surface is called the surface tension which is also responsible for the shape of a liquid droplet. The hydrophobic/hydrophilic characteristics of the solid materials can be estimated by means of water contact angle measurements together with a theory of intermolecular forces.
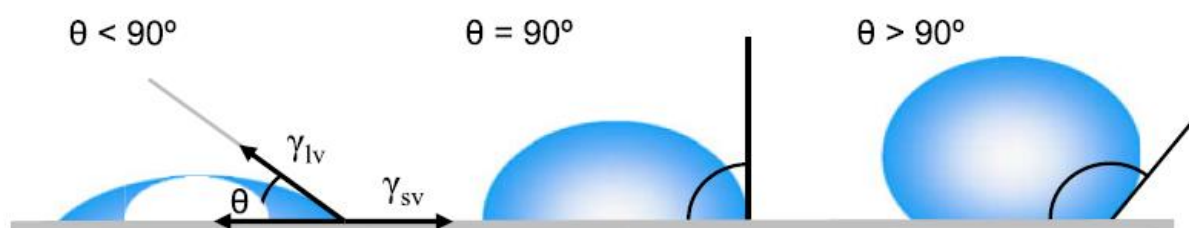

Figure A1.6 Illustration of contact angles formed by sessile liquid drops on a smooth homogeneous solid surface (Yuan and Lee, 2013).

Appendix-II

"Laccase from Aspergillus niger: A novel tool to graft multifunctional materials of interests and their characterisation"
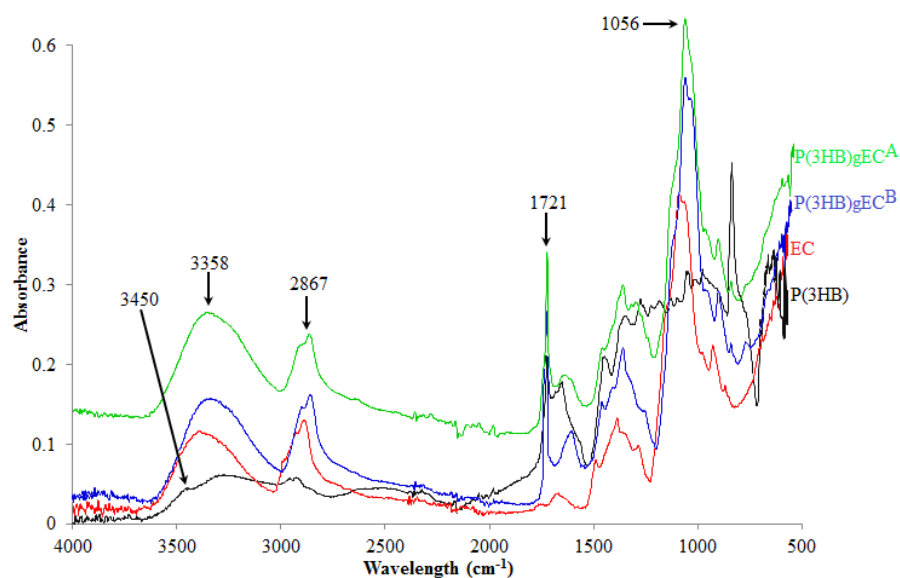
Figure A2.1 FT-IR spectra of P(3HB)-EC based individual polymers and their grafted composites i.e., P(3HB)-g-EC^A (prepared using laccase supplemented with ABTS as a mediator) and P(3HB)-g-EC^B (prepared using pure laccase alone).
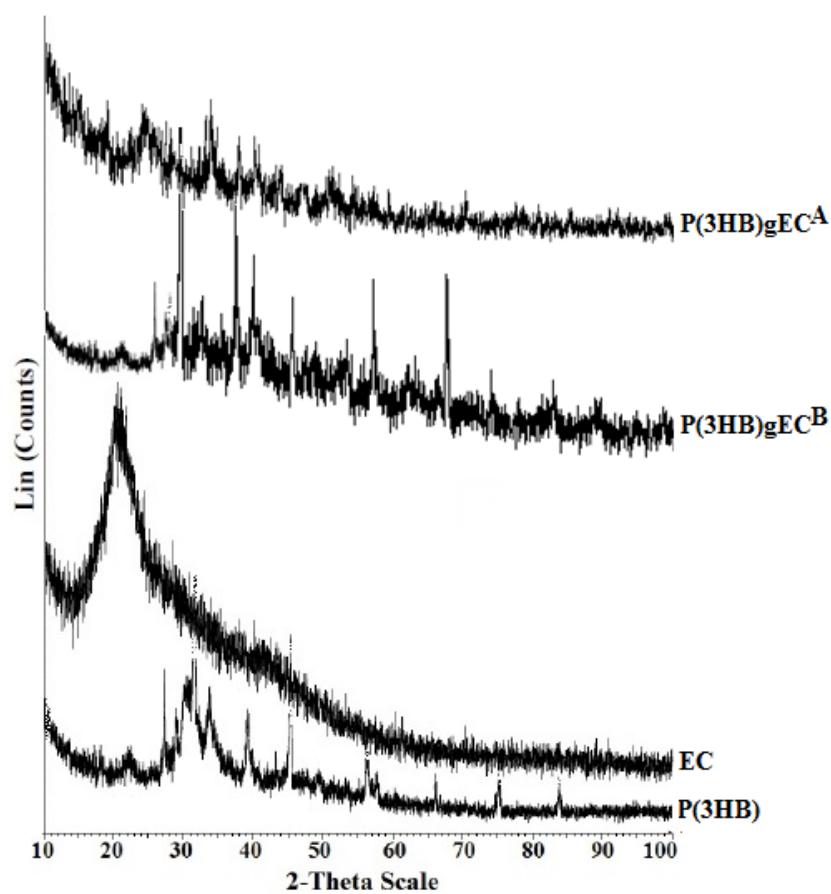

Figure A2.2 XRD profiles of P(3HB)-EC based individual polymers and their grafted composites i.e., P(3HB)-g-EC^A (prepared using laccase supplemented with ABTS as a mediator) and P(3HB)-g-EC^B (prepared using pure laccase alone).
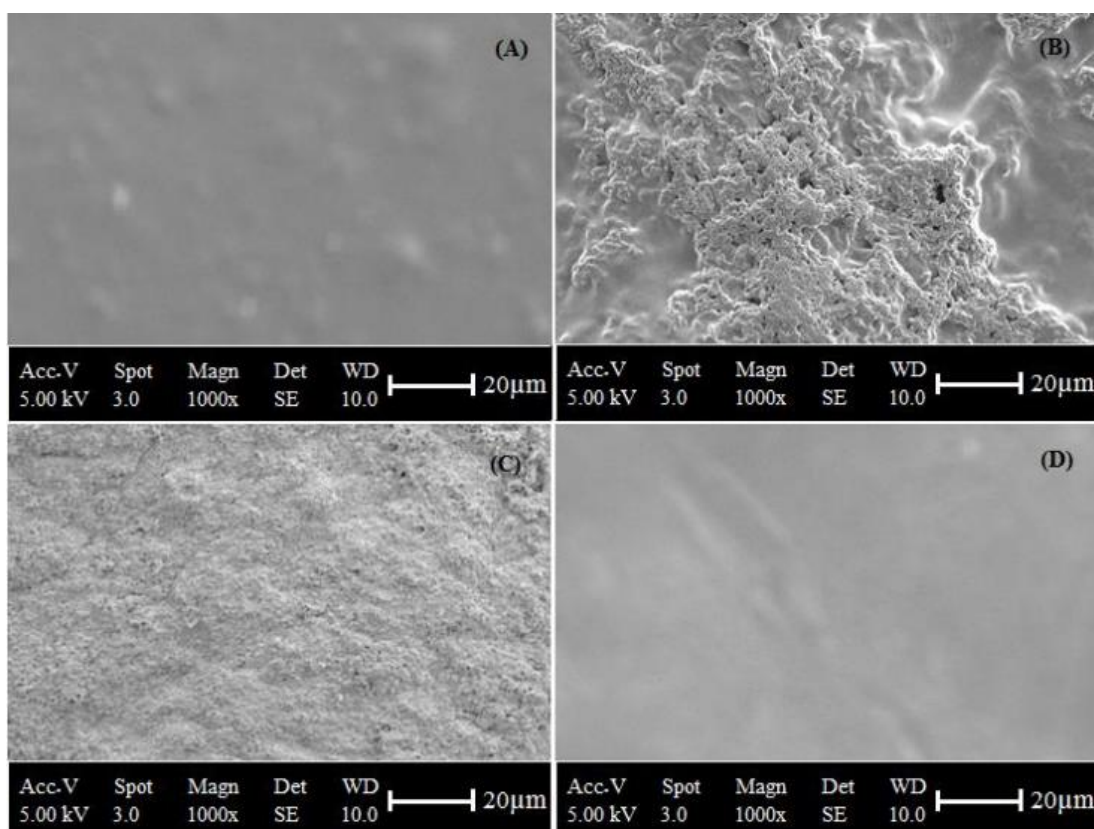
Figure A2.3 SEM micrographs of individual and grafted materials used in the present study: (A) P(3HB)-g-EC^A, (B) P(3HB)-g-EC^B, (C) P(3HB) and (D) EC.

Table A2.1 Thermo- mechanical characteristics of P(3HB)-EC based individual polymers and their grafted composites i.e., P(3HB)-g-EC^A and P(3HB)-g-EC^B.

Samples	T_g (°C)	T_m (°C)	T_c (°C)	ΔH_m (J/g)	TS (MPa)	YM (GPa)	EB (%)
P(3HB)	9±0.05	174±0.45	135±0.18	64±0.02	ND	ND	ND
EC	ND	188±0.09	48±0.05	86±0.69	122±9.85	3.38 ± 0.85	8.2±1.25
P(3HB)-g-EC^A	28±0.33	192±1.21	72±1.25	62±0.93	78±3.35	0.91±2.15	19.2±2.65
P(3HB)-g-EC^B	13±0.96	175±2.32	99±1.34	81±1.15	46±1.33	1.10±2.36	10.4±1.42

Where, ND: Not detected; TS: Tensile strength; YM: Young's modulus and EB: Elongation at break; P(3HB)-g-EC^A : prepared using laccase supplemented with ABTS as a mediator and P(3HB)-g-EC^B :prepared using pure laccase alone.
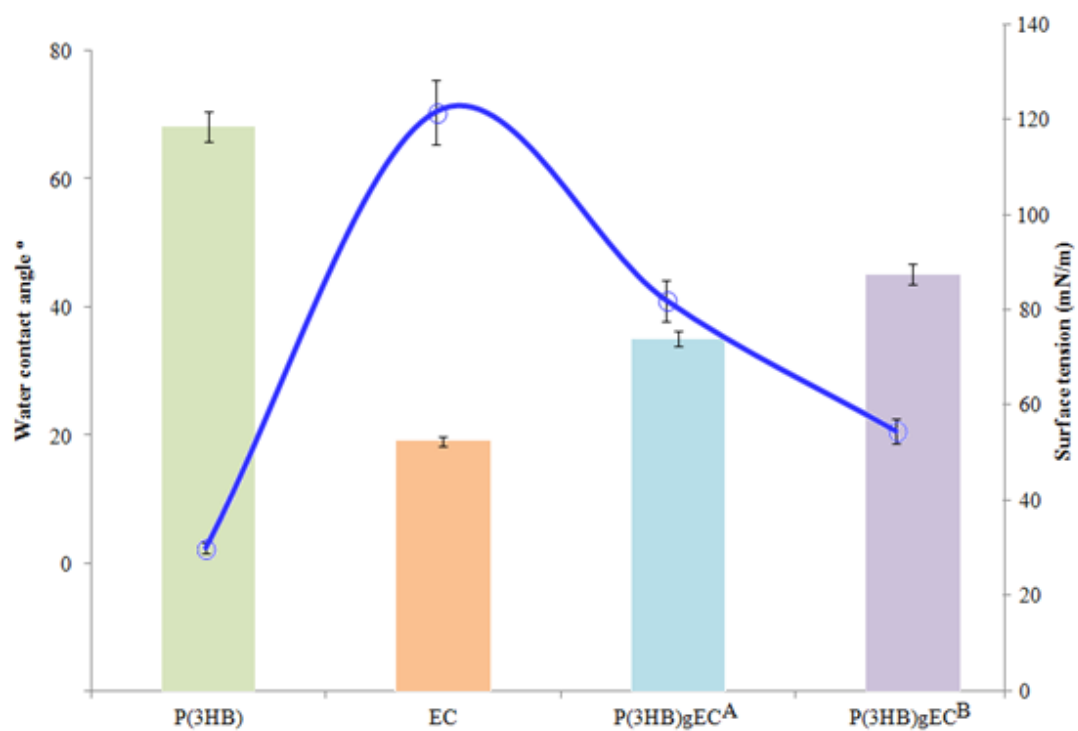
276

Figure A2.4 WCA profile of P(3HB)-EC based individual polymers and their grafted composites i.e., P(3HB)-g-EC^A (prepared using laccase supplemented with ABTS as a mediator) and P(3HB)-g-EC^B (prepared using pure laccase alone).